DEVELOPMENT OF DESIGN SOFTWARE FOR ROTATIONAL PARTS BASED ON ENERGY CONSUMPTION AND CARBON FOOTPRINT ESTIMATION MODEL

A THESIS SUBMITTED TO
THE GRADUATE SCHOOL OF NATURAL AND APPLIED SCIENCES
OF
MIDDLE EAST TECHNICAL UNIVERSITY

BY

MUHTAR URAL ULUER

IN PARTIAL FULFILLMENT OF THE REQUIREMENTS
FOR
THE DEGREE OF DOCTOR OF PHILOSOPHY
IN
MECHANICAL ENGINEERING

JUNE 2024

Approval of the thesis:

DEVELOPMENT OF DESIGN SOFTWARE FOR ROTATIONAL PARTS BASED ON ENERGY CONSUMPTION AND CARBON FOOTPRINT ESTIMATION MODEL

submitted by **MUHTAR URAL ULUER** in partial fulfillment of the requirements for the degree of **Doctor of Philosophy in Mechanical Engineering, Middle East Technical University** by,

Prof. Dr. Naci Emre Altun
Dean, Graduate School of **Natural and Applied Sciences** _______________

Prof. Dr. M. A. Sahir Arıkan
Head of Department, **Mechanical Engineering** _______________

Assoc. Prof. Dr. Ulaş Yaman
Supervisor, **Mechanical Engineering, METU** _______________

Prof. Dr. S. Engin Kılıç
Co-Supervisor, **Manufacturing Engineering, Atılım Uni.** _______________

Examining Committee Members:

Prof. Dr. M. A. Sahir Arıkan
Mechanical Engineering, METU _______________

Assoc. Prof. Dr. Ulaş Yaman
Mechanical Engineering, METU _______________

Assist. Prof. Dr. Orkun Özşahin
Mechanical Engineering, METU _______________

Prof. Dr. Can Çoğun
Mechatronics Engineering, Çankaya University _______________

Assist. Prof. Dr. Bahram Lotfi
Mechanical Engineering, TOBB ETU _______________

Date: 11.06.2024

I hereby declare that all information in this document has been obtained and presented in accordance with academic rules and ethical conduct. I also declare that, as required by these rules and conduct, I have fully cited and referenced all material and results that are not original to this work.

Name, Last name : Muhtar Ural Uluer

Signature :

ABSTRACT

DEVELOPMENT OF DESIGN SOFTWARE FOR ROTATIONAL PARTS BASED ON ENERGY CONSUMPTION AND CARBON FOOTPRINT ESTIMATION MODEL

Uluer, Muhtar Ural
Doctor of Philosophy, Mechanical Engineering
Supervisor: Assoc. Prof. Dr. Ulaş Yaman
Co-Supervisor: Prof. Dr. S. Engin Kılıç

June 2024, 298 pages

This study develops a model to estimate the electrical energy consumption and its environmental impact for a rotational product during manufacturing. Energy consumed for manufacturing processes is investigated under two components: theoretical and auxiliary energy.

Theoretical energy is consumed for actual metal removal processes and it is estimated by using the specific cutting energy and the volume of chip removed for each STEP AP224 feature of the design. Auxiliary energy is consumed by the peripheral equipment of a CNC lathe such as coolant system, spindle motor and axis servos. It is estimated by using power requirement of each auxiliary equipment and their utilization time. Power requirement is based on measurements and empirical findings. Time is calculated from the tool path movements and cutting parameters.

Estimated manufacturing process energy is converted to carbon emissions by using Carbon Emission Signature (CES^{TM}) method. This method utilizes the fractions of primary energy sources that use fossil fuels and a conversion efficiency factor. These fractions are obtained from Turkish Electricity Transmission Company (TEİAŞ) data.

Estimation model is integrated into TurnDesign Eco Edition, a feature modelling software for rotational parts. It estimates energy consumption and carbon footprints of rotational parts in the early design stages, enabling design engineer to make energy aware decisions.

Developed model is verified by measuring energy consumptions of 5 sample parts with different geometries and materials. Measurements are done using a Siemens Sentron PAC3200 power meter, installed on Anatool TP 32 CNC lathe at the Department of Mechanical Engineering, METU.

Keywords: Sustainable Manufacturing, Energy Estimation, Carbon Footprint, Energy Monitoring on CNC Lathe

ÖZ

DÖNEL PARÇALAR İÇİN ENERJİ TÜKETİMİ VE KARBON AYAK İZİ TAHMİN MODELİNE DAYALI BİR TASARIM YAZILIMI GELİŞTİRİLMESİ

Uluer, Muhtar Ural
Doktora, Makina Mühendisliği
Tez Yöneticisi: Doç. Dr. Ulaş Yaman
Ortak Tez Yöneticisi: Prof. Dr. S. Engin Kılıç

Haziran 2024, 298 sayfa

Bu çalışmada, dönel parçaların üretim operasyonları sırasındaki elektrik enerjisi tüketimlerini ve bunun çevresel etkilerini tahmin edecek bir model geliştirilmiştir. Üretim operasyonları için tüketilen enerji iki bileşen altında incelenmiştir: teorik enerji ve yanal enerji.

Teorik enerji operasyon sırasında yapılan fiziksel talaş kaldırma işlemi için harcanan enerjidir. Bu enerji, tasarlanan dönel parçalardaki her STEP AP224 unsuru için spesifik kesme enerjisi ve kaldırılan talaş hacmi kullanılarak tahmin edilmiştir. Yanal enerji CNC tornadaki kesme sıvısı sistemi, hidrolik sistem, yağlama sistemi, iş mili ve eksen servoları gibi çevresel bileşenler tarafından tüketilen enerjidir. Bu enerji, her yanal bileşenin güç gereksinimi ve o bileşenin çalıştığı süre tahmin edilerek hesaplanmıştır. Güç tüketimi ölçümler ve deneysel veri kullanılarak, süreler ise takım yolları ve kesme parametrelerinden yararlanılarak bulunmuştur.

Üretim operasyonları için tahmin edilen enerji, Carbon Emission Signature (CES^{TM}) yöntemiyle karbon salınım değerine dönüştürülmüştür. CES yöntemi, fosil yakıt tüketen enerji kaynaklarının oranları ve bir verimlilik çarpanı kullanır. Fosil yakıtları yakılmasından üretilen eletrik enerjisinin oranı Türkiye Elektrik İletim A.Ş (TEİAŞ) verisinden elde edilmiştir.

Tahmin modeli, dönel parçalar için unsur modelleme yazılımı olan TurnDesign Eco Edition'a entegre edilmiştir. Bu yazılım dönel parçaların erken tasarım aşamalarında enerji tüketimlerini ve karbon ayak izlerini tahmin ederek tasarım mühendisinin eko-tasarım yapmasına olanak sağlamaktadır.

Geliştirilen model, farklı geometri ve malzemelere sahip 5 örnek parçanın enerji tüketimleri ölçülerek doğrulanmıştır. Ölçümler, ODTÜ Makina Mühendisliği Bölümünde bulunan Anatool TP 32 CNC torna tezgahına bağlı bir Siemens Sentron PAC3200 enerji analizörü kullanılarak yapılmıştır.

Anahtar Kelimeler: Sürdürülebilir Üretim, Enerji Tahmini, Karbon Ayakizi, CNC Torna Tezgahında Enerji Ölçümü

In memory of Prof. Dr. Metin Akkök

ACKNOWLEDGEMENTS

I would like to express my deepest gratitude to my supervisors, Assoc. Prof. Dr. Ulaş Yaman and Prof. Dr. S. Engin Kılıç, for their invaluable guidance and support throughout this journey. Their expertise and encouragement have been instrumental in shaping this dissertation.

I am also profoundly thankful to the committee members, Prof. Dr. Can Çoğun, Prof. Dr. Sahir Arıkan and Prof. Dr. Ömer Anlağan. I consider myself fortunate to have had their manufacturing and academic expertise by my side. Their insightful comments and constructive criticisms have been crucial in refining my thesis.

I extend my sincere thanks to the jury members, Assist. Prof. Dr. Bahram Lotfi, for his insights on discrepancies in the verification study and Assist. Prof. Dr. Orkun Özşahin, for his guidance during the experimental investigation of chatter in the sample parts.

My appreciation also goes to the machine shop team: Refik Önder, for his help with designs, advice on parameters and assistance in the manufacture of sample parts, along with Sefa Şahin and Yusuf Papur.

A special thanks to Tansel Yıldız from Arçelik Compressor Plant in Eskişehir for providing the Siemens Sentron PAC32000 used for all the measurements in this study, as well as his expertise in energy monitoring. His support helped overcome a significant bottleneck in this research.

I am grateful to Burç Aral from Erkunt Sanayi A.S. for providing the cast iron workpieces used in the verification part of this study.

To my colleagues and friends, your support and friendship have been a source of strength and encouragement.

Lastly, I am deeply indebted to my parents for their endless support and understanding throughout this journey. Their belief in me has been a constant source of strength and motivation.

TABLE OF CONTENTS

LIST OF TABLES

TABLES

LIST OF FIGURES

FIGURES

CHAPTER 1

INTRODUCTION

Climate change is widely acknowledged as a major environmental challenge at global scale. It is known that climate change and global warming are triggered by the adverse effects of greenhouse gasses (GHG) and among these, CO_2 has the highest impact on greenhouse effect. The core of this environmental issue is the combustion of fossil fuels, representing the primary source of GHG emissions.

According to 2021 data of National Inventory Report (TurkStat, 2023), 71.3% of the GHG in Turkey is originated from energy sector which includes emissions from the combustion of fossil fuels. As given in Figure 1.1, nearly 40% of those emissions are the result of electricity production (1.A.1.). Therefore, if a manufacturing enterprise seeks to decrease its environmental impact through sustainable manufacturing, it is evident that the company should reduce its electricity dependency by increasing the energy efficiency of its manufacturing processes.

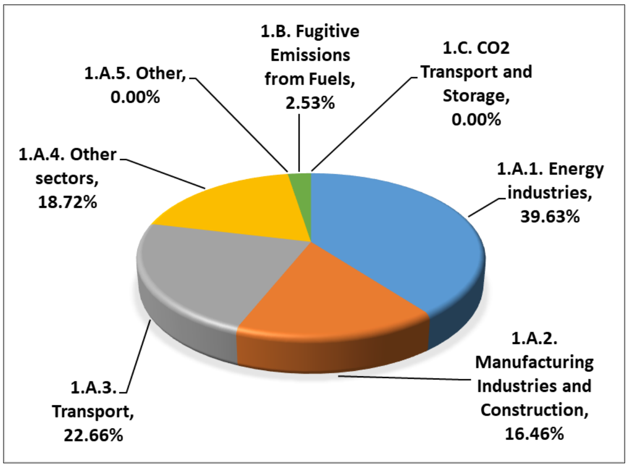

Figure 1.1 Breakdown of GHG Emissions within Energy Sector (TurkStat, 2023).

The growing population and industrialization throughout Turkey lead to a consistent rise in the need for electrical energy (Figure 1.2). According to the report of the Turkish Electricity Transmission Company, the total electricity generation in Turkey was 328,379 GWh in 2022. The Turkish Ministry of Energy and Natural Resources sets an objective of at least a 10% decrease in energy density (energy consumed per national income) by the end of 2023 in the "National Energy Efficiency Action Plan" (ETKB, 2018). The "Energy Efficiency Law" (ETKB, 2007) and the "Regulation on Increasing Efficiency in the usage of Energy Sources and Energy" (ETKB, 2008) are used as bases to achieve this objective.

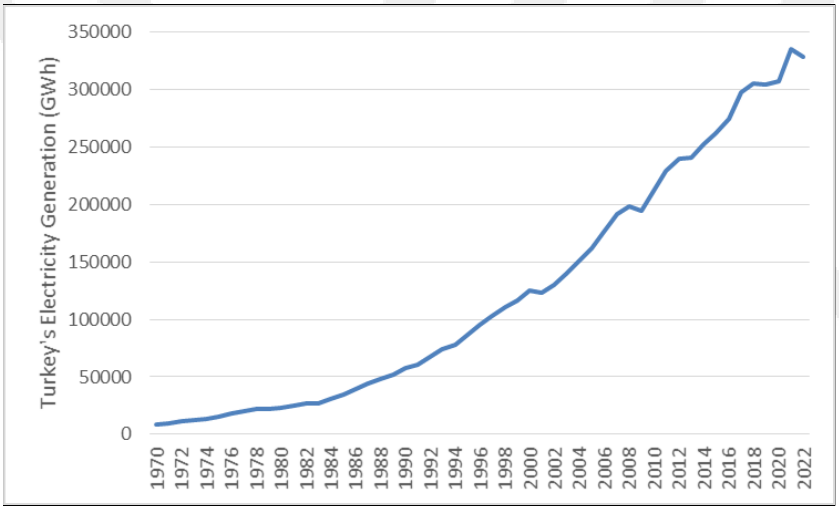

Figure 1.2 Electrical Energy Generation of Turkey (TEİAŞ, 2022a)

Sections 8e, 8f and 8g of "Regulation on Increasing Efficiency in the usage of Energy Sources and Energy" (ETKB, 2008) specify the responsibilities expected from the energy management departments of enterprises as follows:

- Monitoring and evaluating the energy consumptions and costs; preparing periodical reports.
- Acquiring and installing the necessary meters for tracking energy consumptions.

- Tracking the relation between products and energy consumption and preparing proposals for the reduction of energy intensity of the enterprise.

In the context of manufacturing industry, monitoring of energy consumption is only possible during the manufacturing stage, after the design stage of the part is completed. Hauschild et al. (2005) emphasize that the knowledge about the product is increased as the design stage progresses from idea generation towards detailed design. On the other hand, most of the product properties are determined by design decisions, decreasing the possibility of improving the energy consumption and environmental performance of the product. By the time the production starts, most of the design decisions are already made and there is a little improvement potential for the properties of the part. This situation is presented in Figure 1.3. Therefore, a tool is needed which can estimate the energy consumption in the early design stages.

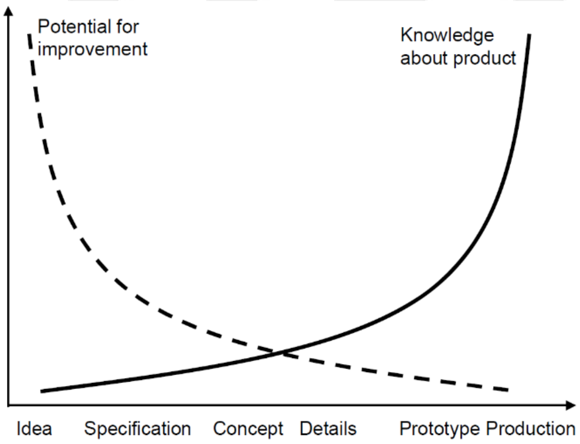

Figure 1.3 Product knowledge vs. improvement potential (Hauschild et al., 2005)

This study aims at developing a method and a software tool for the mechanical product designers, providing information about the energy consumption and carbon footprint of the part. The tool will enable them to make energy aware and environmentally conscious decisions during the design stage, before the process plan is made and part is manufactured.

1.1 Scope and Limitations of the Study

In this study, a method and a software tool is developed to estimate the manufacturing energy requirement and carbon footprint of a rotational part in real time as the design process continues. Estimation is based on material removal in machining operations, cutting tool geometry, cutting parameters and the total cutting time. These requirements generates a need for a process plan and a part program generation. For this purpose a complete CAD/CAPP/CAM system is developed allowing the determination of the estimation parameters. For each design change, CAPP and CAM modules run in the background assuming the current state as the final design and making all the decisions and creating the necessary outputs to manufacture the design.

The estimated energy for the designed part is the electrical energy required by the manufacturing processes. Energy required by the automated material handling equipment such as robots or conveyors and indirect energy required by the services to maintain the environment for the production activities of the part are not in the scope of this study.

A feature modeler is used for the CAD system. Design by features enables a smooth CAD/CAPP/CAM integration without any user intervention. A feature modeler developed by Akkuş and Kılıç (2012) establishes the foundation of the CAD system of this study. The feature library involves outer round features (outer diameter, outer diameter to shoulder), revolved groove, revolved flat, revolved round), transition features (fillet, edge round, chamfer), hole features (round hole, hole, counterbore, countersunk) and excludes knurl and thread features.

CAPP system involves Geometry Extraction and Process Planning modules. Geometry Extraction creates the link between features to toolpaths by defining the outer and inner geometry utilizing feature data. Process planning determines the tools and cutting parameters for different materials. ISO material grouping is used for this study and one subgroup for each P (alloy steel), N (nonferrous material) and K (cast iron) groups is selected for database generation.

The primary component of the CAM system is Part Programming module, responsible for generating the NC code. Cutting time is incrementally calculated during part programming stage as well. Part programs emulate simple and multiple repetitive lathe cycles without toolpath optimization. Outer turning part program can be generated for Type I cycles (steadily increasing contour) only and includes finish turning. Finish cut is not included for grooving operations.

Anatool TP32 CNC lathe is used for calculating the empirical inputs of the auxiliary energy estimation model and verification studies of the entire model. Implementation of the estimation model for other CNC lathes requires a calibration of the software based on measurements for the new CNC lathe.

1.2 Outline

Chapter 2 consists of a literature survey on manufacturing energy requirements of parts and machine tools. Previous studies on manufacturing energy estimations are reviewed under theoretical and empirical models.

Chapter 3 presents the framework and the interdependency of modules of the estimation model. General information on the modules is provided with specific details in the following chapters.

Chapter 4 describes the feature modeler used for the feature data input and design virtualization. STEP AP224 features used in the library of this study are also outlined in this chapter.

Chapter 5 introduces the Geometry Extraction module, essential for converting user-input feature data into usable geometrical information for toolpath generation in the Part Programming module. Point matrices specific to each operation are generated, defining the outer or inner geometry of the part.

Chapter 6 involves the integration of process planning stages into the estimation model. This chapter provides a detailed explanation of the selection of tools and cutting parameters for each operation, establishing a connection between the User Input and the Part Programming modules.

Chapter 7 focuses on the Part Programming module. Firstly, part program structure is explained. Then, toolpaths generated for each operation are detailed. Finally time estimation method for each motion type (G00/G01/G02/G03) of the part program is presented.

Chapter 8 is dedicated to the energy and carbon footprint estimation model. Energy estimation is explained in two different sections: theoretical and auxiliary energy. Another section discusses a method for carbon footprint estimation based on energy values.

Chapter 9 presents the test set-up used for the study giving details about the energy monitoring system and the CNC Lathe used. It also involves the verification studies of the estimation model using 5 sample parts. Drawings for the sample parts, generated part programs and estimation results for those 5 sample parts are presented. Estimation results are compared with the measurements to demonstrate the performance of the developed model.

Chapter 10 finalizes the thesis by providing concluding remarks for the study. Recommendations for possible future works based on the developed model are outlined in this chapter as well.

CHAPTER 2

LITERATURE REVIEW

2.1 Introduction

This literature review provides an overview of energy consumption models and estimation methods in manufacturing. It traces the evolution from basic empirical models to advanced approaches and identifies gaps to shape the thesis scope.

Section 2.2 focuses on models developed for predicting energy consumption in manufacturing processes. These models are essential for understanding the energy requirements of various manufacturing operations. Section 2.3 presents research on techniques for reducing energy consumption during machining operations. This includes optimizing toolpaths, implementing CNC machining practices and selecting energy-efficient cutting tools. Section 2.4 discusses potential gaps in the literature. This section addresses the need for a more integrated CAD/CAM approach with minimal human intervention for accurate energy estimation at the design stage.

2.2 Empirical and Theoretical Energy Modeling

One of the early studies for manufacturing energy estimation is Gutowski et al. (2006). In this study they emphasized that the actual machining takes only a small portion of the total manufacturing energy and auxiliary equipment can dominate energy requirements as shown in Figure 2.1.

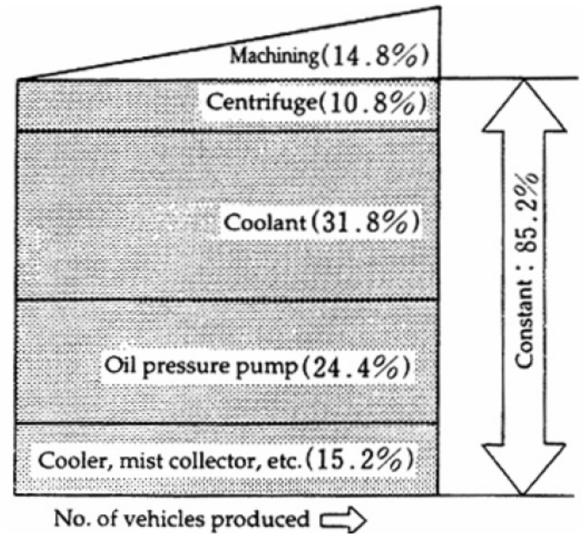

Figure 2.1 Energy of a car production machining line (Gutowski et al., 2006)

A significant amount of energy is needed to start and maintain the equipment in a "ready" state. After reaching this state, extra energy is required that directly correlates with the volume of material being processed. They modeled this by:

$$E = (P_o + k\,\dot{v})\,t \tag{2.1}$$

where P_o is the idle power, $\dot{v}$ is the material removal rate and k is a constant related to the particular manufacturing process. They concluded that the rate of production is the most critical factor affecting the specific electrical energy requirements of manufacturing processes. To minimize energy consumption, the authors suggest redesigning auxiliary equipment and increasing the efficiency of the physical mechanisms involved.

Another important study frequently referenced in the literature was conducted by Li and Kara (2011). They aimed to develop a method to predict the total energy consumption of a CNC turning machine tool. considering not only the energy used for material removal but also the energy consumed by auxiliary units. Using empirical data, the authors established a model based on power measurements. The model uses specific energy consumption (SEC) as the functional unit, defined as the energy consumed to remove 1 cm^3 of material. The primary equation used is:

$$SEC = C_0 + \frac{C_1}{MRR} \tag{2.2}$$

where C_0 and C_1 are coefficients derived from experimental data and MRR is the material removal rate.

It was found that the specific energy consumption depends significantly on the material removal rate, with the energy requirements increasing at lower rates of material removal. The study concluded that optimizing auxiliary equipment and increasing the efficiency of the physical mechanisms involved are essential strategies for reducing energy use. However, the model is highly dependent on experimentally determined coefficients, which may vary between different setups.

Balogun and Mativenga (2013) aimed to develop a model for estimating the direct electrical energy requirements of machining processes. The researchers focused on breaking down the components of energy consumption into distinct states of the machine tool: basic, ready and cutting states. They utilized an empirical approach to measure the power consumption of various machine modules and auxiliary units in these states. The fundamental equation for their energy model, represented as:

$$E_t = P_b\, t_b + (P_b + P_r)\, t_r + P_{air}\, t_{air} + (P_b + P_r + P_{cool} + k\dot{v})\, t_c \tag{2.3}$$

where E_t is the total energy requirement, P_b is the basic power, P_r is the power increment for the ready state, P_{cool} is the coolant pumping power, k is the specific cutting energy, $\dot{v}$ is the material removal rate, t_b, t_r and t_c are the times for the basic, ready and cutting states respectively and t_{air} represents the time for non-cutting moves.

The results indicated that the power requirements for machine tools operating at no load are significantly influenced by the auxiliary units. For instance, the power demand in the ready state for various machines ranged between 28% to 47% of the total power requirement at no load. This highlights the importance of accurately modeling the ready state to estimate total energy demand effectively. Additionally, the study found that fluid pump and spindle movement were major contributors to energy consumption during the machining process.

Liu et al. (2015) conducted a study to predict the energy consumption of the main driving system of a machine tool. The focus was on the spindle motor and mechanical transmission system, as these components primarily determine the energy consumption of the machine. The study categorized the energy consumption periods into start-up, idle and cutting periods. The energy consumption during these periods was modeled using empirical data and formulated into specific equations.

The total energy consumption was calculated using the following model:

$$E = \sum E_s + \sum E_u + \sum E_c \tag{2.4}$$

where E is the total energy consumption, E_s is the start-up energy consumption, E_u is the idle energy consumption and E_c is the cutting energy consumption. The start-up energy consumption was modeled as:

$$E_s = x_1 n^2 + x_2 n + x_3 \tag{2.5}$$

where n is the spindle speed and x_1, x_2 and x_3 are coefficients derived from experimental data. Similarly, the idle period energy consumption was calculated using the equation:

$$E_u = P_u t_u \tag{2.6}$$

where P_u is the idle power and t_u is the idle time. For the cutting periods, the energy consumption was determined by integrating the power over time, given by the equation:

$$E_c = \int (a_2 \, P_c^2 + (1 + a_1) \, P_c + P_u) \, dt \qquad (2.7)$$

where P_c is the cutting power, a_1 and a_2 are machine-specific parameters.

The results demonstrated that the model could predict the energy consumption of the machining process with a prediction error of approximately 8%. This was validated by comparing the predicted energy consumption with actual measurements obtained from an electricity meter during the machining of a specific workpiece.

Kolar et al. (2016) developed a predictive model for estimating the power consumption of the auxiliary units of CNC machine tools. The model was created through an analysis of all installed auxiliary units and their behavior. The core of the model is based on two equations. The first equation expresses the relationship between the active power of a device and its activity:

$$P_i(t) = A(t) \, P_{input} \qquad (2.8)$$

where P_i is the time characteristic of active power of a given auxiliary unit, A(t) is the time characteristic of the activity of the unit and P_{input} is the required active power in normal operation. The second equation represents the summation of energy flows:

$$P_{total}(t) = P_{drive}(t) + P_{air}(t) + \Sigma P_i(t) \qquad (2.9)$$

where P_{total} is the total active power of the machine, P_{drive} is the active power of the machine drives, P_{air} is the equivalent active power of auxiliary units powered by compressed air and P_i is the sum of the active powers of individual auxiliary units.

The results of the study showed that the proposed model could predict the power consumption of machine tool auxiliary units with reasonable accuracy. Calibration of the model with real measurements of the auxiliary units improved the prediction accuracy, reducing the deviation between the predicted and actual energy consumption to around 12%.

Jiang et al. (2019) focus on developing an improved energy consumption model for CNC machine tools, emphasizing the relationship between processing parameters such as spindle speed, feed rate, depth of cut and their impact on energy consumption. The proposed model includes components such as idle power, cutting power and auxiliary power, considering the specific energy consumption (SEC) in different machining states. The new energy consumption model is formulated as follows:

$$SEC = k_0 + \frac{k_1}{MRR} + \frac{k_2 n}{MRR} + \frac{k_3 n^2}{MRR} \tag{2.10}$$

The coefficients k_0, k_1, k_2 and k_3 are the power consumption components. k_0 is the specific energy requirement in the process of the manufacturing operation. k_1 includes machine tool standby power, motor iron loss and motor copper loss, all independent of processing status and time, affected by auxiliary functions and motor properties. k_2 accounts for non-load Kulun friction loss and Coulomb friction torques, proportional to spindle speed. k_3 denotes viscous friction power, including damping coefficients and mechanical friction losses, with a linear relationship to the square of angular velocity. These coefficients are determined through experimental data and regression analysis to fit the model accurately to the observed energy consumption patterns under various processing parameters.

The results demonstrated that the improved model provides higher accuracy in predicting energy consumption compared to previous model of Li and Kara (2011), with an average prediction accuracy of 99.70%.

2.3 Toolpath and Process Optimization

Kong et al. (2011) developed a software-based tool path evaluation system aimed at enhancing environmental sustainability in CNC machining processes. The study focused on modeling energy consumption and greenhouse gas (GHG) emissions related to CNC tool paths by evaluating various components such as acceleration/deceleration of machine tool axes and the direction of axes movement. The core model breaks down the total energy demand into constant, run-time and cutting energy portions:

$$E_{machine} = E_{const} + E_{runtime-transient} + E_{runtime-steady} + E_{cut} \tag{2.11}$$

where $E_{runtime-steady}$ is the energy required when the spindle motor and the axis drives keep a specified value and $E_{runtime-steady}$ is the required energy when the spindle and the axis drives accelerate or decelerate to reach specified values. The cutting energy is calculated by:

$$E_{cut} = K_{cut}\, w\, b\, z^p\, v_f^{1-p}\, n^p \tag{2.12}$$

where K_{cut} and p are empirically determined constants, w is the width of cut, b is the depth of cut, z is the number of flutes on the cutter and v_f is the feed rate and n is the spindle speed.

The results (Figure 2.2) showed that the tool path strategy significantly impacts energy consumption and GHG emissions. Longer toolpaths generally require longer processing time. The energy demand is also proportional to the processing time.

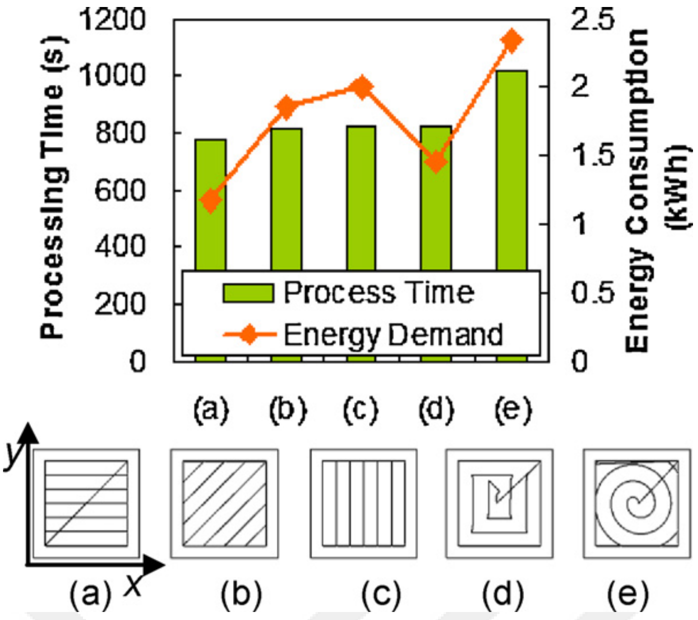

Figure 2.2 Energy consumption and time of various toolpaths (Kong et al., 2011)

He et al. (2011) conducted a study to develop a practical method for estimating the energy consumption from the NC code of a part. The focus was on analyzing the correlation between NC codes and the energy-consuming components of machine tools. The energy consumption components considered in the study included the spindle, axis feed, servos system, tool change system and auxiliary equipment such as coolant pumps and fans. The total energy consumption was modeled using the equation:

$$E_{total} = E_{spindle} + E_{feed} + E_{tool} + E_{cool} + E_{fix} \tag{2.13}$$

where $E_{spindle}$, E_{feed}, E_{tool}, E_{cool} and E_{fix} represent the energy consumption of the spindle, axis feed, tool change system, coolant pump and fixed energy consumption respectively. Further breakdown of the spindle energy consumption $E_{spindle}$ was given by:

$$E_{spindle} = \int_{t_{ms}}^{t_{me}} p_m \, dt + \int_{t_{cs}}^{t_{ce}} p_c \, dt \tag{2.14}$$

where p_m is the power for enabling the operating state of the spindle transmission module and p_c is the power for material removal from the workpiece.

Comparison with actual measurements on both NC milling machines and lathes demonstrated that the proposed method effectively estimated the energy consumption. The energy consumption of various components revealed that the highest energy consumption is attributed to the fan motors and servos system, followed by the coolant pump and spindle motor (Figure 2.3).

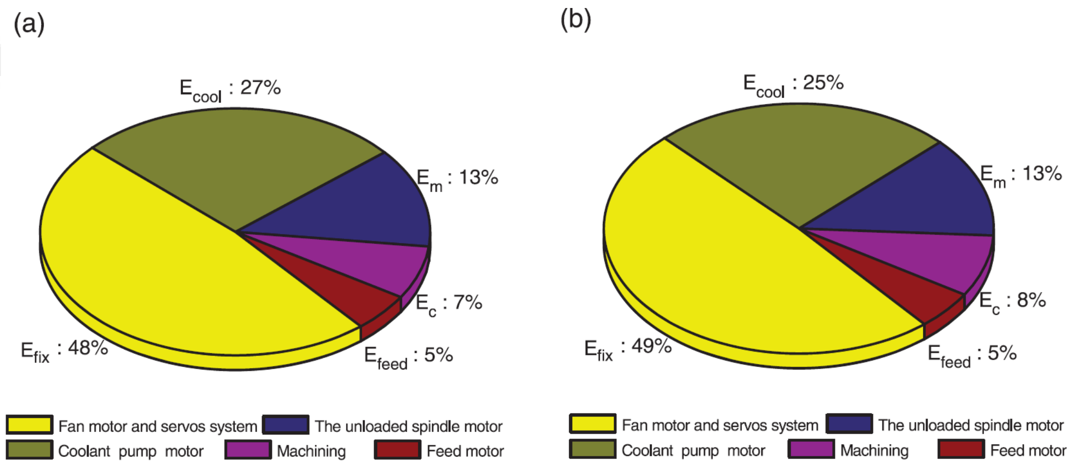

Figure 2.3 Estimated (a) and measured (b) energy percentages (He et al., 2011)

Edem and Mativenga (2017) aimed to develop a model for predicting the energy consumption of CNC machining processes by analyzing the influence of NC codes on energy demand. The study focused on various components of energy consumption, including baseline power, tool change power, spindle run power, cutting power, feed power and coolant power. The energy consumption model is presented in the following equation:

$$E = E_{baseline} + E_{toolchange} + E_{spindlerun} + E_{cut} + E_{feed} + E_{coolant} \quad (2.15)$$

This equation is further detailed in Equation (2.16):

$$E_{total} = P_{baseline}\, t_{baseline} + P_{toolchange}\, t_{toolchange} + P_{spindlerun}\, t_{spindlerun} + P_{cut}\, t_{cut} + P_{feed}\, t_{feed} + P_{coolant}\, t_{coolant} \qquad (2.16)$$

Time values are calculated from the toolpaths whereas power values are input by the user as shown in Figure 2.4.

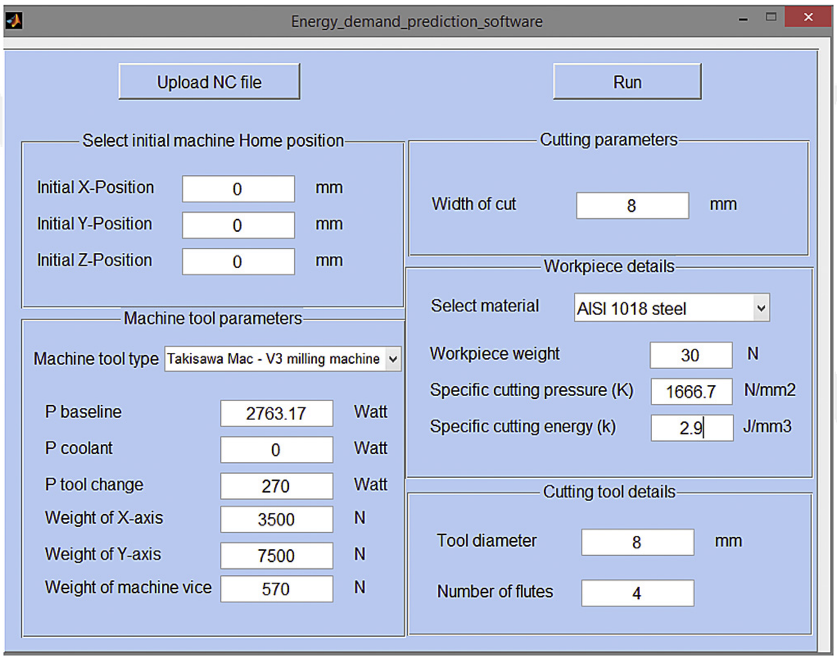

Figure 2.4 GUI for uploading NC program (Edem and Mativenga, 2017)

The study found that baseline energy consumption was the most significant component, accounting for 76% of the total energy demand, while feed axes motions and spindle energy consumption were also substantial contributors.

The study concluded that the proposed model effectively estimates the total electrical energy required for executing NC programs. This model emphasizes the importance of toolpath design in reducing energy consumption, particularly by highlighting the high energy intensity associated with shorter linear and circular toolpath segments due to acceleration and deceleration constraints. The authors suggested that selecting toolpaths with longer linear segments could significantly reduce energy intensity in machining operations.

The study by Boettjer et al. (2021) presents a methodology for machine-specific energy estimation in milling processes at the detailed design stage. The research focuses on enhancing the unit process life cycle inventory (UPLCI) model by incorporating adjustment factors that account for uncertainties in machine tool specifications and specific cutting energy (SCE) of workpiece materials. To model the energy consumption, the total energy is considered as the sum of the basic, idle and machining energies, represented as:

$$E_{total} = P_{basic}t_{basic} + P_{idle}t_{idle} + P_{milling}t_{milling} \quad (2.17)$$

where P_{basic} represents the power demand during the standby mode, which is present from the time the machine is started until it is turned off. t_{basic} is the duration the machine remains in standby mode. P_{idle} corresponds to the power demand in the run-time mode, which includes movement of the tool relative to the workpiece without cutting. t_{idle} is the time period during which this movement occurs. $P_{milling}$ denotes the power required for the actual milling operation and $t_{milling}$ is the duration of the milling process which is calculated using the length of the cut and the feed rate:

$$t_{milling} = \frac{Length\ of\ cut}{feed\ rate} \quad (2.18)$$

where length of cut is the total distance the cutting tool travels through the material.

The power required for milling can be expressed in terms of the volume removal rate (VRR) and the specific cutting energy (SCE):

$$P_{milling} = VRR\ SCE \tag{2.19}$$

To account for machine-specific factors and improve the accuracy of energy estimation, the adjusted UPLCI model introduces adjustment factors:

$$E_{total,a} = K_{basic}\ E_{basic} + \sum\left(K_{idle,s}\ E_{idle,s}\right) + \sum\left(K_{milling,o}\ E_{milling,o}\right) \tag{2.20}$$

In this equation, $E_{total,a}$ represents the total adjusted energy consumption. K_{basic} is the adjustment factor for the basic energy consumption, $K_{idle,s}$ is the adjustment factor for idle energy consumption in a specific state "s" (such as tool change or rapid traverse) and $K_{milling,o}$ is the adjustment factor for milling energy consumption in a specific operation "o" (such as face milling or pocketing). These adjustment factors are computed by comparing actual energy consumption data with those estimated by the original UPLCI model.

The authors measured energy consumption experimentally for a reference test part on specific machine tools to validate the adjusted UPLCI model. Results indicated that the UPLCI model generally overestimated energy consumption across all modes: basic, idle and machining. The adjusted UPLCI model significantly reduced these estimation errors, achieving a higher accuracy in energy consumption predictions for milling processes.

The study by Cheng et al. (2022) presents a detailed methodology for estimating energy consumption in intelligent CNC machining using the STEP-NC program. STEP-NC is a standard designed to replace traditional part programming. The authors propose to extend the STEP-NC data model to include attributes for energy consumption. The extended data model introduces entities such as "energy_usage_label", "machine_tool_energy" and "main_cutting_energy" (Figure 2.5). These entities capture key parameters like standby power, idle power, cutting power and machining time, which are used for calculating energy consumption.

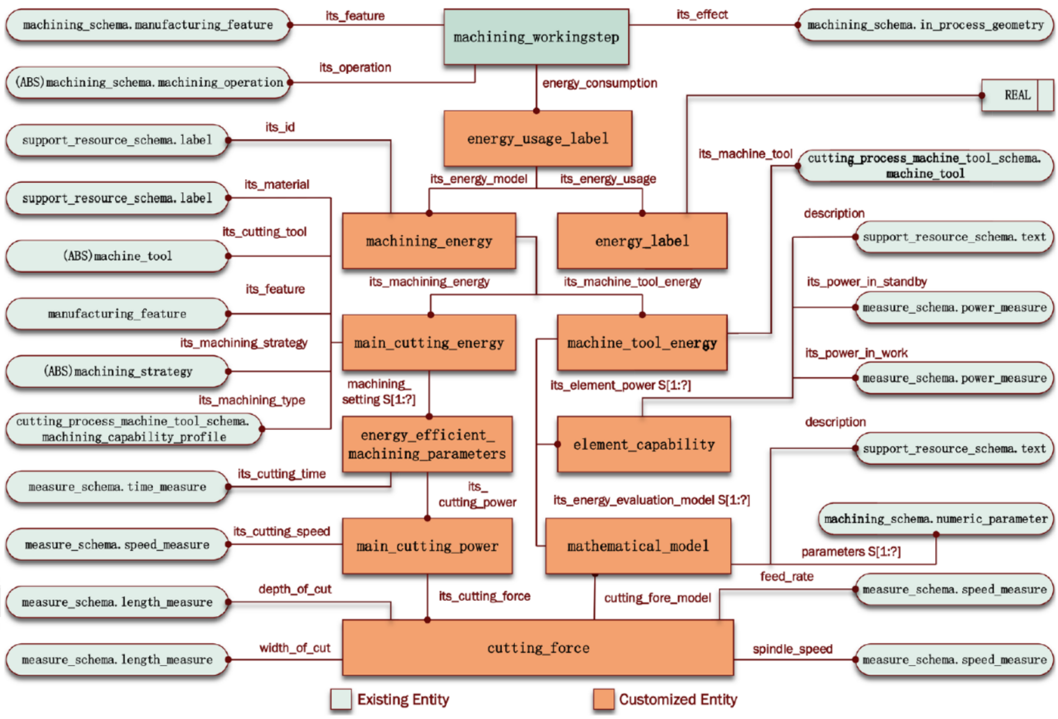

Figure 2.5 "energy_usage_label" entitiy for STEP-NC (Cheng et al.,2022)

The energy estimation method is based on machining features, considering both roughing and finishing operations. The total energy consumption of a part is the sum of the energy consumed in each machining working step, which is broken down into standby energy (E_{st}), air-cutting energy (E_{air}) and effective cutting energy (E_{ef}):

$$E_{feature} = \Sigma E_{ws-roughing} + E_{ws-finishing} \tag{2.21}$$

$$E_{ws} = E_{st} + E_{air} + E_{ef} \tag{2.22}$$

$$E_{part} = \Sigma E_{feature} + \Sigma E_{connect} + \Sigma E_{toolchange} \tag{2.23}$$

where E_{ws} is the energy consumption for a working step, $E_{connect}$ is the energy for connecting movements and $E_{toolchange}$ is the energy for tool changes.

The power components are detailed as follows:

$$E_{st} = P_{st} t_{st} \tag{2.24}$$

$$E_{air} = \left(P_{sp} + P_{st}\right) t_{air} \tag{2.25}$$

$$E_{ef} = P_{ef} t_{ef} = P_{ef} \frac{V}{MRR} \tag{2.26}$$

where P_{sp} is the spindle power and defined with a quadratic equation, P_{st} is the standby power, V is the volume of material removed, MRR is the material removal rate.

The results demonstrated that the proposed methodology could estimate energy consumption with an accuracy above 90%. A limitation of the study is that the platform requires human-computer interaction to convert the solid model of the part into a STEP-NC program, indicating that the link between the solid model and the STEP-NC program is not fully automated.

Pawanr et al. (2022) developed an energy consumption model for cylindrical parts where Variable-Material Removal Rate (VMRR) processes are considered. Variable-Material Removal Rate (VMRR) machining involves processes where the material removal rate changes dynamically during machining, such as in end-facing operations where the cutting velocity decreases as the tool moves towards the center of the part. Authors divided the total energy consumption into different modules:

$$E_{total} = E_{startup} + E_{standby} + E_{acc} + E_{rapid} + E_{idle} + E_{tc} + E_{air} + E_{cool} + E_{cut} \tag{2.27}$$

Cutting energy (E_{cut}) is further divided further into CMRR and VMRR:

$$E_{cut} = E_{cut\_CMRR} + E_{cut\_VMRR} \quad (2.28)$$

In their results, the authors validated the model using experimental data from a LMW-Smarturn CNC lathe machine, achieving an accuracy of over 97%.

Zhao et al. (2022) proposes a cutting tool selection method based on energy consumption as the evaluation criteria. The model is designed with a data structure that is compatible with the STEP-NC framework.The authors developed a model to estimate energy consumption for different cutting tools. The total power (P) consumed is modeled as the sum of a constant base power (C_1) and a variable power component proportional to the cutting power ($P_{cutting}$):

$$P = C_1 + C_2\, P_{cutting} \quad (2.29)$$

Authors derive $P_{cutting}$ from the cutting force F_t, which is a function of cutting depth (a_p), cutting width (a_e), feed per tooth (f_z), tool diameter (D) and number of tooth (Z).

$$F_t = C_F\, k_{fc}\, a_p^{m1}\, a_e^{m2}\, f_z^{m3}\, n^{m4}\, D^{m5}\, \mathrm{Z} \quad (2.30)$$

where m1 to m5 are the corresponding cutting force influence indexes, C_F is the force factor and k_{fc} is the cutting correction factor.

According to the authors, in a single cutting tool machining region, it is unnecessary to directly calculate the total energy consumption when comparing the effects of different cutting tools. Instead, they suggest that the selection criteria should focus on comparing the specific energy consumption (SEC) which is calculated using Equations (2.29) and (2.30):

$$SEC = \frac{P}{MRR} = \frac{C_1 + C_2\,(C_F\, k_{fc}\, a_p^{m1}\, a_e^{m2}\, f_z^{m3}\, n^{m4}\, D^{m5}\, \mathrm{Z})V_c}{MRR} \quad (2.31)$$

Zhao et al. conducted three groups of cutting experiments using a three-axis CNC machine and various cutting tools for validation. They initially performed twelve facing milling operations to acquire machining power coefficients C_1 and C_2. For the test part 1, optimal cutting tools and parameters were recommended by the model and compared against three sets of parameters provided by experienced process planners. The results indicated good prediction accuracy, with measured and predicted values of power and SEC closely aligning. Specifically, the model-based recommendations showed an accuracy of around 99% for both power and SEC.

2.4 Discussion

Most of the estimation studies covered in this chapter focus on machine consumption and efficiency, primarily from the machine tool perspective, with a noticeable gap in the product point of view. Additionally, the literature is heavily weighted towards milling operations, with limited research on turning operations.

Some studies estimate the total energy of parts by analyzing the part program, where the part is already designed and the NC code is generated. These methods focus on process energy estimation for pre-designed parts, but do not provide solutions for estimating energy consumption at the design stage.

STEP models in the literature fail to offer an efficient bridge between part geometry and manufacturing. They often overlook the feature geometries defined in the ISO standard and instead concentrate on STEP-NC, which is mainly related to NC code generation.

A significant gap exists in the development of a complete system that estimates energy consumption accurately at the design stage, before part program generation and manufacturing. This gap highlights the need for a more integrated CAD/CAM approach to energy estimation.

Therefore, the scope of this thesis is to address this gap by seamlessly integrating CAD and CAM for a part designed to be manufactured on a CNC lathe, limiting human intervention to the initial part design stage only. The integration will be automated through feature-based design. This approach aims to provide real-time energy estimation results to the design engineer and enhance the accuracy and efficiency of energy consumption predictions.

CHAPTER 3

GENERAL FRAMEWORK

3.1 Introduction

As previously stated in Chapter 1, the main objective of this study is to develop a method and a software tool which estimates the electrical energy requirement of a rotational part and its corresponding carbon footprint. For reaching this objective, the process energy of the part is investigated in two components, theoretical energy and auxiliary energy.

Theoretical energy is the tool tip energy which is required to remove the given volume of material. It is calculated using the following equation:

$$E_{th} = V_{rem}\, p_s \tag{3.1}$$

where V_{rem} (mm^3) is the volume removed for every feature based on the feature parameters and p_s (J/mm^3) is the specific cutting energy which is defined as the energy to remove a unit volume of material. p_s is calculated by:

$$p_s = (1 - 0.01\,\gamma_0)\,\frac{p_{s1}}{(a_f\,\sin\kappa_r)^{mc}} \tag{3.2}$$

γ_0 represents the cutting rake and κ_r is the cutting edge angle, a_f is the feed engagement (feed per tooth), p_{s1} denotes the specific cutting energy for an uncut chip thickness of 1 mm and mc is a material constant.

Auxiliary energy refers to the additional energy required by peripheral equipment of the machine tool. It can be calculated either of Equation (3.3) and (3.4) according to the characteristic of each component.

$$E_{aux} = P_{aux\_component\_av}\ t_{component} \tag{3.3}$$

$$E_{aux} = E_{aux\_component\_av}\ n_{component} \tag{3.4}$$

where $P_{aux\_component\_av}$ is the average power consumption which is based on measurement results, $t_{component}$ is the use time for the auxiliary equipment, $E_{aux\_component\_av}$ is the average energy requirement of a specific component and $n_{component}$ is the number of times that particular component is used.

To estimate the time in auxiliary energy estimation equation (3.3), toolpaths and cutting parameters must be determined in advance, necessitating the creation of a part program for toolpaths and a process plan for cutting parameters. The need for a process plan also extends to the theoretical energy estimation equations (3.1) and (3.2). Equation (3.2) involves parameters such as p_{s1} and mc, dependent on the material, γ_0 and κ_r, determined by the tool geometry as well as a_f a cutting parameter, all identified within a process plan. V_{rem} calculations in Equation (3.1) require finish allowance (a_{p_finish}) and stock diameter, also determined through a process plan. Consequently, to estimate energy for a rotational part, both a process plan and a part program are essential, highlighting the development of a complete CAD/CAPP/CAM system enabling the determination of estimation parameters.

Figure 3.1 illustrates the general framework of the CAD/CAPP/CAM system, TurnDesign Eco Edition and the interdependency of its modules. Further explanation of each module is presented in the following sections.

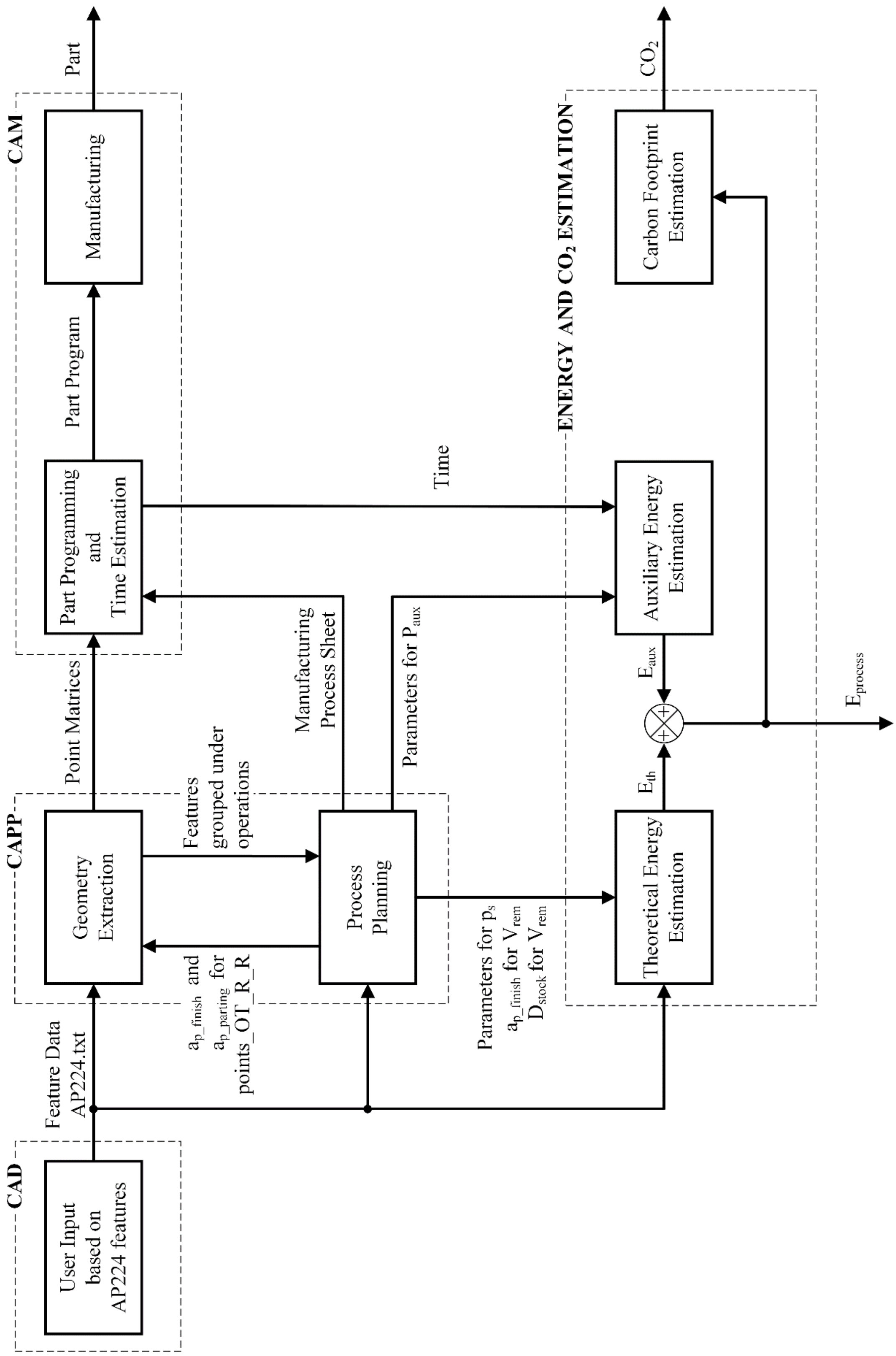

Figure 3.1 General Framework of TurnDesign Eco Edition

3.2 User Input

User Input is the primary module for the CAD subsystem and it uses a feature modeler where product data and its geometric model is created by selecting among predefined features from the feature library. This module collects all the design data input by the user that is used in the subsequent modules of the TurnDesign Eco Edition.

A feature based rotational part modeler, developed by Akkuş and Kılıç (2012) enables visualization of model creation. Developed feature modeler serves for designing rotational parts easily in a user friendly visual environment, by just picking from the pre-defined application specific features.

The feature library is developed using STEP AP224 and refining the machining features defined in AP224 for turning operations. The feature library includes definitions, classifications, attributes, generation techniques and parameters. STEP uses a formal language, EXPRESS, for specifying the features. Feature library of the module is implemented as an object-oriented data type library aligned with the EXPRESS specification of STEP.

This module outputs an STEP Part 21 file, containing all the features and parameters related to the part design. Details of this module are explained in Chapter 4.

3.3 Geometry Extraction

Geometry Extraction module creates a geometrical link between User Input and Part Programming modules. Primary objective of this module is to facilitate the transition from user-input feature data, which includes geometrical parameters related to the features, to a format usable by the Part Programming module for creating toolpaths. This involves conversion of feature data into point matrices, where each matrix represents the specific point coordinates related to machining. These matrices essentially define the exterior and interior contours of the part, guiding the generation of toolpaths in the Part Programming module. The specifics of the Geometry Extraction module are discussed in Chapter 5.

Apart from creating point matrices, the Geometry Extraction module also addresses the task of associating features with the corresponding manufacturing operations. This is achieved by grouping features with similar manufacturing operations under the same point matrix.

3.4 Process Planning

This module sequentially covers stages of process planning, including material selection, stock determination, feature identification, sequencing of manufacturing operations and setups, workholding strategies, machine allocation for each setup and specification of tools and parameters.

The main goal of the Process Planning module is to create a manufacturing bridge with subsequent modules, especially part programming and energy estimation. Its significance lies in providing cutting parameters for part programming, enabling the calculation of cutting time which is a key parameter in the auxiliary energy estimation.

The output of this module is a manufacturing process sheet (MPS) which summarizes all the decisions made for the process plan of the designed part, including the operations, tools and cutting parameters of each operation and the information on stock size and material. Process Planning module is detailed under Chapter 6.

3.5 Part Programming and Time Estimation

Part Programming module plays a critical role in the generation of the NC code for the designed rotational part. A part program generated by TurnDesign Eco Edition includes two fundamental components: toolpaths, derived from point matrices established in the Geometry Extraction module and cutting parameters acquired from the Process Planning module, reported on a Manufacturing Process Sheet (MPS).

Beyond NC code generation, Part Programming module estimates the total machining time for the designed part and usage times for each component of the CNC lathe. This estimation is achieved through calculations of incremental time required for programmed movements in each block.

3.6 Energy and Carbon Footprint Estimation

This is the main module primarily responsible for the estimation and reporting of energy requirement and carbon footprint of the designed part. Using the data gathered from the other modules, estimation module calculates the energy based on Equations (3.1) to (3.4). Corresponding carbon footprint is calculated in this module based on the Carbon Emission Signature (CES^{TM}) method proposed by Jeswiet and Kara (2008). This method involves considering the fractions of coal, natural gas and petroleum within the overall energy sources.

This module gives two outputs. The first one is the summary of the energy and carbon values on the TurnDesign Eco Edition screen. On this screen only high level theoretical, auxiliary and carbon footprint results are presented. The second output is a comprehensive Excel table which drills down all the energy and carbon footprint values for each operation and feature, providing results both in tabular form and in charts.

CHAPTER 4

USER INPUT

4.1 Introduction

The User Input module is the core of the CAD subsystem, utilizing a feature modeler to create the geometric model of a product by selecting predefined features from the feature library. This module gathers all design data input by the user, which is then used in other modules of TurnDesign Eco Edition. A feature-based rotational part modeler, developed by Akkuş and Kılıç (2012), facilitates easy design of rotational parts in a user-friendly visual environment by allowing users to select from predefined application-specific features.

The feature library, developed using STEP AP224, refines machining features for turning operations. It includes definitions, classifications, attributes, generation techniques and parameters, all specified using the formal language EXPRESS. The library is implemented as an object-oriented data type library aligned with the EXPRESS specification of STEP. This module outputs a STEP Part 21 file that contains all features and parameters related to the part design.

4.2 Design by Features

Most CAD systems utilize geometric modeling techniques which provide an incomplete definition of the product. Despite their power of representation of product model, due to the lacking high level information they cannot be used alone for downstream applications such as process planning, manufacturing, CNC programming, inspection, etc. (Shah and Rogers, 1988). There is always a need for another system to translate the implicit geometric data into explicit process planning and manufacturing information adding the design intent of the product.

To eliminate this need and be able to supply geometric tools with a higher level of information, feature modeling was introduced in 1980s. Lacking information elements in geometric modeling were introduced and named as features to create a link between geometric models and downstream applications. This means features make possible understanding the design intent and manufacturing information besides geometric information by providing engineering attributes such as materials, dimensions, tolerances, surface finish, etc. (Akkuş and Kılıç, 2012).

There are several techniques used to create features, either directly or indirectly. The direct creation case named as design by features is using the predefined features in design stage and creating geometry from the feature definitions. The indirect case is feature recognition where features are derived from the geometry of a product created by CAD software. TurnDesign Eco Edition is based on design by features.

Product data and its geometric model are created by selecting among predefined features named feature library. This gives the opportunity of adding the functional design intent and explicit manufacturing information into the product data as well as the geometric modes. This property of design by features makes the high-level communication between design and manufacturing possible without any additional process after the design phase. If there is a complete feature library for product definition the only limit is the creativity of the designer and competence of the feature based design software in using the pre-defined generic features (Amaitik and Kılıç, 2005).

4.3 Feature Library

The Feature Library is a crucial component in the design and manufacturing process, particularly for rotational parts. This section explains the various aspects of the Feature Library, emphasizing its structure, creation and application within the STEP AP224-based system.

4.3.1 STEP

A standardized product data model is required for representation and exchange of information about a product allowing the seamless integration of CAD/CAM systems. In order to address this need, the International Standards Organization (ISO) proposed a “Standard for the Exchange of the Product data” (STEP). Prior to STEP all standards developed for product data representation and exchange failed to supply high-level information for CAPP and CAM systems and only dealt with geometric aspect of design data. Introduction of STEP enabled exchanging not only geometric design data but also the high-level information.

ISO 10303 is an international standard for the computer-interpretable representation and exchange of product data, STEP. The objective is to provide a mechanism that is capable of describing product data throughout the life cycle of a product, independent from any particular system. The nature of this description makes it suitable not only for neutral file exchange, but also as a basis for implementing and sharing product databases and archiving (ISO, 1994).

STEP is organized as a series of parts, each published separately. These parts fall into one of the following series: description methods, integrated resources, application protocols (APs), abstract test suites, implementation methods and conformance testing (ISO, 1994).

4.3.2 EXPRESS Specification

STEP uses a formal specification language, EXPRESS, to specify the product information to be represented. The use of a formal language enables precision and consistency of representation and facilitates development of implementations. (Figure 4.1).

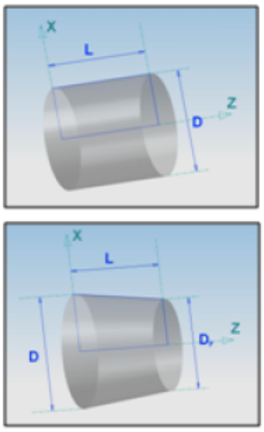


```
ENTITY outer_diameter
  SUBTYPE OF (outer_round);
  diameter : numeric_parameter;
  feature_length : numeric_parameter;
  reduced_size : OPTIONAL taper_select;
END_ENTITY;

TYPE taper_select = SELECT (diameter_taper, angle_taper);
END_TYPE;

ENTITY diameter_taper;
  final_diameter: numeric_parameter;
END_ENTITY;

ENTITY angle_taper;
  angle: numeric_parameter;
END_ENTITY;
```

Figure 4.1 EXPRESS Specification of outer_round

The EXPRESS-G diagrams, a graphical representation of the EXPRESS language, offer a visual understanding of these specifications. Figure 4.2 illustrates the EXPRESS-G representation of outer_round, aiding in the clear depiction of the data structure and relationships.

For example, the EXPRESS-G diagram for the "Outer_diameter_to_shoulder" feature, as shown in the same figure, details the relationships and attributes associated with this feature. This includes parameters such as diameter, length and the location of the feature on the part. These diagrams ensure that every aspect of the feature is defined, facilitating accurate data exchange and interpretation across different CAD/CAM systems.

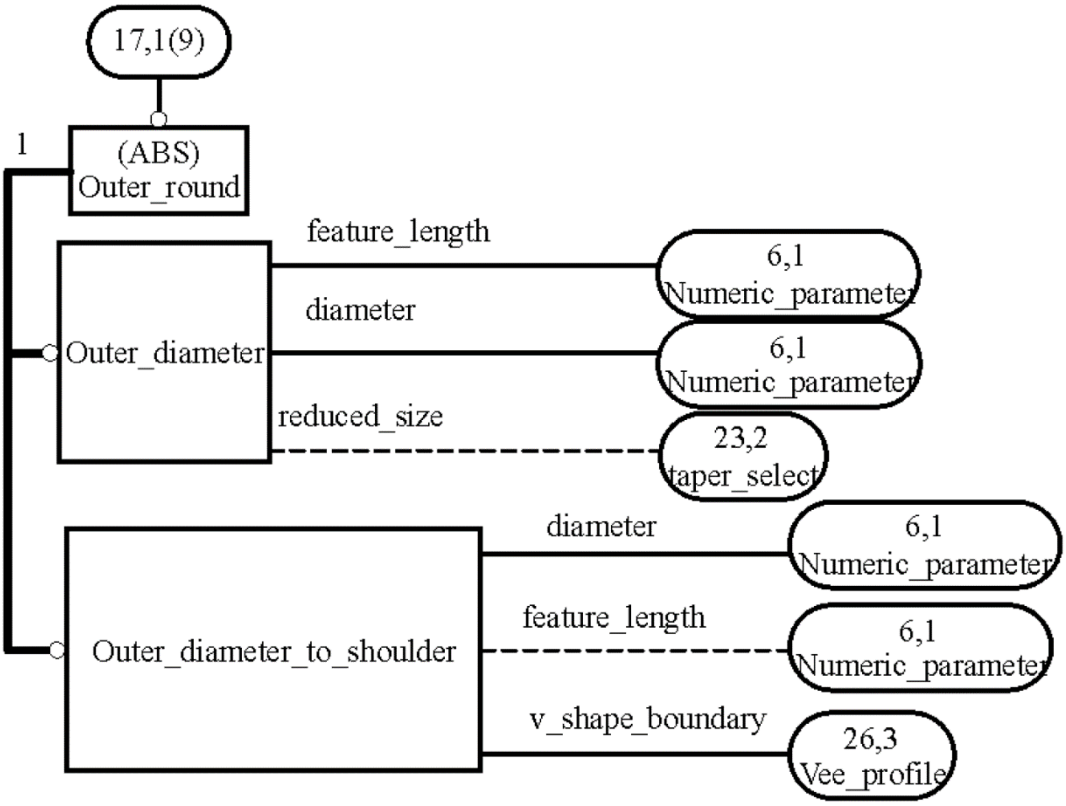

Figure 4.2 EXPRESS-G Specification of outer_round (ISO, 2006)

4.3.3 Extraction of Features from EXPRESS Specification

This section describes the method of extracting and utilizing features from the EXPRESS specifications of STEP's Application Protocols (APs), specifically AP224 and AP238, which are pivotal for mechanical product definitions and numerical controllers, respectively.

The goal is to create a unified and comprehensive feature library that can be used in the design and manufacturing processes. This involves identifying and converting feature definitions from these APs to ensure consistency and completeness.

The first step involves extracting feature definitions from AP224, which primarily uses EXPRESS-G diagrams. This conversion process ensures that the feature definitions are in a format that can be easily integrated into the system's database and utilized by various applications, including the feature modeler and the NC-code generator.

While AP224 provides a robust foundation, it does not cover all the necessary details for some features. Therefore, AP238 is used to supplement missing definitions. AP238 provides a more detailed description of features, especially from the perspective of numerical control. By cross-referencing and integrating information from both APs, a complete and detailed feature library is created.

For instance, the 'Outer_round' feature in AP224 might lack certain details that are present in AP238. By combining the information from both protocols, the system ensures that all aspects of the feature, including geometric data, tolerances and material properties, are fully defined.

4.3.4 Creation of Dynamic Link Library

The creation of a Dynamic Link Library (DLL) is a pivotal step in implementing the feature library within a software environment. A DLL allows the feature library to be compiled into a reusable module that can be linked to various applications.

The aim is to create a object-oriented model for feature definition and usage within a Visual Basic (VB) environment, facilitating the design and manufacturing of rotational parts. The primary goal is to convert the extracted rotational features and their geometric definitions, into a format that can be utilized by a feature modeler developed in VB 6.0. This involves classifying features as individual objects and establishing a hierarchy among them, reflecting their parameters and relationships.

Features are first extracted from AP224 and enriched with tolerance data. These features are then converted from their original EXPRESS-G or EXPRESS specifications into a VB-compatible format. Each feature is represented as a class object in VB and these class objects are organized into a hierarchical structure to reflect their relationships and shared parameters accurately. The class objects are compiled into a DLL using VB 6.0. This DLL, named TurnDESIGN.dll, serves as a package containing all the necessary feature definitions and can be used by both the feature modeler and the NC-code generator.

Every entity defined in STEP AP224 is mapped to a corresponding class in VB. For instance, a machining_feature might be represented as a class with various attributes such as dimensions, geometric tolerances and material properties. Classes are organized into a hierarchical structure, mirroring the relationships and dependencies as defined in AP224. This ensures that parameters and attributes are stored at the appropriate hierarchical levels. Once the class definitions and their hierarchical organization are complete, the classes are compiled into a DLL using VB 6.0. This DLL is then integrated into the feature modeler, allowing it to use the feature definitions directly.

The creation of a DLL streamlines the integration of feature definitions into the system. It ensures that features are represented consistently and can be easily accessed and manipulated within the VB environment. By using a DLL, the system can leverage object-oriented programming principles, enhancing the modularity and maintainability of the code. It also allows for easier updates and expansions, as new features or modifications can be added to the DLL without affecting the overall system structure.

4.3.5 Features of TurnDesign Eco Edition

In this study, AP224 (Mechanical Product Definition for Process Planning using Machining Features) and its feature library is used after refining for the rotational features. For the lacking information in AP224, AP238 (Application Interpreted

Model for Computerized Numerical Controllers) is referred. STEP AP224 contains all the information needed to manufacture the required part. Features and corresponding parameters used in the feature library of this study is given in Table 4.1.

Table 4.1 Feature List

OUTER ROUND	
Outer Diameter	D, L
Tapered Outer Diameter	D, D_F, L
Outer Diameter to Shoulder	D, R, L, α, β, r
REVOLVED FEATURE	
Revolved Flat	R, R_F, L
Revolved Round	R, α, r
Spherical Cap	R, α=90, r=R
Groove	
Partial Circular	R, α, r
Rounded U	R, W
Square U	R, W, α_1, r_1, α_2, r_2
Vee	R, α, β, r
MUTIAXIS FEATURE	
Hole	
Round Hole	D, L, Bottom Condition
Tapered Round Hole	D, D_F, L, Bottom Condition
Counterbore Hole	1^{st} Hole, 2^{nd} Hole
Countersunk Hole	1^{st} Tapered Hole, 2^{nd} Hole
TRANSITION FEATURE	
Edge Round	1^{st} and 2^{nd} feature, r
Fillet	1^{st} and 2^{nd} feature, r
Chamfer	1^{st} and 2^{nd} feature, D_1, α

4.4 Feature Modeler

The feature modeler is a crucial component in the development system for designing rotational parts, utilizing a built-in feature dynamic link library (DLL) and integrating with SolidWorks for 3D visualization. The feature modeler comprises a series of user-friendly forms tailored for each feature in the library. The feature modeler also includes a preprocessor that stores and exchanges design data in real-time.

The architecture of the feature modeler is designed to streamline the rotational part design process. Users select predefined features from the library and input necessary parameters through interactive forms. The forms are designed to be simple yet functional, guiding users through the design process and ensuring that all required data is correctly entered. The system automatically positions features where possible to expedite the design process and minimize the need for user calculations.

The feature creation process within the modeler is divided into two main operations: geometry creation and physical file creation. Geometry creation involves generating a 3D model of the part using SolidWorks, based on the parameters defined for each feature. The system employs a simple method commonly used in CAD—revolving a section 360 degrees around an axis—to create the 3D model. For instance, when creating the 'Outer_diameter_to_shoulder' feature, the system uses parameters such as diameter, length, tilt angle, profile angle and profile radius. The physical file creation aspect is handled by the feature modeler preprocessor, which synchronously generates the feature representing segment in the STEP Part 21 physical file.

Overall, the feature modeler is designed to be an intuitive and efficient tool for designing rotational parts. It leverages the built-in feature DLL and SolidWorks integration to provide a seamless design experience. By automating many aspects of the design process and incorporating robust error handling, the modeler helps users create high-quality, manufacturable parts with ease. The system's ability to generate a neutral STEP Part 21 file ensures compatibility with downstream applications, such as geometry extraction and part programming modules, further streamlining the transition from design to manufacturing.

Feature modeler preprocessor plays a critical role in this process by ensuring that all feature definitions are accurately represented in the STEP Part 21 physical file. This synchronization between feature creation and file generation ensures that the design data is always up-to-date and correctly formatted for use in subsequent stages of the manufacturing process. By adhering to the STEP standards, the system facilitates the seamless exchange of product data between CAD and CAM applications.

4.5 Sample Code

This code segment displayed in Table 4.2 is responsible for setting various parameters for the "outer diameter to shoulder" feature (ODSHLD). User inputs from text boxes TextBox2, TextBox3, TextBox4, TextBox5, TextBox6 and option buttons OptionButton1, OptionButton2 on the form (Figure 4.3) are assigned to the respective feature parameters such as diameter, profile radius, profile angle, tilt angle and length. Each With block assigns a specific parameter's name, value and unit designation.

Table 4.2 Code for parameter extraction from Outer Diameter to Shoulder

```
With ODSHLD(count_feature).diameter ' (***)  Set Diameter
.parameter_name = ODSHLD(count_feature).feature_ID & " DIAMETER AT
PLACEMENT"
.parameter_value = Val(TextBox2.value) * 2
.parameter_unit = measure.designation
End With

With ODSHLD(count_feature).vee.profile_radius ' (***)  Set Profile
Radius for VEE PROFILE
.parameter_name = ODSHLD(count_feature).feature_ID & " PROFILE RADIUS"
.parameter_value = Val(TextBox3.value)
.parameter_unit = measure.designation
End With
```

Table 4.2 (continued)

```
With ODSHLD(count_feature).vee.profile_angle
.parameter_name = ODSHLD(count_feature).feature_ID & " PROFILE ANGLE"
.parameter_value = Val(TextBox4.value)
.parameter_unit = measure.angle_designation
End With

With ODSHLD(count_feature).vee.tilt_angle
.parameter_name = ODSHLD(count_feature).feature_ID & " TILT ANGLE"
.parameter_value = Val(TextBox5.value)
.parameter_unit = measure.angle_designation
End With

With ODSHLD(count_feature).length  ' (***)  Set Feature Length
.parameter_name = ODSHLD(count_feature).feature_ID & " LENGTH"
.parameter_unit = measure.designation
End With

If OptionButton1.value = True Then
ODSHLD(count_feature).length.parameter_value = Val(TextBox6.value)
ODSHLD(count_feature).last_parameter.last_var_type = var_length
Df(count_feature) = ODSHLD(count_feature).diameter.parameter_value + 2 *
(ODSHLD(count_feature).length.parameter_value - ((Di(count_feature) -
ODSHLD(count_feature).diameter.parameter_value) / 2 / Tan(Pi -
(ODSHLD(count_feature).vee.profile_angle.parameter_value +
ODSHLD(count_feature).vee.tilt_angle.parameter_value) *
measure.angle_convertion_factor))) *
Tan(ODSHLD(count_feature).vee.tilt_angle.parameter_value *
measure.angle_convertion_factor)
End If

If OptionButton2.value = True Then  ' Set Final Diameter
Df(count_feature) = Val(TextBox6.value)
ODSHLD(count_feature).last_parameter.last_var_type = var_final_diameter
ODSHLD(count_feature).length.parameter_value = ((Di(count_feature) -
ODSHLD(count_feature).diameter.parameter_value) / 2 / (Tan(Pi -
(ODSHLD(count_feature).vee.profile_angle.parameter_value +
ODSHLD(count_feature).vee.tilt_angle.parameter_value) *
measure.angle_convertion_factor)))
ODSHLD(count_feature).length.parameter_value =
ODSHLD(count_feature).length.parameter_value + ((Df(count_feature) -
ODSHLD(count_feature).diameter.parameter_value) / 2 /
(Tan(ODSHLD(count_feature).vee.tilt_angle.parameter_value *
measure.angle_convertion_factor)))
End If

With ODSHLD(count_feature).vee.first_length
.parameter_name = ODSHLD(count_feature).feature_ID & " FIRST LENGTH"
.parameter_value = (Di(count_feature) -
ODSHLD(count_feature).diameter.parameter_value) / 2 / (Tan(Pi -
(ODSHLD(count_feature).vee.profile_angle.parameter_value +
ODSHLD(count_feature).vee.tilt_angle.parameter_value) *
measure.angle_convertion_factor))
.parameter_unit = measure.designation
End With
With ODSHLD(count_feature).vee.second_length
.parameter_name = ODSHLD(count_feature).feature_ID & " SECOND LENGTH"
.parameter_value = ODSHLD(count_feature).length.parameter_value -
ODSHLD(count_feature).vee.first_length.parameter_value
.parameter_unit = measure.designation
End With
```

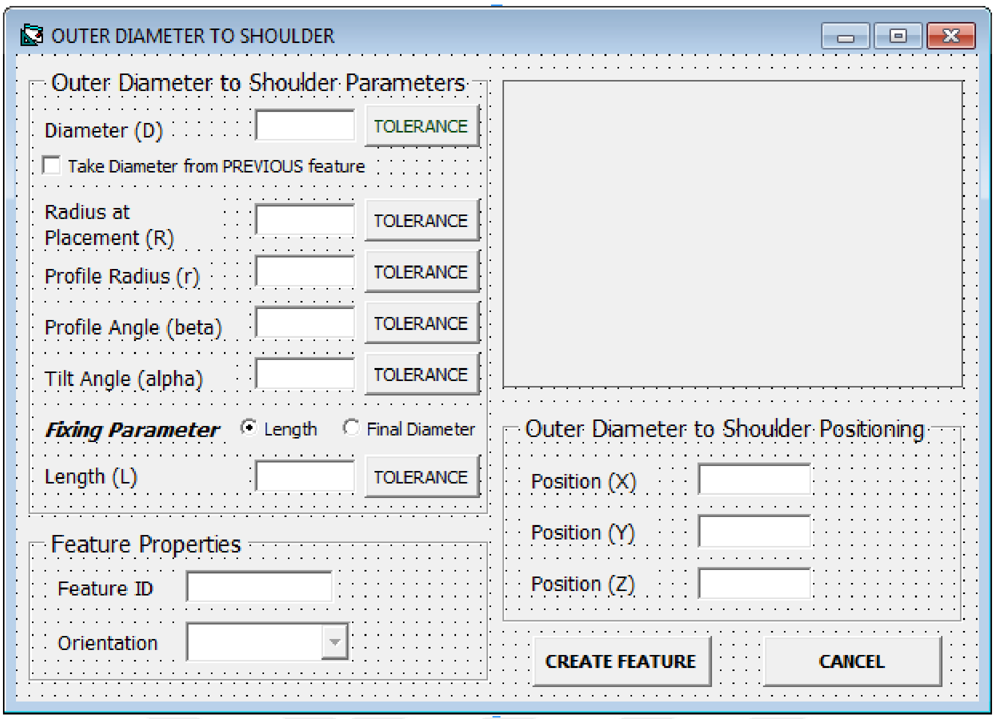

Figure 4.3 VB6 form for Outer Diameter to Shoulder

4.6 Output

The main output of this module is the AP224 file which involves all the feature data for the current design. The file structure is divided into two parts: the Header section and the Data section. The Header section contains information about the exchange structure itself, while the Data section includes the actual data to be transferred. The structure starts with the special token "ISO-10303-21;", followed by the Header and Data sections. It ends with the token "END-ISO-10303-21;" immediately after the Data section. AP224 file for the first sample part, SP1-AL6013, is given as an example in Figure 4.4.

The second output from the user input module is the solid model created on SolidWorks, displayed in the TurnDesign Eco Edition interface. The feature tree on

```
ISO-10303-21;

HEADER;
FILE_DESCRIPTION(('ISO-10303-224,FEATURE BASED ROTATIONAL PART CREATED BY',
'TurnDESIGN Eco Edition'),'1');
FILE_NAME(('SP1-AL6013-2024sp.part21','2024-6-23 T00:25:41',
('Designed by: URAL ULUER','METU-ME','ANKARA TURKIYE')
FILE_SCHEMA(('ROTATIONAL PART', 'PART FOR 2-AXIS TURNING'));
ENDSEC;

DATA;
#1=MATERIAL($,'Non-Ferrous Metal N16',$,$,$);
#2=OUTER_DIAMETER('OD1',#3,#4,#5,$);
#3=ORIENTATION((0,0,0),(1,0,0,0,1,0,0,0,1));
#4=NUMERIC_PARAMETER('OD1 DIAMETER',MM,28,$);
#5=NUMERIC_PARAMETER('OD1 LENGTH',MM,30,$);
#6=OUTER_DIAMETER('OD2',#7,#8,#9,$);
#7=ORIENTATION((0,0,30),(1,0,0,0,1,0,0,0,1));
#8=NUMERIC_PARAMETER('OD2 DIAMETER',MM,16,$);
#9=NUMERIC_PARAMETER('OD2 LENGTH',MM,10,$);
#10=OUTER_DIAMETER('OD3',#11,#12,#13,#14);
#11=ORIENTATION((0,0,40),(1,0,0,0,1,0,0,0,1));
#12=NUMERIC_PARAMETER('OD3 DIAMETER',MM,16,$);
#13=NUMERIC_PARAMETER('OD3 LENGTH',MM,10,$);
#14=DIAMETER_TAPER(#15);
#15=NUMERIC_PARAMETER('OD3 FINAL DIAMETER',MM,12,$);
#16=OUTER_DIAMETER('OD4',#17,#18,#19,$);
#17=ORIENTATION((0,0,50),(1,0,0,0,1,0,0,0,1));
#18=NUMERIC_PARAMETER('OD4 DIAMETER',MM,12,$);
#19=NUMERIC_PARAMETER('OD4 LENGTH',MM,10,$);
#20=GROOVE('SQRUGRV1',#21,#22,#23,#24);
#21=ORIENTATION((9,0,16),(1,0,0,0,1,0,0,0,1));
#22=DIRECTION(-1,0,0);
#23=NUMERIC_PARAMETER('SQRUGRV1 GROOVE RADIUS',MM,9,$);
#24=SQUARE_U_PROFILE($,#25,#26,#27,#28,#29);
#25=NUMERIC_PARAMETER('SQRUGRV1 WIDTH',MM,22,$);
#26=NUMERIC_PARAMETER('SQRUGRV1 FIRST RADIUS',MM,0,$);
#27=NUMERIC_PARAMETER('SQRUGRV1 FIRST ANGLE',DEGREES,90,$);
#28=NUMERIC_PARAMETER('SQRUGRV1 SECOND RADIUS',MM,0,$);
#29=NUMERIC_PARAMETER('SQRUGRV1 SECOND ANGLE',DEGREES,90,$);
#30=ROUND_HOLE('RNDHOL1',#31,$,#32,#33,$,#34);
#31=ORIENTATION((0,0,60),(1,0,0,0,1,0,0,0,1));
#32=LINEAR_PATH(#35,#36);
#33=NUMERIC_PARAMETER('RNDHOL1 DIAMETER',MM,8,$);
#34=CONICAL_HOLE_BOTTOM(#37,#39);
#35=NUMERIC_PARAMETER('RNDHOL1 DISTANCE',MM,9,$);
#36=DIRECTION(0,0,-1);
#37=NUMERIC_PARAMETER('RNDHOL1 CONICAL BOTTOM TIP ANGLE',MM,140,$);
#38=NUMERIC_PARAMETER('RNDHOL1 CONICAL BOTTOM TIP RADIUS',MM,0.0001,$);
#39=CONSTANT_RADIUS_FILLET('FILLET1','OD1','OD2',#40,$,$);
#40=NUMERIC_PARAMETER('FILLET1 RADIUS',MM,5,$);
ENDSEC;
END-ISO-10303-21;
```

Figure 4.4 AP224 file for SP1-AL6013

the left lists all features and their parameters. Figure 4.5 shows the solid model for the first sample part, SP1-AL6013, generated by the feature modeler of TurnDesign Eco Edition.

The final output is an Excel sheet that lists all the features of the designed part. Although this information is also available in the AP224 file, the Excel table is maintained for quick reporting and easy reference. The feature list output for the sample part shown in Figure 4.5 is presented in Figure 4.6.

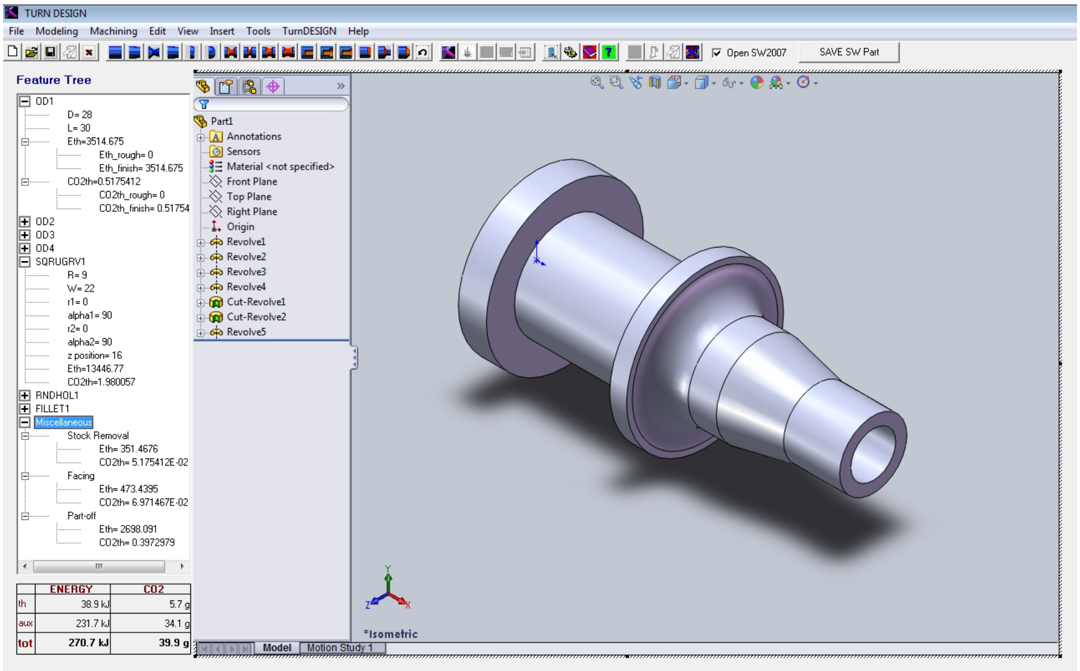

Figure 4.5 Solidworks 3D model for SP1-AL6013

No	Feature	Parameters
1	OD1	D = 28 L = 30
2	OD2	D = 16 L = 10
3	OD3	D = 16 Df = 12 L = 10
4	OD4	D = 12 L = 10
5	SQRUGRV1	R = 9 W = 22 Depth = 5 r1 = 0 alpha1 = 90 r2 = 0 alpha2 = 90 z position = 16
6	RNDHOL1	D = 8 L = 9 conical bottom alpha = 140 r_tip = 0.0001
7	FILLET1	1st Feature = OD1 2nd Feature = OD2 r = 5

Figure 4.6 Feature and parameter list for SP1-AL6013

CHAPTER 5

GEOMETRY EXTRACTION

5.1 Introduction

Feature data input by the user involves parameters related to the feature geometry and cannot be directly employed in Part Programming module. The primary objective of Geometry Extraction module is to convert this feature data into geometrical information usable for generating toolpaths in the Part Programming module. For this purpose, point matrices are created for each operation. Point matrices are the combination point coordinates of a particular feature relevant to machining. Depending on the feature characteristic, these points define the outer or inner geometry of the part and are used to calculate the target coordinates the tool will travel.

The secondary objective of the Geometry Extraction module is to link the features to manufacturing operations. This is achieved by grouping features machined with the same manufacturing operation under the same point matrix. In conventional designs where geometrical modeling is utilized, this step is a component of process planning effort. However, in the implemented feature modeling approach, the coupling of features with operations had to be addressed within the Geometry Extraction module due to how the point matrices are generated. This establishes a bridge between features and manufacturing operations, forming the basis for the subsequent process planning stages outlined in Chapter 6 Process Planning.

Figure 5.1 illustrates the input and output structure of the Geometry Extraction module. Next section describes the general structure of the point matrices. In Sections 5.3 to 5.5, point matrix generation is explained for different features.

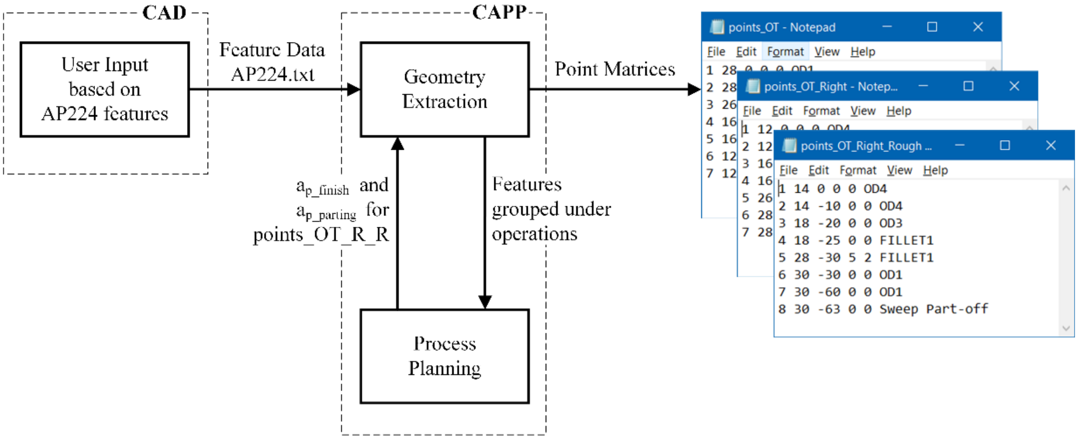

Figure 5.1 Geometry Extraction Module: Inputs and Outputs

5.2 Point Matrices

Point matrices, corresponding features and linked operations are presented in Table 5.1.

Table 5.1 Point Matrix List

Point Matrix Name	Features	Operation
points_OT	Outer Diameter, Tapered Outer Diameter, Outer Diameter to Shoulder, Revolved Flat, Revolved Round, Spherical Cap, Edge Round, Fillet, Chamfer	Outer Turning
points_RNDUGRV	Rounded U Groove	Grooving
points_CIRCGRV	Partial Circular Groove	Grooving
points_VEEGRV	Vee Groove	Grooving
points_SQRUGRV	Square U Groove	Grooving
points_RNDHOL	Round Hole	Drilling
points_CBORHOL	Counterbored Hole	Counterboring
points_CSKHOL	Countersunk Hole	Countersinking

Each matrix provides information about 6 items for a single point for outer turning and drilling operations. :

[#, X, Z, R, 2/3, feature_ID]

where

#: point number

X: X axis coordinate (for diameter programming)

Z: Z axis coordinate (reference point on left face of the part)

R: Radius (0 if NA)

2/3: Curvature parameter. If G02/CW = 2, if G03/CCW =3, if G00/G01 = 0

feature_ID: unique ID of the current feature (ex: ODSHLD1 for 1st outer diameter to shoulder feature)

An additional parameter is allocated for the tool dimeter for drilling operations:

[#, X, Z, R, 2/3, feature_ID, ϕ]

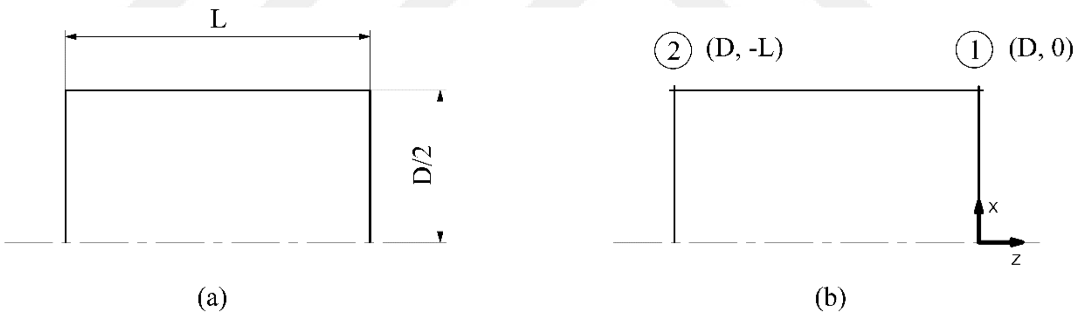

Figure 5.2 Points for Outer Diameter

Outer Diameter feature is given in Figure 5.2 as an example. The user inputs length (L) and diameter (D) parameters. However, those two parameters cannot be directly used in the part programming module and must be converted into a format which involves X and Z coordinates for part programming of outer turning operation. Therefore, Outer Diameter feature is broken down into two end points and corresponding coordinates $(X_1,Z_1) = (D,0)$ and $(X_2,Z_2) = (D,-L)$ are saved in the point matrix of the outer turning operation. Those coordinates will be used for the tool tip destinations in the part program.

In the following sections point matrix calculations are shown for a feature under each operation. Outer Diameter to Shoulder, Square U Groove and Round Hole are selected for outer turning, grooving and drilling operations respectively.

5.3 Point Matrix for Outer Diameter to Shoulder

For Outer Diameter to Shoulder feature, the outer geometry is broken down into 4 points as shown in Figure 5.3. Placement of the feature at (0, z_{pos}) is indicated by the coordinate axis in Figure 5.3. z_{pos} is a parameter used in TurnDesign Eco Edition to represent the position of each feature on Z axis. It is calculated based on the lengths of the preceding features. If Outer Diameter to Shoulder is the first feature for outer turning operations, then z_{pos} is zero. Parameters of Outer Diameter to Shoulder, D, R, L, α, β, r, are based on STEP AP224 (ISO 10303-224, 2006).

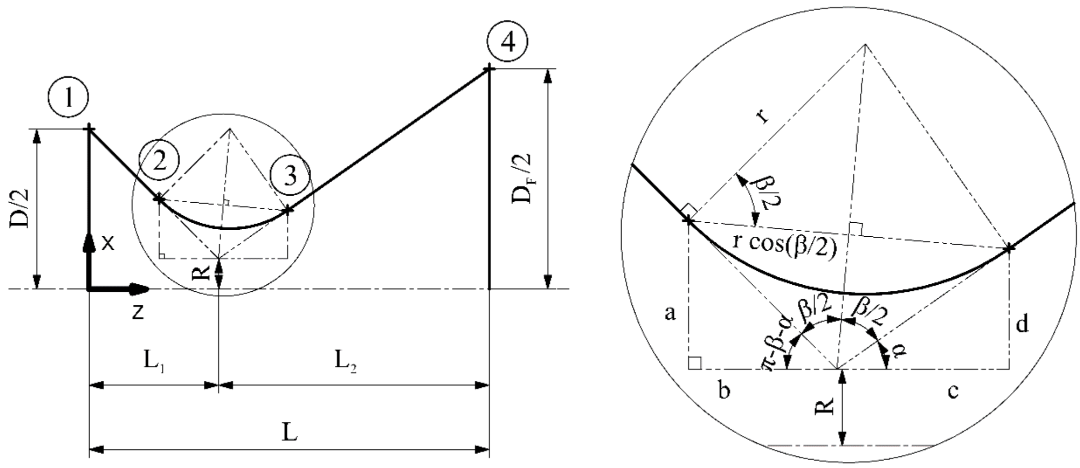

Figure 5.3 Points for Outer Diameter to Shoulder

First Point (P_1)

$$P_{1x} = D \tag{5.1}$$

$$P_{1z} = z_{pos} \tag{5.2}$$

Second Point (P_2)

X coordinates of second point (P_{2x}) is calculated from the following equations:

$$P_{2x} = 2\,(R + a) \tag{5.3}$$

$$a = r\,\frac{\cos(\beta/2)}{\sin(\beta/2)}\,\sin(\pi - \beta - \alpha) \tag{5.4}$$

$$a = \frac{r}{\tan(\beta/2)}\,\sin(\beta + \alpha) \tag{5.5}$$

$$P_{2x} = 2\left(R + \frac{r}{\tan(\beta/2)}\,\sin(\beta + \alpha)\right) \tag{5.6}$$

Z coordinates of second point (P_{2z}) is calculated from the following equations:

$$P_{2z} = z_{pos} + L_1 - b \tag{5.7}$$

$$L_1 = \frac{D/2 - R}{\tan(\pi - \beta - \alpha)} \tag{5.8}$$

$$b = r\,\frac{\cos\,(\beta/2)}{\sin\,(\beta/2)}\,\cos(\pi - \beta - \alpha) \tag{5.9}$$

$$b = -\frac{r}{\tan\,(\beta/2)}\,\cos(\beta + \alpha) \tag{5.10}$$

$$P_{2z} = z_{pos} + \frac{D_i/2 - R}{\tan(\pi - \beta - \alpha)} + \frac{r}{\tan\,(\beta/2)}\,\cos(\beta + \alpha) \tag{5.11}$$

Second Point (P_3)

X coordinates of third point (P_{3x}) is calculated from the following equations:

$$P_{3x} = 2\,(R + d) \tag{5.12}$$

$$d = r\,\frac{\cos(\beta/2)}{\sin(\beta/2)}\,\sin\alpha \tag{5.13}$$

$$d = \frac{r}{\tan(\beta/2)}\sin\alpha \tag{5.14}$$

$$P_{3x} = 2\left(R + \frac{r}{\tan(\beta/2)}\,\sin\alpha\right) \tag{5.15}$$

Z coordinates of third point (P_{3z}) is calculated from the following equations:

$$P_{2z} = z_{pos} + L_1 - c \tag{5.16}$$

$$L_1 = \frac{D/2-R}{\tan(\pi-\beta-\alpha)} \tag{5.17}$$

$$c = r\,\frac{\cos(\beta/2)}{\sin(\beta/2)}\cos\alpha \tag{5.18}$$

$$c = \frac{r}{\tan(\beta/2)}\cos\alpha \tag{5.19}$$

$$P_{3z} = z_{pos} + \frac{D/2-R}{\tan(\pi-\beta-\alpha)} + \frac{r}{\tan(\beta/2)}\cos\alpha \tag{5.20}$$

Fourth Point (P_4)

$$P_{4x} = D_F \tag{5.21}$$

$$P_{4z} = z_{pos} + L \tag{5.22}$$

Outer Diameter to Shoulder is machined by outer turning and these calculated points are saved under points_OT matrix (Table 5.1). After addition of each feature, current state of the design is assumed to be the final part and two other matrices are generated using points_OT. The representations for those two matrices are given in Figure 5.4, assuming the design has only Outer Diameter to Shoulder feature.

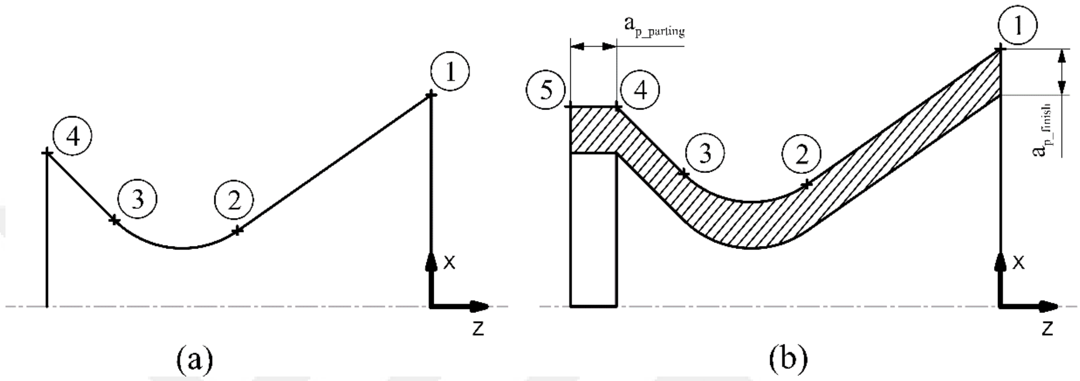

Figure 5.4 Representation of points_OT_R and points_OT_R_R for a feature

The first matrix is points_OT_R (Figure 5.4a). The "R" in the matrix name denotes the origins association with the right side. This point matrix is generated by reversing the order of points for Z axis in points_OT matrix. The rightmost point for the design becomes the first point making its Z coordinate zero. This rearrangement enables a better integration with the nature of RHS programming for a CNC lathe.

The second matrix is points_OT_R_R (Figure 5.4b). Additional "R" in the matrix name stands for roughing. This point matrix is generated to account for the finish allowance for rough outer turning operation. points_OT_R_R is used as the primary guide for roughing operations since it constructs the bottom contour for the roughing excess. Points from points_OT_R are shifted by finish allowance (a_{p_finish}) in X axis to determine the points of points_OT_R_R.

Besides the allowance for finishing, points_OT_R_R adds an extra point to the end of points_OT_R. The new point is added to the left of the last point, at a distance equal to the width of the parting tool ($a_{p\_parting}$). Rough and finish outer turning operations will be done up to this newly added point (Point 5 in Figure 5.4b) past the last point of the design (Point 4 in Figure 5.4b). The aim is to eliminate any excess material that might remain after the parting operation due to the potential deflection of the RHS tool and different tool offsets of RHS and parting tools.

5.4 Point Matrix for Square U Groove

Contour of Square U Groove feature is defined by the 6 points as illustrated in Figure 5.5. The origin that determines the placement of the feature is at (0, zpos). z_{pos} is a parameter used in TurnDesign Eco Edition to indicate the position of each feature on Z axis. For Square U Groove, the user defines z_{pos} when designing the groove. STEP AP224 (ISO 10303-224, 2006) parametrizes this feature with attributes R, W, α_1, r_1, α_2, r_2 and depth.

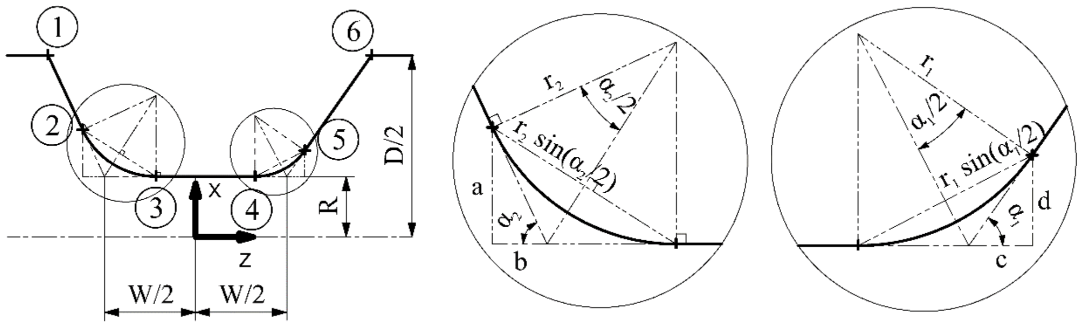

Figure 5.5 Points for Square U Groove

Depth of the groove is not a user input, it is calculated based on position on Z axis (z_{pos}) and radius at placement (R). First, diameter (D) of the corresponding feature on which the Square U Groove is generated is determined. This is achieved by comparing the z_{pos} of the groove with the z_{pos} of features defining the current outer contour in a loop structure. This process enables the calculation of the depth in the next step using the following equation:

$$Depth = D/2 - R \tag{5.23}$$

First Point (P_1)

$$P_{1x} = D \tag{5.24}$$

$$P_{1z} = z_{pos} - \frac{W}{2} - \frac{D/2-R}{\tan\alpha_2} \tag{5.25}$$

Second Point (P_2)

X coordinates of second point (P_{2x}) is calculated from the following equations:

$$P_{2x} = 2\,(R + a) \tag{5.26}$$

$$a = r_2\,\frac{\sin(\alpha_2/2)}{\cos(\alpha_2/2)}\sin\alpha_2 \tag{5.27}$$

$$P_{2x} = 2\,(R + r_2\tan(\alpha_2/2)\sin\alpha_2) \tag{5.28}$$

Z coordinates of second point (P_{2z}) is calculated from the following equations:

$$P_{2z} = z_{pos} - \frac{W}{2} - b \tag{5.29}$$

$$b = r_2\,\frac{\sin(\alpha_2/2)}{\cos(\alpha_2/2)}\cos\alpha_2 \tag{5.30}$$

$$P_{2z} = z_{pos} - W/2 - r_2\tan(\alpha_2/2)\cos\alpha_2 \tag{5.31}$$

Third Point (P_3)

$$P_{3x} = 2\,R \tag{5.32}$$

$$P_{3z} = z_{pos} - \frac{W}{2} - r_2\,\frac{\sin(\alpha_2/2)}{\cos(\alpha_2/2)} \tag{5.33}$$

$$P_{3z} = z_{pos} - \frac{W}{2} + r_2\tan(\alpha_2/2) \tag{5.34}$$

Fourth Point (P_4)

$$P_{4x} = 2\,R \tag{5.35}$$

$$P_{4z} = z_{pos} + \frac{W}{2} - r_1\,\frac{\sin(\alpha_1/2)}{\cos(\alpha_1/2)} \tag{5.36}$$

$$P_{4z} = z_{pos} + \frac{W}{2} - r_1\tan(\alpha_1/2) \tag{5.37}$$

Fifth Point (P_5)

X coordinates of fifth point (P_{5x}) is calculated from the following equations:

$$P_{5x} = 2\,(R + d) \tag{5.38}$$

$$d = r_1\,\frac{\sin(\alpha_1/2)}{\cos(\alpha_1/2)}\,\sin\alpha_1 \tag{5.39}$$

$$P_{5x} = 2\,(R + r_1\tan(\alpha_1/2)\sin\alpha_1) \tag{5.40}$$

Z coordinates of fifth point (P_{5z}) is calculated from the following equations:

$$P_{5z} = z_{pos} + \frac{W}{2} + c \tag{5.41}$$

$$c = r_1 \frac{\sin(\alpha_1/2)}{\cos(\alpha_1/2)} \cos \alpha_1 \tag{5.42}$$

$$P_{5z} = z_{pos} + W/2 + r_1 \tan(\alpha_1/2) \cos \alpha_1 \tag{5.43}$$

Sixth Point (P_6)

$$P_{1x} = D \tag{5.44}$$

$$P_{1z} = z_{pos} + \frac{W}{2} + \frac{D/2 - R}{\tan(\alpha_1)} \tag{5.45}$$

These points are saved under points_SQRUGRV matrix which will be used for the toolpath generation for grooving operation (Table 5.1). An additional points_SQRUGRV_R matrix is generated using points_SQRUGRV after each new feature introduced to the design. The illustration of the points for this new matrix is given in Figure 5.6.

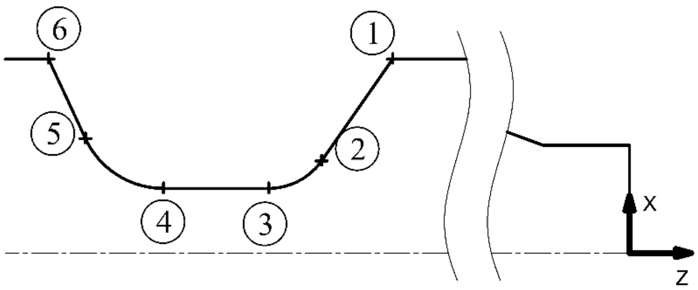

Figure 5.6 Representation of points_SQRUGRV_R

The "R" in points_SQRUGRV_R denotes that the origin is associated with the rightmost face of the design. This point matrix is generated by transferring the origin to its new position and reversing the order of points for Z axis in points_SQRUGRV matrix. This rearrangement facilitates integration with the nature of RHS programming for a CNC lathe. Unlike Outer Diameter to Shoulder feature, a second additional matrix is not generated for Square U Groove feature because grooving operations do not include a finish cut.

5.5 Point Matrix for Round Hole

Point matrix for Round Hole (points_RNDHL) includes the tip point of the hole. This is due to the characteristic of a drilling operation toolpath where motion occurs only in -Z direction after the drill is positioned at a safe distance on X=0 axis. Placement of the feature is at (0, 0) which corresponds to the rightmost surface of the designed part. This also eliminates the need for a points_RNDHL_R matrix and saved point can be directly used for RHS programming in Part Programming module. In addition, since drilling does not involve a finish operation, points_RNDHL_R_R is not needed as well.

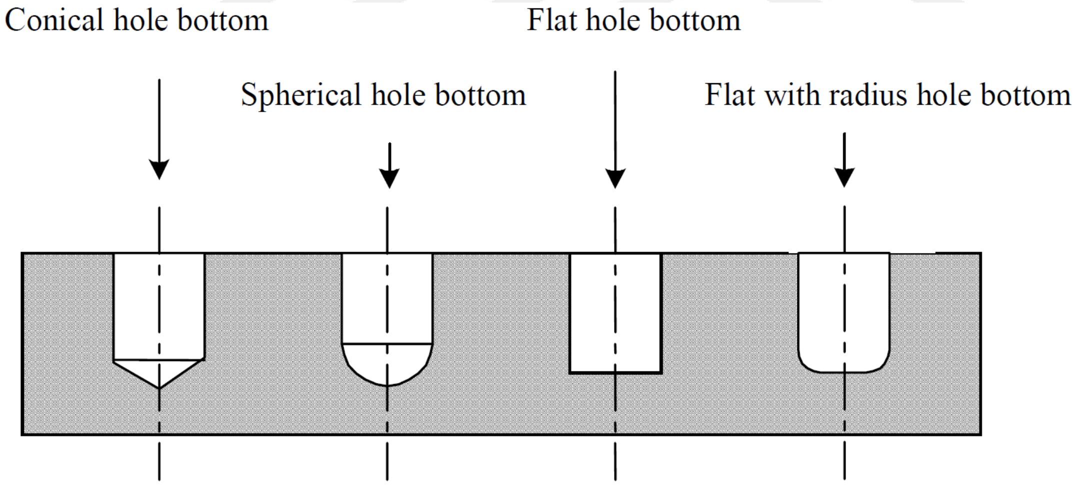

Figure 5.7 Round Hole Blind Bottom Conditions (ISO 14649-10, 2004)

Based on STEP AP224 (ISO 10303-224, 2006), parameters of Round Hole feature are D, L and Bottom Condition. Bottom conditions are grouped under Through Bottom Condition and Blind Bottom Condition. Blind Bottom Condition further branches down into Conical, Flat, Flat with Radius and Spherical Hole Bottom Conditions as shown in Figure 5.7. Even if Flat, Flat with Radius and Spherical Hole Bottom Conditions are primarily used for milling applications, they are added to this study for the sake of completeness.

5.5.1 Through Bottom Condition

For the calculation of the point position of a Round Hole having a Through Bottom Condition, the maximum length of the designed part (L_{max}), clearance length (L_c) and the horizontal length of the conical part of the drill (L_{cone}) are employed. The conical length calculation excludes the rounded portion of the tool tip and it is compensated with the clearance length. A clearance length of 1 mm is utilized to ensure that internal taper on the left end of the hole is avoided.

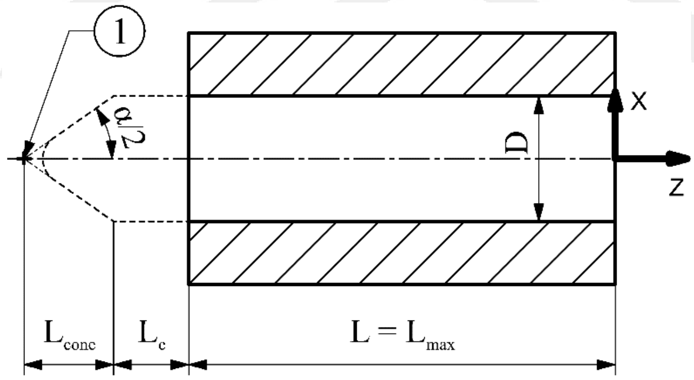

Figure 5.8 Point for Round Hole, Bottom Condition: Through

$$P_{1x} = 0 \tag{5.46}$$

$$P_{1z} = -L_{max} - L_c - L_{cone} \tag{5.47}$$

$$P_{1z} = -L_{max} - 1 - \frac{D}{2\tan(\alpha/2)} \tag{5.48}$$

5.5.2 Conical Bottom Condition

Based on STEP AP224 (ISO 10303-224, 2006) there are two additional attributes regarding conical bottom condition: Tip angle (α) and tip radius (r). This bottom condition is demonstrated in Figure 5.9. Since length of the hole is the cylindrical portion, X and Z coordinates of the tool tip are calculated using the equations below:

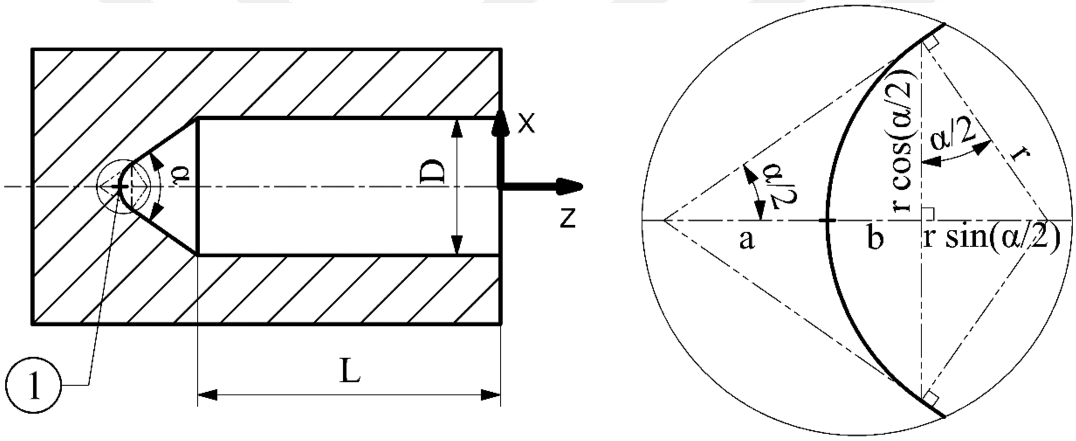

Figure 5.9 Point for Round Hole, Bottom Condition: Conical

$$P_{1x} = 0 \tag{5.49}$$

$$P_{1z} = -L - \frac{D}{2\tan(\alpha/2)} + a \tag{5.50}$$

$$a + b = \frac{r\cos(\alpha/2)}{\tan(\alpha/2)} \tag{5.51}$$

$$b = r - r\sin(\alpha/2) \tag{5.52}$$

$$P_{1z} = -L - \frac{D}{2\tan(\alpha/2)} + \frac{r\cos(\alpha/2)}{\tan(\alpha/2)} - r + r\sin(\alpha/2) \tag{5.53}$$

5.5.3 Other Bottom Conditions

Point matrices of the holes having Flat Hole Bottom, Flat with Radius Hole Bottom and Spherical Bottom Conditions are identical and only account for the length of the hole.

$$P_{1x} = 0 \tag{5.54}$$

$$P_{1z} = -L \tag{5.55}$$

5.6 Sample Code

Geometry Extraction module of TurnDesign Eco Edition loops through all geometric features of the current design and groups each feature under the relevant manufacturing operations using "Case" statement of Visual Basic. The grouping structure is outlined in Table 5.1. Within each "Case", points defining the contour of the respective feature are calculated. Once all the points for a manufacturing operation are determined, they are printed and saved in the corresponding point matrix.

Table 5.2 demonstrates one of those "Case" statements for Outer Diameter to Shoulder feature. point_OT matrix is generated by inputting the items including point number, X and Z coordinates (as per Equations 5.1 to 5.22), radius, circular interpolation (G02/G03) and feature ID. This process is elaborated under Section 5.3 Point Matrix for Outer Diameter to Shoulder.

Table 5.2 Code for point matrix of Outer Diameter to Shoulder

```
Case "ODSHLD":

beta(i) = ODSHLD(i).vee.profile_angle.parameter_value  '****for profile
angle=beta
Rp(i) = ODSHLD(i).diameter.parameter_value / 2         '****for radius
at placement=Rp

points_OT(total_point_no_OT + 1, 0) = total_point_no_OT + 1
points_OT(total_point_no_OT + 1, 1) = Di(i)
points_OT(total_point_no_OT + 1, 2) = z_pos(i)
points_OT(total_point_no_OT + 1, 3) = 0
points_OT(total_point_no_OT + 1, 4) = 0
points_OT(total_point_no_OT + 1, 5) = feature_ID(i)

points_OT(total_point_no_OT + 2, 0) = total_point_no_OT + 2
points_OT(total_point_no_OT + 2, 1) = 2 * (rad(i) / Tan(beta(i) *
measure.angle_convertion_factor / 2) * Sin((beta(i) + alpha_e(i)) *
measure.angle_convertion_factor) + Rp(i))
points_OT(total_point_no_OT + 2, 2) = z_pos(i) + (Di(i) / 2 - Rp(i)) /
(Tan(Pi - (alpha_e(i) + beta(i)) * measure.angle_convertion_factor)) +
(rad(i) / Tan(beta(i) * measure.angle_convertion_factor / 2) *
Cos((beta(i) + alpha_e(i)) * measure.angle_convertion_factor))
points_OT(total_point_no_OT + 2, 3) = rad(i) 'G02 and radius value
points_OT(total_point_no_OT + 2, 4) = 2
points_OT(total_point_no_OT + 2, 5) = feature_ID(i)

points_OT(total_point_no_OT + 3, 0) = total_point_no_OT + 3
points_OT(total_point_no_OT + 3, 1) = 2 * (rad(i) / Tan(beta(i) *
measure.angle_convertion_factor / 2) * Sin(alpha_e(i) *
measure.angle_convertion_factor) + Rp(i))
points_OT(total_point_no_OT + 3, 2) = z_pos(i) + (Di(i) / 2 - Rp(i)) /
(Tan(Pi - (alpha_e(i) + beta(i)) * measure.angle_convertion_factor)) +
(rad(i) / Tan(beta(i) * measure.angle_convertion_factor / 2) *
Cos(alpha_e(i) * measure.angle_convertion_factor))
points_OT(total_point_no_OT + 3, 3) = 0 'G01 and no radius value
points_OT(total_point_no_OT + 3, 4) = 0
points_OT(total_point_no_OT + 3, 5) = feature_ID(i)

points_OT(total_point_no_OT + 4, 0) = total_point_no_OT + 4
points_OT(total_point_no_OT + 4, 1) = Df(i)
points_OT(total_point_no_OT + 4, 2) = z_pos_end(i)
points_OT(total_point_no_OT + 4, 3) = 0
points_OT(total_point_no_OT + 4, 4) = 0
points_OT(total_point_no_OT + 4, 5) = feature_ID(i)

total_point_no_OT = total_point_no_OT + 4

End If
```

After generating all the points for the points_OT matrix, which represents the entire outer contour of the features to be manufactured through outer turning operations, the matrix is reorganized to shift the reference position to the right face of the design. The first section of the code, as presented in Table 5.3, illustrates the generation of the points_OT_R matrix by reversing the order of points in the points_OT matrix. In the second part of the code, a file named points_OT_Right.txt is created and the points_OT_R matrix is written into this text file.

Table 5.3 Code for points_OT_R and output text file generation

```
'Reverse points_OT to make right most point ZERO for RHS machining
For j = total_point_no_OT To 1 Step -1
points_OT_R(total_point_no_OT - points_OT(j, 0) + 1, 0) =
total_point_no_OT - points_OT(j, 0) + 1
points_OT_R(total_point_no_OT - points_OT(j, 0) + 1, 1) = points_OT(j,
1)
points_OT_R(total_point_no_OT - points_OT(j, 0) + 1, 2) = points_OT(j,
2) - points_OT(total_point_no_OT, 2)
points_OT_R(total_point_no_OT - points_OT(j, 0) + 1, 3) = points_OT(j,
3)
points_OT_R(total_point_no_OT - points_OT(j, 0) + 1, 4) = points_OT(j,
4)
points_OT_R(total_point_no_OT - points_OT(j, 0) + 1, 5) = points_OT(j,
5)
Next j


Dim iFileNo11 As Integer
iFileNo11 = FreeFile
Open "C:\Users\ural\Desktop\points_OT_Right.txt" For Output As
#iFileNo11

For j = 1 To total_point_no_OT
Print #iFileNo11, points_OT_R(j, 0) & " " & points_OT_R(j, 1) & " " &
points_OT_R(j, 2) & " " & points_OT_R(j, 3) & " " & points_OT_R(j, 4) &
" " & points_OT_R(j, 5)
Next j

Close #iFileNo11
```

The generation of the point matrix points_OT_R_R to accommodate finish allowance for rough outer turning is detailed in the first part of Table 5.4. In the second part, the additional point is appended to the end of points_OT_R_R to eliminate the material left after the parting operation. Finally, the points_OT_R_R matrix is printed in a file named points_OT_Right_Rough.txt. For details and the structure of the points_OT_R_R matrix, please refer to Section 5.3 Point Matrix for Outer Diameter to Shoulder.

Table 5.4 Code for points_OT_R_R and output text file generation

```
'Increase X values of points_OT_R matrix finish allowance much: 2 *
a_p(3) to define points_OT_R_R matrix
For j = 1 To total_point_no_OT
points_OT_R_R(j, 0) = points_OT_R(j, 0)
points_OT_R_R(j, 1) = points_OT_R(j, 1) + 2 * a_p(3)
points_OT_R_R(j, 2) = points_OT_R(j, 2)
points_OT_R_R(j, 3) = points_OT_R(j, 3)
points_OT_R_R(j, 4) = points_OT_R(j, 4)
points_OT_R_R(j, 5) = points_OT_R(j, 5)
Next j

'Add an extra point for part-off sweep CUU_stockremoval
points_OT_R_R(total_point_no_OT + 1, 0) = total_point_no_OT + 1
points_OT_R_R(total_point_no_OT + 1, 1) =
points_OT_R_R(total_point_no_OT, 1)
points_OT_R_R(total_point_no_OT + 1, 2) =
points_OT_R_R(total_point_no_OT, 2) - a_p(20)
points_OT_R_R(total_point_no_OT + 1, 3) = 0
points_OT_R_R(total_point_no_OT + 1, 4) = 0
points_OT_R_R(total_point_no_OT + 1, 5) = "Sweep Part-off"


Dim iFileNo12 As Integer
iFileNo12 = FreeFile
Open "C:\Users\ural\Desktop\points_OT_Right_Rough.txt" For Output As
#iFileNo12

For j = 1 To total_point_no_OT + 1
Print #iFileNo12, points_OT_R_R(j, 0) & " " & points_OT_R_R(j, 1) & " "
& points_OT_R_R(j, 2) & " " & points_OT_R_R(j, 3) & " " &
points_OT_R_R(j, 4) & " " & points_OT_R_R(j, 5)
Next j

Close #iFileNo12
```

5.7 Output

The output of Geometry Extraction module of TurnDesign Eco Edition software is point matrices as text (.txt) files. They demonstrate the significant points of the geometry for toolpath generation. General data structure of those matrices are explained in Section 5.2 Point Matrices. Figures below presents the point matrices for the first specimen: SP1-AL6013. Technical information about SP1-AL6013 can be found under Chapter 9 Test Set-Up And Verification.

Figure 5.10 shows the point matrices defining the outer contour of SP1-AL6013. These point matrices are:

- Figure 5.10 (a): points_OT saved as point_OT.txt
- Figure 5.10 (b): points_OT_R saved as point_OT_Right.txt
- Figure 5.10 (c): points_OT_R_R saved as point_OT_Right_Rough.txt

Details of each matrix is explained in Section 5.3 Point Matrix for Outer Diameter to Shoulder. Point matrices in Figure 5.10 (b) and Figure 5.10 (c) are inputs used for toolpath generation of finish and rough outer turning operations respectively.

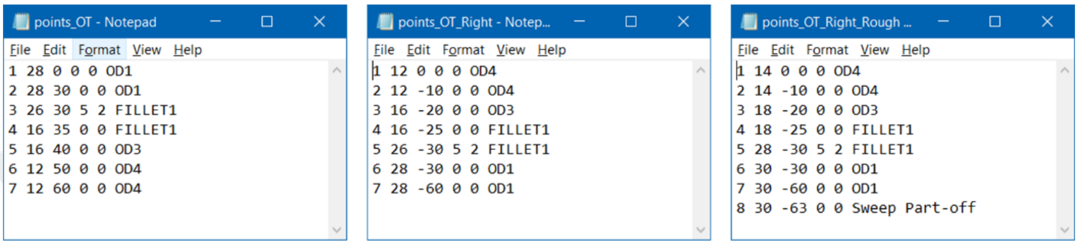

(a) (b) (c)

Figure 5.10 Point matrices for SP1-AL6013: Outer Turning

Figure 5.11 shows the point matrices defining the groove contour of SP1-AL6013. These point matrices are:

- Figure 5.11 (a): points_SQRUGRV saved as points_ SQRUGRV.txt
- Figure 5.11 (b): points_SQRUGRV_R saved as points_SQRUGRV_Right.txt

Details of each matrix is explained in Section 5.4 Point Matrix for Square U Groove. Toolpaths and part program of the grooving operation are directly based on the point matrix shown in Figure 5.11 (b).

In Figure 5.12 the point of Round Hole feature which corresponds to the tip of the hole for SP1-AL6013 is shown. Information saved in points_RNDHOL matrix internally is printed as points_RNDHOL.txt file. Details of point matrix for drilling operation can be found in Section 5.5 Point Matrix for Round Hole.

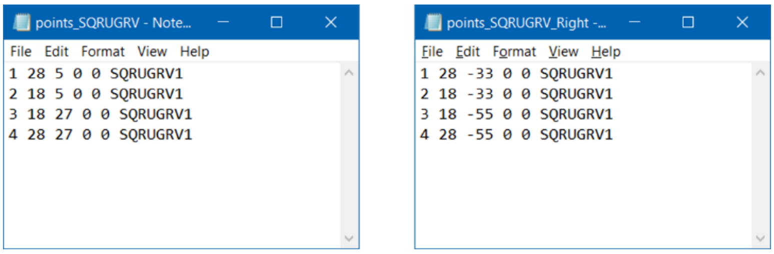

(a) (b)

Figure 5.11 Point matrices for SP1-AL6013: Grooving

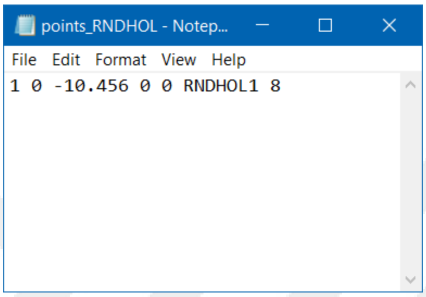

Figure 5.12 Point matrix for SP1-AL6013: Drilling

CHAPTER 6

PROCESS PLANNING

6.1 Introduction

This chapter outlines the stages of the process planning module which serves an important role for establishing the link between design and part programming. Stages of a typical process plan involve the determination of the following items:

- Material and Stock
- Features
- Manufacturing Operations
- Sequence of Operations and Setups
- Workholding for Setups
- Machine for each Setup
- Tools and Parameters

The main objective of this module is providing data for the part programming and energy estimation modules. Cutting parameters are the direct input for part programming which calculates the cutting time. Cutting time, in turn, is used in Section 8.3 Auxiliary Energy Estimation for calculating the energy requirement of each auxiliary component of the CNC lathe. Specific cutting energy, calculated after the tool and cutting parameters are determined, is an input for Section 8.2 Theoretical Energy Estimation module. Figure 6.1 illustrates the input and output structure of the Process Planning module.

All the stages mentioned above are covered in Sections 6.2 to 6.8. Section 6.9 includes a portion of the code for the Process Planning module. Finally, Section 6.10 presents the output of this module, the Manufacturing Process Sheet (MPS).

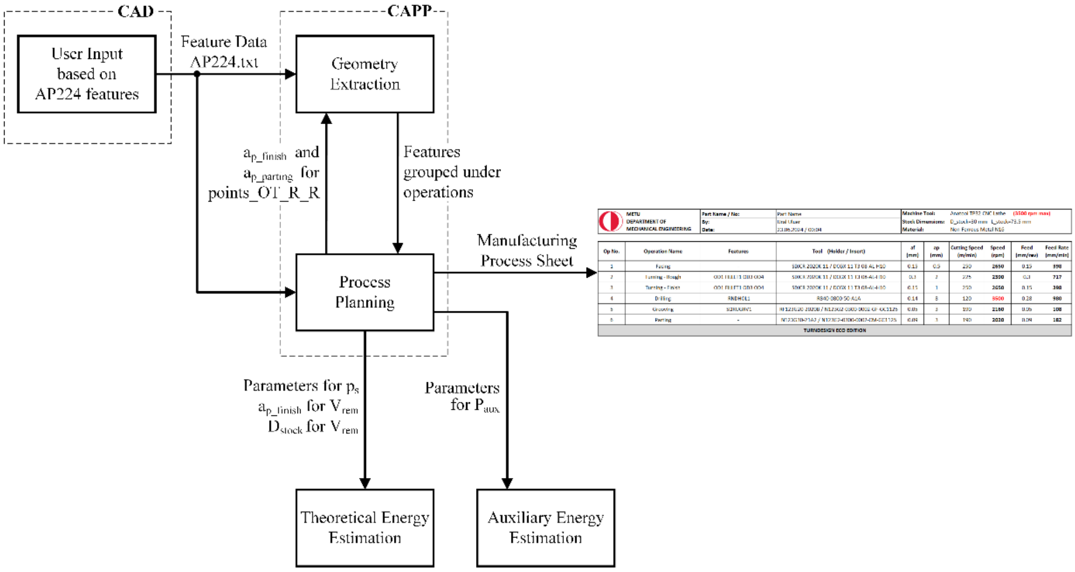

Figure 6.1 Process Planning Module: Inputs and Outputs

6.2 Material and Stock

Material is selected by the user among 22 material groups based on SECO tool catalogues (Seco, 2023). TurnDesign Eco Edition has an expandable material database but for this study only the following material groups are used:

- P3: Low alloy general structural steels, 0.25% < C < 0.67%wt
- K13: Low alloy cast iron. Malleable cast iron. Nodular cast iron.
- N16: Aluminum alloys, Si < 9%

Stock size (L_{stock} and D_{stock}) is calculated based on the maximum diameter and length of the designed part. Stock size is updated as the designed part changes based on the following equations:

$$L_{stock} = L_{clearance} + L_{max} + a_{p\_facing} \tag{6.1}$$

where

$L_{clearance}$: Allowance left at the end of the part before the chuck

L_{max}: Length of the designed part
a_{p_facing}: Allowance left for facing

$$D_{stock} = D_{max} + D_{allowance} \tag{6.2}$$

where
D_{max}: Diamater of the designed part
$D_{allowance}$: Allowance left on diameter for turning operations

6.3 Features

This study adopts a feature based approach for the part design. Unlike conventional process planning where the second stage includes feature identification from the designed part, part is generated using features in the design stage. Therefore feature identification stage in process planning is irrelevant for this study. Features are based on ISO 10303-224 (2006) and ISO 10303-238 (2007) and selected by the user from the feature library. Detailed information on feature modeler and feature based design are provided in Chapter 4 User Input.

6.4 Manufacturing Operations

Manufacturing operations for rotational parts are facing, outer turning, center drilling, drilling, grooving and parting. Features of the designed part are grouped under each operation in Geometry Extraction module which is explained under Chapter 5. Depending on the point matrices of Geometry Extraction, this submodule determines the presence of each operation for the design. Some additional remarks for each operation are as follows:

- Facing removes 0.5 mm of material thickness. Finish turning parameters will be used for facing operation as well.

- Outer turning operations involve rough and finish passes. Allowance is left only on Z axis for finishing.
- Center drilling is performed for hole diameters exceeding 8 mm.
- Pecking is employed for hole depths greater than 5 times the hole diameter.
- Grooving involves rough machining square U grooves by plunge cutting. Finish pass is not executed.
- Parting width is selected as 3 mm.

6.5 Sequence of Operations and Setups

Parts which require a single setup are considered in the scope of the thesis. Manufacturing operations follow the sequence below (Figure 6.2). This sequence is common for turning operations since it minimizes the tool change and has a potential to reduce the machining time.

- Facing
- Outer Turning-rough
- Outer Turning-finish
- Center drilling
- Drilling
- Grooving
- Parting

6.6 Workholding for Setups

In the context of this thesis study, only parts held in the chuck have been taken into consideration. The parts designed and manufactured are assumed to be short, eliminating the need for additional support with a tailstock. It is also assumed that the overhang of the part can be managed within the current setup without affecting stability or machining accuracy.

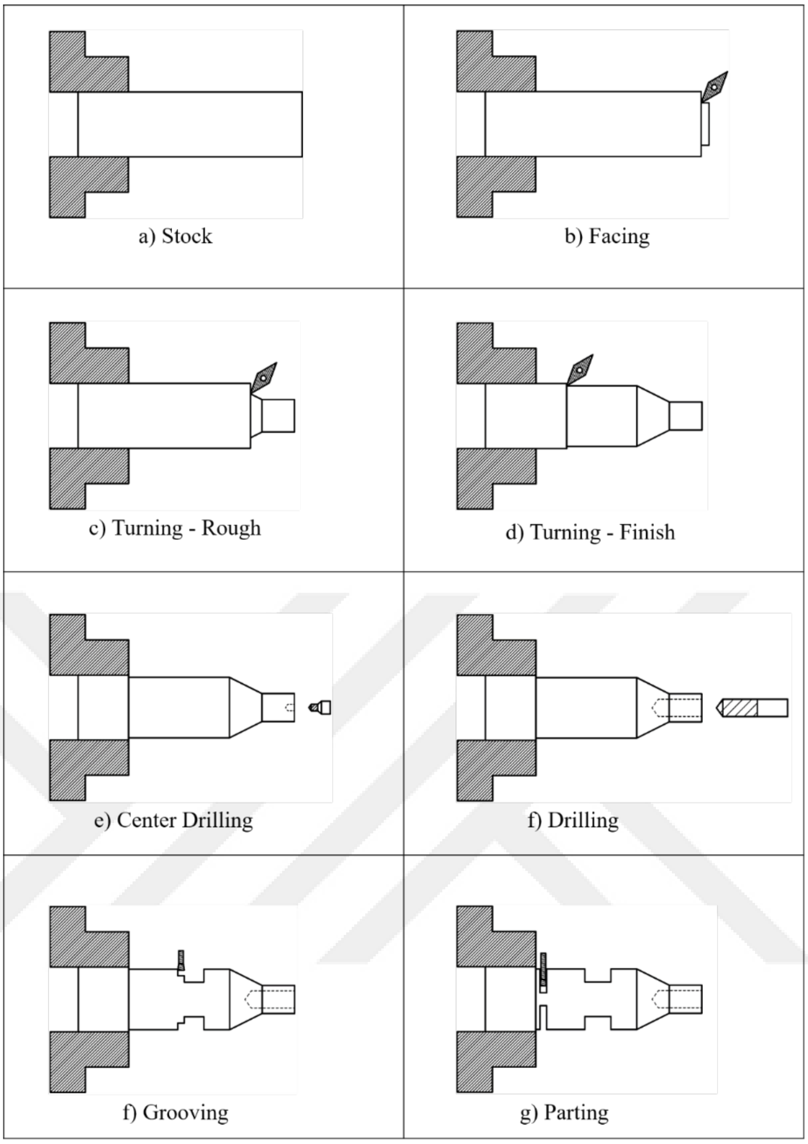

Figure 6.2 Sequence of operations

6.7 Machine for each Setup

This study is based on and verified with Anatool TP 32 CNC lathe in the Department of Mechanical Engineering at METU. Power and energy parameters of this CNC are input under Power and Energy Calibration module in TurnDesign Eco Edition. Measurement methods which can be used as the calibration for other CNCs are presented in Section 8.3 Auxiliary Energy Estimation.

6.8 Tools and Parameters

In the final stage of the process planning module, the tools and cutting parameters for each manufacturing operation are determined. Selection procedure is grouped under 3 sections: Outer Turning, Grooving and Parting, Drilling. After determining the tools and parameters, database is generated in TurnDesign Eco Edition for each material and manufacturing operation combination.

6.8.1 Tool Selection for Outer Turning Operations

In the tool selection process for outer turning operations, the assumptions and limitations concerning material, part geometry and cutting conditions are initially introduced in Section 6.8.1.1 Selection Criteria. Subsequently, Section 6.8.1.2 Insert Selection and Section 6.8.1.3 Toolholder Selection provide the insert and toolholder parameters based on the alphanumeric ISO representation, with explanations for the selection of each alphanumeric code.

6.8.1.1 Selection Criteria

Material: Tools will be selected based on three material groups based on SECO tool catalogues (Seco, 2023):

- P3: Low alloy general structural steels, 0.25% < C < 0.67%wt
- K13: Low alloy cast iron. Malleable cast iron. Nodular cast iron.
- N16: Aluminum alloys, Si < 9%

Part Geometry: Small parts will be machined (Ø < 60 mm). This assumption is made for limiting the study from small to medium sized CNC lathes. Bigger sized CNC lathes may have additional auxiliary equipment and different energy consumption characteristics.

Operations and Cutting Conditions: Selected tools will be used for facing, longitudinal turning and profiling operations. Since small parts are machined, cutting conditions are taken as medium and finish cutting.

Brand: Toolholder and insert selection will be based on Sandvik Coromant Turning Tools.

6.8.1.2 Insert Selection

Indexable outer turning inserts are selected based on the code defined in ISO 1832:2017. A designation taken from Sandvik Turning Tools Catalogue (Sandvik, 2009) is presented here for an example (Figure 6.3):

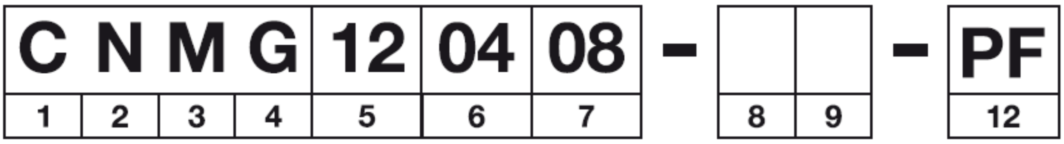

Figure 6.3 Sample code for turning insert (Sandvik, 2009)

where:
1: Insert shape
2: Insert clearance angle (α_n)
3: Tolerances
4: Insert type
5: Insert size
6: Insert thickness
7: Nose radius
12: Geometry
13: Grade (Not given in ISO designation)

Clearance angle (α_n) is the first step for selecting the insert because it also narrows down the tool family alternatives. Clearance angle is determined considering the cutting conditions. Negative inserts ($\alpha_n = 0$) are used mostly for rough machining. Positive inserts ($\alpha_n > 0$) generate lower cutting forces and tool deflections so they are preferred for medium and finish machining. The first and the most common choice for positive inserts is $\alpha_n = 7°$ (Sandvik, 2017b). Therefore a **C** type clearance angle will be used for this study.

Considering the clearance angle (positive insert) and the manufacturing operations (Facing, longitudinal turning, profiling) CoroTurn 107 is selected as the tool family as shown in Figure 6.4.

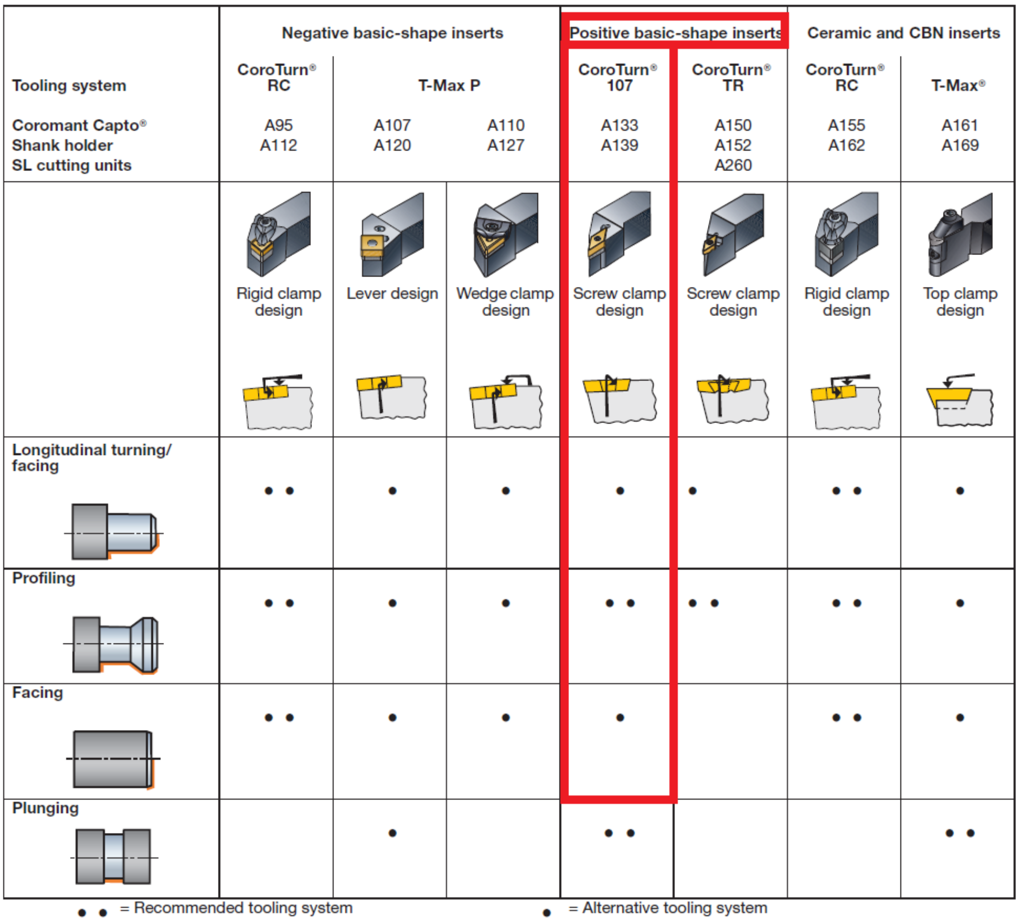

Figure 6.4 Turning tool family selection (Sandvik, 2009)

Insert shape is determined according to the cutting conditions and manufacturing processes. **D** shape having a point angle of 55° is selected so that a single insert can be used for all operations of a given design. Figure 6.5 shows that D shape can be used for light roughing to finishing operations and it is suitable for the manufacturing operations defined in the selection criteria (Sandvik, 2017b).

Insert shape	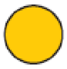	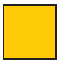	 80°	 80°		 55°	 35°
Roughing strength	●	●	●	○	○		
Light roughing/semi-finishing		○	●	●	●	●	
Finishing			○	○	●	●	●
Longitudinal turning			●	○	○	●	●
Profiling			○	○	○	●	●
Facing	○	●	●	○	○	○	
Operational versatility	○		●	○	○	●	○
Limited machine power			○	○	●	●	●
Vibration tendencies				○	●	●	●
Hard material	●	●					
Intermittent machining	●	●	○	○	○		
Small lead angle			●	●	●	●	
Large lead angle	●	●		●	●		

Figure 6.5 Insert shape selection (Sandvik, 2017b)

Geometry which defines the design and chip breaker of an insert, depends on the stock material and cutting conditions. Geometry of the insert is usually defined by using 2 letters, first one indicating the material code and the second one indicating the cutting conditions. Selected geometry will set the range for the depth of cut and feed values for acceptable chip breaking.

Three different material groups will be used (**P, K, N**) and cutting conditions are limited to medium to finish cutting for this study. Since D shape insert can be used for machining both medium and finish cuts, single insert will be used for those two cutting conditions. For general purpose use **M** (medium) is selected as cutting condition which is available for steel and cast iron. Standard geometry for aluminum is **AL**. Therefore, geometry codes for three different materials groups are **PM, KM and AL** for steel, cast iron and aluminum respectively.

Grade of an insert shows its wear resistance and toughness. It depends on the stock material group, manufacturing operations and cutting conditions. Figure 6.6 shows the range of grades with respect to cutting conditions of 01 to 50 for Steels (Sandvik, 2017b). For this study grades for average cutting conditions will be used. Figure 6.7 presents all the available grades for different material groups and machining conditions (Sandvik, 2009). To avoid above average cutting speed recommendations, grades **GC4235** for P, **GC3215** for K and **H10** for N are selected (Figure 6.7).

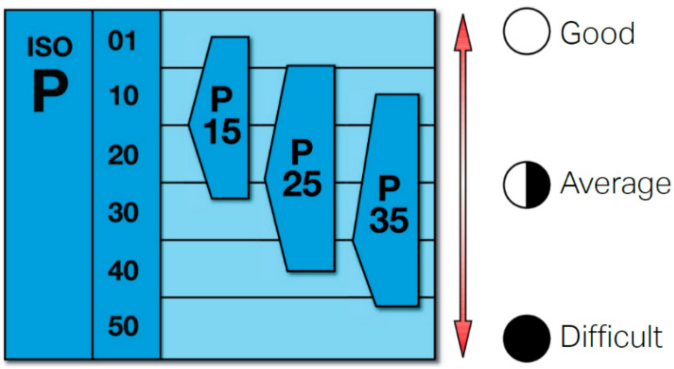

Figure 6.6 Simplified grade chart for a material (Sandvik, 2017b)

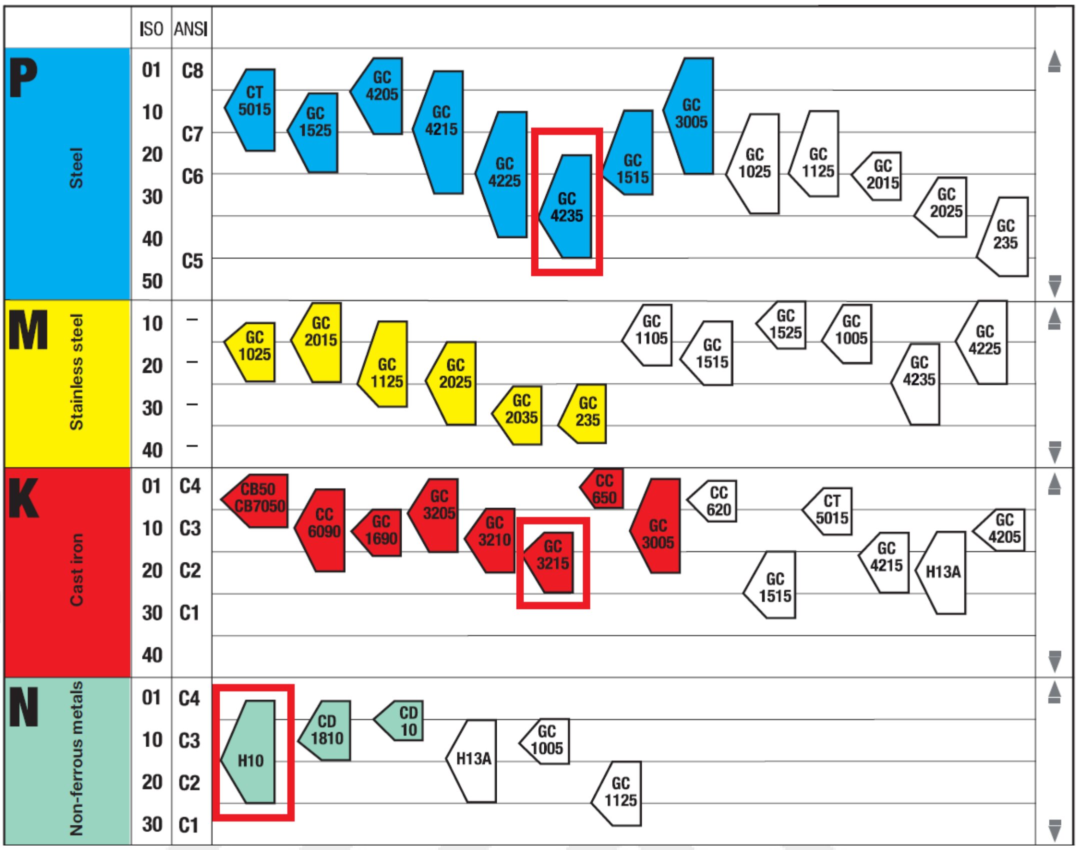

Figure 6.7 Grade charts for general turning: P, M, K, N groups (Sandvik, 2009)

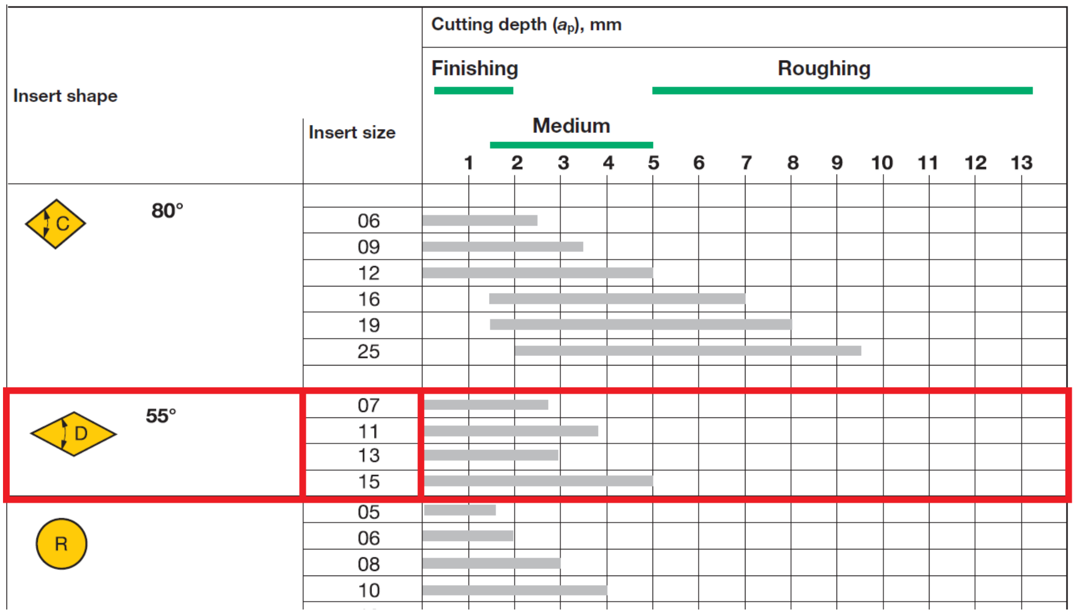

Figure 6.8 Insert size (Sandvik, 2009)

Insert size defines the cutting edge length of that insert. Cutting edge length, in turn, determines the maximum depth of cut that could be used with the given insert. For this study maximum depth of cut value will be 3 mm. Therefore cutting edge length of the insert for a D shape should be **11** as shown in Figure 6.8 (Sandvik, 2009).

Nose radius (r_ε) is the last item to select the insert code. Large nose radius values lead to a stronger cutting edge and a better surface finish. Therefore among the alternatives, inserts with a larger nose radius are selected. According to the Sandvik Training Handbook (2017b) first choice for medium cutting with CoroTurn 107 is **08**.

After above codes are determined, insert alternatives are narrowed down to one for each material group. Selected inserts are shown in Figure 6.9 (Sandvik, 2009) and summarized in Table 6.1.

CoroTurn® 107

Rhombic 55°

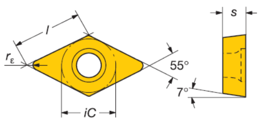

				P									M							K					N				S				
			Ordering code	GC 1025	GC 1125	GC 1515	GC 1525	GC 4205	GC 4215	GC 4225	GC 4235	CT 5015	GC 1025	GC 1105	GC 1125	GC 2015	GC 2025	GC 2035	GC 235	GC 3005	GC 3205	GC 3210	GC 3215	- H13A	GC 1005	GC 1025	GC 1810	- H10	GC 1005	GC 1025	GC 1105	- H13A	GC S05F
Medium	DCMT-PM	07	DCMT 07 02 04-PM			☆	☆		☆	★	☆	☆																					
			DCMT 07 02 08-PM			☆	☆		☆	★	☆	☆																					
		11	DCMT 11 T3 04-PM			☆	☆	☆	☆	★	☆	☆																					
			DCMT 11 T3 08-PM			☆	☆	☆	☆	★	☆	☆																					
			DCMT 11 T3 12-PM			☆	☆	☆	☆	★	☆	☆																					
	DCMT-KM	07	DCMT 07 02 04-KM																	☆			★	☆								★	
			DCMT 07 02 08-KM																	☆			★	☆								★	
		11	DCMT 11 T3 04-KM																	☆		★	☆	☆								★	
			DCMT 11 T3 08-KM																	☆		★	☆	☆								★	
Aluminium	DCGX-AL	07	DCGX 07 02 02-AL																								★	☆					
			DCGX 07 02 04-AL																						☆		★	☆					
		11	DCGX 11 T3 02-AL																								★	☆					
			DCGX 11 T3 04-AL																						☆		★	☆					
			DCGX 11 T3 08-AL																						☆		★	☆					

Figure 6.9 Selected turning inserts for material groups (Sandvik, 2009)

Table 6.1 Selected inserts for material groups

Material	Insert
P3: Low alloy general structural steels, 0.25% < C < 0.67%wt	DCMT 11 T3 08 - PM - GC4235
K13: Low alloy cast iron. Malleable cast iron. Nodular cast iron.	DCMT 11 T3 08 - KM - GC3215
N16: Aluminum alloys, Si < 9%	DCGX 11 T3 08 - AL - H10

6.8.1.3 Toolholder Selection

Shank type toolholders are selected based on the code defined in ISO 1832:2017. A designation taken from Sandvik Turning Tools Catalogue (2009) is presented here for an example (Figure 10):

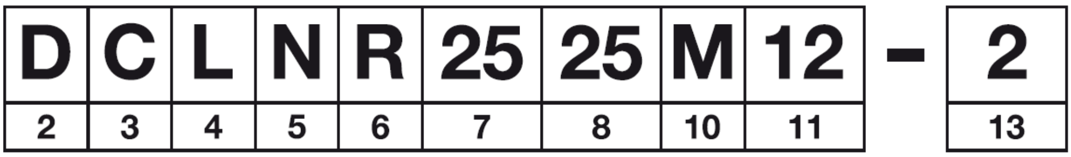

Figure 6.10 Sample code for shank type toolholder (Sandvik, 2009)

where:

2: Clamping system

3: Insert shape (Determined by insert selection)

4: Holder style

5: Insert clearance angle (α_n Determined by insert selection)

6: Hand of tool

7: Shank height

8: Shank width

10: Shank tool length

11: Insert size (Determined by insert selection)

13: Clamping system ceramics

Clearance angle (α_n) and **insert shape** which are determined by the insert selection narrows down the toolholder alternatives. In 6.8.1.2 Insert Selection section, clearance angle is selected as **C** and the insert shape is selected as **D.**

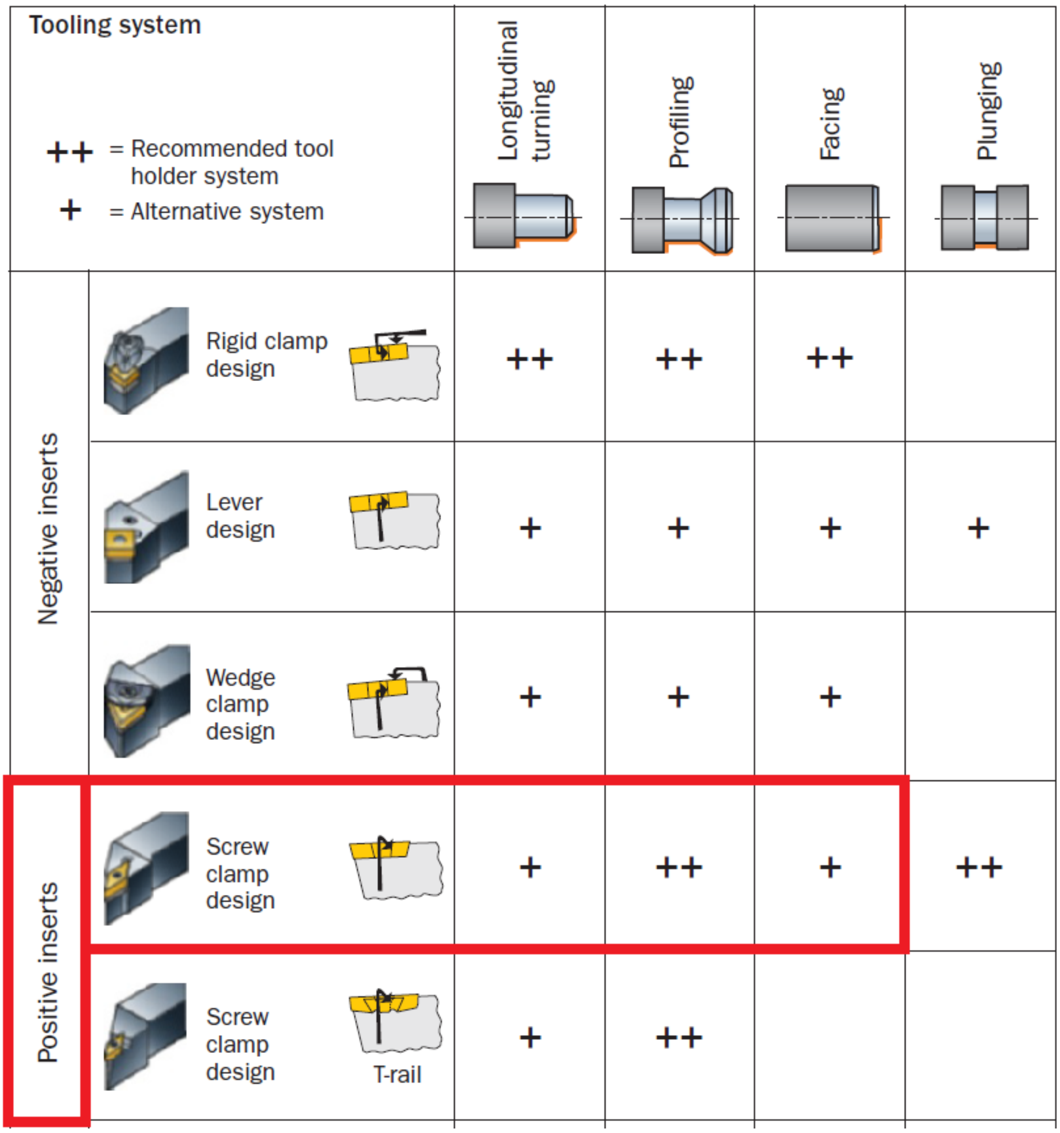

Tooling system ++ = Recommended tool holder system + = Alternative system		Longitudinal turning	Profiling	Facing	Plunging
Negative inserts	Rigid clamp design	++	++	++	
Negative inserts	Lever design	+	+	+	+
Negative inserts	Wedge clamp design	+	+	+	
Positive inserts	Screw clamp design	+	++	+	++
Positive inserts	Screw clamp design T-rail	+	++		

Figure 6.11 Clamping system for toolholder (Sandvik, 2017b)

Clamping system is automatically selected after the clearance angle and manufacturing operations are determined (Figure 6.11). Clearance angle is 7° which implies a positive insert and operations defined in the selection criteria (Facing, longitudinal turning, profiling) sets the clamping system as **S - screw clamp design** (Sandvik, 2017b).

Holder style is defined by the cutting edge angle, κ_r. Large cutting edge angle increases chip thickness leading a decrease in power requirement and decreases the radial force component which reduces the vibration tendency. Therefore a large cutting edge angle is favorable. Selection of the cutting edge angle depends on the manufacturing operation and the workpiece geometry. For longitudinal turning and profiling **93°** cutting edge angle is commonly used. 93° cutting edge angle corresponds to a **J** type tooldholder (Figure 6.12). Once the holder style (κ_r) and insert shape (point angle) are defined, minor cutting edge angle (κ_r') is can be determined by the following equation:

$$\kappa_r' = 180 - \kappa_r - point\ angle \tag{6.3}$$

Shank height and **shank width** dimensions are determined by the turret of the CNC lathe. Those values are specified in the user manual of the CNC. For this study, shank height and width are set as **20 x 20 mm** which are taken from Anatool TP 32 CNC lathe manual. 20 x 20 mm shank dimensions are commonly used on other CNC lathe turrets, as well.

Insert size (cutting edge length = **11**) set by the insert selection, reduces the toolholder to a single alternative (Figure 6.13 and Table 4.1) (Sandvik, 2009).

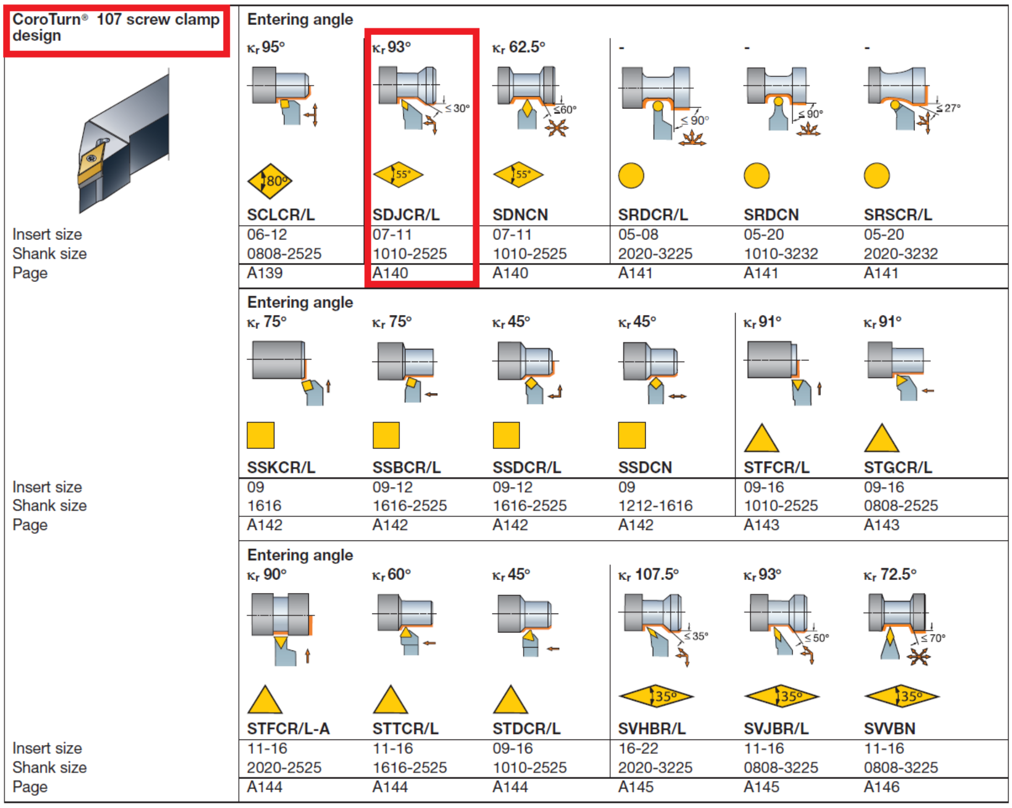

CoroTurn® 107 screw clamp design	Entering angle					
	κr 95°	κr 93°	κr 62.5°	-	-	-
	SCLCR/L	SDJCR/L	SDNCN	SRDCR/L	SRDCN	SRSCR/L
Insert size	06-12	07-11	07-11	05-08	05-20	05-20
Shank size	0808-2525	1010-2525	1010-2525	2020-3225	1010-3232	2020-3232
Page	A139	A140	A140	A141	A141	A141

	Entering angle					
	κr 75°	κr 75°	κr 45°	κr 45°	κr 91°	κr 91°
	SSKCR/L	SSBCR/L	SSDCR/L	SSDCN	STFCR/L	STGCR/L
Insert size	09	09-12	09-12	09	09-16	09-16
Shank size	1616	1616-2525	1616-2525	1212-1616	1010-2525	0808-2525
Page	A142	A142	A142	A142	A143	A143

	Entering angle					
	κr 90°	κr 60°	κr 45°	κr 107.5°	κr 93°	κr 72.5°
	STFCR/L-A	STTCR/L	STDCR/L	SVHBR/L	SVJBR/L	SVVBN
Insert size	11-16	11-16	09-16	16-22	11-16	11-16
Shank size	2020-2525	1616-2525	1010-2525	2020-3225	0808-3225	0808-3225
Page	A144	A144	A144	A145	A145	A146

Figure 6.12 Shank type toolholder family selection (Sandvik, 2009)

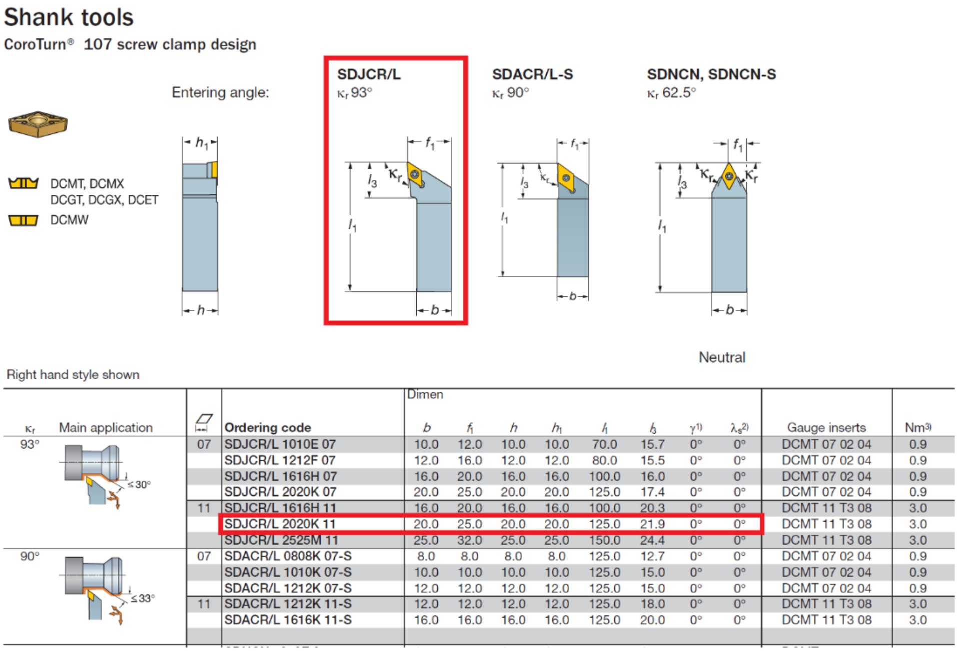

κr	Main application		Ordering code	b	f1	h	h1	l1	l3	γ1)	λs2)	Gauge inserts	Nm3)
93°		07	SDJCR/L 1010E 07	10.0	12.0	10.0	10.0	70.0	15.7	0°	0°	DCMT 07 02 04	0.9
			SDJCR/L 1212F 07	12.0	16.0	12.0	12.0	80.0	15.5	0°	0°	DCMT 07 02 04	0.9
			SDJCR/L 1616H 07	16.0	20.0	16.0	16.0	100.0	16.0	0°	0°	DCMT 07 02 04	0.9
			SDJCR/L 2020K 07	20.0	25.0	20.0	20.0	125.0	17.4	0°	0°	DCMT 07 02 04	0.9
		11	SDJCR/L 1616H 11	16.0	20.0	16.0	16.0	100.0	20.3	0°	0°	DCMT 11 T3 08	3.0
			SDJCR/L 2020K 11	20.0	25.0	20.0	20.0	125.0	21.9	0°	0°	DCMT 11 T3 08	3.0
			SDJCR/L 2525M 11	25.0	32.0	25.0	25.0	150.0	24.4	0°	0°	DCMT 11 T3 08	3.0
90°		07	SDACR/L 0808K 07-S	8.0	8.0	8.0	8.0	125.0	12.7	0°	0°	DCMT 07 02 04	0.9
			SDACR/L 1010K 07-S	10.0	10.0	10.0	10.0	125.0	15.0	0°	0°	DCMT 07 02 04	0.9
			SDACR/L 1212K 07-S	12.0	12.0	12.0	12.0	125.0	15.0	0°	0°	DCMT 07 02 04	0.9
		11	SDACR/L 1212K 11-S	12.0	12.0	12.0	12.0	125.0	18.0	0°	0°	DCMT 11 T3 08	3.0
			SDACR/L 1616K 11-S	16.0	16.0	16.0	16.0	125.0	20.0	0°	0°	DCMT 11 T3 08	3.0

Figure 6.13 Selected shank type toolholder (Sandvik, 2009)

Table 6.2 Selected shank type toolholder

Toolholder	γ_n	λ_s	κ_r	κ_r'	α_n
SDJCR 2020K 11	0	0	93	32	7

6.8.2 Parameter Selection for Outer Turning Operations

For outer turning operations, cutting parameters that define the productivity are depth of cut (a_p), feed (a_f) and cutting speed (V_c). Selection of those parameters are presented in the following sections.

6.8.2.1 Depth of Cut (a_p)

Insert size (cutting edge length) is selected based on the maximum depth of cut value required for the manufacturing operations. Selected insert size sets the maximum depth of cut value that could be used in all manufacturing operations (Figure 6.8).

Depth of cut value should be larger than the nose radius (r_ε) of the insert to avoid vibration tendency.

Insert geometry sets the range for the depth of cut values to have proper chip breaking (Sandvik, 2009, 2017b). Recommended a_p values are presented in Figure 6.14.

Considering the criteria above, following limitations are set for the depth of cut values:

1) $a_p < 4$ mm
2) $a_p > r_\varepsilon = 0.8$ mm
3) DCMT 11 T3 08 - PM $0.5 < a_p < 3$ mm
   DCMT 11 T3 08 - KM $0.5 < a_p < 3$ mm
   DCGX 11 T3 08 - AL $0.5 < a_p < 5.5$ mm

Selected tools will be used for both roughing and finishing operations so a_p values presented in Table 6.3 will be used in the part program.

CoroTurn® 107 insert for turning

Insert	Depth of cut a_p = mm Rec	Min	Max.	Cutting feed f_n = mm/r Rec	Min	Max.
DCGW11T304S01530F	0.1	0.07	0.4	0.1	0.05	0.2
DCGW11T304S02030F	0.1	0.07	0.2	0.1	0.05	0.2
DCGW11T304T01020F	0.1	0.07	0.4	0.1	0.05	0.2
DCGW11T308S01020F	0.2	0.07	0.4	0.15	0.05	0.3
DCGW11T308S01020FWH	0.2	0.07	0.8	0.2	0.05	0.3
DCGW11T308S01520FWH	0.2	0.07	0.4	0.2	0.05	0.3
DCGW11T308S01530F	0.2	0.07	0.8	0.15	0.05	0.3
DCGW11T308S02030F	0.2	0.07	0.4	0.15	0.05	0.3
DCGW11T308T01020F	0.2	0.07	0.8	0.15	0.05	0.3
DCGW11T312S01020F	0.2	0.07	0.6	0.2	0.05	0.3
DCGW11T312S01530F	0.2	0.07	1.2	0.15	0.05	0.3
DCGX070202-AL	1	0.3	4	0.12	0.05	0.15
DCGX070204-AL	1.5	0.5	4	0.2	0.1	0.3
DCGX11T302-AL	1	0.3	5.5	0.12	0.05	0.15
DCGX11T304-AL	1.5	0.5	5.5	0.2	0.1	0.3
DCGX11T308-AL	1.5	0.5	5.5	0.3	0.15	0.6
DCMT070202-KF	0.26	0.06	1.5	0.06	0.03	0.11
DCMT070202-MF	0.26	0.06	1.5	0.06	0.03	0.11
DCMT070202-PF	0.26	0.06	1.5	0.06	0.05	0.11
DCMT070202-UF	0.4	0.1	1.5	0.07	0.05	0.15
DCMT070204-KF	0.26	0.08	1.5	0.08	0.05	0.17
DCMT070204-KM	0.6	0.19	2.25	0.11	0.06	0.17
DCMT070204-MF	0.26	0.08	1.5	0.08	0.05	0.17
DCMT070204-MM	0.6	0.19	2.25	0.11	0.06	0.17
DCMT070204-PF	0.26	0.08	1.5	0.08	0.05	0.17
DCMT070204-PM	0.6	0.19	2.25	0.11	0.06	0.17
DCMT070204-UF	0.4	0.2	1.5	0.1	0.05	0.2

Insert	Depth of cut a_p = mm Rec	Min	Max.	Cutting feed f_n = mm/r Rec	Min	Max.
DCMT070204-UM	1	0.3	2.5	0.2	0.06	0.3
DCMT070204-UM	1	0.5	2.5	0.2	0.08	0.3
DCMT070208-KM	0.6	0.38	2.25	0.15	0.08	0.23
DCMT070208-MM	0.6	0.38	2.25	0.15	0.08	0.23
DCMT070208-PM	0.6	0.38	2.25	0.15	0.08	0.23
DCMT070208-UM	1	0.5	2.5	0.25	0.12	0.35
DCMT11T302-KF	0.35	0.08	2	0.08	0.04	0.15
DCMT11T302-MF	0.35	0.08	2	0.08	0.04	0.15
DCMT11T302-PF	0.35	0.08	2	0.08	0.05	0.15
DCMT11T304-KF	0.35	0.11	2	0.11	0.06	0.23
DCMT11T304-KM	0.8	0.25	3	0.15	0.08	0.23
DCMT11T304-MF	0.35	0.11	2	0.11	0.06	0.23
DCMT11T304-MM	0.8	0.25	3	0.15	0.08	0.23
DCMT11T304-PF	0.35	0.11	2	0.11	0.06	0.23
DCMT11T304-PM	0.8	0.25	3	0.15	0.08	0.23
DCMT11T304-UF	0.4	0.2	2	0.1	0.05	0.2
DCMT11T304-UM	1.25	0.5	4	0.2	0.08	0.3
DCMT11T304-UR	2	1	4	0.25	0.15	0.3
DCMT11T308-KF	0.35	0.15	2	0.15	0.08	0.3
DCMT11T308-KM	0.8	0.5	3	0.2	0.1	0.3
DCMT11T308-KR	2	1	4	0.25	0.12	0.35
DCMT11T308-MF	0.35	0.15	2	0.15	0.08	0.3
DCMT11T308-MM	0.8	0.5	3	0.2	0.1	0.3
DCMT11T308-MR	2	1	4	0.25	0.12	0.35
DCMT11T308-PF	0.35	0.15	2	0.15	0.08	0.3
DCMT11T308-PM	0.8	0.5	3	0.2	0.1	0.3
DCMT11T308-PR	2	1	4	0.25	0.12	0.35

Figure 6.14 Recommended depth of cut and cutting feed (Sandvik, 2017b)

Table 6.3 Selected depth of cut values

Material	**Insert**	**Toolholer**	**a_p rough (mm)**	**a_p finish (mm)**
P3	DCMT 11 T3 08 - PM - GC4235	SDJCR 2020K 11	1.5	0.8
K13	DCMT 11 T3 08 - KM - GC3215	SDJCR 2020K 11	1.5	0.8
N16	DCGX 11 T3 08 - AL - H10	SDJCR 2020K 11	2	1

6.8.2.2 Feed (a_f)

Insert geometry sets the range for the feed values to have proper chip breaking (Sandvik, 2009, 2017b). Recommended a_f values are presented in Figure 6.14.

A specified surface roughness on the part design could also set the feed value according the equation below (Boothroyd and Knight, 1989):

$$R_a = \frac{0.0321 \cdot a_f^2}{r_\varepsilon} \tag{6.4}$$

Surface roughness values are not in the scope of this study, so considering only the first criterion above, following limitations are set for the feed values:

DCMT 11 T3 08 - PM $0.1 < a_p < 0.3$ mm/rev

DCMT 11 T3 08 - KM $0.1 < a_p < 0.3$ mm/rev

DCGX 11 T3 08 - AL $0.15 < a_p < 0.6$ mm /rev

Selected tools will be used for both roughing and finishing operations so larger a_f values will be used for roughing and smaller values for finishing operations in the part program (Table 6.4):

Table 6.4 Selected feed values

Material	**Insert**	**Toolholder**	**a_f rough (mm/rev)**	**a_f finish (mm/rev)**
P3	DCMT 11 T3 08 - PM - GC4235	SDJCR 2020K 11	0.2	0.1
K13	DCMT 11 T3 08 - KM - GC3215	SDJCR 2020K 11	0.2	0.1
N16	DCGX 11 T3 08 - AL - H10	SDJCR 2020K 11	0.3	0.15

6.8.2.3 Cutting Speed (V_c)

Cutting speed depends on the material, grade and selected feed values. Grade which is defined primarily by the insert coating has a significant effect on speed. For example, because of their different technology and wear resistance, two main coating technologies, PVD and CVD result in different cutting speed recommendation ranges.

Selected grades in Section 6.8.1.2 Insert Selection are the ideal ones for the given cutting conditions. Therefore the recommended speed ranges (Figure 6.15) are above the industry averages which will lead to underestimation of cutting times. In order to compensate for the probability of using lower quality grades (for example PVD instead of CVD), lower limits of the recommendations are used for finishing operations and 90% of the lower limit is used for roughing (Table 6.5).

GENERAL TURNING Cutting data

Cutting speed recommendations

The recommendations are valid for use with cutting fluid.

ISO	CMC No.	Material	Specific cutting force k_c 0.4 N/mm²	Hardness Brinell HB	TO GC4225 0.1-0.4-0.8	GC2015 0.1-0.4-0.8	GC4235 0.1-0.4-0.8	GC2025 0.1-0.4-0.8
P		**Unalloyed steel**						
	01.1	C = 0.1–0.25%	2000	125	510-345-245	440-300-210	425-275-200	295-200-14
	01.2	C = 0.25–0.55%	2100	150	455-305-215	400-270-190	380-245-180	265-180-13
	01.3	C = 0.55–0.80%	2200	170	425-290-205	370-250-175	365-235-170	250-170-12

ISO	CMC No.	Material	Specific cutting force k_c 0.4 N/mm²	Hardness Brinell HB	GC3210 0.2-0.4-0.6	GC3215 0.2-0.4-0.6	GC3005 0.2-0.4-0.6	GC4205 0.2-0.4-0.6
K		**Malleable cast iron**						
	07.1	Ferritic (short chipping)	940	130	385-315-265	260-215-185	250-210-185	365-295-25
	07.2	Pearlitic (long chipping)	1100	230	315-255-215	210-175-150	235-190-150	295-245-20
		Grey cast iron						
iron	08.1	Low tensile strength	1100	180	445-360-305	300-250-210	275-245-225	400-335-29
	08.2	High tensile strength	1150	220	355-290-245	240-200-170	260-225-200	320-275-24

ISO	CMC No.	Material	Specific cutting force k_c 0.4 N/mm²	Hardness Brinell HB	<<<< WEAR RESISTANCE CD10	CD1810	H10
					h_{ex}, mm ≈ feed f_n, mm/r 0.05-0.4	0.15-0.8	0.15-0.8
					Cutting speed (v_c), m/min		
N		**Aluminium alloys**					
	30.11	Wrought or wrought and coldworked, non-aging	500	60	2 000 (2500-250)1)	2 000 (2500-250)1)	2 000 (2500-250)1)
	30.12	Wrought or wrought and aged	800	100	2 000 (2500-250)1)	2 000 (2500-250)1)	2 000 (2500-250)1)

Figure 6.15 Cutting speed recommendations (Sandvik, 2009)

Table 6.5 Selected cutting speed values

Material	Insert	Toolholder	V_c rough (m/min)	V_c finish (m/min)
P3	DCMT 11 T3 08 - PM - GC4235	SDJCR 2020K 11	162	180
K13	DCMT 11 T3 08 - KM - GC3215	SDJCR 2020K 11	153	170
N16	DCGX 11 T3 08 - AL - H10	SDJCR 2020K 11	225	250

6.8.2.4 Spindle Speed (n) and Feed Rate (V_f)

Spindle speed (n) is calculated by the following equation for outer turning operations:

$$n = \frac{1000\, V_c}{\pi\, D_{stock}} \tag{6.5}$$

Feed rate (V_f) is found by:

$$V_f = a_f\, n \tag{6.6}$$

6.8.3 Tool Selection for Grooving and Parting Operations

In the tool selection process for grooving and parting operations, Section 6.8.3.2 Insert Selection initially introduces the assumptions and limitations related to material, part shape and cutting conditions. Afterward, Sections 6.8.3.2 Insert Selection and 6.8.3.3 Toolholder Selection are used to present the insert and toolholder parameters based on codes from the Sandvik Turning Tools Catalogue (Sandvik, 2017a) and explanations for why each code is chosen are provided.

6.8.3.1 Selection Criteria

Material: Tools will be selected based on three material groups based on SECO tool catalogues (Seco, 2023):

- P3: Low alloy general structural steels, 0.25% < C < 0.67%wt
- K13: Low alloy cast iron. Malleable cast iron. Nodular cast iron.
- N16: Aluminum alloys, Si < 9%

Part and Feature Geometry: Following assumptions are made for the part geometry regarding grooving and parting operations:

- Maximum parting diameter is 60 mm.
- Minimum groove width is 3 mm.
- Maximum groove depth is 20 mm.

Operations and Cutting Conditions: Based on the classification of Sandvik Training Handbook (2017b), for grooving, if the groove depth falls between 6 and 50 mm, it is considered medium grooving. In the case of parting, if the maximum diameter is between 40 and 60 mm, it is classified as deep parting.

For grooves which are wider than the insert width, G75 grooving cycle is emulated which involves consecutive plunge cuts in radial direction only. This type of grooving is referred as "Multiple Plunge Grooving" in Sandvik Training Handbook.

Tool family which is used for parting and grooving operations can also perform turning, profiling, face grooving and undercutting. Face grooving and under cutting is not in the scope of this study. Turning and profiling operations require axial feed and they will be done by using conventional turning inserts which are covered in Section 6.8.1 Tool Selection for Outer Turning Operations. Finish cut will not be performed for grooving operations. Since small parts are machined, low to medium feeds will be used for grooving and parting operations.

Brand: Toolholder and insert selection will be based on Sandvik Coromant Turning Tools.

6.8.3.2 Insert Selection

The first step of selecting the inserts for grooving and parting tools is determining the insert family. Insert family is based on the manufacturing operations. As stated in the Operations and Cutting Conditions section, only medium grooving and deep parting operations will be performed.

According to Figure 6.16 (Sandvik 2017b), CoroCut1 and CoroCut2 family, which are combined as CoroCut 1-2 in the new Sandvik Turning Tools catalogue (2017a), is the best choice for both grooving and deep parting operations.

Figure 6.16 Grooving and parting tool family selection (Sandvik 2017b)

Although there are dedicated insert families for specific manufacturing operations (for example CoroCut QD family for deep grooving), **CoroCut 1-2** family is preferred since it is the first choice system for all parting and grooving operations and Corocut 1-2 family is more commercially available compared the other dedicated geometries.

Grooving and parting inserts are specified based on the code defined in Sandvik Turning Tools Catalogue (Sandvik, 2017a). A sample code is presented here for an example (Figure 6.17):

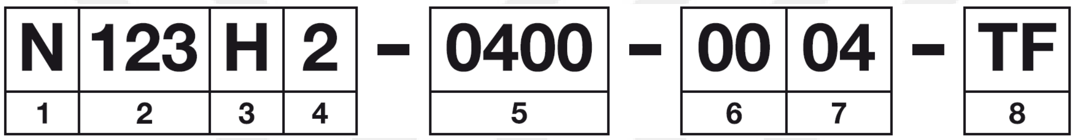

Figure 6.17 Sample code for CoroCut 1-2 insert (Sandvik, 2017a)

where:
1: Hand of insert
2: Main code (For Corocut 1-2-3 inserts)
3: Seat size
4: Number of edges
5: Insert width
6: Front angle
7: Corner radius
8: Geometry
9: Grade (Not given in Sandvik CoroCut 1-2 designation)

In order to select the relevant insert group under CoroCut 1-2 family, **geometry** of the insert should be determined. Geometry which defines the design and chip breaker of the insert, depends on manufacturing operation, cutting conditions and stock material. Geometry of the insert is usually defined by using 2 letters, first one giving information about the type of operation and occasionally stock material and the second one indicating the cutting conditions (Figure 6.18, Sandvik 2017b). Selected geometry will set the range for the radial feed values along with the insert width.

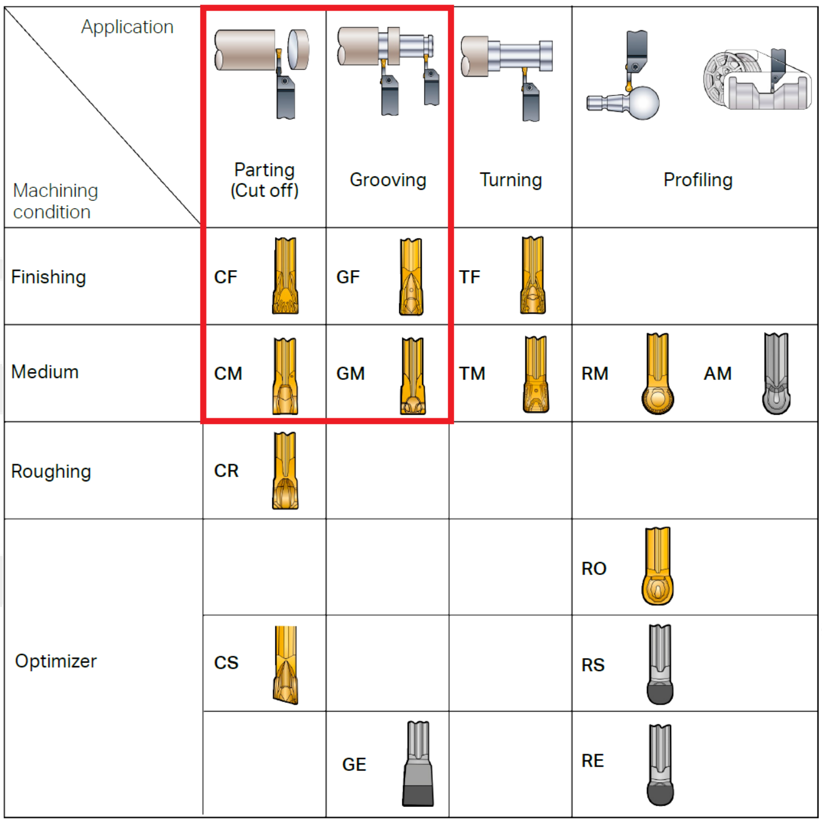

Figure 6.18 Geometry overview for grooving/parting inserts (Sandvik 2017b)

Three different material groups will be used (P, K, N) and cutting conditions are limited to medium to finish cutting for this study. As explained in Operations and Cutting Conditions under Section 6.8.3.1 Selection Criteria, operations are grooving and parting only. Geometry recommendations of Sandvik Turning Handbook (2017c) are presented in Figure 6.19. Cast iron (K) recommendation is not available and is found as CM from the Sandvik CoroCut 1-2 "How to use" website. Selected geometries are summarized in Table 6.6.

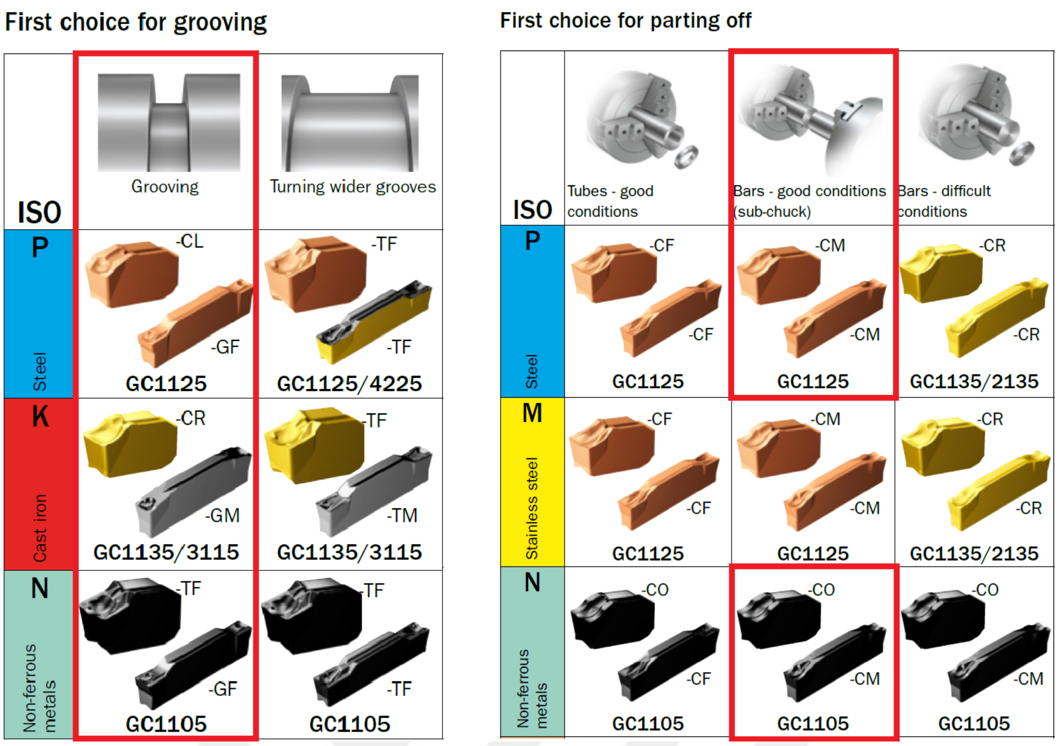

Figure 6.19 Geometry/grade recommendations: CoroCut 1-2 (Sandvik 2017c)

Table 6.6 Selected geometries for CoroCut 1-2 inserts

Material	Grooving	Parting
P3	GF	CM
K13	GM	CM
N16	GF	CM

Number of edges depends on the manufacturing operation and maximum cutting depth of the insert. Most of the inserts have 2 edges for machining economics. Number of edges is determined automatically for the specified insert geometry. Based on Sandvik Turning Tools catalogue (2017a), number of edges is **2** for the selected geometries in Table 6.6.

Hand of insert and **front angle** are closely related. If front angle is 0, hand of insert is neutral (N). If front angle has a positive value, hand of insert could be left (L) or right (R) according to the inclination. Front angle is used for pip size reduction in parting operations but it also increases the cutting force and decreases chip control. Neutral inserts are recommended for parting by Sandvik Training Handbook (2017b). Front angle is always 0 for grooving inserts. Therefore for both parting and grooving operations **neutral (N)** inserts with **0°** front angle are selected.

Seat size is determined by **insert width**. For grooving operations groove size determines the insert width. Minimum groove width is 3 mm as stated in Part and Feature Geometry under Section 6.8.3.1 Selection Criteria, therefore insert width cannot be greater than 3 mm. For wider grooves multiple plunge grooving will be done. Since there will not be finishing operation for single cut grooves and in order to minimize the machining time for wider grooves, maximum insert width of **3 mm is selected for grooving**. For parting operations maximum stock diameter determines the insert size. Maximum parting diameter is 60 mm as stated in Part and Feature Geometry under Section 6.8.3.1 Selection Criteria. According to Figure 6.20 (Sandvik, 2017c), **3 mm insert is selected for parting**. Based on the seat sizes given Sandvik Turning Tools catalogue (2017a), 3.00 to 3.99 mm insert width for both grooving and parting operations falls under **seat size G**.

D mm (inch)	CW mm
–10 (–0.4)	1.0
10–25 (0.4–1.0)	1.5
25–40 (1.0–1.6)	2.0
40–50 (1.6–2.0)	2.5
50–65 (2.0–2.6)	3.0

Figure 6.20 Insert width (CW) values based on stock diameter (Sandvik, 2017c)

Corner radius will be selected based on the feed rates for the operations. Since low to medium feeds are used for grooving and parting operations, minimum available corner radius values are preferred. Considering the items above and based on the remaining alternatives in Sandvik Turning Tools catalogue (2017a) **02** (0.2 mm) is used for GF and CM geometries and **03** (0.3 mm) is used for GM geometry.

Grade of an insert shows its wear resistance and toughness. It depends on the stock material, manufacturing operations and cutting conditions. GC1125 is a commercially available PVD coated grade which the first choice for grooving and parting operations of steel (Figure 6.19). Recommendations for grooving of cast iron (K) is a CVD coated grade (GC3115) from Figure 6.19 and results in above average cutting speed recommendations. This study is intended for general purpose machining therefore a PVD coating is preferred for cast iron (K) as well. Recommendation for parting of cast iron (K) is not available in Figure 6.19. For aluminum alloys the recommended grade is GC1105 in Figure 6.19. However, the cutting speed values of that grade is missing in the Sandvik Turning Tools catalogue (2017a). As a result, recommendations of Sandvik Turning Handbook (2017c) in Figure 6.19 could only be followed for steel (P). Instead of using those grades, a common PVD coated grade is selected for all material groups which is going to reduce the number of tools and give higher production versatility. Based on the grade recommendations of Sandvik Turning Tools catalogue (2017a), even if it is not the first choice, GC1125 can also be used for the parting and grooving operations of cast iron (K) and aluminum alloys (N). Therefore, **GC1125** is selected for each material/operation configuration. Corresponding grades are shown in the grade charts for grooving and parting operations in Figure 6.21, as well.

After grades are determined, insert alternatives are narrowed down to one for each material group. Selected inserts are shown in Figure 6.22, Figure 6.23 for grooving and in Figure 6.24 for parting (Sandvik, 2017a). Codes are presented in Table 6.7 as a summary.

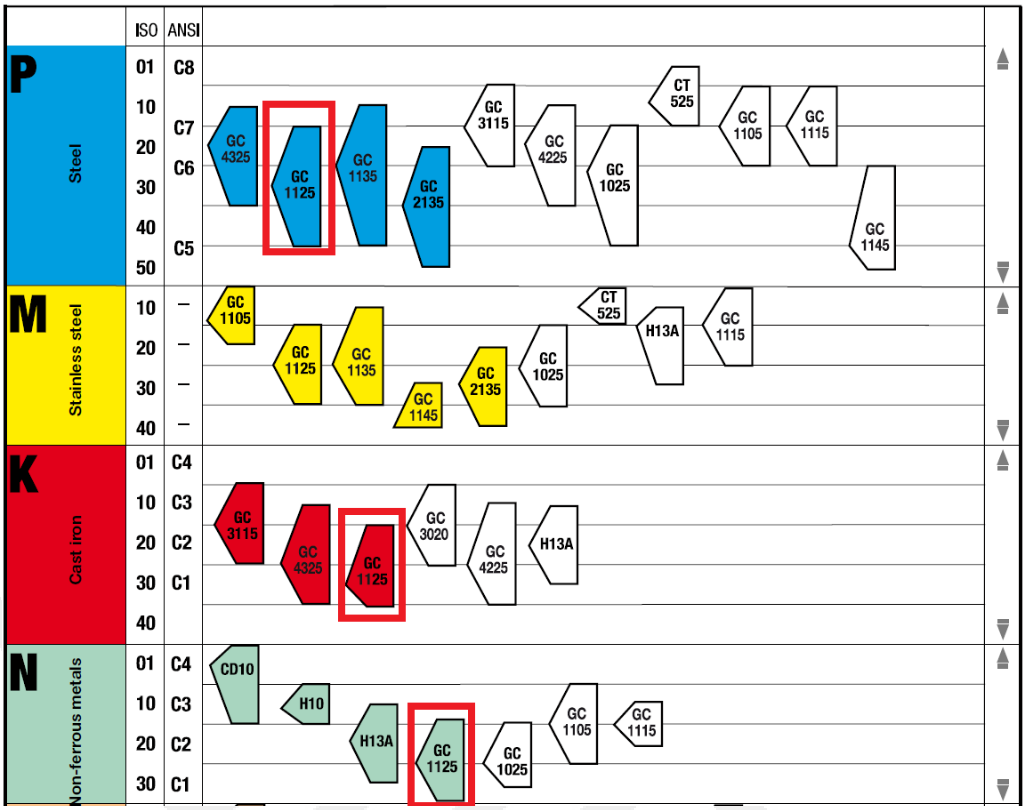

Figure 6.21 Grade charts of grooving/parting: P,M,K,N groups (Sandvik, 2009)

CoroCut® 1-2 insert for grooving

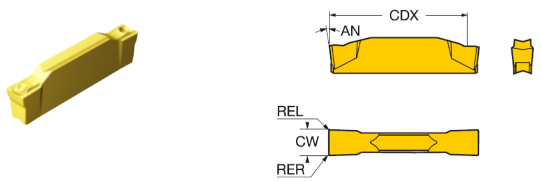

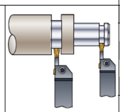

SSC	CW	REL	RER	CDX	Ordering code	P 1105	P 1125	P 2135	P 525	M 1105	M 1125	M 2135	M H13A	K 1125	K 2135	K H13A	N 1105	N 1125	N 2135	N H13A	S 1105	S 1125	S 2135	S H13A	Dimensions, mm AN
D	1.5	0.10	0.10	13.3	N123D2-0150-0001-GF	☆	★		☆	☆	★			★			★	☆			★	☆			5°
E	2.0	0.20	0.20	19.2	N123E2-0198-0002-GF		★				★			★				★				★			7°
	2.0	0.20	0.20	19.2	N123E2-0200-0002-GF	☆	☆	★	☆	☆	☆	★	☆	★	☆	☆	☆	☆	☆	★	★	☆	☆	☆	7°
	2.0	0.40	0.40	19.2	N123E2-0200-0004-GF	☆	★			☆	★		☆	★		☆	☆	☆		★	★	☆		☆	7°
	2.2	0.20	0.20	19.2	N123E2-0224-0002-GF	☆	★			☆	★			★			★	☆			★	☆			7°
F	2.4	0.20	0.20	19.2	N123F2-0239-0002-GF	☆	★			☆	★		☆	★		☆	☆	☆		★	★	☆		☆	7°
	2.4	0.40	0.40	19.2	N123F2-0239-0004-GF	☆	★			☆	★			★			★	☆			★	☆			7°
	2.5	0.30	0.30	19.1	N123F2-0246-0003-GF	☆	★		☆	☆	★		☆	★		☆	☆	☆		★	★	☆		☆	7°
	2.7	0.20	0.20	19.2	N123F2-0267-0002-GF		★				★			★				★				★			7°
	2.8	0.30	0.30	19.1	N123F2-0279-0003-GF	☆	★			☆	★			★			★	☆			★	☆			7°
G	3.0	0.20	0.20	19.2	N123G2-0300-0002-GF	☆	☆	★	☆	☆	☆	★	☆	★	☆	☆	☆	☆	☆	★	★	☆	☆	☆	7°
	3.0	0.40	0.40	19.2	N123G2-0300-0004-GF	☆	★			☆	★		☆	★		☆	☆	☆		★	★	☆		☆	7°
	3.1	0.20	0.20	19.2	N123G2-0310-0002-GF		★				★			★				★				★			7°
	3.2	0.20	0.20	19.2	N123G2-0318-0002-GF	☆	★		☆	☆	★		☆	★		☆	☆	☆		★	★	☆		☆	7°
	3.2	0.40	0.40	19.2	N123G2-0318-0004-GF		★				★			★				★				★			7°
	3.2	0.80	0.80	19.2	N123G2-0318-0008-GF	☆	★			☆	★			★			★	☆			★	☆			7°
	3.6	0.30	0.30	19.1	N123G2-0361-0003-GF	☆	★			☆	★		☆	★		☆	☆	☆		★	★	☆		☆	7°
H	4.0	0.20	0.20	24.4	N123H2-0396-0002-GF	☆	★			☆	★			★			★	☆			★	☆			7°

Figure 6.22 Selected grooving inserts for material group P, N (Sandvik,2017a)

CoroCut® 1-2 insert for grooving

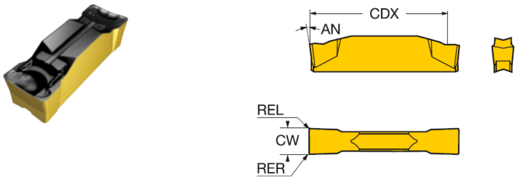

	SSC	CW	REL	RER	CDX	Ordering code	P			M				K					N			S				Dimensions, mm
							1125	1145	2135	1125	1145	2135	H13A	1125	2135	3115	4325	H13A	1125	2135	H13A	1125	1145	2135	H13A	AN
Medium	E	2.0	0.20	0.20	18.8	N123E2-0200-0002-GM	☆	☆	★	☆	☆	★	☆	☆	☆	☆	★	☆	☆	☆	★	★	☆	☆	☆	7°
		2.4	0.20	0.20	18.4	N123E2-0239-0002-GM	☆		★	☆		★	☆	☆	☆	☆	★	☆	☆	☆	★	★		☆	☆	7°
	G	3.0	0.30	0.30	18.2	N123G2-0300-0003-GM	☆	☆	★	☆	☆	★	☆	☆	☆	☆	★	☆	☆	☆	★	★	☆	☆	☆	7°
		3.2	0.30	0.30	18.0	N123G2-0318-0003-GM	☆	☆	★	☆	☆	★	☆	☆	☆	☆	★	☆	☆	☆	★	★	☆	☆	☆	7°
	H	4.0	0.30	0.30	23.0	N123H2-0400-0003-GM	☆	☆	★	☆	☆	★	☆	☆	☆	☆	★	☆	☆	☆	★	★	☆	☆	☆	7°
	J	4.8	0.30	0.30	22.6	N123J2-0475-0003-GM	☆		★	☆		★	☆	☆	☆	☆	★	☆	☆	☆	★	★		☆	☆	7°
		5.0	0.40	0.40	22.9	N123J2-0500-0004-GM	☆	☆	★	☆	☆	★	☆	☆	☆	☆	★	☆	☆	☆	★	★	☆	☆	☆	7°
	K	6.0	0.40	0.40	22.7	N123K2-0600-0004-GM	☆	☆	★	☆	☆	★	☆	☆	☆	☆	★	☆	☆	☆	★	★	☆	☆	☆	7°
		6.4	0.25	0.25	22.6	N123K2-0635-0003-GM	☆	☆	★	☆	☆	★	☆	☆	☆	☆	★	☆	☆	☆	★	★	☆	☆	☆	7°
	L	7.9	0.30	0.30	28.7	N123L2-0792-0003-GM	★			★				☆			★		★			★				7°
		8.0	0.50	0.50	28.4	N123L2-0800-0005-GM	☆		★	☆		★	☆	☆	☆	☆	★	☆	☆	☆	★	★		☆	☆	7°
	M	9.1	0.80	0.80	28.0	N123M2-0900-0008-GM	★			★				☆			★		★			★				7°
		10.0	0.80	0.80	28.0	N123M2-1000-0008-GM	★			★				☆			★		★			★				7°

Figure 6.23 Selected grooving inserts for material group K (Sandvik, 2017a)

CoroCut® 1-2 insert for parting

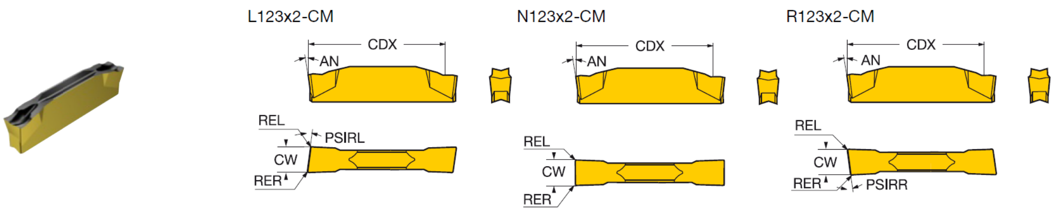

	SSC	CW	REL	RER	CDX	PSIRL	PSIRR	Ordering code	P					M				K				N				S				Dimensions, mm
									1105	1125	1145	2135	525	1105	1125	1145	2135	1125	1145	3115	4325	1105	1125	1145	2135	1105	1125	1145	2135	AN
Medium	E	2.0	0.20	0.20	19.0	5°		L123E2-0200-0502-CM		★	☆	☆			☆	☆	★	★	☆				★	☆	☆		☆	★	☆	7°
	F	2.5	0.20	0.20	18.9	5°		L123F2-0250-0502-CM		★	☆	☆			☆	☆	★	★	☆				★	☆	☆		☆	★	☆	7°
	G	3.0	0.20	0.20	18.8	5°		L123G2-0300-0502-CM		★	☆	☆			☆	☆	★	★	☆	☆	☆		★	☆	☆		☆	★	☆	7°
	H	4.0	0.20	0.20	24.1	5°		L123H2-0400-0502-CM		★	☆	☆			☆	☆	★	★	☆				★	☆	☆		★	★	☆	7°
	J	5.0	0.20	0.20	24.1	5°		L123J2-0500-0502-CM		★		☆			☆		★	★					★		☆		★		☆	7°
	E	2.0	0.20	0.20	19.0		5°	R123E2-0200-0502-CM		★	☆	☆			☆	☆	★	★	☆				★	☆	☆		☆	★	☆	7°
	F	2.5	0.20	0.20	18.9		5°	R123F2-0250-0502-CM		★	☆	☆			☆	☆	★	★	☆				★	☆	☆		☆	★	☆	7°
	G	3.0	0.20	0.20	18.8		5°	R123G2-0300-0502-CM		★	☆	☆			☆	☆	★	★	☆	☆	☆		★	☆	☆		☆	★	☆	7°
	H	4.0	0.20	0.20	24.1		5°	R123H2-0400-0502-CM		★	☆	☆			☆	☆	★	★	☆				★	☆	☆		☆	★	☆	7°
	J	5.0	0.20	0.20	24.1		5°	R123J2-0500-0502-CM		★		☆			☆		★	★					★		☆		★		☆	7°
	D	1.5	0.20	0.20	12.9			N123D2-0150-0002-CM	☆	★	☆	☆		☆	☆	☆	★	★	☆			★	☆	☆	☆	☆	☆	★	☆	7°
	E	2.0	0.20	0.20	19.0			N123E2-0200-0002-CM	☆	★		☆	☆	☆	☆		★	★		☆	☆	★	☆		☆	☆	★		☆	7°
	F	2.5	0.20	0.20	18.9			N123F2-0250-0002-CM	☆	★		☆		☆	☆		★	★		☆	☆	★	☆		☆	☆	★		☆	7°
	G	3.0	0.20	0.20	18.9			N123G2-0300-0002-CM	☆	★		☆	☆	☆	☆		★	★		☆	☆	★	☆		☆	☆	★		☆	7°
	H	4.0	0.20	0.20	24.1			N123H2-0400-0002-CM	☆	★		☆	☆	☆	☆		★	★		☆	☆	★	☆		☆	☆	★		☆	7°
	J	5.0	0.20	0.20	24.1			N123J2-0500-0002-CM		★		☆			☆		★	★					★		☆		★		☆	7°

Figure 6.24 Selected parting inserts for material groups (Sandvik, 2017a)

Table 6.7 Selected grooving and parting inserts for material groups

Material	Grooving Insert	Parting Insert
P3	N123G2-0300-0002-GF-GC1125	N123G2-0300-0002-CM-GC1125
K13	N123G2-0300-0003-GM-GC1125	N123G2-0300-0002-CM-GC1125
N16	N123G2-0300-0002-GF-GC1125	N123G2-0300-0002-CM-GC1125

6.8.3.3 Toolholder Selection

There are mainly two type of toolholders for grooving and parting operations: Shank holders and blades. Proper holder type is selected based on the manufacturing operation, maximum cutting depth for grooving and maximum diameter for parting. Shank holders are more rigid and can be used for both axial and radial feed. Axial feed makes them suitable for grooving, turning, profiling, face grooving and undercutting operations. They are used for small diameters. Blades can only be used for radial feed. Their thin geometry enables deep grooving and parting operations.

As explained in Part and Feature Geometry and Operations and Cutting Conditions under Section 6.8.3.1 Selection Criteria, medium grooving and deep parting operations will be performed for this study. Sandvik Training Handbook (2017b) recommends shank holders for grooving operations and blades for deep parting operations.

Shank Holder Selection for Grooving:

Shank type toolholders are specified based on the code defined in Sandvik Turning Tools Catalogue (Sandvik, 2017a). A sample code is presented here for an example (Figure 6.25):

R	F	123	E	08	-	1616	B	-	007	064	B
2	3	4	5	6		7	8		10	12	13

Figure 6.25 Sample code for shank toolholder for grooving (Sandvik, 2017a)

where:

2: Hand of tool

3: Holder style

4: Main code (for Corocut 1-2-3 inserts)

5: Insert seat size

6: Machining limitations (Maximum cutting depth)

7: Shank width/height

8: Clamping system

10: Holder angle (for profiling or undercutting)

12: Min. diameter for first cut (for face grooving)

13: Type of curve (for face grooving)

Seat size which is determined by the insert and **shank width/height** which are determined by the turret of the CNC lathe narrow down the toolholder alternatives. In Section 4.2 Insert Selection, seat size is selected as **G**. Shank width/height are specified as **2020** according to the technical specifications given in Anatool TP 32 CNC lathe manual. 20 x 20 shank dimensions are commonly used on other CNC lathe turrets, as well.

Maximum cutting depth is selected according to the maximum groove depth of the designed part. The maximum depth is specified as 20 mm in Part and Feature Geometry under Section 6.8.3.1 Selection Criteria. Once the seat size and shank dimensions are decided, only two alternatives remain for cutting depth in Sandvik Turning Tools catalogue (2017a): 10 and 20 mm. Therefore **20** is selected for the maximum cutting depth.

Hand of tool is selected based on the manufacturing operation and the workpiece geometry. For multiple plunge grooving (6.8.3.1 Selection Criteria) either Neutral or Right/Left type can be used. Although this study is limited to multiple plunge grooving, most of the time Corocut inserts are used both for turning and grooving. Therefore, **R** type is selected for general purpose machining.

Holder style is selected as **F** which represents 0° angle. Other holder styles are for face grooving and undercutting operations which are not in the scope of this study.

Clamping system is **B** which is typical for shank type toolholders. B type represents screw clamping which gives enough strength for axial feed.

Based on the codes above, shank toolholder is selected as **RF123G20-2020B** for grooving operations. Selected holder is shown in Figure 6.27 (Sandvik, 2017a), as well.

Blade Selection for Parting:

Blade type toolholders are specified based on the code defined in Sandvik Turning Tools Catalogue (Sandvik, 2017a). A sample code is presented here for an example (Figure 6.26):

N	123	F	55	-	25	A	2
2	4	5	6		7	8	9

Figure 6.26 Sample code for blade toolholder for parting (Sandvik, 2017a)

where:

2: Hand of tool

4: Main code (for Corocut 1-2-3 inserts)

CoroCut® 1-2 shank tool for parting and grooving

Screw clamp design

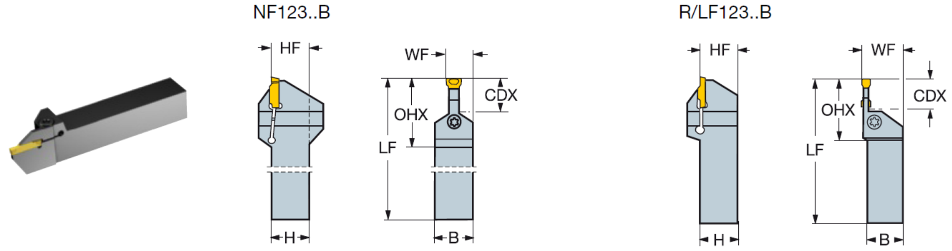

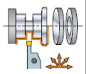

SSC	CZC_{MS}	CDX	OHX	Ordering code	B	H	LF	WF	HF	NM	KG	MIID
					Dimensions, mm							
F	16 x 16	10.0	29.0	R/LF123F10-1616B	16.0	16.0	125.0	17.0	16.0	3.0	0.26	N123F2-0250-0002-CM
	16 x 16	20.0	22.4	R/LF123F20-1616B	16.0	16.0	125.0	17.0	16.0	4.0	0.25	N123F2-0250-0002-CM
	20 x 20	10.0	29.0	R/LF123F10-2020B	20.0	20.0	125.0	21.0	20.0	3.0	0.35	N123F2-0250-0002-CM
	20 x 20	20.0	22.4	R/LF123F20-2020B	20.0	20.0	125.0	21.0	20.0	4.0	0.36	N123F2-0250-0002-CM
	25 x 25	10.0	29.0	R/LF123F10-2525B	25.0	25.0	150.0	26.0	25.0	3.0	0.72	N123F2-0250-0002-CM
	25 x 25	20.0	22.4	R/LF123F20-2525B	25.0	25.0	150.0	26.0	25.0	4.0	0.67	N123F2-0250-0002-CM
	32 x 25	20.0	40.0	R/LF123F20-3225B	25.0	32.0	170.0	26.0	32.0	4.0	0.99	N123F2-0250-0002-CM
G	16 x 16	10.0	22.4	R/LF123G10-1616B	16.0	16.0	125.0	17.0	16.0	3.5	0.26	N123G2-0300-0003-TF
	16 x 16	20.0	41.0	R/LF123G20-1616B	16.0	16.0	125.0	17.0	16.0	5.0	0.26	N123G2-0300-0003-TF
	20 x 20	10.0	22.4	R/LF123G10-2020B	20.0	20.0	125.0	21.0	20.0	3.5	0.40	N123G2-0300-0003-TF
	20 x 20	20.0	41.0	R/LF123G20-2020B	20.0	20.0	125.0	21.0	20.0	5.0	0.36	N123G2-0300-0003-TF
	25 x 25	10.0	22.4	R/LF123G10-2525B	25.0	25.0	150.0	26.0	25.0	3.5	0.73	N123G2-0300-0003-TF
	25 x 25	20.0	41.0	R/LF123G20-2525B	25.0	25.0	150.0	26.0	25.0	5.0	0.68	N123G2-0300-0003-TF
	32 x 25	10.0	30.0	R/LF123G10-3225B	25.0	32.0	170.0	26.0	32.0	3.5	1.05	N123G2-0300-0003-TF
	32 x 25	20.0	41.0	R/LF123G20-3225B	25.0	32.0	170.0	26.0	32.0	5.0	0.99	N123G2-0300-0003-TF
	32 x 32	20.0	41.0	R/LF123G20-3232B	32.0	32.0	170.0	33.0	32.0	5.0	1.24	N123G2-0300-0003-TF
H	16 x 16	13.0	34.0	R/LF123H13-1616B	16.0	16.0	125.0	17.0	16.0	4.5	0.21	N123H2-0400-0004-TF
	16 x 16	25.0	47.0	R/LF123H25-1616B	16.0	16.0	125.0	17.0	16.0	7.0	0.26	N123H2-0400-0004-TF
	20 x 20	13.0	34.0	R/LF123H13-2020BM	20.0	20.0	125.0	21.0	20.0	4.5	0.41	N123H2-0400-0004-TF
	20 x 20	25.0	47.0	R/LF123H25-2020BM	20.0	20.0	125.0	21.0	20.0	7.0	0.40	N123H2-0400-0004-TF
	25 x 25	13.0	34.0	R/LF123H13-2525BM	25.0	25.0	150.0	26.0	25.0	4.5	0.73	N123H2-0400-0004-TF
	25 x 25	25.0	47.0	R/LF123H25-2525BM	25.0	25.0	150.0	26.0	25.0	7.0	0.68	N123H2-0400-0004-TF
	32 x 25	13.0	34.0	R/LF123H13-3225BM	25.0	32.0	170.0	26.0	32.0	4.5	1.05	N123H2-0400-0004-TF
	32 x 25	25.0	47.0	R/LF123H25-3225BM	25.0	32.0	170.0	26.0	32.0	7.0	0.97	N123H2-0400-0004-TF
	32 x 32	13.0	34.0	R/LF123H13-3232BM	32.0	32.0	170.0	33.0	32.0	4.5	1.31	N123H2-0400-0004-TF
	32 x 32	25.0	47.0	R/LF123H25-3232BM	32.0	32.0	170.0	33.0	32.0	7.0	1.22	N123H2-0400-0004-TF

SSC = To correspond with SSC on insert. R = Right hand, L = Left hand

Figure 6.27 Shank type toolholder for grooving operation (Sandvik, 2017a)

5: Insert seat size

6: Machining limitations (Maximum cutting depth)

7: Blade dimension

8: Clamping system

9: Number of insert seats

Number of insert seats should be determined first while selecting the suitable blade. Single ended blades are generally preferred for larger parting diameters. They are thicker in order to provide stiffness for large diameter parting. On the other hand, double ended blades are preferred for productivity. Double ended blades with **2** insert seats are selected since they are more commercially available and maximum parting diameter of this study falls within the range of double ended blades.

Seat size which should correspond to seat size of the insert is the starting item for blade selection. In Section 6.8.3.2 Insert Selection, insert seat size is selected as **G**.

Maximum cutting depth is selected according to the maximum parting diameter of the designed part. Maximum parting diameter is limited to 60 mm in Part and Feature Geometry under Section 6.8.3.1 Selection Criteria. Therefore, maximum cutting depth should be bigger than or equal to half of the maximum parting diameter. Once the seat size is decided, only two alternatives remain for cutting depth in Sandvik Turning Tools catalogue (2017a): 30 and 55 mm. Since 55 mm will create excessive overhang, **30** is selected for the maximum cutting depth.

Hand of tool is selected based on the manufacturing operation requirements. For Corocut 1-2 family, double ended blades are Neutral and single ended blades are either Right or Left. Since double ended blades are selected, **N** type toolholder will be used.

Blade dimension is automatically determined according to the selected specifications of the blade. Based on seat size and maximum cutting depth blade dimension is specified as **21**. Blade dimension and shank width/height of the CNC lathe turret sets the specifications of the tool block for blades. Tool block is a connector used for attaching the blade to the turret.

Clamping system is **A** which is typical for parting blades. A type represents spring clamping which enables quick insert change.

Based on the codes above, blade is selected as **N123G30-21A2** for grooving operations. Selected holder is shown in Figure 6.28 (Sandvik, 2017a), as well.

CoroCut® 1-2 blade for parting

Spring lock design

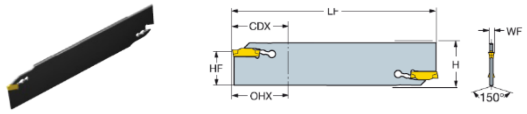

Double ended parting blade

	SSC	CZC_{MS}	CDX	OHX	Ordering code	H	LF	WF	HF	KG	MIID
						Dimensions, mm					
	F	21	30.0	30.0	N123F30-21A2	25.9	110.0	2.3	21.4	0.05	N123F2-0250-0002-CM
		25	55.0	55.0	N123F55-25A2	31.9	150.0	2.3	25.0	0.09	N123F2-0250-0002-CM
	G	21	30.0	30.0	N123G30-21A2	25.9	110.0	2.7	21.4	0.06	N123G2-0300-0003-TF
		25	55.0	55.0	N123G55-25A2	31.9	150.0	2.3	25.0	0.10	N123G2-0300-0003-TF
	H	25	55.0	55.0	N123H55-25A2	31.9	150.0	3.7	25.0	0.13	N123H2-0400-0004-TF
	J	25	55.0	55.0	N123J55-25A2	31.9	150.0	4.8	25.0	0.16	N123J2-0500-0002-CM
	K	25	55.0	55.0	N123K55-25A2	31.9	150.0	5.8	25.0	0.18	N123K2-0600-0004-CR

Figure 6.28 Blade for parting operation (Sandvik, 2017a)

6.8.4 Parameter Selection for Grooving and Parting Operations

In grooving and parting operations, the productivity is determined by the cutting parameters, which include feed (a_f) and cutting speed (V_c). The depth of cut (a_p) for these operations is defined by the insert width. The selection of these parameters is explained in the following sections.

6.8.4.1 Feed (a_f)

Insert geometry and insert width sets the range for feed values to have proper chip breaking (Sandvik, 2017a). For this study, both grooving and parting operations require radial feed only (See 6.8.3.1 Selection Criteria). However, some geometries can be used for turning or profiling which require axial feed, as well. For those inserts, geometry and insert width sets the range of radial feed, axial feed and depth of cut. Since for this section, operations are limited to grooving and parting, axial feeds and depth of cut values are irrelevant.

Recommended a_f values for the selected insert geometries are presented in Figure 6.29 (Sandvik, 2017a).

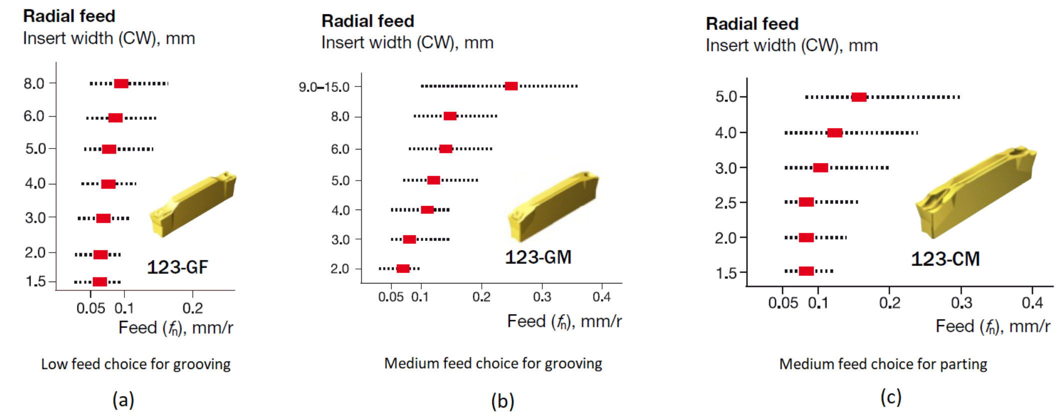

Figure 6.29 Feed recommendations for grooving and parting (Sandvik, 2017a)

There is not a finishing cycle for grooving operation as stated in Section 6.8.3.1 Selection Criteria. Therefore in order to obtain the best surface quality with the roughing cut, smallest possible feed values will be selected. All of the specified inserts for grooving and parting have a width value of 3 mm. For the selected geometries **GF, GM and CM, 0.05, 0.06 and 0.09 mm/rev** radial feed values are determined respectively based on Figure 6.29. Feed values and the corresponding inserts are presented in Table 6.8 for grooving and in Table 6.9 for parting operations.

Table 6.8 Selected feed values for grooving operations

Material	**Insert**	**Toolholder**	**a_f (mm/rev)**
P3	N123G2-0300-0002-GF-GC1125	RF123G20-2020B	0.05
K13	N123G2-0300-0003-GM-GC1125	RF123G20-2020B	0.06
N16	N123G2-0300-0002-GF-GC1125	RF123G20-2020B	0.05

Table 6.9 Selected feed values for parting operations

Material	Insert	Toolholder	a_f (mm/rev)
P3	N123G2-0300-0002-CM-GC1125	N123G30-21A2	0.09
K13	N123G2-0300-0002-CM-GC1125	N123G30-21A2	0.09
N16	N123G2-0300-0002-CM-GC1125	N123G30-21A2	0.09

6.8.4.2 Cutting Speed (V_c)

Cutting speed depends on the material, grade and selected feed values. Recommended ranges for cutting speed are shown in Figure 6.30 (Sandvik, 2017a). A comparison with the speed recommendations of other tool manufacturers (Seco, 2012 and Iscar 2017a) for the same operations reveals that the speed ranges given in Figure 6.30 are above average. In order to comply with the industry averages, lower limit of each range is used. Selected speeds are presented in Table 6.10 for grooving and in Table 6.11 for parting operations.

Table 6.10 Selected cutting speed values for grooving operations

Material	Insert	Toolholder	V_c (m/min)
P3	N123G2-0300-0002-GF-GC1125	RF123G20-2020B	115
K13	N123G2-0300-0003-GM-GC1125	RF123G20-2020B	90
N16	N123G2-0300-0002-GF-GC1125	RF123G20-2020B	190

PARTING AND GROOVING Cutting data

Cutting speed recommendations

The recommendations are valid for use with cutting fluid.

ISO P MC No.	CMC No.	Steel Material	Specific cutting force k_{c1} N/mm²	Hardness Brinell HB	GC1115 0.05-0.5	GC1125 0.05-0.5	GC1025 0.05-0.5
		Unalloyed					
P1.1.Z.AN	01.1	C = 0.1–0.25%	1500	125	360-180	295-145	235-115
P1.2.Z.AN	01.2	C = 0.25–0.55%	1600	150	325-145	265-115	210-90
P1.3.Z.AN	01.3	C = 0.55–0.80%	1700	170	290-130	235-105	185-85

ISO K MC No.	CMC No.	Cast iron Material	Specific cutting force k_{c1} N/mm²	Hardness Brinell HB	GC1125 0.05-0.5	GC1025 0.05-0.5	H13A 0.05-0.5
		Malleable					
	07.1	Ferritic (short chipping)	790	130	255-125	205-100	100-85
K1.1.C.NS	07.2	Pearlitic (long chipping)	900	230	170-95	140-75	70-55
		Grey					
K2.1.C.UT	08.1	Low tensile strength	890	180	210-110	170-85	80-65
K2.2.C.UT	08.2	High tensile strength	970	220	175-90	140-70	80-60

ISO N MC No.	CMC No.	Non-ferrous material Material	Specific cutting force k_{c1} N/mm²	Hardness Brinell HB	GC1125 0.05-0.8	GC1025 0.05-0.8	H13A 0.05-0.8
		Aluminium alloys					
N1.2.Z.UT	30.11	Wrought or wrought and coldworked, non-aging	400	60	1500 (1900 - 190)	1500 (1900 - 190)	1500 (1900 - 190)
N1.2.Z.AG	30.12		650	100	1500 (1900 - 190)	1500 (1900 - 190)	1500 (1900 - 190)

Figure 6.30 Cutting speed recommendations:Parting/grooving (Sandvik, 2017a)

Table 6.11 Selected cutting speed values for parting operations

Material	Insert	Toolholder	V_c (m/min)
P3	N123G2-0300-0002-CM-GC1125	N123G30-21A2	115
K13	N123G2-0300-0002-CM-GC1125	N123G30-21A2	90
N16	N123G2-0300-0002-CM-GC1125	N123G30-21A2	190

6.8.4.3 Spindle Speed (n) and Feed Rate (V_f)

Spindle speed (n) is calculated by the following equation for grooving and parting operations:

$$n = \frac{1000\, V_c}{\pi\, D} \tag{6.7}$$

where D is the diameter of the corresponding feature on which the groove is generated for grooving operation and stock diameter for parting operation.

Feed rate (V_f) is found by:

$$V_f = a_f\, n \tag{6.8}$$

6.8.5 Tool Selection for Drilling

In the tool selection process for drilling operations, the assumptions and limitations related to material, part geometry and cutting conditions are first introduced in Section 6.8.5.1 Selection Criteria. The drill parameters are subsequently provided in Section 6.8.5.2 Drill Selection based on the code defined in Sandvik Solid Round Tools Catalogue (Sandvik, 2017d).

6.8.5.1 Selection Criteria

Material: Tools will be selected based on three material groups based on SECO tool catalogues (Seco, 2023):

- P3: Low alloy general structural steels, 0.25% < C < 0.67%wt
- K13: Low alloy cast iron. Malleable cast iron. Nodular cast iron.
- N16: Aluminum alloys, Si < 9%

Feature Geometry: Hole diameters and hole depths involve the following assumptions in order to decrease the programming effort:

- Hole diameters are limited to 6, 8, 10 and 12 mm.
- Hole length to hole diameter ratio is assumed to be smaller than 5 times the diameter value: Hole depth < 5 x Hole Diameter

Operations and Cutting Conditions: For drilling, if the hole length is less than 5 times the diameter, standard drilling is used. Otherwise, peck drilling is employed. Additionally, center drilling is applied when the hole diameter is greater than 8.

Brand: Drill selection will be based on Sandvik Coromant Solid Round Tools Catalogue (2017d). Solid carbide center drills are not available in Sandvik Catalogue. Therefore, a commercially available HSS center drill is selected based on data from CNC Programming Handbook (Smid, 2008).

6.8.5.2 Drill Selection

The first step of drill selection is determining the product family. Based on Figure 6.31, solid carbide or indexable inserts should be preferred considering the material groups (P, K and N) given in Section 6.8.5.1 Selection Criteria.

ISO material group		P	M	K	N	S	H
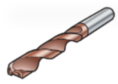	Solid carbide drills	•••	•••	•••	•••	•••	•••
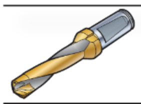	Exchangeable tip drills	•••	•••	•••	•	•	•
	Indexable insert drills	•••	•••	•••	•••	•••	•••

Figure 6.31 Drills families based on ISO material groups (Sandvik, 2017b)

Figure 6.32 shows the diameter ranges for different product families. The largest hole has a diameter value of 12 mm and since all the drills should support 5xD, solid carbide drills is the best option for this study.

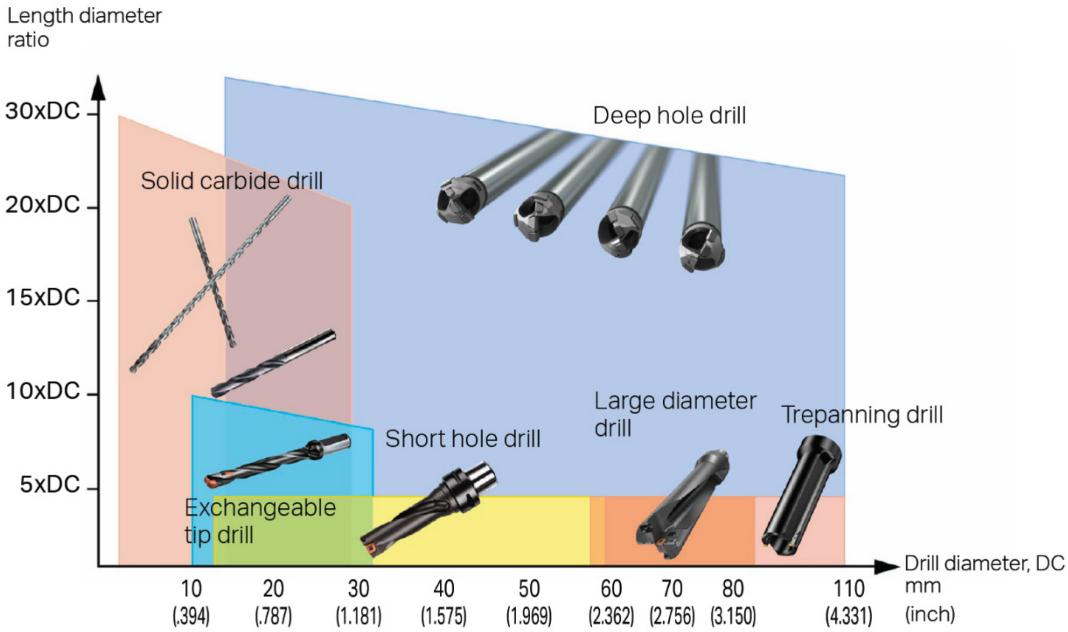

Figure 6.32 Drill families based on diameter ranges (Sandvik, 2017b)

	R840	R841	861-GP	861-GM	862-GM	854	856	863	452
Drill type	Solid carbide drill	Solid carbide drill	Pilot drill	Solid carbide drill for deep holes	Solid carbide drill for micro holes	Solid carbide drill	Solid carbide drill	Solid carbide drill	Drill for hand-held applications
DC mm	0.30-20.00	3.35-17.50	3.00-12.00	3.00-20.00	1.85-2.95	4.00-12.70	4.00-12.70	4.83-11.14	2.50-12.70
DC inch	.012-.787	.132-.689	.118-.472	.118-.787	.073-.116	.157-.500	.157-.500	.190-.439	.098-.50
ISO application area	P N M S K H	P N M S K H	P N M K	P N M K	P N M S K	O	O	M O N S	P S K O N
ULDR	2-7 x DC	2-3 x DC	3 x DC	12-30 x DC	8-12 x DC	4-5 x DC	5 x DC	3-18 x DC	4-20 x DC

Figure 6.33 Product groups for solid carbide drills (Sandvik, 2017d)

There are different product groups under solid carbide drills. The most suitable group is determined based on feature geometry and material. **R840** which is the first choice for all materials will be used. R840 is also suitable for 5D hole depths as given in Figure 6.33.

R840 solid carbide drills are specified based on the code defined in Sandvik Solid Round Tools Catalogue (Sandvik, 2017d). A sample code is presented here for an example (Figure 6.34):

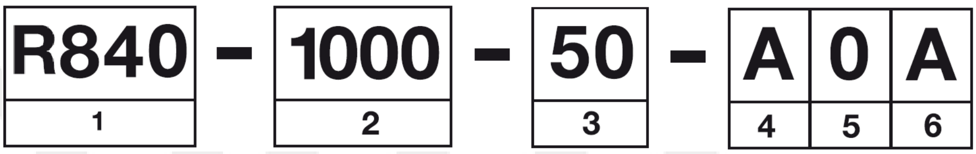

Figure 6.34 Sample code for R840 solid carbide drill (Sandvik, 2017d)

where:
1: Product family
2: Cutting diameter
3: Length/Diameter ratio
4: Shank type
5: Coolant

In order to select the relevant drills under R840 family, **coolant** and **shank type** should be determined first. According to Sandvik Training Handbook (2017b), internal coolant should always be used at hole depths above 3 times the diameter. Since it is stated that 5xD drills will be used in Section 6.8.5.1 Selection Criteria, drills with **internal coolant (1)** will be selected. Shank type is determined by the toolholder on the CNC lathe. For this study shank type is selected as **cylindrical (A)** which is based on Anatool TP 32 CNC lathe. Cylindrical shanks are commonly preferred to whistle notch shanks on other CNC lathes, as well.

After selecting the codes above, drill alternatives are narrowed down to one for each diameter value. **Grades** for all drills are the same and determined automatically as **1220**.

Solid carbide center drills are not available in Sandvik Catalogue. Therefore, a commercially available HSS center drill is selected based on data from CNC Programming Handbook (Smid, 2008).

Selected HSS drill is shown in Figure 6.35 (Smid, 2008), solid drills are shown in Figure 6.36 (Sandvik, 2017a) and summarized in Table 6.12.

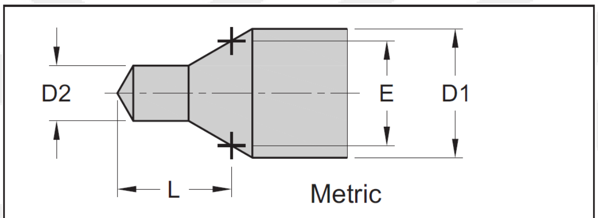

Number	D1	D2	E	L
# 1	3.175	1.194	2.600	2.700
# 2	4.775	1.981	3.800	4.100
# 3	6.350	2.794	5.100	5.600
# 4	7.925	3.175	6.400	6.800
# 5	11.125	4.775	8.900	9.700
# 6	12.700	5.537	10.200	11.000
# 7	15.875	6.350	12.700	13.700
# 8	19.050	7.925	15.200	16.500

Figure 6.35 Selected HSS center drill (Smid, 2008)

Table 6.12 Selected R840 solid carbide drills

Drill Diameter (mm)	**Drill Code**
Ø6	R840-0600-50-A1A
Ø8	R840-0800-50-A1A
Ø10	R840-1000-50-A1A
Ø12	R840-1200-50-A1A

CoroDrill® R840 solid carbide drills

HA shank

Internal coolant supply

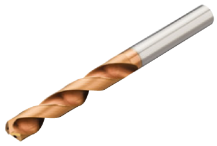

TCHA H9
CNSC 4

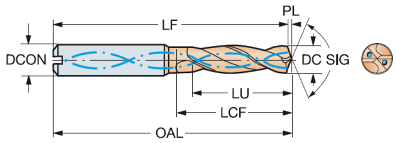

Dimensions, mm, inch

DC	DC"	LU	LU"	ULDR	CZC_{MS}	Ordering code	P 1220	M 1220	K 1220	N 1220	S 1220	H 1220	DCON	DCON"	OAL	OAL"	LF	LF"	LCF	LCF"	PL	PL"	SIG	CP Bar	Kg	BSG
5.90	.232	17.4	.685	2	6	R840-0590-30-A1A	☆	☆	☆	☆	☆	☆	6.00	.236	66	2.598	65.0	2.559	28	1.102	1.0	.039	140°	20	0.030	DIN 6537 K
5.90	.232	30.5	1.201	5	6	R840-0590-50-A1A	☆	☆	☆	☆	☆	☆	6.00	.236	82	3.228	81.0	3.189	44	1.732	1.0	.039	140°	20	0.036	DIN 6537 L
5.90	.232	39.4	1.551	6	6	R840-0590-70-A1A	☆	☆	☆	☆	☆	☆	6.00	.236	93	3.661	92.0	3.622	50	1.969	1.0	.039	140°	20	0.040	COROMANT
5.95	.234	17.3	.681	2	6	R840-0595-30-A1A	☆	☆	☆	☆	☆	☆	6.00	.236	66	2.598	65.0	2.559	28	1.102	1.0	.039	140°	20	0.040	DIN 6537 K
5.95	.234	30.8	1.213	5	6	R840-0595-50-A1A	☆	☆	☆	☆	☆	☆	6.00	.236	82	3.228	81.0	3.189	44	1.732	1.0	.039	140°	20	0.030	DIN 6537 L
5.95	.234	39.3	1.547	6	6	R840-0595-70-A1A	☆	☆	☆	☆	☆	☆	6.00	.236	93	3.661	92.0	3.622	50	1.969	1.0	.039	140°	20	0.041	COROMANT
6.00	.236	19.0	.748	3	6	R840-0600-30-A1A	☆	☆	☆	☆	☆	☆	6.00	.236	66	2.598	65.0	2.559	28	1.102	1.0	.039	140°	20	0.040	DIN 6537 K
6.00	.236	31.0	1.220	5	6	R840-0600-50-A1A	☆	☆	☆	☆	☆	☆	6.00	.236	82	3.228	81.0	3.189	44	1.732	1.0	.039	140°	20	0.040	DIN 6537 L
6.00	.236	41.0	1.614	6	6	R840-0600-70-A1A	☆	☆	☆	☆	☆	☆	6.00	.236	93	3.661	92.0	3.622	50	1.969	1.0	.039	140°	20	0.041	COROMANT
6.10	.240	19.3	.760	3	8	R840-0610-30-A1A	☆	☆	☆	☆	☆	☆	8.00	.315	79	3.110	78.0	3.071	34	1.339	1.0	.039	140°	20	0.064	DIN 6537 K
7.94	.313	56.7	2.232	7	8	R840-0794-70-A1A	☆	☆	☆	☆	☆	☆	8.00	.315	105	4.134	103.6	4.079	67	2.638	1.4	.055	140°	20	0.076	COROMANT
8.00	.315	25.4	1.000	3	8	R840-0800-30-A1A	☆	☆	☆	☆	☆	☆	8.00	.315	79	3.110	77.6	3.055	41	1.614	1.4	.055	140°	20	0.076	DIN 6537 K
8.00	.315	41.4	1.630	5	8	R840-0800-50-A1A	☆	☆	☆	☆	☆	☆	8.00	.315	91	3.583	89.6	3.528	53	2.087	1.4	.055	140°	20	0.065	DIN 6537 L
8.00	.315	56.6	2.228	7	8	R840-0800-70-A1A	☆	☆	☆	☆	☆	☆	8.00	.315	105	4.134	103.6	4.079	67	2.638	1.4	.055	140°	20	0.066	COROMANT
8.10	.319	25.7	1.012	3	10	R840-0810-30-A1A	☆	☆	☆	☆	☆	☆	10.00	.394	89	3.504	87.6	3.449	47	1.850	1.4	.055	140°	20	0.066	DIN 6537 K
9.92	.391	71.1	2.799	7	10	R840-0992-70-A1A	☆	☆	☆	☆	☆	☆	10.00	.394	133	5.236	131.3	5.169	84	3.307	1.7	.067	140°	20	0.120	COROMANT
10.00	.394	31.7	1.248	3	10	R840-1000-30-A1A	☆	☆	☆	☆	☆	☆	10.00	.394	89	3.504	87.3	3.437	47	1.850	1.7	.067	140°	20	0.070	DIN 6537 K
10.00	.394	48.0	1.890	4	10	R840-1000-50-A1A	☆	☆	☆	☆	☆	☆	10.00	.394	103	4.055	101.3	3.988	61	2.402	1.7	.067	140°	20	0.180	DIN 6537 L
10.00	.394	71.0	2.795	7	10	R840-1000-70-A1A	☆	☆	☆	☆	☆	☆	10.00	.394	133	5.236	131.3	5.169	84	3.307	1.7	.067	140°	20	0.120	COROMANT
10.10	.398	32.0	1.260	3	12	R840-1010-30-A1A	☆	☆	☆	☆	☆	☆	12.00	.472	102	4.016	100.3	3.949	55	2.165	1.7	.067	140°	20	0.120	DIN 6537 K
11.90	.469	85.3	3.358	7	12	R840-1190-70-A1A	☆	☆	☆	☆	☆	☆	12.00	.472	151	5.945	149.0	5.866	101	3.976	2.0	.079	140°	20	0.150	COROMANT
12.00	.472	38.1	1.500	3	12	R840-1200-30-A1A	☆	☆	☆	☆	☆	☆	12.00	.472	102	4.016	99.9	3.933	55	2.165	2.1	.083	140°	20	0.150	DIN 6537 K
12.00	.472	56.6	2.228	4	12	R840-1200-50-A1A	☆	☆	☆	☆	☆	☆	12.00	.472	118	4.646	115.9	4.563	71	2.795	2.1	.083	140°	20	0.119	DIN 6537 L
12.00	.472	86.1	3.390	7	12	R840-1200-70-A1A	☆	☆	☆	☆	☆	☆	12.00	.472	151	5.945	148.9	5.862	101	3.976	2.1	.083	140°	20	0.190	COROMANT
12.10	.476	38.4	1.512	3	14	R840-1210-30-A1A	☆	☆	☆	☆	☆	☆	14.00	.551	107	4.213	104.9	4.130	60	2.362	2.1	.083	140°	20	0.149	DIN 6537 K

Figure 6.36 Selected R840 solid carbide drills (Sandvik, 2017a)

6.8.6 Parameter Selection for Drilling

Feed (a_f) and cutting speed (V_c) are main cutting parameters for estimating the drilling time. The depth of cut (a_p) of drilling operation is equal to the drill diameter. Selection method of these two parameters are shown in the next sections.

6.8.6.1 Feed (a_f)

Feed range is determined based on the material, grade and drill diameter. Feed recommendations increase with increasing diameter value. Since grade is the same for R840 solid carbide product family, it does not have an effect on the selected feed.

Unlike turning and grooving operations, for drilling feed value is twice the feed engagement (or feed per tooth, a_f). Recommendations in Sandvik Catalogue (2017d) are feed values (mm/revolution) and they are used directly because the input for the study is mm/revolution, as well.

Recommended ranges for feed are shown in Figure 6.37 (Sandvik, 2017d). A comparison with the feed recommendations of other tool manufacturers (Seco, 2015 and Iscar 2017b) for the same drill diameters reveals that the feed values given in Figure 6.37 are above average. In order to comply with the industry averages, some of the selected values are taken from Seco Holemaking catalogue (2015). Selected feeds are presented in Table 6.13.

CoroDrill® R840, R841 and R846 for drill diameters 3-20 mm

ISO	CMC No.	Material	Hardness Brinell HB	Grades	Cutting speed (v_c), m/min	Drill diameter, mm 3.00–6.00	6.01–10.00	10.01–14.00	14.01–20.00
						Feed f_n mm/r 3)			
P		Unalloyed steel							
	01.0	C = 0.05–0.10 %	125	1220	80-140	0.10-0.25	0.15-0.34	0.20-0.40	0.22-0.45
	01.1	C = 0.1–0.25%	125	1220	80-140	0.10-0.25	0.15-0.34	0.20-0.40	0.22-0.45
	01.2	C = 0.25–0.55%	150	1220	80-140	0.10-0.25	0.15-0.34	0.20-0.40	0.22-0.45
	01.3	C = 0.55–0.80%	170	1220	70-130	0.10-0.25	0.15-0.34	0.20-0.40	0.22-0.45
K		**Malleable cast iron**							
	07.1	Ferritic (short chipping)	130	1220	90-150	0.15-0.30	0.25-0.40	0.35-0.60	0.40-0.60
				1210	100-160	0.15-0.30	0.25-0.40	0.35-0.60	0.40-0.60
	07.2	Pearlitic (long chipping)	230	1220	70-130	0.15-0.25	0.20-0.35	0.30-0.55	0.35-0.55
				1210	100-150	0.15-0.25	0.20-0.35	0.30-0.55	0.35-0.55
		Grey cast iron							
	08.1	Low tensile strength	180	1220	90-150	0.15-0.30	0.25-0.40	0.35-0.60	0.40-0.60
				1210	140-200	0.15-0.30	0.25-0.40	0.35-0.60	0.40-0.60
	08.2	High tensile strength	260	1220	70-130	0.15-0.25	0.20-0.35	0.30-0.55	0.35-0.55
				1210	100-140	0.15-0.25	0.20-0.35	0.30-0.55	0.35-0.55
		Nodular cast iron, SG iron							
	09.1	Ferritic	160	1220	80-110	0.15-0.30	0.25-0.40	0.35-0.60	0.40-0.60
				1210	110-150	0.15-0.30	0.25-0.40	0.35-0.60	0.40-0.60
	09.2	Pearlitic	250	1220	70-100	0.15-0.25	0.20-0.35	0.30-0.55	0.35-0.55
				1210	100-140	0.15-0.25	0.20-0.35	0.30-0.55	0.35-0.55
	CGI			1210	90-130	0.15-0.30	0.20-0.40	0.30-0.60	0.35-0.60
N		**Aluminium alloys**							
	30.11	Wrought or wrought and coldworked, non-aging	60	N20D	120-230	0.15-0.25	0.20-0.40	0.30-0.50	0.40-0.60
	30.21	Cast, non-aging	75	N20D	120-230	0.15-0.25	0.20-0.40	0.30-0.50	0.40-0.60
		Copper and copper alloys							
	33.1	Free cutting alloys, ≥1% Pb	110	N20D	90-150	0.15-0.25	0.20-0.40	0.30-0.50	0.40-0.60
	33.2	Brass, leaded bronzes, ≤1% Pb	90	N20D	90-150	0.15-0.25	0.20-0.40	0.30-0.50	0.40-0.60

Figure 6.37 Feed and cutting speed recommendations: R840 solid carbide drills

HSS center drill is selected from CNC Programming Handbook (Smid, 2008) in Figure 6.35. Feeds are based on the values for Ø3 mm drill in Figure 6.37. Since those values are for solid carbide drills, 20% reduction is done to suit an HSS drill. Therefore feed values for **P3, K13, N16** material groups are **0.08**, **0.12** and **0.12** mm/rev respectively.

Table 6.13 Selected feed values (mm/rev) for drilling

Diameter (mm)	**Drill Code**	**Feed for P3**	**Feed for K13**	**Feed for N16**
Ø6	R840-0600-50-A1A	0.17	0.18	0.22
Ø8	R840-0800-50-A1A	0.20	0.22	0.28
Ø10	R840-1000-50-A1A	0.24	0.26	0.32
Ø12	R840-1200-50-A1A	0.26	0.28	0.38

6.8.6.2 Cutting Speed (V_c)

Cutting speed depends on the material and grade. Since grade is the same for R840 solid carbide product family, it does not have an effect on the selected speed. Recommended speed ranges are shown in Figure 6.37 for different material groups. Even if drills with internal coolant are selected in Section 6.8.5.2 Drill Selection, in order to make the values more generic and add allowance for external coolant as well, lowest values are selected in the range. Speed values are summarized in Table 6.14.

Table 6.14 Selected cutting speed values for drilling operations

Material	**V_c (m/min)**
P3	80
K13	70
N16	120

HSS center drill is selected from CNC Programming Handbook (Smid, 2008) in Figure 6.35. Cutting speeds are based on the lowest limit of recommendation range of the handbook presented in Figure 6.38.

Metric - m/min	Drilling		Tapping	Milling - Rough		Milling - Finish		Turning	
Material	HSS	Carbide	HSS	HSS	Carbide	HSS	Carbide	Carbide Rough	Carbide Finish
Aluminum	55 60	90 - 115	25 - 35	60 - 90	135 - 180	75 - 105	120 - 240	120 - 240	150 - 270
Brass - Soft	40 - 45	75 - 100	20 - 30	45 - 60	60 - 75	60 - 90	90 - 210	105 - 210	135 - 260
Cast Iron - Medium	12 18	35 - 45	8 - 15	15 - 25	55 - 75	25 - 30	60 - 90	60 - 90	75 - 135
Steel - Mild	10 15	18 - 27	10 - 20	18 - 30	45 - 60	23 - 40	75 - 105	75 - 105	100 - 145
Stainless Steel (Free machining)	8 - 18	25 - 37	5 - 10	10 - 15	55 - 67	12 - 25	60 - 100	75 - 120	85 - 150

Figure 6.38 Selected cutting speed values for center drilling (Smid, 2008)

6.8.6.3 Spindle Speed (n) and Feed Rate (V_f)

Spindle speed (n) is calculated by the following equation for drilling operations:

$$n = \frac{1000\, V_c}{\pi\, D_{drill}} \tag{6.9}$$

Feed rate (V_f) is found by:

$$V_f = 2\, a_f\, n \tag{6.10}$$

6.9 Sample Code

Following code (Table 6.15) is taken from the process planning module of TurnDesign Eco Edition. It shows the tool and cutting parameter input for N16 (Aluminum alloys) material group for rough turning and grooving operations:

Table 6.15 Code for process planning module

```
'TURNING ROUGH-----------------------------------------------------------
op_name(2) = "Turning - Rough"
nc_tool(2) = "T01"
holder(2) = "SDJCR 2020K 11"
tool(2) = "DCGX 11 T3 08-AL-H10"

v_c(2) = 225
a_f(2) = 0.3
a_p(2) = 2
n(2) = CInt(1000 * v_c(2) / Pi / Dstock_current / 10) * 10 'round to
nearest 10
If n(2) > n_max Then n(2) = n_max
v_f(2) = a_f(2) * n(2)

gamma_n(2) = 0
kappa_r(2) = 93
kappa_rp(2) = 32
lambda_s(2) = 0
alpha_n(2) = 7

ps1(2) = 800 / 1000
mc(2) = 0.25
ps(2) = (1 - 0.01 * gamma_n(2)) * ps1(2) / (a_f(2) * Sin(kappa_r(2) *
measure.angle_convertion_factor)) ^ mc(2)

'GROOVING----------------------------------------------------------------
If grooving_present = 1 Then
op_name(19) = "Grooving"
nc_tool(19) = "T19"
holder(19) = "RF123G20-2020B"
tool(19) = "N123G2-0300-0002-GF-GC1125"

v_c(19) = 190
a_f(19) = 0.05
a_p(19) = 3
n(19) = CInt(1000 * v_c(19) / Pi / points_SQRUGRV_R(1, 1) / 10) * 10
'round to nearest 10
If n(19) > n_max Then n(19) = n_max
v_f(19) = a_f(19) * n(19)

gamma_n(19) = 0
kappa_r(19) = 90
kappa_rp(19) = 0
lambda_s(19) = 0
alpha_n(19) = 7

ps1(19) = 800 / 1000
mc(19) = 0.25
ps(19) = (1 - 0.01 * gamma_n(19)) * ps1(19) / (a_f(19) * Sin(kappa_r(19)
* measure.angle_convertion_factor)) ^ mc(19)
End If
```

For each operation first part of the code is allocated for the operation name, tool number and tool name. For example, holder(2) and tool(2) parameters for the rough turning operation are the toolholder and the insert selected in Sections 6.8.1.3 Toolholder Selection and 6.8.1.2 Insert Selection.

Second part of the code inputs the cutting parameters. Rotational speed (n) and feed speed (V_f) are calculated based on those parameters. v_c(2), a_f(2) and a_p(2) for rough turning are taken from Section 6.8.2 Parameter Selection for Outer Turning Operations.

Third part of the code includes the tool angles. For rough turning those angles were presented in Table 6.2 for the selected toolholder. These angles are mainly used for the specific energy (p_s) calculation in the fourth part. Material constants (p_{s1} and mc) taken from SECO tool catalogue (Seco, 2023) are given in the fourth part as well. Those are the remaining two inputs for the specific cutting energy calculation. Specific cutting energy will be the input for Theoretical Energy Estimation (Section 8.2) module.

6.10 Output

The output of the process planning module of TurnDesign Eco Edition software is a Manufacturing Process Sheet (MPS). The MPS presents the operations, their sequence, machined features, tool specifications and cutting parameters for a given operation. A sample MPS for the first specimen: SP1-AL6013 is given in Figure 6.39.

METU DEPARTMENT OF MECHANICAL ENGINEERING	Part Name / No:	Part Name	Machine Tool:	Anatool TP32 CNC Lathe (3500 rpm max)
	By:	Ural Uluer	Stock Dimensions:	D_stock=30 mm L_stock=73.5 mm
	Date:	23.06.2024 / 00:04	Material:	Non-Ferrous Metal N16

Op No.	Operation Name	Features	Tool (Holder / Insert)	af (mm)	ap (mm)	Cutting Speed (m/min)	Speed (rpm)	Feed (mm/rev)	Feed Rate (mm/min)
1	Facing	-	SDJCR 2020K 11 / DCGX 11 T3 08-AL-H10	0.15	0.5	250	**2650**	0.15	**398**
2	Turning - Rough	OD1 FILLET1 OD3 OD4	SDJCR 2020K 11 / DCGX 11 T3 08-AL-H10	0.3	2	225	**2390**	0.3	**717**
3	Turning - Finish	OD1 FILLET1 OD3 OD4	SDJCR 2020K 11 / DCGX 11 T3 08-AL-H10	0.15	1	250	**2650**	0.15	**398**
4	Drilling	RNDHOL1	R840-0800-50-A1A	0.14	8	120	**3500**	0.28	**980**
5	Grooving	SQRUGRV1	RF123G20-2020B / N123G2-0300-0002-GF-GC1125	0.05	3	190	**2160**	0.05	**108**
6	Parting	-	N123G30-21A2 / N123G2-0300-0002-CM-GC1125	0.09	3	190	**2020**	0.09	**182**
TURNDESIGN ECO EDITION									

Figure 6.39 Manufacturing Process Sheet for SP1-AL6013

CHAPTER 7

PART PROGRAMMING

7.1 Introduction

The Part Programming module is responsible for generating the NC code (or part program) for the designed part. A part program involves two fundamental components: toolpaths and cutting parameters for each manufacturing operation. Toolpaths are generated based on point matrices established in the Geometry Extraction module. Cutting parameters necessary for the part program are obtained from Process Planning module which are all reported on a Manufacturing Process Sheet (MPS) as an output. Figure 7.1 illustrates the input and output structure of the Part Programming module.

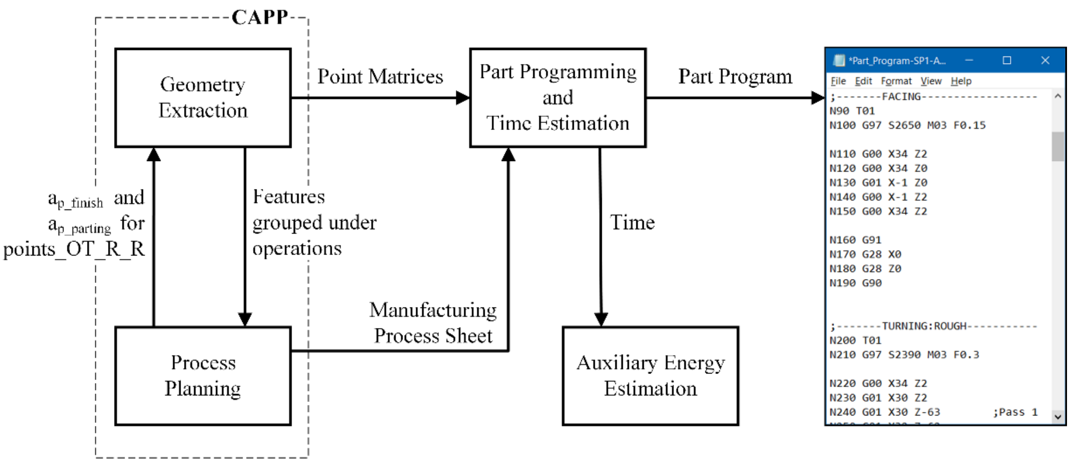

Figure 7.1 Part Programming Module: Inputs and Outputs

Besides NC code generation, part programming estimates the total machining time for the designed part along with the usage times for each component of the CNC lathe. This is achieved by calculating the incremental time required for the programmed movement in each block and adding up to the total cutting time or equipment usage time. The time data serves as input for the auxiliary energy estimation module.

Part programming is divided into submodules, each dedicated to a specific manufacturing operation. Coding for operations requiring multiple passes are based on multiple repetitive cycles outlined in Table 7.1. In the following section, toolpath generation of each manufacturing operation is presented after explaining the general structure of the part program.

Table 7.1 Emulated Lathe Cycles

Operation	**Lathe Cycle**
Outer Turning - Rough	G71 - Stock Removal Cycle
Outer Turning - Finish	G70 - Contour Finishing Cycle
Drilling with Pecking	G83 - Deep Hole Drilling Cycle (Chip Removal)
Grooving	G75 - Groove Cutting Cycle

7.2 Part Program Structure

The structure of the part program involves three key sections: the header, manufacturing operations and program termination.

The CNC lathe part program begins with essential information like the creation date, time and programmer details (Table 7.2). It includes specifications about the raw material such as stock diameter (D_stock), stock length (L_stock), CNC lathe model. Preparatory commands like G21 (Metric system), G18 (ZX plane), G95 (feed/revolution) and G40 (tool nose radius offset cancel) get the machine ready for subsequent manufacturing operations. Turret is positioned to machine zero by G28 commands and program zero is set on the right face by G54 offset. Coolant activation (M07) is included in the header section because it is assumed to be on during entire machining for all material types.

Table 7.2 Header of Part Program

Part Program: Header	**Explanation**
;DATE......................... dd.mm.yyyy ;TIME.......................... hh:mm ;PROGRAMMER....... Ural Uluer	Program information
;D_stock...................... ## mm ;L_stock...................... ## mm ;MACHINE..........TP32 CNC Lathe	Material and machine information
N10 G291	ISO mode
N20 G91 N30 G28 X0 N40 G28 Z0 N50 G90	N20-N50: Send turret to machine zero
N60 G21 G18 G95 G40	Preparatory commands
N70 M07	Coolant on
N80 G54	Work offset

Each manufacturing operation in the program follows a systematic sequence (Table 7.3). It starts by specifying the tool number (T), spindle speed (S), rotation direction (M03) and feed rate (F). Cutting parameters found in Section 6.8 Tools and Parameters are input for F and S values.

Toolpaths for material removal consistently start and end at a safe point, guaranteeing secure tool positioning. Safe point (X_{sp}, Z_{sp}) is calculated by the following equations:

$$X_{sp} = D_{stock} + safe\_allowance\_X \tag{7.1}$$

$$Z_{sp} = safe\_allowance\_Z \quad (7.2)$$

For this study, the determination of the safe point ensures that the tool maintains a 2 mm clearance in both the X and Z axes. Consequently, safe allowances of 4 mm and 2 mm are utilized for the X and Z axes, respectively.

The tool moves either rapidly (G00), linearly (G01) or by circular interpolation (G02/G03) to remove material in between safe point blocks. Prior to generating any block in between safe points, the current position of the tool is first stored as (X_{old}, Z_{old}). This position is critical for calculating the toolpath length which in turn will be used for time estimation. The target position (X_{new}, Z_{new}) is determined based on the operation and part geometry and is subsequently printed in the block with a unique line number. Detailed information about the toolpath of individual operations can be found under Section 7.3 Toolpaths for Operations.

The final segment of each operation positions the tool to the machine zero location, preparing the turret for the next tool change and operation. Sending to machine zero is done on X and Z axes separately irrespective of the manufacturing operation to avoid any tool collision.

Table 7.3 Operations in Part Program

Part Program: Operations	**Explanation**
N90 T## N100 G97 S#### M03 F#.## N110 G00 X_{sp} Z_{sp} … N150 G00 X_{sp} Z_{sp} N160 G91 N170 G28 X0 N180 G28 Z0 N190 G90	Tool number Cutting parameters Start toolpath at safe point Toolpaths for material removal Complete operation toolpath at safe point N160-N190: Send turret to mahine zero

The conclusion of the CNC lathe part program is marked by the M09 command, indicating the end of coolant flow. Subsequently, the M30 command serves as a program stop and reset, concluding the machining process and preparing the machine for new tasks (Table 7.4).

Table 7.4 Termination of Part Program

Part Program: Termination	Explanation
N1490 M09 N1500 M30	M09: Coolant off M30: Program end

7.3 Toolpaths for Operations

This section explores the toolpaths used in different turning operations, including facing, outer turning (both rough and finish), drilling, grooving and parting. Data primarily utilized in this section is derived from the point matrices generated in Chapter 5 Geometry Extraction.

7.3.1 Facing

The toolpath for facing is illustrated in Figure 7.2. Solid lines represent cutting feed (G01), while dashed lines represent rapid positioning (G00).

1: Tool moves from machine zero position to the safe point with G00.

$(X_{new}, Z_{new}) = (X_{sp}, Z_{sp})$

2: Tool moves from the safe point to the starting point for facing operation on the Z-axis with G00.

$(X_{new}, Z_{new}) = (X_{sp}, 0)$

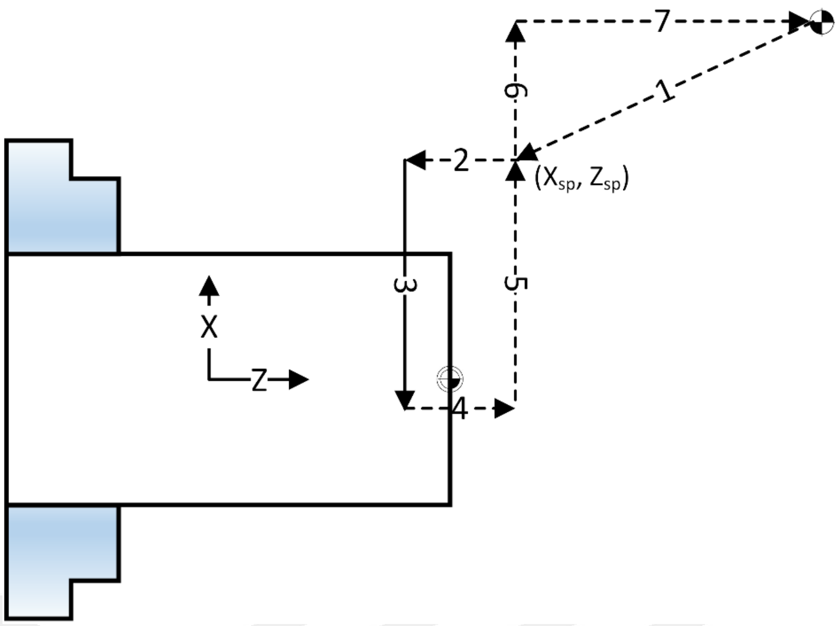

Figure 7.2 Toolpath for facing

3: Tool moves down to complete face cut with G01

$(X_{new}, Z_{new}) = (-1, 0)$

4: Tool retracts to the safe point on the Z-axis with G00

$(X_{new}, Z_{new}) = (-1, Z_{sp})$

5: Tool retracts to the safe point on the X-axis with G00

$(X_{new}, Z_{new}) = (X_{sp}, Z_{sp})$

6 and 7: Tool is sent back to machine zero first in X then in Z axis.

7.3.2 Outer Turning

Outer turning operation involves rough and finish machining. Rough machining emulates Stock Removal Cycle (G71) in two major steps. First step removes the stock for the calculated number of passes. The second step sweeps the outer profile with finish allowance added as a last pass. Finish machining emulates the Contour Finishing Cycle (G70) which removes the finishing allowance left on diameter. The toolpath for outer turning operation is presented in Figure 7.3.

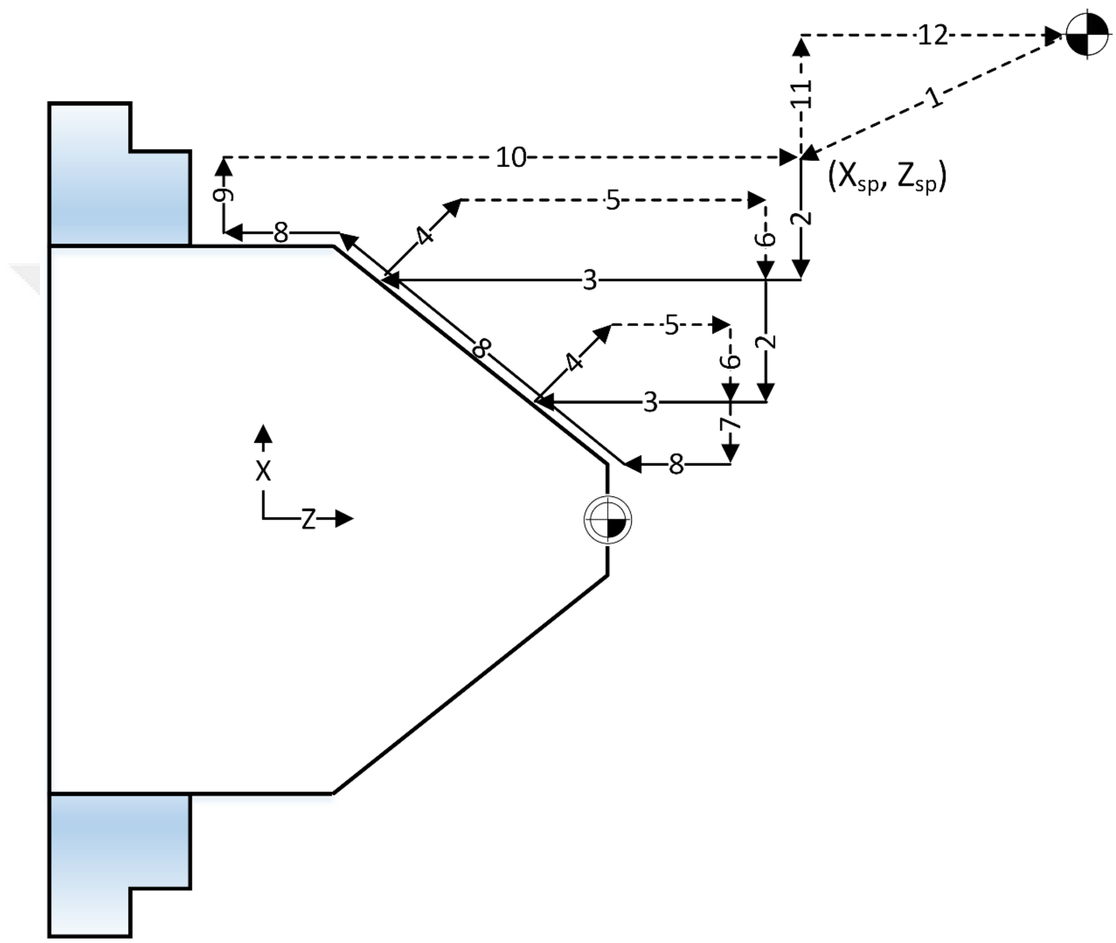

Figure 7.3 Toolpath for outer turning

Before rough machining movements are executed, the number of passes is calculated using the equation below:

$$n_{pass\_rough} = Int\left(\frac{X_{sp} - points\_OT\_R\_R(1,1)}{2\ a_{p\_rough}}\right) \tag{7.3}$$

where X_{sp} is the X coordinate of safe point, points_OT_R_R(1,1) is the X coordinate of the rightmost point with finish allowance (explained under Section 5.3) and a_{p_rough} is the depth of cut for the rough turning operation found in Section 6.8.2.1 Depth of Cut (a_p).

1: Tool moves from machine zero position to the safe point with G00.

$(X_{new}, Z_{new}) = (X_{sp}, Z_{sp})$

The movements for material removal (2-6) are repetitive and they are executed in a loop until the number of passes for rough turning (n_{pass_rough}) is reached.

2: Tool moves down to i^{th} multiple of the depth of cut, where i represents the current number of roughing pass, positioning itself for the longitudinal cut. G01 is used for safety reasons.

$(X_{new}, Z_{new}) = (X_{sp} - 2i \cdot a_{p\_rough}, Z_{sp})$

3: Tool moves longitudinally for the rough cut with G01 until it reaches to contour limit. Z_{limit} is calculated based on the boundary, i.e. horizontal, vertical, taper or circular.

$(X_{new}, Z_{new}) = (X_{sp} - 2i \cdot a_{p\_rough}, Z_{limit})$

4: Tool retracts from the contour limit at 45 degrees with G01. Retraction amount ($turn_{retract}$) is taken as 1 mm on both axes.

$(X_{new}, Z_{new}) = (X_{sp} - 2\ i\ a_{p\_rough} + 2\ turn_{retract}, Z_{limit} + turn_{retract})$

5: Tool moves back to the safe point on Z axis with G00 preparing for the next plunge.

$(X_{new}, Z_{new}) = (X_{sp} - 2\ i\ a_{p\_rough} + 2\ turn_{retract}, Z_{sp})$

6: Tool moves down to the previous cutting depth with G00.

$(X_{new}, Z_{new}) = (X_{sp} - 2\ i\ a_{p\_rough}, Z_{sp})$

After completing the calculated number of passes for the rough cutting, the second step is executed where all of the points of points_OT_R_R matrix is visited for sweeping the rough outer contour.

7: Tool moves down to the lowest level of the rough contour on X axis with G01, positioning itself for the final pass of rough cut.
(X_{new}, Z_{new}) = (points_OT_R_R(1, 1), Z_{sp})

8: Tool sweeps rough contour following the coordinates of the points in points_OT_R_R matrix. Positioning of the tool is done either by linear interpolation (G01) or circular interpolation (G02/G03) depending on the curvature parameter of the target point, i.e. points_OT_R_R(i, 4) where i represents the current point.
(X_{new}, Z_{new}) = (points_OT_R_R(i, 1), points_OT_R_R(i, 2))

9: Tool retracts to the safe point along X axis with G01.
(X_{new}, Z_{new}) = (X_{sp}, points_OT_R_R(total_point_no_OT + 1, 2))
where total_point_no_OT + 1 corresponds to the extra point added as explained in Section 5.3.

10: Tool returns to the safe point along Z axis with G00.
$(X_{new}, Z_{new}) = (X_{sp}, Z_{sp})$

11 and 12: Tool is sent back to machine zero first in X then in Z axis.

Toolpath for finish machining resembles the last step for roughing. Similar movements to those described between steps 7-12 are executed. The tool sweeps the contour defined by points_OT_R matrix, giving the final shape to the part by removing the finish allowance on the outer contour.

7.3.3 Drilling

Drilling toolpath depends on the operation requirements. In cases where pecking is unnecessary, it mimics a fixed drilling cycle. Center drilling similarly follows the pattern of a fixed drilling cycle. On the other hand, when pecking is required, the toolpath replicates the G83 - Deep Hole Drilling Cycle. The subsequent sections elaborate on the specific toolpaths for these two alternatives.

7.3.3.1 Drilling without Pecking

The toolpaths for drilling and center drilling are illustrated in Figure 7.4. Solid lines represent cutting feed (G01), while dashed lines represent rapid positioning (G00).

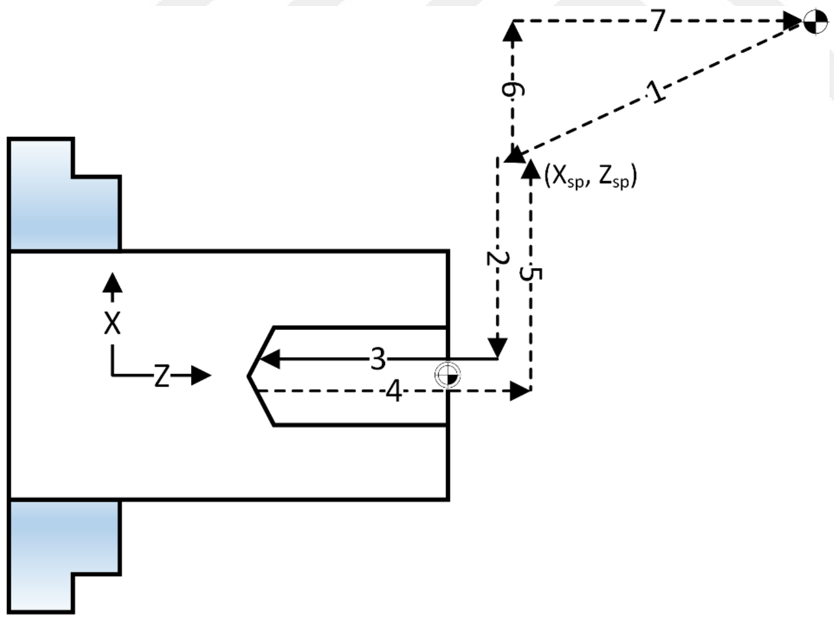

Figure 7.4 Toolpath for drilling without pecking

1: Tool moves from machine zero position to the safe point with G00.
$(X_{new}, Z_{new}) = (X_{sp}, Z_{sp})$

2: Tool moves from the safe point to the starting point for drilling operation on the X axis with G00.

$(X_{new}, Z_{new}) = (0, Z_{sp})$

3: Tool drills down to the hole bottom with G01. Hole bottom position for drilling is taken from the points_RNDHOL matrix. For center drilling, a depth parameter ($depth_{centerdrill}$) of 7 mm, determined from Figure 6.35, is used for the selected center drill.

$(X_{new}, Z_{new}) = (0, points\_RNDHOL(1, 2))$ for drilling

$(X_{new}, Z_{new}) = (0, depth_{centerdrill})$ for center drilling

4: Tool retracts to the safe point on the Z axis with G00.

$(X_{new}, Z_{new}) = (0, Z_{sp})$

5: Tool retracts to the safe point on the X axis with G00.

$(X_{new}, Z_{new}) = (X_{sp}, Z_{sp})$

6 and 7: Tool is sent back to machine zero first in X, then in Z axis.

7.3.3.2 Drilling with Pecking

The initial step in generating the peck drilling toolpath involves calculating the necessary parameters used for the tool motions. The first parameter is the number of pecking required calculated by the following equation:

$$n_{peck} = Int\left(\frac{Z_{sp} - points\_RNDHOL(1,2)}{depth_{peck}}\right) \tag{7.4}$$

where Z_{sp} is the Z coordinate of safe point, points_RNDHOL(1,2) is the Z coordinate of the hole depth (explained under Section 5.5) and $depth_{peck}$ is the depth of each peck. Peck depth corresponds to the Q value in standard G83 cycle and is found by:

$$depth_{peck} = 3\, points\_RNDHOL(1,6) \tag{7.5}$$

where points_RNDHOL(1,6) is the diameter of the hole and 3 is an industry average multiple for calculating the peck depth.

Another parameter, peck clearance ($clearance_{peck}$) serves as a safety buffer in the toolpath generation. After each peck, the drill rapidly traverses (G00) to the depth of the previous peck minus the clearance before advancing with the cutting feed (G01). Peck clearance is aligned with the parameter "d" for the standard G83 cycle and it is typically set at 1 mm internally by the CNC controller. Therefore, 1 mm clearance is used for toolpath generation, as well.

The int_{peck} parameter determines whether the term in parentheses in Equation (7.4) yields an integer value ($int_{peck} = 1$) or not ($int_{peck} = 0$). This parameter plays a crucial role in concluding the peck loop during toolpath generation.

Figure 7.5 shows a representative toolpath for drilling which requires two full pecks and one partial peck for the remaining material at the bottom. Details of the toolpath execution are given in the tool movements between 1 and 11.

1: Tool moves from machine zero position to the safe point with G00.
$(X_{new}, Z_{new}) = (X_{sp}, Z_{sp})$

2: Tool moves from the safe point to the starting point for peck drilling operation on the X axis with G00.
$(X_{new}, Z_{new}) = (0, Z_{sp})$

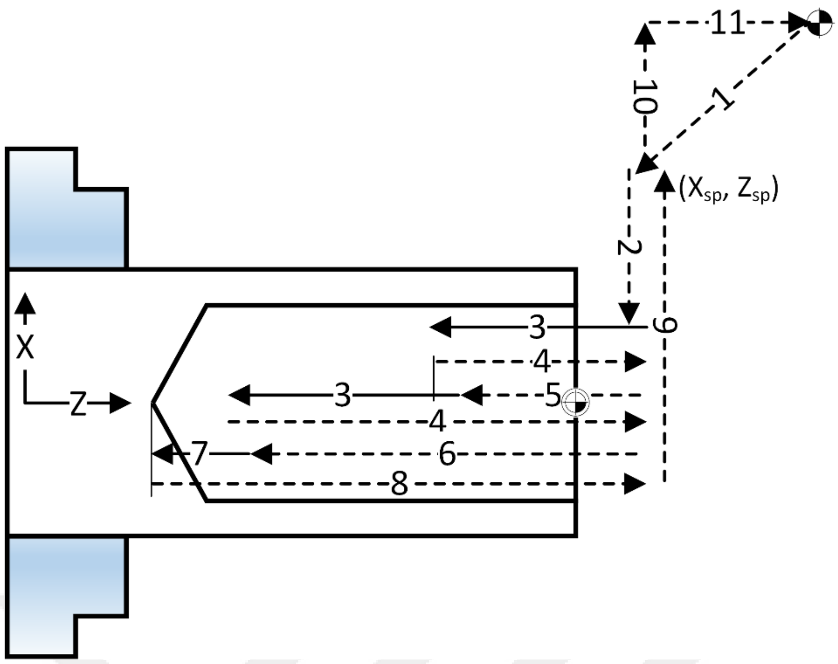

Figure 7.5 Toolpath for peck drilling

Tool movements between 3 and 5 are repeated in a loop until the number of pecks (n_{peck}) is reached.

3: Tool drills down to i^{th} multiple of the peck depth with G01, where i represents the current number of peck.

$(X_{new}, Z_{new}) = (0, -i\ depth_{peck} + Z\_sp)$

4: Tool retracts to the safe point on the Z axis with G00.

$(X_{new}, Z_{new}) = (0, Z_{sp})$

5: Tool rapidly traverses (G00) to previous depth on Z axis by putting a safety buffer of $clearance_{peck}$ set at 1 mm preparing for the next material removal cut. This movement is not executed for the last peck, i.e. $i = n_{peck}$.

$(X_{new}, Z_{new}) = (0, -i\ depth_{peck} + Z\_sp + clearance_{peck})$

After completing the calculated number of pecks, if the last peck did not reach the hole bottom, a final partial peck is executed. Therefore, the following tool movements between 6 and 8 are executed only if $int_{peck} = 0$. Because if $int_{peck} = 1$ it indicates that the drill has already reached the hole bottom at the end of the previous loop and the peck drilling operation is finalized.

6: Tool rapidly traverses (G00) to previous depth on Z axis by putting a safety buffer of $clearance_{peck}$ set at 1 mm preparing for the partial peck.

$(X_{new}, Z_{new}) = (0, - n_{peck}\ depth_{peck} + Z\_sp + clearance_{peck})$

7: Tool drills down to the hole bottom with G01. Information for the hole bottom position is available in the points_RNDHOL matrix.

$(X_{new}, Z_{new}) = (0, points\_RNDHOL(1, 2))$

8: Tool retracts to the safe point on the Z axis with G00.

$(X_{new}, Z_{new}) = (0, Z_{sp})$

After the final peck is completed, the tool is first retracted to the safe point and then to the machine zero.

9: Tool retracts to the safe point on the X axis with G00.

$(X_{new}, Z_{new}) = (X_{sp}, Z_{sp})$

10 and 11: Tool is sent back to machine zero first in X, then in Z axis.

7.3.4 Grooving

The toolpath for grooving, replicates Groove Cutting Cycle (G75) and excludes a finishing cut. Geometry for toolpath generation is based on points_SQRUGRV matrix.

Prior to toolpath generation, necessary parameters are calculated. The first parameter is the number of plunges required to complete the machining of the groove:

$$n_{plunge} = Int\left(1 + \frac{\mathrm{W_{groove}} - \mathrm{a_{p\_groove}}}{infeed_Z}\right) \tag{7.6}$$

where 1 is for the initial plunge and the other terms account for the remaining plunges after each infeed in Z axis. a_{p_groove} is equal to the width of the parting tool (Section 6.8.4) and W_{groove} is the width of the groove. W_{groove} is calculated as follows:

$$W_{groove} = points\_SQRUGRV\_R(1,2) - points\_SQRUGRV\_R(4,2) \tag{7.7}$$

In the equation above, points_SQRUGRV_R(1,2) and points_SQRUGRV_R(4,2) are the Z coordinates of the first and last points of the groove respectively.

Tool starts plunging from the right wall of the groove and moves to the left wall incrementally after each plunge. This incremental movement is called the infeed amount in Z axis ($infeed_Z$) and found by the following equation:

$$infeed_Z = 0.6\, a_{p\_groove} \tag{7.8}$$

Besides the safe point (X_{sp}, Z_{sp}), a start point (X_{start}, Z_{start}) is defined for the grooving operation. This need arises because X_{sp} is computed based on the stock diameter, while grooves may be placed at smaller diameters on the designed part. Therefore, retracting to X_{sp} would be impractical for every plunge. Consequently, a closer level to the part geometry in X axis (X_{start}) is defined a so that after each plunge tool retracts X_{start} instead of X_{sp}.

$$X_{start} = points\_SQRUGRV\_R(1,1) + clearance_{plunge} \tag{7.9}$$

$$Z_{start} = points\_SQRUGRV\_R(1,2) - a_{p\_groove} \tag{7.10}$$

where points_SQRUGRV_R(1,1) and points_SQRUGRV_R(1,2) are the X and Z coordinates of the upper point on the right wall of the groove. $clearance_{plunge}$ is the clearance distance from the top surface of the groove in X axis and taken as 2 mm on diameter for this study. Since the reference point for a grooving tool is on its left face, the starting point on Z axis is positioned at a distance equivalent to the groove width (a_{p_groove}) away from the right wall.

The int_{plunge} parameter assesses if the expression in parentheses in Equation (7.6) results in an integer value ($int_{plunge} = 1$) or not ($int_{plunge} = 0$). This parameter is pivotal in deciding whether any excessive material remains on the groove left wall and if an extra plunge is needed to complete the grooving operation.

Figure 7.6 demonstrates a grooving operation where three normal and one extra plunges are done. Details of the movements from 1 to 13 are presented below.

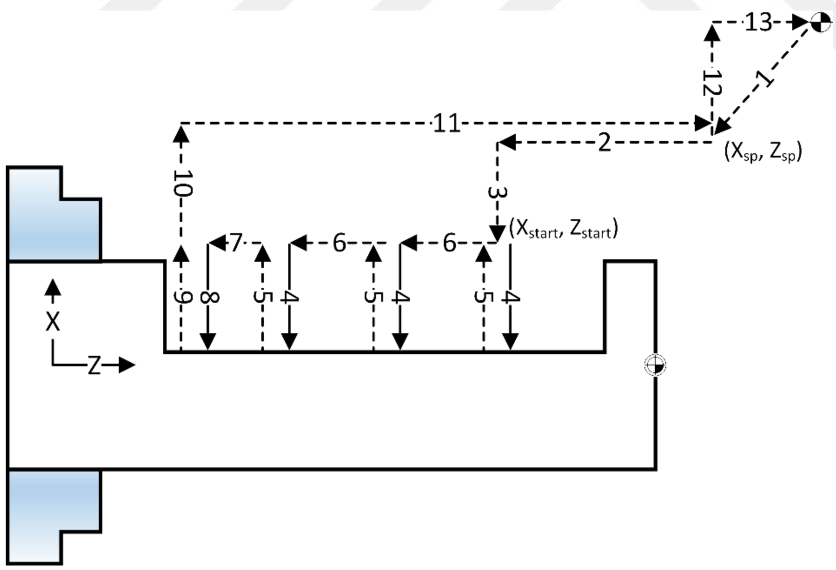

Figure 7.6 Toolpath for grooving

1: Tool moves from machine zero position to the safe point with G00.

$(X_{new}, Z_{new}) = (X_{sp}, Z_{sp})$

2: Tool positions to the starting point of grooving operation on the Z axis with G00.

$(X_{new}, Z_{new}) = (X_{sp}, Z_{start})$

3: Tool positions to the starting point for grooving operation on the X axis with G00.

$(X_{new}, Z_{new}) = (X_{start}, Z_{start})$

Tool movements occurring between steps 4 and 6 are carried out in a loop until the number of plunges (n_{plunge}) is reached.

4: Tool plunges to the groove depth with G01. Current plunge number is represented by i.

(X_{new}, Z_{new}) = (points_SQRUGRV_R(2, 1), Z_{start} - (i-1) $infeed_Z$)

5: Tool retracts to the starting point on the Z axis with G00.

$(X_{new}, Z_{new}) = (X_{start}, Z_{start} - (i-1)\ infeed_Z)$

6: Tool rapidly traverses (G00) in Z axis to position itself for the next plunge. This movement is omitted for the last plunge, i.e. $i = n_{plunge}$.

$(X_{new}, Z_{new}) = (X_{start}, Z_{start} - i\ infeed_Z)$

Following the completion of the specified number of plunges (n_{plunge}), an extra plunge is performed if the left wall of the groove has not been reached and there is residual material on the wall. Therefore, movements from 7 to 9 are executed only when int_{plunge} equals 0.

7: Tool positions for the last plunge on Z axis by rapidly traversing to the left wall.

(X_{new}, Z_{new}) = (X_{start}, points_SQRUGRV_R(4, 2))

8: Tool plunges to the groove depth with G01.

(X_{new}, Z_{new}) = (points_SQRUGRV_R(2, 1), points_SQRUGRV_R(4, 2))

9: Tool retracts to the start point on the X axis with G00.

$(X_{new}, Z_{new}) = (X_{start}$, points_SQRUGRV_R(4, 2))

After the final plunge is completed, the tool is first retracted to the safe point and then to the machine zero.

10: Tool retracts to the safe point on the X axis with G00.

$(X_{new}, Z_{new}) = (X_{sp}$, points_SQRUGRV_R(4, 2))

11: Tool retracts to the safe point on the Z axis with G00.

$(X_{new}, Z_{new}) = (X_{sp}, Z_{sp})$

12 and 13: Tool is sent back to machine zero first in X, then in Z axis.

7.3.5 Parting

The toolpath for parting is illustrated in Figure 7.7. Solid lines represent cutting feed (G01), while dashed lines represent rapid positioning (G00).

1: Tool moves from machine zero position to the safe point with G00.

$(X_{new}, Z_{new}) = (X_{sp}, Z_{sp})$

2: Tool moves from the safe point to the starting point for parting operation on the Z-axis with G00.

$(X_{new}, Z_{new}) = (X_{sp}, 0)$

3: Tool moves down to complete parting cut with G01

$(X_{new}, Z_{new}) = (-1, 0)$

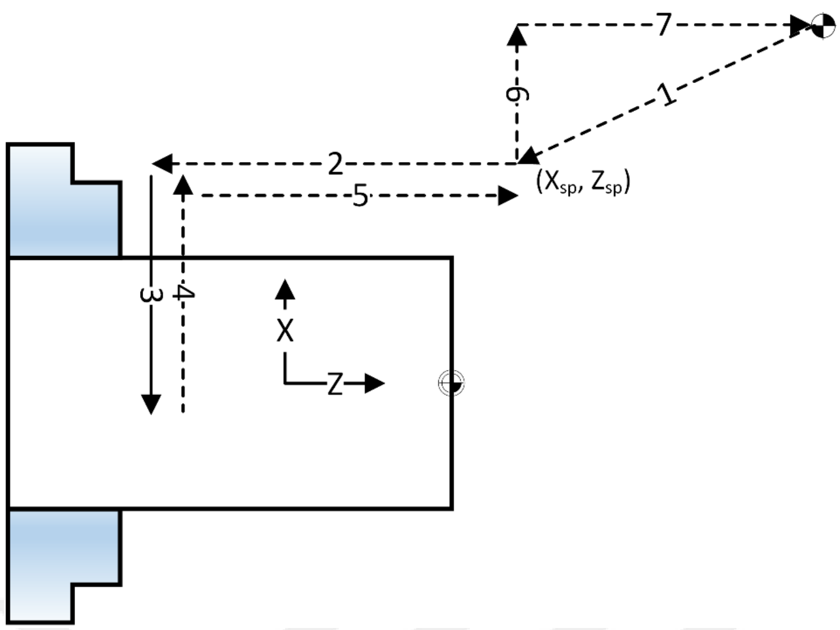

Figure 7.7 Toolpath for parting

4: Tool retracts to the safe point on the Z-axis with G00

$(X_{new}, Z_{new}) = (-1, Z_{sp})$

5: Tool retracts to the safe point on the X-axis with G00

$(X_{new}, Z_{new}) = (X_{sp}, Z_{sp})$

6 and 7: Tool is sent back to machine zero first in X then in Z axis.

7.4 Time Estimation

Based on the distance traveled by the tool and the cutting parameters, a time value (t_{step}) is estimated for each block in the part program. This estimation is iteratively applied under every block code and a total cutting time (t_c) is calculated by accumulating all the t_{step} values, providing an ongoing measure of the overall cutting duration.

After the part program of each manufacturing operation is completed, the total cutting time is used to compute the time required for each operation from the following equation:

$$t_{op}(n) = t_c - \sum_{i=1}^{n-1} t_{op}(i) \qquad (7.11)$$

The utilization time of servo motors are calculated in each applicable block, as well. Separate time parameters are used for the X and Z axis servos, to save the time required for their rapid motions (G00) and cutting motions (G01, G02/G03). Relevant time parameters of servo motors are incrementally increased by t_{step} depending on the axis and characteristic of the tool motion (cutting or rapid).

Following sections explain the methods of t_{step} calculations for G00, G01, G02/G03 tool motions, machine zero return and tool change.

7.4.1 Linear Interpolation: G01

Linear distance (L_{step}) traveled by the tool for a block containing G01 and time needed for that motion (t_{step}) are calculated as:

$$L_{step} = \sqrt{\left(\frac{X_{new} - X_{old}}{2}\right)^2 + (Z_{new} - Z_{old})^2} \qquad (7.12)$$

$$t_{step} = 60\,\frac{L_{step}}{V_f} \qquad (7.13)$$

where V_f is the feed rate in mm/min of the specific operation and is calculated in Section 6.8 Tools and Parameters.

7.4.2 Circular Interpolation: G02/G03

Arc length (s_{step}) traveled by the tool for a G02 or G03 block and the corresponding time (t_{step}) for the tool travel are calculated by the following equations. A representation of the lengths and points used in calculations is shown in Figure 7.8.

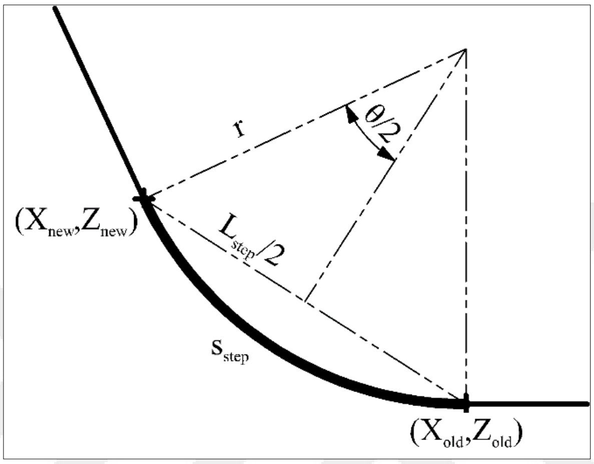

Figure 7.8 G02 (Clockwise) circular interpolation

$$L_{step} = \sqrt{\left(\frac{X_{new} - X_{old}}{2}\right)^2 + (Z_{new} - Z_{old})^2} \tag{7.14}$$

$$s_{step} = r\,\theta \tag{7.15}$$

$$\theta = 2 \arcsin\left(\frac{L_{step}}{2\,r}\right) \tag{7.16}$$

$$s_{step} = 2\,r \arcsin\left(\frac{L_{step}}{2\,r}\right) \tag{7.17}$$

$$t_{step} = 60\,\frac{s_{step}}{V_f} \tag{7.18}$$

7.4.3 Rapid Positioning: G00

Unlike linear and circular interpolations where feed rates are slow, rapid positioning uses the maximum feed rate which is 30000 mm/min for both axes. Time required to reach this maximum feed rate is high, so assuming that the entire tool movement is completed at 30000 mm/min for a G00 block would be misleading. Consequently, acceleration is involved in the time (t_{step}) estimations for G00.

Acceleration is incorporated into time estimation in two different cases (Figure 7.9). First case assumes the linear distance (L_{step}) traveled by the tool provides enough time for feed rate to reach its maximum value (V_{max}). For the second case linear distance is not sufficient enough and feed rate reaches to a value (V') smaller than maximum feed rate (V_{max}) of the axis motor.

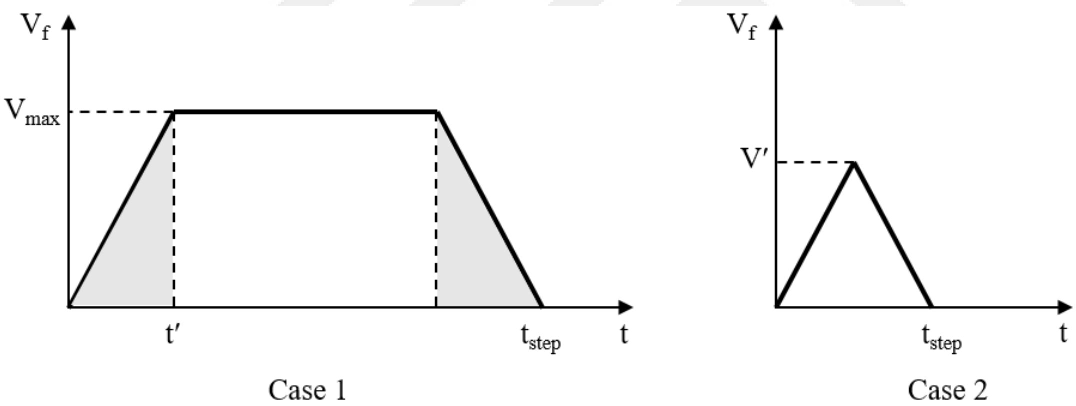

Figure 7.9 Acceleration modeling

In order to distinguish between those cases, L_{step}' is employed, representing the linear distance traveled when the feed rate starts from 0, reaches V_{max} and then decelerates to 0 again, a triangular speed profile peaking at V_{max}. If L_{step} of any G00 block exceeds L_{step}' it indicates that feed rate will reach V_{max} and tool will travel at that speed for a certain duration before decelerating to 0, describing Case 1. Conversely, if L_{step} is smaller than L_{step}', it signifies that V_{max} is not reached. Instead, the feed rate peaks at V′ followed by deceleration. This type of tool movement is categorized under Case 2. L_{step}' is determined using the following equations:

$$L'_{step} = 2\ \frac{1}{2}\frac{V_{max}}{60}\ t' = \frac{V_{max}}{60}\ t' \tag{7.19}$$

$$a = \frac{V_{max}}{60\ t'} \tag{7.20}$$

$$L'_{step} = \frac{V_{max}^2}{3600\ a} \tag{7.21}$$

Subsequently, linear distance (L_{step}) traveled by the tool for a block containing G00 and time needed for that motion (t_{step}) for Case 1 and Case 2 are calculated as follows:

$$L_{step} = \sqrt{\left(\frac{X_{new} - X_{old}}{2}\right)^2 + \ (Z_{new} - Z_{old})^2} \tag{7.22}$$

t_{step} for Case 1: $L_{step} > L'_{step}$

The area under the graph in Figure 7.9 gives L_{step}:

$$L_{step} = \frac{V_{max}}{60}\ t_{step} - 2\ \left(\frac{1}{2}\ \frac{V_{max}}{60}\ t'\right) \tag{7.23}$$

Substituting t′ from Equation (7.20) into Equation (7.23) and solving for t_{step} gives the following equations:

$$L_{step} = \frac{V_{max}}{60}\ t_{step} - \frac{V_{max}^2}{3600\ a} \tag{7.24}$$

$$t_{step} = \frac{60\ L_{step}}{V_{max}} + \frac{V_{max}}{60\ a} \tag{7.25}$$

t_{step} for Case 2: $L_{step} < L'_{step}$

L_{step} is calculated by the area under the graph in Figure 7.9:

$$L_{step} = \frac{1}{2}\frac{V'}{60}\, t_{step} \tag{7.26}$$

t_{step} is obtained in Equation (7.28) by substituting V′ from the Equation (7.27) into Equation (7.26):

$$a = \frac{V'}{60(t_{step}/2)} \tag{7.27}$$

$$t_{step} = 2\sqrt{\frac{L_{step}}{a}} \tag{7.28}$$

Table 7.5 Time estimation comparisons: without and with acceleration

		Without Acceleration			**With Acceleration 1000 mm/s^2**		
	Time [s]	**Est. [s]**	**Error [%]**	**Error [s]**	**Est. [s]**	**Error [%]**	**Error [s]**
Facing	**8.4**	7	17	**1.4**	9	-7	**-0.6**
Turning - Rough	**112.8**	107	5	**5.8**	111	2	**1.8**
Turning - Finish	**55.5**	53	5	**2.5**	56	-1	**-0.5**
Center Drilling	**8**	6	25	**2**	8	0	**0**
Drilling	**8.9**	7	21	**1.9**	9	-1	**-0.1**
Grooving	**98.1**	90	8	**8.1**	95	3	**3.1**
Parting	**27.7**	26	6	**1.7**	28	-1	**-0.3**
	319.4	**296**	**7**	**23.4**	**316**	**1**	**3.4**

The numerical value of acceleration is not available in the user manual of Anatool TP32 CNC Lathes, therefore a value is found using experimental approach. In Table 7.5 two scenarios are presented for a sample part: without and with acceleration. Actual cutting time is indicated in the second column as 319.4 seconds. In the first scenario acceleration is neglected and the total cutting time is estimated as 296 seconds, resulting in a 7% error. After several trial and errors, the total cutting time is refined to 316 seconds by involving an acceleration value of 1000 mm/s^2 (approximately 0.1g), reducing the total error to 1%. As a result, a constant acceleration of 1000 mm/s^2 is included into the time estimation for rapid positioning.

7.4.4 Machine Zero Return

Tool motion for each manufacturing operation starts by sending the tool from machine zero to the safe point and ends by returning the tool from safe point to machine zero. Despite the coordinates of the safe point being known for any given part program, the machine zero position varies among CNC manufacturers and across different machines. To eliminate the necessity for exact distance calculations between the safe point and machine zero, the time required for travel between these two points is assumed to be constant (t_{MCzero}). This value is determined through experimental observations for the Anatool TP32 CNC lathe and a similar approach could be adopted for other CNC lathes.

The numerical value of t_{MCzero} is found by executing an NC code that transitions the tool from machine zero to the safe point and back to the machine zero 10 times. The total time for these movements is measured as 20 seconds. Therefore the duration of a single motion to or from the machine zero is calculated as 1 second. In the part program, whenever a machine zero send or return is executed, t_{step} is considered equivalent to t_{MCzero}:

$$t_{step} = t_{MCzero} = 1\ s \tag{7.29}$$

7.4.5 Tool Change

Every time a tool change occurs in the part program, a constant tool change time (t_{ch}) is assigned to each of those blocks. Tool change time depends on the turret size, number of tools and the location of the tool on the turret. Rather than considering all these parameters, an average tool change time (t_{ch}) is found by experimental observations on the Anatool TP32 CNC lathe.

For the calculation of this parameter, 20 tool change commands are executed. To adopt a conservative approach, the indexing time is maximized by selecting two opposite tools (T3 and T8). The total measurement time is recorded as 31 seconds. Consequently, the average tool change time (t_{ch}) is calculated as 1.55 seconds and t_{step} is set to t_{ch} when a tool change block is added to the part program.

$$t_{step} = t_{ch} = 1.55\ s \tag{7.30}$$

7.5 Sample Code

The initiation steps of the part program are outlined in the code presented in Table 7.6. The first section of the Part Programming module for TurnDesign Eco Edition, begins by creating a "Part_Program.txt" file. The file is saved and closed upon completion of the Part Programming module. The subsequent section of the code shows the header structure of the part program where relevant information for the design is registered for further reference. The information is printed block by block using the "Print" statements. Each line of the code corresponds to a specific detail and block numbers (e.g., N10, N20) are used for sequencing and referencing in the NC code. The third section of the code introduces standard preparatory commands essential for CNC lathe operations.

Table 7.6 Code for part program generation: header

```
Dim iFileNo20 As Integer
iFileNo20 = FreeFile
Open "C:\Users\ural\Desktop\Part_Program.txt" For Output As #iFileNo20

'HEADER---------------------------------------------------------
Print #iFileNo20, ";DATE............ " & Format(Now, "dd.mm.yyyy")
Print #iFileNo20, ";TIME............ " & Format(Now, "hh:mm")
Print #iFileNo20, ";PROGRAMMER....... " & "Ural Uluer"
Print #iFileNo20, ""

Print #iFileNo20, ";D_stock.......... " & Dstock_current & " mm"
Print #iFileNo20, ";L_stock.......... " & Lmax_current + a_p(1) +
a_p(20) + 10 & " mm"
Print #iFileNo20, ";MACHINE.......... " & "Anatool TP32 CNC Lathe"
Print #iFileNo20, ""
Print #iFileNo20, ""

'PREPARATORY FUNCTIONS------------------------------------------
Print #iFileNo20, "N10 " & "G291"
Print #iFileNo20, "N20 " & "G91"
Print #iFileNo20, "N30 " & "G28" & " " & "X" & "0"
Print #iFileNo20, "N40 " & "G28" & " " & "Z" & "0"
Print #iFileNo20, "N50 " & "G90"
Print #iFileNo20, "N60 " & "G21 G18 G95 G40"
Print #iFileNo20, "N70 " & "M07"
Print #iFileNo20, "N80 " & "G54"
Print #iFileNo20, ""
Print #iFileNo20, ""
```

Table 7.7 provides the code segment utilized for generating part program of facing. In the first section, tool change and cutting parameters are printed in the part program file. Subsequent sections process each tool movement explained in Section 7.3.1. A block is printed in the text file including the G code (G00/G01) and target point (X_{new} and Z_{new}) followed by the incremental time calculations of the movement. The total time for the facing operation is saved in the t_op array at the end of the code.

Table 7.7 Code for part program generation: facing operation

```
'FACING---------------------------------------------------------
Print #iFileNo20, ";-------FACING------------------------------------"

'Tool Speed feed
Print #iFileNo20, "N" & blockno & " " & nc_tool(1): blockno=blockno + 10
Print #iFileNo20, "N" & blockno & " " & "G97 S" & n(1) & " " & "M03" & "
" & "F" & a_f(1): blockno = blockno + 10
Print #iFileNo20, ""
n_ch = n_ch + 1
```

Table 7.7 (continued)

```
t_step = t_ch
t_c_current = t_c_current + t_step


X_sp = Dstock_current + safe_allowance_X
Z_sp = 0 + safe_allowance_Z

'position to safe point
X_new = X_sp
Z_new = Z_sp
Print #iFileNo20, "N" & blockno & " " & "G00" & " " & "X" & X_new & " "
& "Z" & Z_new: blockno = blockno + 10
t_step = t_MCzero
t_c_current = t_c_current + t_step
t_servox00 = t_servox00 + t_step
t_servoz00 = t_servoz00 + t_step

'position to starting point Z-axis
X_old = X_new
Z_old = Z_new
X_new = X_sp
Z_new = 0
Print #iFileNo20, "N" & blockno & " " & "G00" & " " & "X" & X_new & " "
& "Z" & Z_new: blockno = blockno + 10
If Sqr(((X_new - X_old) / 2) ^ 2 + (Z_new - Z_old) ^ 2) > v_rapidz ^ 2 /
(3600 * accel) Then
t_step = Sqr(((X_new - X_old) / 2) ^ 2 + (Z_new - Z_old) ^ 2) / v_rapidz
* 60 + v_rapidz / (accel * 60)
End If
If Sqr(((X_new - X_old) / 2) ^ 2 + (Z_new - Z_old) ^ 2) <= v_rapidz ^ 2
/ (3600 * accel) Then
t_step = 2 * Sqr(Sqr(((X_new - X_old) / 2) ^ 2 + (Z_new - Z_old) ^ 2) /
accel)
End If
t_c_current = t_c_current + t_step
t_servoz00 = t_servoz00 + t_step

'move down: facing
X_old = X_new
Z_old = Z_new
X_new = -1
Z_new = 0
Print #iFileNo20, "N" & blockno & " " & "G01" & " " & "X" & X_new & " "
& "Z" & Z_new: blockno = blockno + 10
t_step = Sqr(((X_new - X_old) / 2) ^ 2 + (Z_new - Z_old) ^ 2) / v_f(1) *
60
t_c_current = t_c_current + t_step
t_servox01 = t_servox01 + t_step

'Retract to safe point Z-axis: Z_sp
X_old = X_new
Z_old = Z_new
X_new = -1
Z_new = Z_sp
Print #iFileNo20, "N" & blockno & " " & "G00" & " " & "X" & X_new & " "
& "Z" & Z_new: blockno = blockno + 10
If Sqr(((X_new - X_old) / 2) ^ 2 + (Z_new - Z_old) ^ 2) > v_rapidz ^ 2 /
(3600 * accel) Then
t_step = Sqr(((X_new - X_old) / 2) ^ 2 + (Z_new - Z_old) ^ 2) / v_rapidz
* 60 + v_rapidz / (accel * 60)
```

Table 7.7 (continued)

```
End If
If Sqr(((X_new - X_old) / 2) ^ 2 + (Z_new - Z_old) ^ 2) <= v_rapidz ^ 2
/ (3600 * accel) Then
t_step = 2 * Sqr(Sqr(((X_new - X_old) / 2) ^ 2 + (Z_new - Z_old) ^ 2) /
accel)
End If
t_c_current = t_c_current + t_step
t_servoz00 = t_servoz00 + t_step

'Retract to safe point X-axis: X_sp
X_old = X_new
Z_old = Z_new
X_new = X_sp
Z_new = Z_sp
Print #iFileNo20, "N" & blockno & " " & "G00" & " " & "X" & X_new & " "
& "Z" & Z_new: blockno = blockno + 10
If Sqr(((X_new - X_old) / 2) ^ 2 + (Z_new - Z_old) ^ 2) > v_rapidx ^ 2 /
(3600 * accel) Then
t_step = Sqr(((X_new - X_old) / 2) ^ 2 + (Z_new - Z_old) ^ 2) / v_rapidx
* 60 + v_rapidx / (accel * 60)
End If
If Sqr(((X_new - X_old) / 2) ^ 2 + (Z_new - Z_old) ^ 2) <= v_rapidx ^ 2
/ (3600 * accel) Then
t_step = 2 * Sqr(Sqr(((X_new - X_old) / 2) ^ 2 + (Z_new - Z_old) ^ 2) /
accel)
End If
t_c_current = t_c_current + t_step
t_servox00 = t_servox00 + t_step

'send to machine zero
Print #iFileNo20, ""
Print #iFileNo20, "N" & blockno & " " & "G91": blockno = blockno + 10
Print #iFileNo20, "N" & blockno & " " & "G28" & " " & "X" & "0": blockno
= blockno + 10
Print #iFileNo20, "N" & blockno & " " & "G28" & " " & "Z" & "0": blockno
= blockno + 10
Print #iFileNo20, "N" & blockno & " " & "G90": blockno = blockno + 10
Print #iFileNo20, ""
Print #iFileNo20, ""
t_step = t_MCzero
t_c_current = t_c_current + t_step
t_servox00 = t_servox00 + t_step
t_servoz00 = t_servoz00 + t_step

t_op(1) = t_c_current
```

7.6 Output

The initial output of the Part Programming module is the NC code of the designed part which is saved as a text (.txt) file. This file is manufacturing-ready and can be seamlessly loaded onto the CNC lathe, provided that the tool numbers in the code match those loaded on the lathe turret. Figure 7.10 shows the NC code for the facing operation and 2 passes of the rough turning operation of SP1-AL6013. For the complete part program of the sample part, please refer to Chapter 9 Test Set-Up And Verification.

*Part_Program-SP1-AL6013_v0-2024sp - Notepad

File Edit Format View Help

```
;-------FACING------------------------------------
N90 T01
N100 G97 S2650 M03 F0.15

N110 G00 X34 Z2
N120 G00 X34 Z0
N130 G01 X-1 Z0
N140 G00 X-1 Z2
N150 G00 X34 Z2

N160 G91
N170 G28 X0
N180 G28 Z0
N190 G90


;-------TURNING:ROUGH-----------------------------
N200 T01
N210 G97 S2390 M03 F0.3

N220 G00 X34 Z2
N230 G01 X30 Z2
N240 G01 X30 Z-63        ;Pass 1
N250 G01 X32 Z-62
N260 G00 X32 Z2
N270 G00 X30 Z2

N280 G01 X26 Z2
N290 G01 X26 Z-29.898        ;Pass 2
N300 G01 X28 Z-28.898
N310 G00 X28 Z2
N320 G00 X26 Z2
```

Figure 7.10 Part Program for SP1-AL6013

The Part Programming module also provides an estimate of the time required for each auxiliary equipment and manufacturing operation, presented in an Excel file. This file is the primary output of the estimation algorithm and contains the energy and carbon footprint estimations as well. Figure 7.11 illustrates a snippet of this larger Excel file showing the time outputs for the first specimen: SP1-AL6013. The complete estimation output can be found in Section 8.6 for a more in-depth examination of the results.

Spindle		OP Time [s]
1	Facing	7
2	Turning - Rough	27
3	Turning - Finish	15
4	Drilling	5
5	Grooving	47
6	Parting	11
Total		**112**

Servo		Time [s]
Servo X	Rapid	16
Servo X	Feed	66
Servo Z	Rapid	18
Total		**-**

Lubrication	Lubrication #
	0.03

Cutting Fluid	ON Time [s]
	112

Turret	Tool Change #
	6

Standby	ON Time [s]
	112

Chuck	Clamp #
	1

Figure 7.11 Time estimations for SP1-AL6013

CHAPTER 8

ENERGY AND CARBON FOOTPRINT ESTIMATION MODEL

8.1 Introduction

Energy required for production of a part (E_{part}) can be broken down into three components:

$$E_{part} = \sum E_{process} + \sum E_{handling} + \sum E_{indirect} \quad (8.1)$$

where $E_{process}$ is the energy requirement of the manufacturing processes, $E_{handling}$ is the energy required by the automated material handling equipment such as robots and conveyors, $E_{indirect}$ is the allocated indirect energy requirement of the services to maintain the environment for the production activities of the part. The primary objective of this module is the estimation and reporting of the energy requirements and carbon emissions of the manufacturing processes of the designed part.

Process energy $E_{process}$ can be broken down further to obtain the following equation for a single feature (Rahimifard et al., 2010):

$$E_{process} = E_{th} + E_{aux} \quad (8.2)$$

where E_{th} is the theoretical energy which is consumed during the actual metal removal processes and E_{aux} is the energy which is consumed during the operation of the auxiliary equipment of the CNC lathe.

Theoretical energy estimations are based on the volume removed for each feature and the specific cutting energy for the operations involved. Volume is calculated using feature parameters from the User Input module. The specific cutting energy is determined by material constants, tool geometry and cutting parameters from the Process Planning module.

Auxiliary energy estimation uses average power or energy values and usage time or frequency, depending on the component. These average values are specific to the CNC lathe and are obtained from the Process Planning module. The usage time and frequency are calculated based on the NC code generated in the Part Programming module.

This module generates two outputs. The first output is a high level summary of theoretical and auxiliary energy values displayed on the TurnDesign Eco Edition user interface. The second output is an Excel report that details all the energy and carbon footprint results in different categories. The outputs are explained under Section 8.6.

Figure 8.1 illustrates the input and output structure of the Energy and Carbon Footprint Estimation module. Two submodules, Theoretical and Auxiliary Energy Estimation are explained under Section 8.2 and Section 8.3 respectively.

8.2 Theoretical Energy Estimation

Theoretical energy which is the energy required at the tool tip to remove a given volume of chip is calculated by the following equation for each feature:

$$E_{th} = V_{rem}\, p_s \tag{8.3}$$

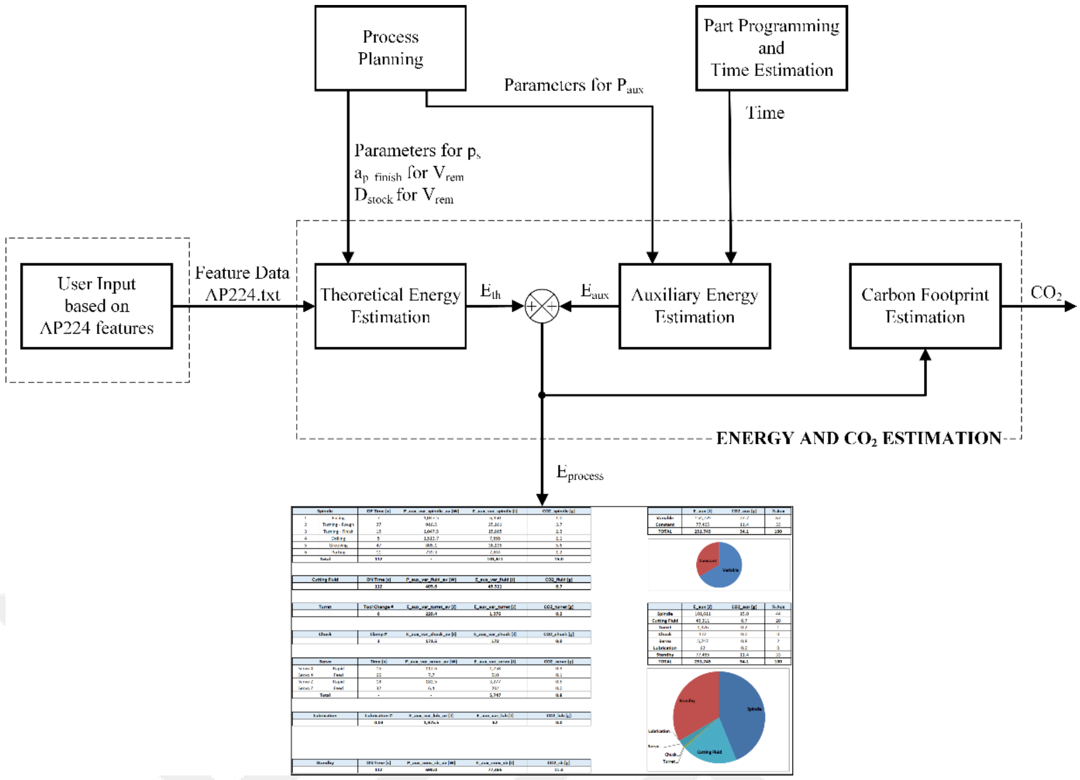

Figure 8.1 Energy and CO_2 Estimation Module: Inputs and Outputs

where V_{rem} (mm^3) is the volume removed for every feature based on the feature parameters from User Input module (Chapter 4) and p_s (J/mm^3) is the specific cutting energy for each operation based on the parameters found in Process Planning module (Chapter 6).

Specific cutting energy which is defined as the energy to remove a unit volume of material is calculated by:

$$p_s = (1 - 0.01\ \gamma_0)\ \frac{p_{s1}}{a_c^{mc}} \tag{8.4}$$

Sequentially, the uncut chip thickness (a_c) can be determined using the following equation:

$$a_c = a_f \sin \kappa_r \tag{8.5}$$

In Equation (8.4), γ_0 represents the cutting rake and κ_r is the cutting edge angle both of which are defined by the tool geometry. a_f is the feed engagement (feed per tooth), determined for each operation based on the tool selection. p_{s1} denotes the specific cutting energy for an uncut chip thickness of 1 mm and mc is a material constant They depend on the machined material. Their values which are taken from Iscar tool catalogues (Iscar, 2017a) are presented in Table 8.1.

Table 8.1 p_{s1} ad mc values

Material	p_{s1} (J/mm^3)	mc
P3	1.675	0.24
K13	1.350	0.28
N16	0.8	0.25

Theoretical energy is investigated under two groups. First group contains the calculations for each feature associated with the operation for each feature. The second group involves miscellaneous operations independent of features. These are facing, parting and stock removal.

8.2.1 Theoretical Energy Estimation for Features

The removed volume for each feature is defined parametrically by applying the theorem on volume of a body of revolution. According to this theorem, the volume of a body of revolution is equal to the product of the generating area and the distance traveled by the centroid of that area during the generation of the body. Therefore:

$$V_{rem} = 2\pi \, \bar{r} \, A_{rem} \tag{8.6}$$

Aligned with the above equation, removed volume calculations for Outer Diameter to Shoulder (Figure 8.2) are shown below. Calculations for the remaining features can be found in Appendix A.

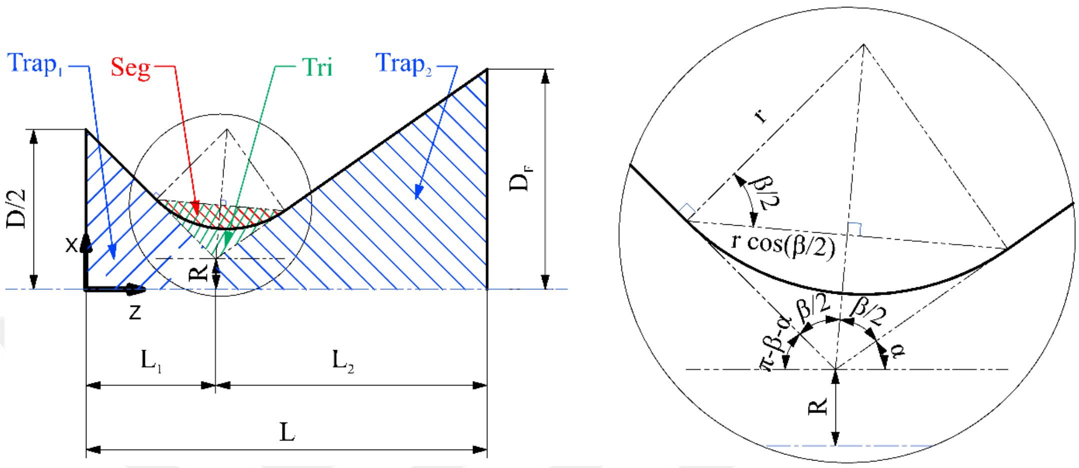

Figure 8.2 Volume removed for Outer Diameter to Shoulder

The horizontal lengths (L_1 and L_2) and the altitude of the triangular section (h), required for volume removal calculations, are provided below:

$$h = r\,\frac{\cos(\beta/2)}{\tan(\beta/2)} = r\,\frac{\cos^2(\beta/2)}{\sin(\beta/2)} \tag{8.7}$$

$$L_1 = \frac{D/2-R}{\tan(\pi-\beta-\alpha)} \tag{8.8}$$

$$L_2 = \frac{D_F/2-R}{\tan\alpha} \tag{8.9}$$

Volume removed for Outer Diameter to Shoulder feature can be found by:

$$V_{rem} = V_{rec} - V_{trap1} - V_{trap2} - V_{tri} + V_{seg} \tag{8.10}$$

The volume generated when the trapezoidal sections are rotated 360 degrees around their horizontal side at can be calculated by the following two equations:

$$V_{trap1} = \frac{\pi}{12}(D^2 + 2\,D\,R + 4R^2)\,L_1 \tag{8.11}$$

$$V_{trap2} = \frac{\pi}{12}(4\,R^2 + 2\,R\,D_F + D_F^2)\,L_2 \tag{8.12}$$

Substituting L_1 and L_2 from Equations (8.8) and (8.9):

$$V_{trap1} = \frac{\pi}{12}(D^2 + 2\,D\,R + 4R^2)\,\frac{D/2-R}{\tan(\pi-\beta-\alpha)} \tag{8.13}$$

$$V_{trap2} = \frac{\pi}{12}(4\,R^2 + 2\,R\,D_F + D_F^2)\,\frac{D_F/2-R}{\tan\alpha} \tag{8.14}$$

The volume obtained when the triangular section is rotated around the centerline can be calculated by:

$$V_{tri} = 2\,\pi\,\bar{r}_{tri}\,A_{tri} \tag{8.15}$$

The centroid of a triangle is at one-third of its altitude. Therefore, the y coordinate of the centroid of the triangular section of Figure 8.2 is calculated as:

$$\bar{r}_{tri} = \frac{2}{3}\,h\,\sin\left(\frac{\beta}{2}+\alpha\right) + R \tag{8.16}$$

Substituting h from Equation (8.7) yields:

$$\bar{r}_{tri} = \frac{2}{3}\,r\,\frac{\cos^2(\beta/2)}{\sin(\beta/2)}\,\sin\left(\frac{\beta}{2}+\alpha\right) + R \tag{8.17}$$

The area of the triangular section is calculated by:

$$A_{tri} = \frac{1}{2}\ 2\,r\ \cos(\beta/2)\ h \tag{8.18}$$

Substituting h from Equation (8.7):

$$A_{tri} = r^2\ \frac{\cos^3(\beta/2)}{\sin(\beta/2)} \tag{8.19}$$

The volume generated when the circular segment is rotated around the centerline is:

$$V_{seg} = 2\ \pi\ \bar{r}_{seg}\ A_{seg} \tag{8.20}$$

Distance of the centroid of the circular segment from the center point is found by:

$$\bar{y} = \frac{4r}{3}\ \frac{\sin^3(\pi/2-\beta/2)}{\pi-\beta-\sin(\pi-\beta)} \tag{8.21}$$

$$\bar{r}_{seg} = \left(\frac{r}{\sin(\beta/2)} - \bar{y}\right)\ \sin\left(\frac{\beta}{2} + \alpha\right) + R \tag{8.22}$$

$$\bar{r}_{seg} = \left(\frac{r}{\sin(\beta/2)} - \frac{4r}{3}\ \frac{\sin^3(\pi/2-\beta/2)}{\pi-\beta-\sin(\pi-\beta)}\right)\ \sin\left(\frac{\beta}{2} + \alpha\right) + R \tag{8.23}$$

The area of the segment is calculated by the following equation:

$$A_{seg} = \frac{r^2}{2}\ [\pi - \beta - \sin(\pi - \beta)] \tag{8.24}$$

8.2.2 Theoretical Energy Estimation for Miscellaneous Operations

Besides the features, material is removed for other manufacturing operations as well, including facing, parting and stock removal. Volumes removed for these operations are shown in Figure 8.3 and calculated in Equations (8.25) to (8.28).

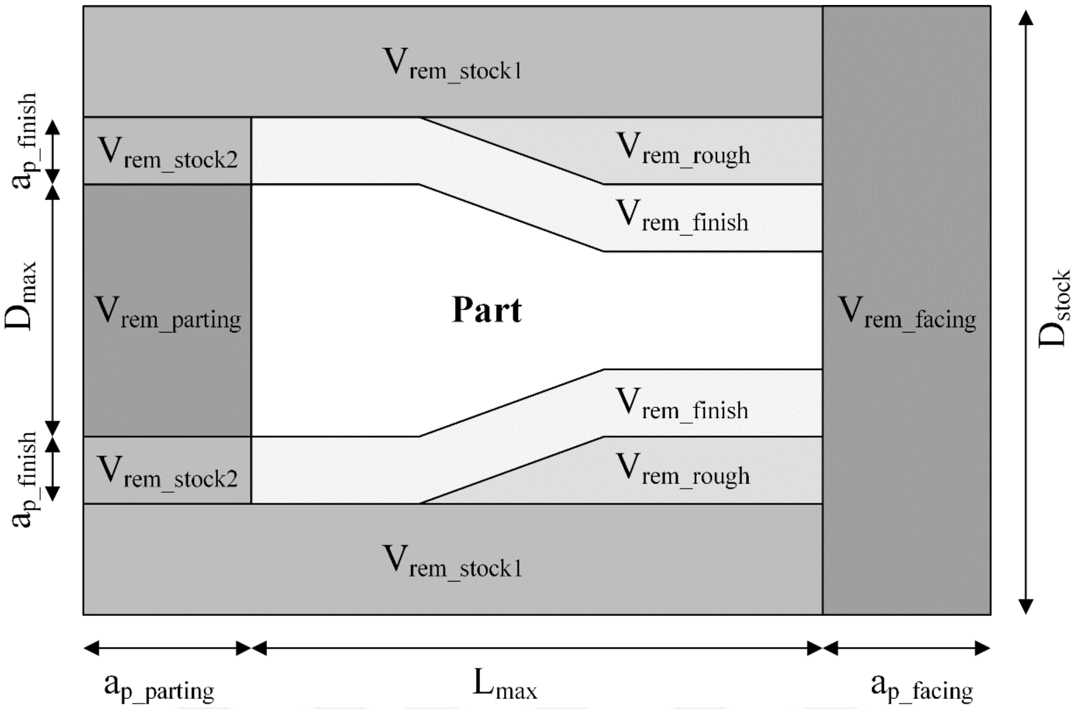

Figure 8.3 Miscellaneous operations

$$V_{rem\_facing} = \frac{\pi}{4} D_{stock}^2 \ a_{p\_facing} \tag{8.25}$$

$$V_{rem\_parting} = \frac{\pi}{4} D_{max}^2 \ a_{p\_parting} \tag{8.26}$$

Stock removal operation is divided into two different volumes. First volume is removed during rough outer turning of the part. This operation brings the stock diameter down to the finish allowance level.

$$V_{rem\_stock1} = \frac{\pi}{4} \left[D_{stock}^2 - \left(D_{max} + 2 \ a_{p\_finish}\right)^2\right] \ \left(L_{max} + a_{p\_parting}\right) \tag{8.27}$$

Second volume is removed during the finish turning of the outer contour. It corresponds to the last sweep motion towards the extra point added to the contour as explained in Section 5.3. Since this volume does not belong to any feature, it is grouped under the stock removal operation.

$$V_{rem\_stock2} = \frac{\pi}{4} \left(D_{max} + 2\, a_{p\_finish}\right)^2 \; a_{p\_parting} - V_{rem\_parting} \tag{8.28}$$

Rough and finish turning operations have different specific cutting energy values so the theoretical energy for stock removal operation is calculates as follows:

$$E_{th\_stock} = V_{rem\_stock1} \; p_{s\_rough} + V_{rem\_stock2} \; p_{s\_finish} \tag{8.29}$$

8.3 Auxiliary Energy Estimation

Auxiliary energy is investigated under two categories: variable (E_{aux_var}) and constant (E_{aux_cons}).

$$E_{aux} = E_{aux\_var} + E_{aux\_cons} \tag{8.30}$$

Variable auxiliary energy is time dependent and may change during the operation of the machine tool. Energy consumed by servo motors, spindle motor or the energy consumed by the turret for each tool change are examples of variable auxiliary energy. This energy can be calculated using either Equation (8.31) or (8.32) according to the specific characteristics of each component:

$$E_{aux\_var\_component} = P_{aux\_var\_component\_av} \; t_{component} \tag{8.31}$$

$$E_{aux\_var\_component} = E_{aux\_var\_component\_av} \; n_{component} \tag{8.32}$$

where $E_{aux\_var\_component}$ is the auxiliary energy consumption, $P_{aux\_var\_component\_av}$ is the average power requirement which is based on measurement results and $t_{component}$ is the use time for a specific auxiliary equipment. $E_{aux\_var\_component\_av}$ in Equation (8.32) is the average energy consumption of a specific component and it is used when

$P_{aux\_var\_component\_av}$ cannot be measured or would be incorrect to use. $n_{component}$ is the number of times that particular component is used.

Constant auxiliary energy is due to the auxiliary components of the machine tools which consume energy even if the machine is in standby mode. Lighting and the embedded computer for the CNC machine tools are two examples for constant auxiliary energy. It is calculated using the equation below:

$$E_{aux\_cons} = P_{aux\_cons\_av} \cdot t_c \tag{8.33}$$

where $P_{aux\_const\_av}$ is the average power requirement of the component and t_c is the total cutting time for the part.

Time estimations which will be used in Equations (8.31) to (8.33) are presented in Section 7.4. This section describes the auxiliary equipment and their average power/energy requirement calculations based on the measurements from Anatool TP32 CNC Lathe. All these measurements aim to isolate the power/energy requirements of an individual auxiliary equipment by operating each equipment separately and eliminating the influence of other auxiliary components. The methodology and corresponding measurements serves as a guide for calibration of the energy estimation model for other CNC lathes, as well.

The Anatool TP32 CNC Lathe includes five main auxiliary systems: (1) spindle assembly, (2) servo motors for axis movements, (3) cutting fluid system, (4) lubrication system for axis slideways and (5) hydraulic system for clamping, turret and tailstock assembly movements. Figure 8.4 illustrates the general structure of the lathe. As noted in Section 6.6, the tailstock is not considered in this study. Consequently, the classification of auxiliary components based on Equation (8.30) is as follows:

$$E_{aux\_var} = E_{aux\_var\_spindle} + E_{aux\_var\_fluid} + E_{aux\_var\_turret} + E_{aux\_var\_chuck} + E_{aux\_var\_servo} + E_{aux\_var\_lub} \quad (8.34)$$

$$E_{aux\_cons} = E_{aux\_cons\_sb} \quad (8.35)$$

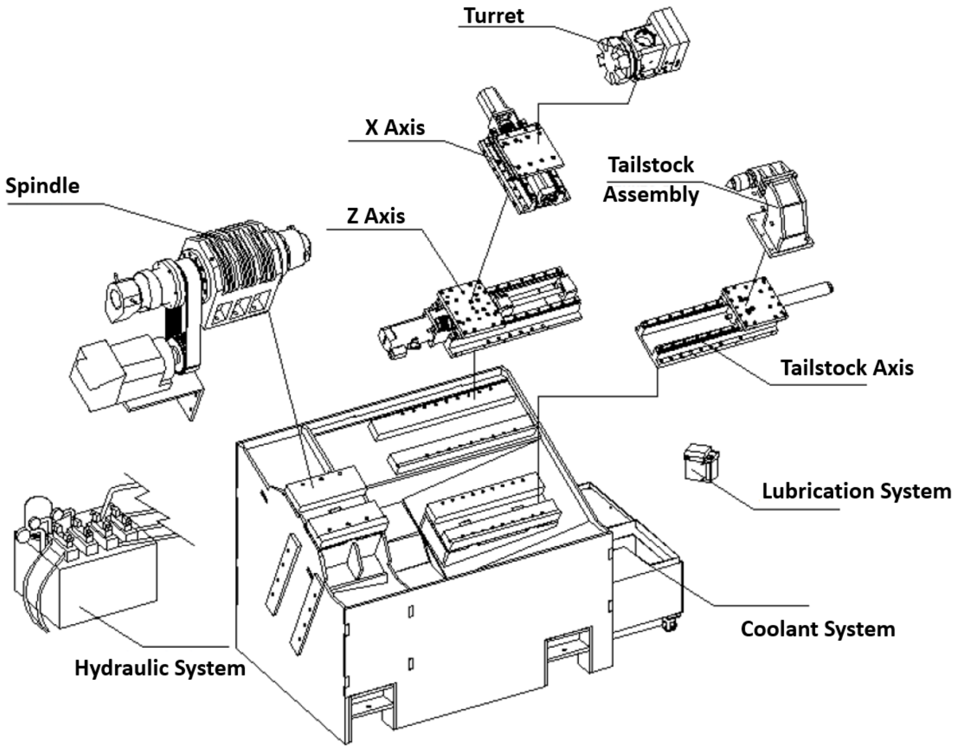

Figure 8.4 General structure of Anatool TP 32 (Anatool Machine Tools, 2009)

8.3.1 Spindle Assembly

Variable auxiliary energy requirement of the spindle assembly ($E_{aux\_var\_spindle}$) is calculated using the following equation:

$$E_{aux\_var\_spindle} = P_{aux\_var\_spinde\_av}\ t_{op} \quad (8.36)$$

where $P_{aux\_var\_spindle\_av}$ represents the average variable auxiliary power consumption of the spindle assembly at a specific rotational speed and t_{op} denotes the time required for a particular operation. The values of t_{op} is determined from Equation (7.11), while $P_{aux\_var\_spindle\_av}$ is based on measurements detailed in the following section.

8.3.1.1 Method

The average power consumption of spindle assembly increases with higher rotational speeds. To capture this, measurements are taken at increments of 125 rpm, ranging from 0 to 3500 rpm, with each increment lasting 60 seconds. The measurement at 0 rpm represents the standby mode. During measurements only spindle is rotated while the internal lamp is open and a 30 mm aluminum (Al1030) part is clamped.

The difference between power consumption measurements of the spindle assembly and the standby state provides the average variable auxiliary power consumption of the spindle ($P_{aux\_var\_servo\_av}$) in W for each rotational speed increment:

$$P_{aux\_var\_spindle\_av} = \left(E_{spindle} - E_{sb}\right)/t \tag{8.37}$$

where $E_{spindle}$ is the energy required by the spindle assembly in J, for 60 seconds at each rotational speed value. E_{sb} is the energy required at standby mode in J for 60 seconds and t is the measurement time period of 60 seconds.

8.3.1.2 Results

The results of the measurements are displayed in Table 8.2. $P_{aux\_var\_spindle\_av}$ values for each rotational speed are calculated using Equation (8.37) and shown in the last column. Figure 8.5 illustrates the second-order polynomial fit applied to these values.

Table 8.2 Power/Energy requirement of spindle assembly

n (rpm)	t (s)	E (J)	P (W)	$P_{aux\_var\_spindle\_av}$ (W)
0 (Standby)	60	42966.2	716.1	
125	60	44067.0	734.4	18
250	60	45894.5	764.9	49
375	60	47965.8	799.4	83
500	60	50064.3	834.4	118
625	60	52397.7	873.3	157
750	60	54645.1	910.8	195
875	60	57765.6	962.8	247
1000	60	60350.3	1005.8	290
1125	60	63538.9	1059.0	343
1250	60	66384.9	1106.4	390
1375	60	69747.7	1162.5	446
1500	60	73228.4	1220.5	504
1625	60	76648.4	1277.5	561
1750	60	80038.7	1334.0	618
1875	60	83608.6	1393.5	677
2000	60	86681.6	1444.7	729
2125	60	90765.1	1512.8	797
2250	60	94717.4	1578.6	863
2375	60	99003.6	1650.1	934
2500	60	102334.6	1705.6	989
2625	60	106937.9	1782.3	1066
2750	60	109988.7	1833.1	1117
2875	60	113222.9	1887.0	1171
3000	60	117120.3	1952.0	1236
3125	60	121211.8	2020.2	1304
3250	60	123764.8	2062.7	1347
3375	60	129065.4	2151.1	1435
3500	60	132408.9	2206.8	1491

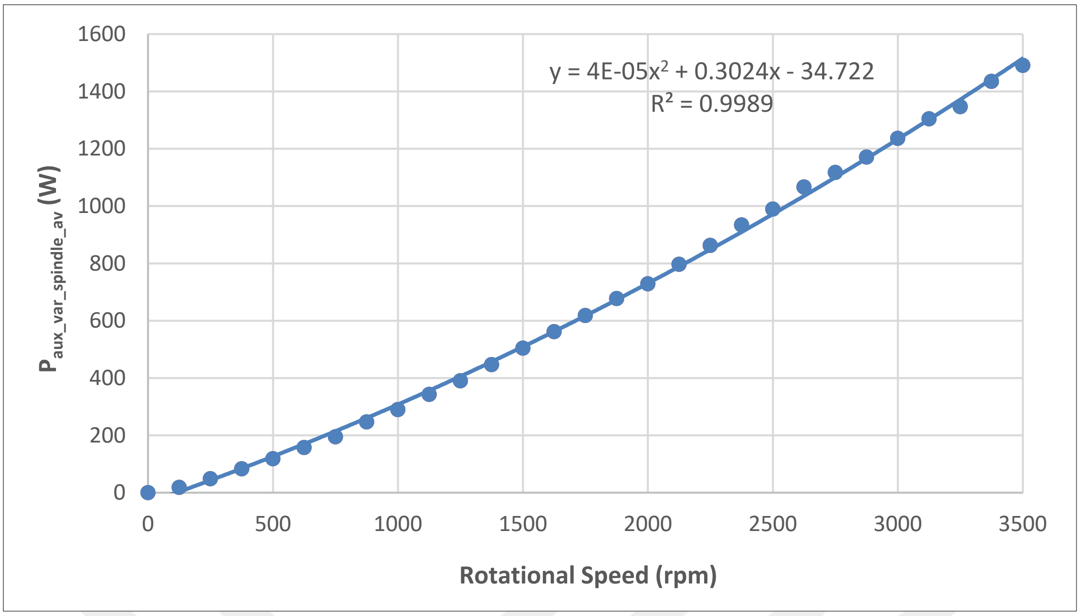

Figure 8.5 Auxiliary power consumption for spindle assembly

Based on the polynomial fit result, average variable auxiliary power consumption of spindle assembly ($P_{aux\_var\_spinde\_av}$) for a specific rotational speed will be estimated using the following quadratic equation, where n is the rotational speed in rpm of the spindle:

$$P_{aux\_var\_spindle\_av} = 0.00004\,n^2 + 0.3024\,n - 34.722 \tag{8.38}$$

8.3.2 Cutting Fluid System

Cutting fluid system is responsible for the coolant supply during machining. Estimation model assumes that the cutting fluid is active throughout all operations of the part. Therefore, the variable auxiliary energy requirement of the cutting fluid system ($E_{aux\_var\_fluid}$) is calculated using the following equation:

$$E_{aux\_var\_fluid} = P_{aux\_var\_fluid\_av}\ t_c \tag{8.39}$$

where $P_{aux\_var\_fluid\_av}$ is the average variable auxiliary power consumption of the cutting fluid system which is estimated based on the measurements taken on the CNC lathe. These measurements are presented in the next section. t_c is the total cutting time calculated based on the toolpaths and machining parameters as explained previously in Section 7.4.

8.3.2.1 Method

Energy and power measurements are taken for 300 seconds at two different states to isolate the impact of cutting fluid. The initial measurement is carried out with the cutting fluid activated, while the second one is performed with the cutting fluid turned off, representing the machine standby mode. During both measurements a 30 mm aluminum part (Al 6013) is clamped in chuck without spindle rotation and the internal machine light is kept on.

The difference between power consumption of two measurements gives the average variable auxiliary power consumption of cutting fluid system ($P_{aux\_var\_fluid\_av}$) in W:

$$P_{aux\_var\_fluid\_av} = \left(E_{fluid} - E_{sb}\right)/t \quad (8.40)$$

where E_{fluid} is the energy requirement in J for 300 seconds when cutting fluid is on, E_{sb} is the energy requirement in J for 300 seconds at standby when cutting fluid is off and t is the time period (300 seconds) for which the measurements are taken.

8.3.2.2 Results

Results of the measurements are presented in Figure 8.6 and Table 8.3. Using Equation (8.40), $P_{aux\_var\_fluid\_av}$ is calculated as 403.6 W.

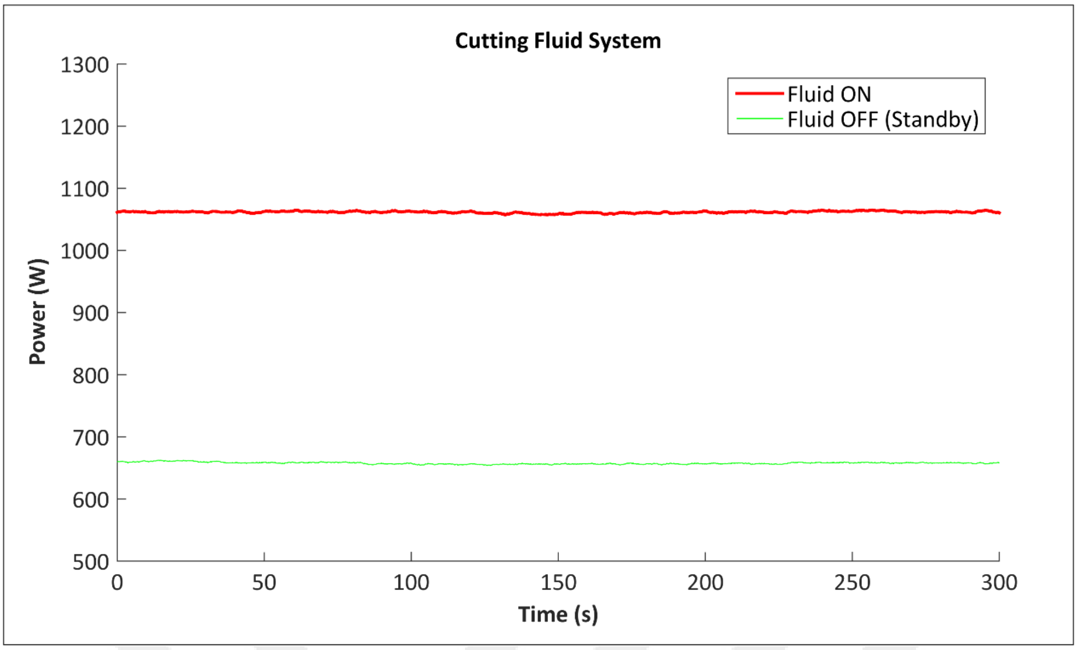

Figure 8.6 Power consumption for cutting fluid

Table 8.3 Average variable auxiliary power consumption of cutting fluid

	t (s)	E (J)	P (W)	$P_{aux\_var\_fluid\_av}$ (W)
Fluid OFF (Standby)	300	197283.6	657.6	
Fluid ON	300	318373.3	1061.2	**403.6**

8.3.3 Servo Motors for X and Z Axes

Servo motors control the axis motions. Their variable auxiliary energy requirements ($E_{aux\_var\_servo}$) are analyzed in two groups: rapid traverse (G00) and linear interpolation (G01) for each axis. Energy estimations are based on average power consumptions, calculated using the following four equations:

$$E_{aux\_var\_servoX00} = P_{aux\_var\_servoX00\_av}\ t_{servoX00} \tag{8.41}$$

$$E_{aux\_var\_servoZ00} = P_{aux\_var\_servoZ00\_av}\ t_{servoZ00} \tag{8.42}$$

$$E_{aux\_var\_servoX01} = P_{aux\_var\_servoX01\_av}\ t_{servoX01} \tag{8.43}$$

$$E_{aux\_var\_servoZ01} = P_{aux\_var\_servoZ01\_av}\ t_{servoZ01} \tag{8.44}$$

where $P_{aux\_var\_servo\_av}$ components represent the average auxiliary power consumption of the servo motors, estimated from measurements on the CNC lathe. The methodology for these measurements is explained in the following section. t_{servo} components denote the usage time of the servo motors for rapid traverse (G00) or linear interpolation (G01) motions throughout the machining process. These time values are updated at each step of the part program if the servo motors are active for the programmed block (Section 7.4).

8.3.3.1 Method

For rapid traverse energy measurements, two set of data are collected to determine the average auxiliary power consumption of each servo motor. In the first set of measurements, 30 reciprocations are executed using G00 along the X axis and 25 reciprocations along the Z axis (Table 8.4). The servo motors on the Anatool TP32 CNC lathe have a rapid traverse speed of 30000 mm/min (Anatool Machine Tools, 2009). Upon analyzing the collected data, the total time values of X and Z reciprocations are found to be 30.2 and 35.4 seconds, respectively (Table 8.5 and Table 8.6). In the second set of measurements, energy requirements are measured at standby mode for the time periods found in the first measurement set.

Table 8.4 Servo Motors: Rapid Traverse Measurements

Servo	# of reciprocations	Distance per Reciprocation (mm)
X Axis - G00	30	200 mm (between X-40 and X160)
Z Axis - G00	25	400 mm (between Z-50 and Z150)

For linear interpolation, energy measurements are taken at feed rate increments of 100 mm/min, ranging from 0 to 1400 mm/min. Using G01 command, the same coordinates are programmed for reciprocations in each axis, as shown in Table 8.4, but with a limited duration of approximately 40 seconds each. The number of reciprocations executed for each increment is determined based on this 40-second limit and the specific feed rate. 0 mm/min measurement represents the power consumption in standby mode.

During all measurements a 30 mm aluminum part (Al 6013) is clamped in chuck without spindle rotation and the internal machine light is kept on.

Difference between power consumption measurements of the servo motors and the standby state provides the average variable auxiliary power consumption of servo motors ($P_{aux\_var\_servo\_av}$) in W:

$$P_{aux\_var\_servo\_av} = (E_{servo} - E_{sb})/t \tag{8.45}$$

where E_{servo} is the energy requirement of servo motors in J for completing the reciprocations, E_{sb} is the energy requirement in J at standby mode and t is the time period for which the measurements are taken.

8.3.3.2 Results

Results of rapid traverse (G00) energy measurements are given in Figure 8.7 and Table 8.5 for X axis and Figure 8.8 and Table 8.6 for Z axis. Using Equation (8.45), $P_{aux\_var\_servoX00\_av}$ is calculated as 112.6 W and $P_{aux\_var\_servoZ00\_av}$ is 182.5 W.

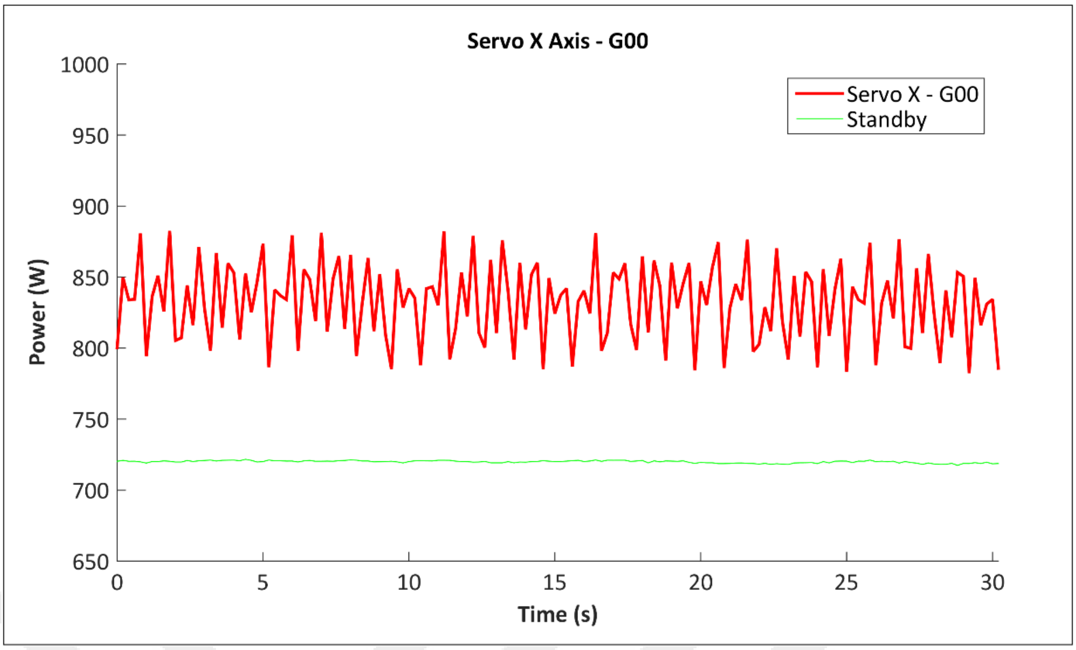

Figure 8.7 Power consumption for X Axis servo motor: G00

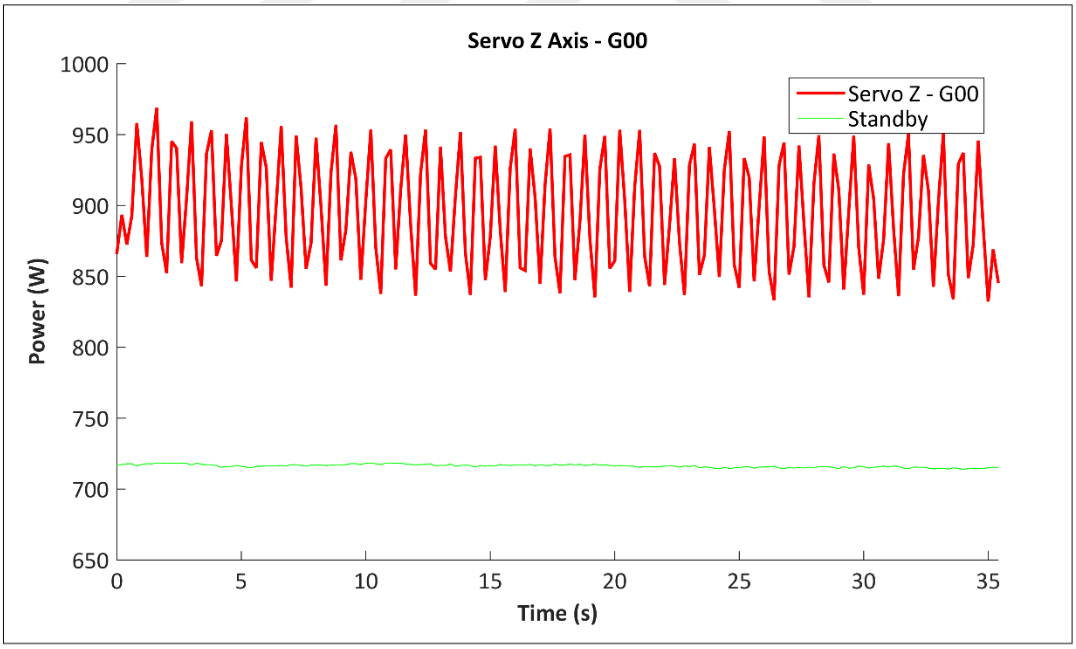

Figure 8.8 Power consumption for Z Axis servo motor: G00

Table 8.5 Average variable auxiliary power of X Axis servo motor: G00

	t (s)	E (J)	P (W)	$P_{aux\_var\_servoX00\_av}$ (W)
Standby	30.2	21645.2	716.7	
Servo X - G00	30.2	25045.5	829.3	**112.6**

Table 8.6 Average variable auxiliary power of Z Axis servo motor: G00

	t (s)	E (J)	P (W)	$P_{aux\_var\_servoZ00\_av}$ (W)
Standby	35.4	25364.2	716.5	
Servo Z - G00	35.4	31824.6	899.0	**182.5**

Results of linear interpolation (G01) energy measurements are presented in Table 8.7 and Figure 8.9 for X axis and Table 8.8 and Figure 8.10 for Z axis. $P_{aux\_var\_servo\_av}$ values for each feed rate are calculated using Equation (8.45) and presented in the last column of the tables.

It is evident from Figure 8.9 and Figure 8.10 that there is not a straightforward correlation between the feed rate and the individual variable auxiliary power consumption values. Consequently, the averages of these values, 7.7 W for the X axis and 6.4 W for the Z axis, are utilized for the $P_{aux\_var\_servo\_av}$ components from the following equations:

$$P_{aux\_var\_servoX01\_av} = \sum E_{servoX01} / \sum t_{servoX01} - E_{sb}/t_{sb} \tag{8.46}$$

$$P_{aux\_var\_servoZ01\_av} = \sum E_{servoZ01} / \sum t_{servoZ01} - E_{sb}/t_{sb} \tag{8.47}$$

Table 8.7 Power/Energy requirement of X Axis servo motor: G01

V_f (mm/min)	t (s)	E (J)	P (W)	$P_{aux\_var\_servoX01\_av}$ (W)
0 (Standby)	38	27007.9	710.7	
100	36	25472.0	707.6	-3.2
200	40	28669.3	716.7	6.0
300	39	28020.7	718.5	7.7
400	39	28098.6	720.5	9.7
500	40	28887.7	722.2	11.5
600	36	26106.6	725.2	14.4
700	39	28074.8	719.9	9.1
800	39	28150.7	721.8	11.1
900	37	26798.5	724.3	13.5
1000	40	28652.0	716.3	5.6
1100	39	27791.3	712.6	1.9
1200	36	25747.5	715.2	4.5
1300	35	25122.2	717.8	7.0
1400	40	28780.7	719.5	8.8
TOTAL	**535**	**384372.5**	-	**7.7**

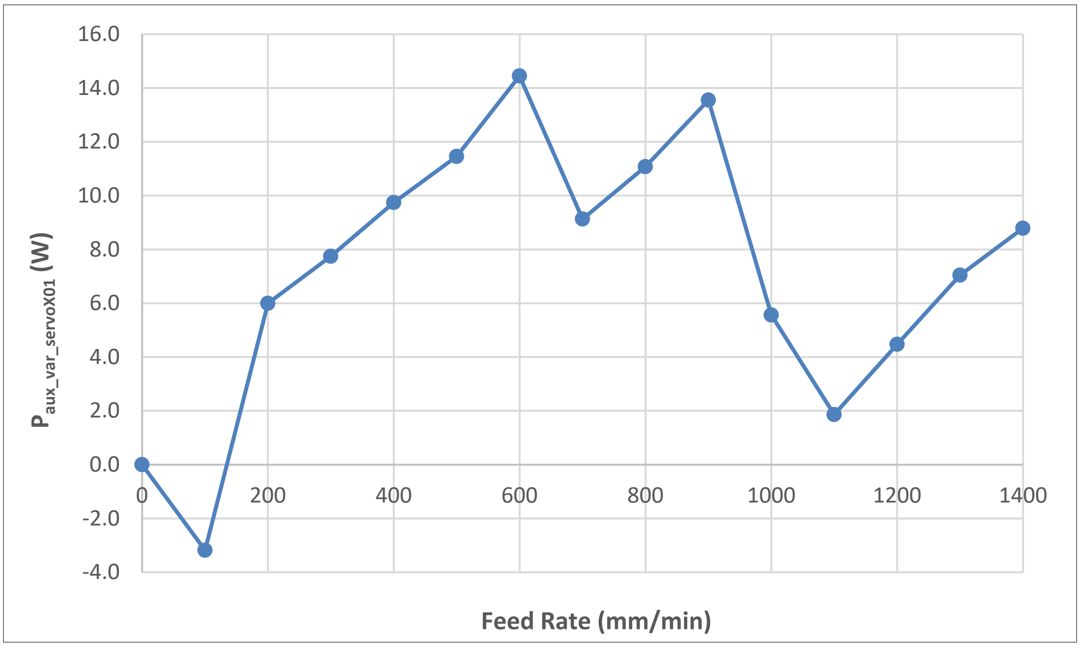

Figure 8.9 Auxiliary power consumption for X Axis servo motor: G01

Table 8.8 Power/Energy requirement of Z Axis servo motor: G01

V_f (mm/min)	t (s)	E (J)	P (W)	$P_{aux\_var\_servoZ01\_av}$ (W)
0 (Standby)	39	27899.7	715.4	
100	38	27306.0	718.6	3.2
200	38	27256.8	717.3	1.9
300	39	28113.7	720.9	5.5
400	40	29007.2	725.2	9.8
500	38	27300.2	718.4	3.0
600	39	27908.2	715.6	0.2
700	40	28890.2	722.3	6.9
800	38	27625.4	727.0	11.6
900	36	25922.0	720.1	4.7
1000	37	26856.2	725.8	10.5
1100	38	27419.5	721.6	6.2
1200	39	28312.4	726.0	10.6
1300	35	25351.7	724.3	9.0
1400	37	26714.9	722.0	6.6
TOTAL	**532**	**383984.5**	**-**	**6.4**

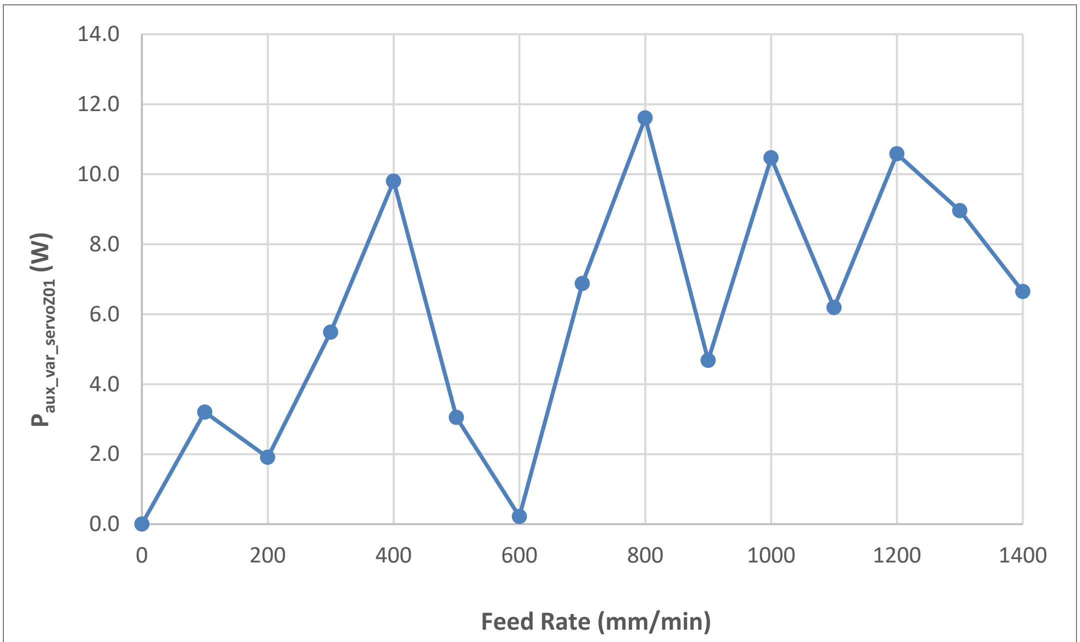

Figure 8.10 Auxiliary power consumption for Z Axis servo motor: G01

8.3.4 Turret

Turret indexing is not continuous during the cutting time and it occurs when the tool change command is activated. This leads to a non-uniform power consumption profile. It can be seen from Figure 8.11 that each tool change creates a power spike for about 4 seconds. For this reason, it is not feasible to use the average power value ($P_{aux\_var\_turret\_av}$) for the variable auxiliary energy estimation of turret. Instead, estimation is based on the average energy requirement ($E_{aux\_var\_turret\_av}$) of turret per tool change:

$$E_{aux\_var\_turret} = E_{aux\_var\_turret\_av} \; n_{ch} \tag{8.48}$$

where n_{ch} is the number of tool changes required for manufacturing a specific part tracked within the Part Programming module. $E_{aux\_var\_turret\_av}$ is based on CNC lathe measurements, detailed in the following section.

8.3.4.1 Method

Two different set of power and energy measurements are taken to find the average energy requirement of each tool change. For the first measurement, 10 tool change commands are executed at 10 seconds apart. A wait time of 10 seconds is added at the start and end. Turret of Anatool TP32 CNC Lathe can accommodate up to 10 tools and it utilizes bi-directional rotation enabling fast indexing of the target tool. In order to adopt a conservative approach, the indexing time is maximized by selecting two opposite tools (T3 and T8) on the turret. Total measurement time is recorded as 124 seconds. For the second measurement, power consumption and energy requirement are measured at standby mode for 124 seconds. During both measurements a 30 mm aluminum part (Al 6013) is clamped in chuck without spindle rotation and the internal machine light is kept on.

The difference between energy requirements per tool change of two measurements gives the average variable auxiliary energy requirement of the turret indexing ($E_{aux\_var\_turret\_av}$) in J:

$$E_{aux\_var\_turret\_av} = (E_{turret} - E_{sb})/n_{ch} \tag{8.49}$$

where E_{turret} is the energy requirement in J for 10 tool changes in 124 seconds, E_{sb} is the energy requirement in J for 124 seconds at standby and n_{ch} is 10 which is the total number of tool changes during measurements are taken.

8.3.4.2 Results

Results of the measurements are presented in Figure 8.11 and Table 8.9. Using Equation (8.49), $E_{aux\_var\_turret\_av}$ is calculated as 229.4 J.

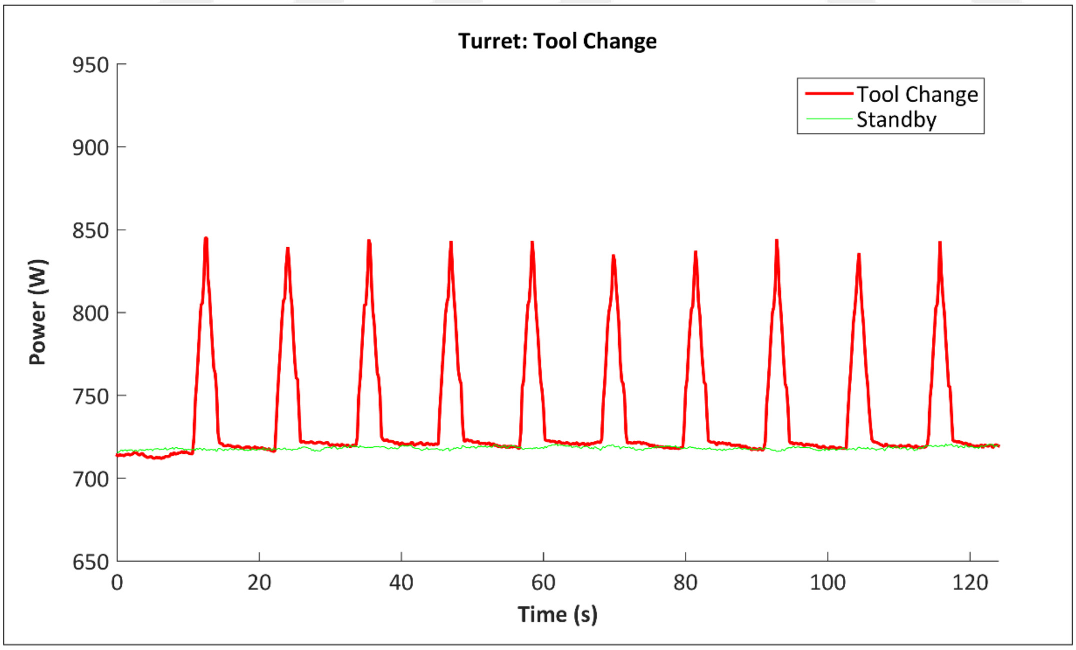

Figure 8.11 Power consumption for turret indexing

Table 8.9 Average variable auxiliary energy requirement of turret

	t (s)	E (J)	P (W)	$E_{aux\_var\_turret\_av}$ (J)
Standby	124	89052.1	718.2	
Tool Change	124	91345.7	736.7	**229.4**

8.3.5 Chuck

The pressure for the clamping system is maintained by the hydraulic system, which is a component of standby energy (Section 8.3.7 Standby Mode). However, each clamping action, i.e., chuck opening or closing, results in an additional power spike as shown in Figure 8.12. To estimate the energy required for these non-uniform power spikes, an average energy for each clamping pair (1 chuck open and 1 chuck close) is calculated instead of using the average power approach. Using this value, the variable auxiliary energy of chuck ($E_{aux\_var\_chuck}$) can be estimated as:

$$E_{aux\_var\_chuck} = E_{aux\_var\_chuck\_av} \ n_{clamp} \qquad (8.50)$$

where n_{clamp} denotes the number of clamping pairs required for manufacturing a specific part. Depending on the design, some parts may require more than one setup if two ends of the part require machining. However, as stated in Section 6.5, this study only considers parts manufactured in a single setup. Therefore, in this study, n_{clamp} is 1. $E_{aux\_var\_chuck\_av}$ is the average energy requirement for each clamping pair. The methodology for calculating $E_{aux\_var\_chuck\_av}$ is presented in the following section.

8.3.5.1 Method

Two different sets of power and energy measurements are taken to determine the average energy requirement of each clamping pair. For the first measurement, a 30 mm aluminum part (Al 6013) is clamped in chuck without spindle rotation. 5 clamping pairs are executed, with 20 seconds between each. After the chuck open command is executed, the chuck is kept in open state for 10 seconds. A wait time of 20 seconds is added at the start and end of the entire cycle. Total measurement time is recorded as 170 seconds. The summary of the first measurement cycle is as follows:

5 x (Wait 20s + Chuck open + Wait 10s + Chuck close) + Wait 20s

For the second measurement, power consumption and energy requirement are measured at standby mode for 170 seconds. A 30 mm aluminum part (Al 6013) is clamped in chuck all through the second measurement. During both measurements the internal machine light is kept on.

The difference between energy requirements divided by the total number of clamping pairs gives the average variable auxiliary energy requirement of the chuck per clamping pair ($E_{aux\_var\_chuck\_av}$) in J:

$$E_{aux\_var\_chuck\_av} = (E_{chuck} - E_{sb})/n_{clamp} \quad (8.51)$$

where E_{chuck} is the energy requirement in J for 5 clamping pairs in 170 seconds, E_{sb} is the energy requirement in J for 170 seconds at standby and n_{clamp} is 5 which is the total number of clamping pairs for the taken measurements.

8.3.5.2 Results

Results of the measurements are presented in Figure 8.12 and Table 8.10. Using Equation (8.51), $E_{aux\_var\_chuck\_av}$ is calculated as 171.5 J.

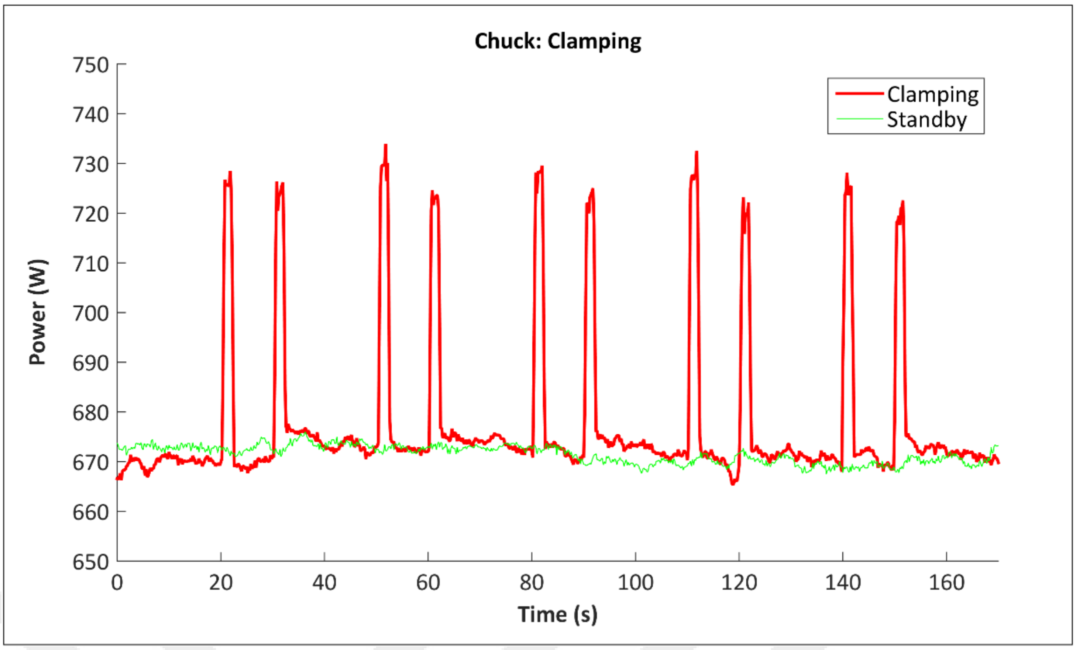

Figure 8.12 Power consumption for chuck

Table 8.10 Average variable auxiliary energy requirement of chuck

	t (s)	E (J)	P (W)	$E_{aux\_var\_chuck\_av}$ (J)
Standby	170	114235.0	672.0	
Clamping	170	115092.6	677.0	**171.5**

8.3.6 Lubrication System

Lubrication system is responsible for X and Z axis slideways lubrication. It operates intermittently at intervals set by the operator. For Anatool TP 32 CNC lathe, intervals can be set between 0 and 150 minutes by adjusting the knob on the lubrication pump (Figure 8.13). Shorter intervals are suitable for frequent use of the CNC lathe.

Figure 8.13 Lubricator on Anatool TP 32 CNC Lathe

Each lubrication creates a discrete power profile, as seen in Figure 8.14. This profile makes the lubrication system unsuitable for power based energy estimation. Instead, the variable auxiliary energy estimation of the lubrication system ($E_{aux\_var\_lub}$) is based on the average energy requirement approach:

$$E_{aux\_var\_lub} = E_{aux\_var\_lub\_av} \; n_{lub} \tag{8.52}$$

where $E_{aux\_var\_lub\_av}$ represents the average energy required for each axis lubrication. The methodology for calculating $E_{aux\_var\_lub\_av}$ is explained in the following section. n_{lub} denotes the number of lubrications during the manufacture of the designed part. Each lubrication takes approximately 11 seconds. Depending on the total cutting time of the part, lubrication may not occur during machining (e.g., if the total cutting time for a part is 3 minutes and lubrication interval is 30 minutes). To allocate the effect of lubrication to the process energy of the part, fraction of the lubrication energy proportional to the machining time of the designed part is used. Therefore, n_{lub} becomes:

$$n_{lub} = \frac{t_c}{t_{lub\_interval}} \tag{8.53}$$

where t_c is the total cutting time of the designed part and $t_{lub\_interval}$ is the interval set by the operator. For this study, it is set to 60 minutes, the default value of CNC lathe.

8.3.6.1 Method

Two different set of power and energy measurements are taken to isolate the average energy requirement of each lubrication. For the first measurement, 5 lubrications are made manually by setting the knob at 0 minutes. Each lubrication takes around 11 seconds and the time between lubrications is 20 seconds. A wait time of 20 seconds is added at the end of the whole cycle. Total measurement time is recorded as 174 seconds. The summary of the first measurement cycle is as follows:

5 x (Wait 20 seconds + Lubrication:~11 seconds) + Wait 20 seconds

In the second measurement, power consumption and energy requirements are recorded in standby mode for 174 seconds. Throughout this period, a 30 mm aluminum part (Al 6013) remained clamped in the chuck. The internal machine light was kept on during both measurements.

The difference in energy requirements, divided by the total number of lubrications provides the average variable auxiliary energy requirement for each lubrication ($E_{aux\_var\_lub\_av}$) in J:

$$E_{aux\_var\_lub\_av} = (E_{lub} - E_{sb})/n_{lub} \tag{8.54}$$

where E_{lub} is the energy requirement in J for 5 lubrications in 174 seconds, E_{sb} is the energy requirement in J for 174 seconds at standby and n_{lub} is 5 which is the total number of lubrications for the taken measurements.

8.3.6.2 Results

Results of the measurements are presented in Figure 8.14 and Table 8.13. Using Equation (8.54), $E_{aux\_var\_lub\_av}$ is calculated as 1975.5 J.

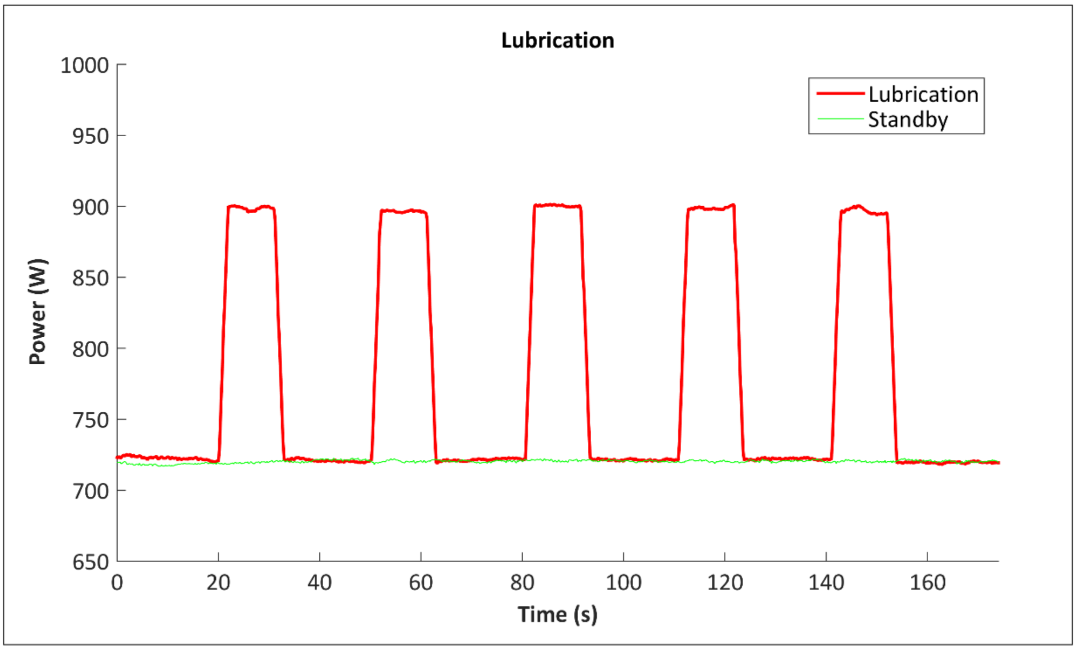

Figure 8.14 Power consumption for lubrication

Table 8.11 Average variable auxiliary energy requirement of lubrication

	t (s)	E (J)	P (W)	$E_{aux\_var\_lub\_av}$ (J)
Standby	174	125322.6	720.2	
Lubrication	174	135199.8	777.0	**1975.5**

8.3.7 Standby Mode

Standby mode in a CNC lathe refers to a state where the machine is powered on but not actively performing any machining operations. It occurs when all preparatory operations are completed after start-up and the machine is idle at a steady state.

Standby energy is the energy consumed by a manufacturing system when it is not actively engaged in production but remains powered on and operational. This includes energy used by components such as hydraulic systems for maintaining pressure build up, internal machine lighting and other auxiliary systems that continue to draw power even when idle.

Standby energy requirement ($E_{aux\_cons\_sb}$) is the only component for the constant auxiliary energy component of the estimation model and it is calculated using the formula below:

$$E_{aux\_cons\_sb} = P_{aux\_cons\_sb\_av}\ t_c \tag{8.55}$$

where $P_{aux\_cons\_sb\_av}$ is the average constant auxiliary power consumption at the standby mode derived from the new and previous measurements taken on the CNC lathe, as outlined in the next section. t_c represents the total cutting time calculated from toolpaths and machining parameters, as explained earlier in Section 7.4.

8.3.7.1 Method

Power consumption and energy requirements are measured at standby mode for 300 seconds. Throughout this period, a 30 mm aluminum part (Al 6013) is clamped in the chuck and the internal machine light is kept on. Besides this measurement, to calculate an overall average constant auxiliary power consumption, all standby measurements collected for other auxiliary equipment are considered, as well.

8.3.7.2 Results

Results of the new and previous measurements for corresponding sections are summarized in Table 8.12. $P_{aux\_cons\_sb\_av}$ is calculated as 690 W using the following equation:

$$P_{aux\_cons\_sb\_av} = \sum E_{sb} / \sum t_{sb} \tag{8.56}$$

where E_{sb} are the energy values of each standby mode measurement in J and t_{sb} are the corresponding time periods for the measurements taken.

Table 8.12 Average constant auxiliary power consumption of standby mode

Section	Components at Standby	t_{sb} (s)	E_{sb} (J)	$P_{aux\_cons\_sb\_av}$ (W)
8.3.1.2	**Spindle Assembly**	60	42966.2	716.1
8.3.2.2	**Cutting Fluid System**	300	197283.6	657.6
8.3.3.2	**Servo X Axis - G00**	30.2	21645.2	716.7
8.3.3.2	**Servo Z Axis - G00**	35.4	25364.2	716.5
8.3.3.2	**Servo X Axis - G01**	38	27007.9	710.7
8.3.3.2	**Servo Z Axis - G01**	39	27899.7	715.4
8.3.4.2	**Turret**	124	89052.1	718.2
8.3.5.2	**Chuck**	170	114235.0	672.0
8.3.6.2	**Lubrication System**	174	125322.6	720.2
8.3.7.2	**Standby**	300	205969.3	686.6
TOTAL		1270.6	876745.8	**690.0**

8.4 Carbon Footprint Estimation

According to the GHG protocol (WBCSD and WRI, 2004), in order to achieve emission reduction goals, first organizational boundaries should be set and then operational boundaries should be determined. Operational boundaries encompass scope 1, scope 2 and scope 3 emissions (Figure 8.15). Scope 1 covers direct emissions from sources owned or controlled by a company. Scope 2 includes indirect emissions originating from the generation of purchased electricity used by a company. These emissions occur at the facility where electricity is generated. Scope 3 comprises indirect emissions resulting from a company's activities but originating from sources not owned or controlled by the company. Scope 3 emissions involve both upstream and downstream emissions and represent the largest opportunity for GHG reductions.

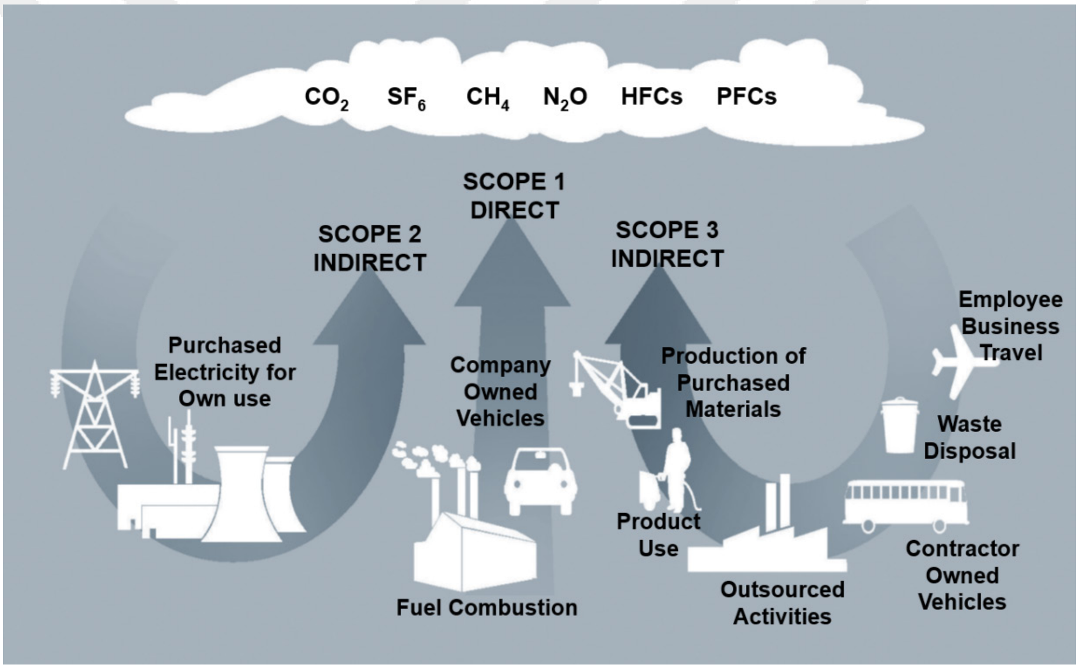

Figure 8.15 GHG emission sources (WBCSD and WRI, 2004)

According to 2021 data from National Inventory Report (TurkStat, 2023), 71.3% of the GHG in Turkey originate from the fossil fuel combustion in energy sector with 39.63% of those emissions attributed to electricity production. It is evident that, for an enterprise aiming to reduce its environmental impact through sustainable manufacturing, decreasing electricity dependency and improving energy efficiency in manufacturing processes are essential. Therefore this study focuses on Scope 2 indirect GHG emissions resulting from purchased electricity used by the company.

Jeswiet and Kara (2008) have proposed a method for estimating carbon footprints in a system that uses electric power grids. This method proposes a Carbon Emission Signature (CES™) that has a unit of kg CO_2/GJ. CES™ depends on the primary energy supplies of a power grid. The carbon emitted for manufacturing processes of a single part ($CE_{process}$) can be estimated by multiplying the electrical energy required for manufacturing that part ($E_{process}$) by the Carbon Emission Signature (CES):

$$CE_{process} = E_{process}\ CES \tag{8.57}$$

In the estimation model, Equation (8.57) is broken down into CE_{th} and CE_{aux} components to report the amount of carbon emitted as a result of the theoretical and auxiliary energy requirements, respectively.

CES can be calculated by the following equation:

$$CES = \frac{1}{\eta}\ (112 \cdot \%C + 49 \cdot \%NG + 66 \cdot \%P) \tag{8.58}$$

where C (coal), NG (natural gas) and P (petroleum) are the fractions of primary energy sources. Coefficients 112, 49 and 66 are the kilograms of carbon released per gigajoule of heat for each case. Lastly η is the efficiency of energy conversion.

The distribution of gross electricity generation by primary energy resources in Turkey is presented in Table 8.13 (TEİAŞ, 2022b). Based on the data fractions for C, NG and P are 34.6%, 22.9% and 0.1% respectively. Using a conversion efficiency of 0.34, CES for Turkey can be calculated as 147.3 kg CO_2/GJ.

Table 8.13 Turkey's electricity generation by primary resources (TEİAŞ,2022b)

Primary Resources	**E (GWh)**	**E (GWh)**	**%**
Hard coal+Asphaltite	6037.9		
Imported Coal	62541.3		
Lignite	45140.3		
Coal Total		113719.5	**34.6**
Fuel oil	382.5		
Diesel oil	10.4		
LPG	1.5		
Naphtha	0.0		
Liquid Fuels Total		394.4	**0.1**
Natural Gas		75058.7	**22.9**
Waste Heat		1364.4	**0.4**
Renew.+Waste	8088.2		
Hydro	66802.5		
Geothermal	11118.8		
Wind	34945.4		
Solar	16887.6		
Renewable Total		137842.5	**42.0**
TOTAL		**328379.3**	**100.0**

8.5 Sample Code

The theoretical energy (E_{th}) estimation module of TurnDesign Eco Edition is activated whenever a new feature is added to the design. It loops through all current features of the design, grouping and processing each under a "Case" statement. Each "Case" statement is dedicated to a specific feature and includes parametric volume removal calculations, theoretical energy and CO_2 emission estimations (detailed in Section 8.2.1). After processing all features, the final part of the code adds these results to the feature tree of TurnDesign Eco Edition for visualization.

Table 8.14 illustrates a sample "Case" statement for the Outer Diameter to Shoulder feature. The initial section of the code integrates Equations (8.10) to (8.24) to calculate the material removal volume for rough outer turning operation. The second section computes the total removed volume for the feature using the same equations. Lastly, the final section estimates E_{th} and CO_2 based on removed volume calculations, specific cutting energy values from Equation (8.4) and CES^{TM} value (referred to as CO2_conv in the code) from Equation (8.58).

Table 8.14 Code for E_{th} calculation of Outer Diameter to Shoulder

```
Case "ODSHLD":
'Volume removed: rough
Di_finish(i) = Di(i) + 2 * a_p(3)
Df_finish(i) = Df(i) + 2 * a_p(3)
Rp_finish(i) = Rp(i) + a_p(3)

Vrect_rough(i) = Pi / 4 * (Dmax + 2 * a_p(3)) ^ 2 * (z_pos_end(i) -
z_pos(i))

Vtrap1_rough(i) = Pi / 12 * (Di_finish(i) ^ 2 + 2 * Di_finish(i) *
Rp_finish(i) + 4 * Rp_finish(i) ^ 2) * (Di_finish(i) / 2 - Rp_finish(i))
/ (Tan(Pi - (alpha_e(i) + beta(i)) * measure.angle_convertion_factor))

Vtrap2_rough(i) = Pi / 12 * (Df_finish(i) ^ 2 + 2 * Df_finish(i) *
Rp_finish(i) + 4 * Rp_finish(i) ^ 2) * (Df_finish(i) / 2 - Rp_finish(i))
/ (Tan(alpha_e(i) * measure.angle_convertion_factor))

Atri_rough(i) = rad(i) ^ 2 * (Cos(beta(i) *
measure.angle_convertion_factor / 2)) ^ 3 / Sin(beta(i) *
measure.angle_convertion_factor / 2)
rtri_rough(i) = 2 / 3 * rad(i) * (Cos(beta(i) *
measure.angle_convertion_factor / 2)) ^ 2 / Sin(beta(i) *
measure.angle_convertion_factor / 2) * Sin((beta(i) / 2 + alpha_e(i)) *
measure.angle_convertion_factor) + Rp_finish(i)
Vtri_rough(i) = 2 * Pi * rtri_rough(i) * Atri_rough(i)

Aseg_rough(i) = rad(i) ^ 2 / 2 * (Pi - beta(i) *
measure.angle_convertion_factor - Sin(Pi - beta(i) *
measure.angle_convertion_factor))
rseg_rough(i) = (rad(i) / Sin(beta(i) * measure.angle_convertion_factor
/ 2) - 4 * rad(i) / 3 * (Sin(Pi / 2 - beta(i) *
measure.angle_convertion_factor / 2)) ^ 3 / (Pi - beta(i) *
measure.angle_convertion_factor - Sin(Pi - beta(i) *
measure.angle_convertion_factor))) * Sin((beta(i) / 2 + alpha_e(i)) *
measure.angle_convertion_factor) + Rp_finish(i)
Vseg_rough(i) = 2 * Pi * rseg_rough(i) * Aseg_rough(i)

Vr_rough(i) = Vrect_rough(i) - Vtrap1_rough(i) - Vtrap2_rough(i) -
Vtri_rough(i) + Vseg_rough(i)

'Volume removed: all
Vrect(i) = Pi / 4 * (Dmax + 2 * a_p(3)) ^ 2 * (z_pos_end(i) - z_pos(i))

Vtrap1(i) = Pi / 12 * (Di(i) ^ 2 + 2 * Di(i) * Rp(i) + 4 * Rp(i) ^ 2) *
(Di(i) / 2 - Rp(i)) / (Tan(Pi - (alpha_e(i) + beta(i)) *
measure.angle_convertion_factor))
```

Table 8.14 (continued)

```
Vtrap2(i) = Pi / 12 * (Df(i) ^ 2 + 2 * Df(i) * Rp(i) + 4 * Rp(i) ^ 2) *
(Df(i) / 2 - Rp(i)) / (Tan(alpha_e(i) *
measure.angle_convertion_factor))

Atri(i) = rad(i) ^ 2 * (Cos(beta(i) * measure.angle_convertion_factor /
2)) ^ 3 / Sin(beta(i) * measure.angle_convertion_factor / 2)
rtri(i) = 2 / 3 * rad(i) * (Cos(beta(i) *
measure.angle_convertion_factor / 2)) ^ 2 / Sin(beta(i) *
measure.angle_convertion_factor / 2) * Sin((beta(i) / 2 + alpha_e(i)) *
measure.angle_convertion_factor) + Rp(i)
Vtri(i) = 2 * Pi * rtri(i) * Atri(i)

Aseg(i) = rad(i) ^ 2 / 2 * (Pi - beta(i) *
measure.angle_convertion_factor - Sin(Pi - beta(i) *
measure.angle_convertion_factor))
rseg(i) = (rad(i) / Sin(beta(i) * measure.angle_convertion_factor / 2) -
4 * rad(i) / 3 * (Sin(Pi / 2 - beta(i) * measure.angle_convertion_factor
/ 2)) ^ 3 / (Pi - beta(i) * measure.angle_convertion_factor - Sin(Pi -
beta(i) * measure.angle_convertion_factor))) * Sin((beta(i) / 2 +
alpha_e(i)) * measure.angle_convertion_factor) + Rp(i)
Vseg(i) = 2 * Pi * rseg(i) * Aseg(i)

Vr(i) = Vrect(i) - Vtrap1(i) - Vtrap2(i) - Vtri(i) + Vseg(i)

Vr_finish(i) = Vr(i) - Vr_rough(i)



'Eth and CO2 calculations
Eth_rough(i) = Vr_rough(i) * ps(2)
Eth_finish(i) = Vr_finish(i) * ps(3)
CO2th_rough(i) = Eth_rough(i) * CO2_conv
CO2th_finish(i) = Eth_finish(i) * CO2_conv

Eth(i) = Eth_rough(i) + Eth_finish(i)
CO2th(i) = CO2th_rough(i) + CO2th_finish(i)
```

After the loop for features is completed and the results are added to the feature tree, theoretical energy calculations for miscellaneous operations are performed, as detailed in Section 8.2.2. Code for these calculations are presented in Table 8.15 under three categories: stock removal, facing and parting. Each category involves volume calculations, theoretical energy requirement and CO_2 emission estimations. These values for stock removal, facing and parting are then added to the feature tree under a "Miscellaneous" group for visualization and easy reference by the user.

Table 8.15 Code for E_{th} calculation of miscellaneous operations

```
'Calculate MISC Eth & CO2

'*****Dstock to Dmax + 2 * a_p(3)
Vr_stock_normal = Pi / 4 * (Dstock_current ^ 2 - (Dmax + 2 * a_p(3)) ^
2) * (Lmax_current + a_p(20))
Vr_stock_sweep = Pi / 4 * (Dmax + 2 * a_p(3)) ^ 2 * a_p(20) - Vr_partoff
Vr_stock = Vr_stock_normal + Vr_stock_sweep
Eth_stock = Vr_stock_normal * ps(2) + Vr_stock_sweep * ps(3)
CO2th_stock = Eth_stock * CO2_conv

'*****Facing
Vr_facing = Pi / 4 * Dstock_current ^ 2 * a_p(1)
Eth_facing = Vr_facing * ps(1)
CO2th_facing = Eth_facing * CO2_conv

'*****Part-off
Vr_partoff = Pi / 4 * Dmax ^ 2 * a_p(20)
Eth_partoff = Vr_partoff * ps(20)
CO2th_partoff = Eth_partoff * CO2_conv
```

Similar to the E_{th} module, the auxiliary energy (E_{aux}) estimation module runs when a new feature is added to the current design. The module is presented in Table 8.16. Initial section of the code calculates the variable and constant auxiliary components along with the corresponding CO_2 emissions using the equations from Section 8.3. The final section of the code aggregates these findings into the auxiliary energy estimation and the total energy requirement for the manufacturing processes, which is the major output of the estimation model.

Table 8.16 Code for E_{aux} calculation

```
Public Sub calc_energy_aux()

'E_aux_var components
E_aux_var_spindle_tot = 0
For j = 1 To 20
E_aux_var_spindle(j) = P_aux_var_spindle_av(j) * t_op(j)
CO2_aux_var_spindle(j) = E_aux_var_spindle(j) * CO2_conv
E_aux_var_spindle_tot = E_aux_var_spindle_tot + E_aux_var_spindle(j)
CO2_aux_var_spindle_tot = E_aux_var_spindle_tot * CO2_conv
Next j

E_aux_var_fluid = P_aux_var_fluid_av * t_c_current
CO2_aux_var_fluid = E_aux_var_fluid * CO2_conv

E_aux_var_turret = E_aux_var_turret_av * n_ch
CO2_aux_var_turret = E_aux_var_turret * CO2_conv
```

Table 8.16 (continued)

```
E_aux_var_chuck = E_aux_var_chuck_av * 1 'no of clamps=1 ie 1 setup
CO2_aux_var_chuck = E_aux_var_chuck * CO2_conv

E_aux_var_servox = P_aux_var_servox00_av * t_servox00 +
P_aux_var_servox01_av * t_servox01
E_aux_var_servoz = P_aux_var_servoz00_av * t_servoz00 +
P_aux_var_servoz01_av * t_servoz01
CO2_aux_var_servox = E_aux_var_servox * CO2_conv
CO2_aux_var_servoz = E_aux_var_servoz * CO2_conv

E_aux_var_lub = E_aux_var_lub_av * t_c_current / t_lub_interval
CO2_aux_var_lub = E_aux_var_lub * CO2_conv


'E_aux_cons components
E_aux_cons_sb = P_aux_cons_sb_av * t_c_current
CO2_aux_cons_sb = E_aux_cons_sb * CO2_conv


'E_aux_var and E_aux_cons
E_aux_var = E_aux_var_spindle_tot + E_aux_var_fluid + E_aux_var_turret +
E_aux_var_chuck + E_aux_var_servox + E_aux_var_servoz + E_aux_var_lub
CO2_aux_var = E_aux_var * CO2_conv

E_aux_cons = E_aux_cons_sb
CO2_aux_cons = E_aux_cons * CO2_conv


'E_aux
E_aux = E_aux_var + E_aux_cons
CO2_aux = E_aux * CO2_conv


'E_tot
E_tot = E_aux + E_th
CO2_tot = E_tot * CO2_conv


End Sub
```

The code that inputs average auxiliary power and energy values is illustrated in Table 8.17. Derived from measurements on the TP32 CNC lathe, as detailed in Section 8.3, these values are used in the auxiliary energy estimation module for each component. Since these values are specific to this lathe, they are integrated into the model within the machine definition submodule of the Process Planning module. If TurnDesign Eco Edition is employed with a different CNC lathe, this part of the code can be recalibrated for the new machine by adjusting the parameters shown in the table.

Table 8.17 Code for average power or energy components of TP32 lathe

```
'Power and Energy Calibration for TP32 Anatool
For j = 1 To 20
P_aux_var_spindle_av(j) = 0.00004 * n(j) ^ 2 + 0.3024 * n(j) - 34.722
Next j
P_aux_var_fluid_av = 403.6
E_aux_var_turret_av = 229.4
E_aux_var_chuck_av = 171.5
P_aux_var_servox00_av = 112.6
P_aux_var_servox01_av = 7.7
P_aux_var_servoz00_av = 182.5
P_aux_var_servoz01_av = 6.4
E_aux_var_lub_av = 1975.5

P_aux_cons_sb_av = 690
```

8.6 Output

Energy and carbon footprint estimation modules of TurnDesign Eco Edition produce two main outputs. The first is displayed in real time on the visual interface of TurnDesign Eco Edition, providing current information on energy requirement and CO_2 emissions for the ongoing design. These values update instantly with any design changes made. The second output is an Excel report, providing a thorough breakdown of all estimation model results, along with pie charts for visualization. While this report is also updated in real time, its primary purpose is detailed analysis after the design process is complete.

Energy outputs on the visual interface are displayed on the left pane, as shown in Figure 8.16. The table at the bottom left provides high level energy and CO_2 results for the current design, detailing total, theoretical and auxiliary energy values. Above it, the feature tree lists design features alongs with their theoretical energy and CO_2 emissions.

The second major output is the Excel report which presents all the energy requirement and carbon emission outputs of the estimation model in details. The report generates three tabs: Theoretical Energy (Figure 8.17), Auxiliary Energy (Figure 8.18) and Process Energy (Figure 8.19). Each tab breaks down the

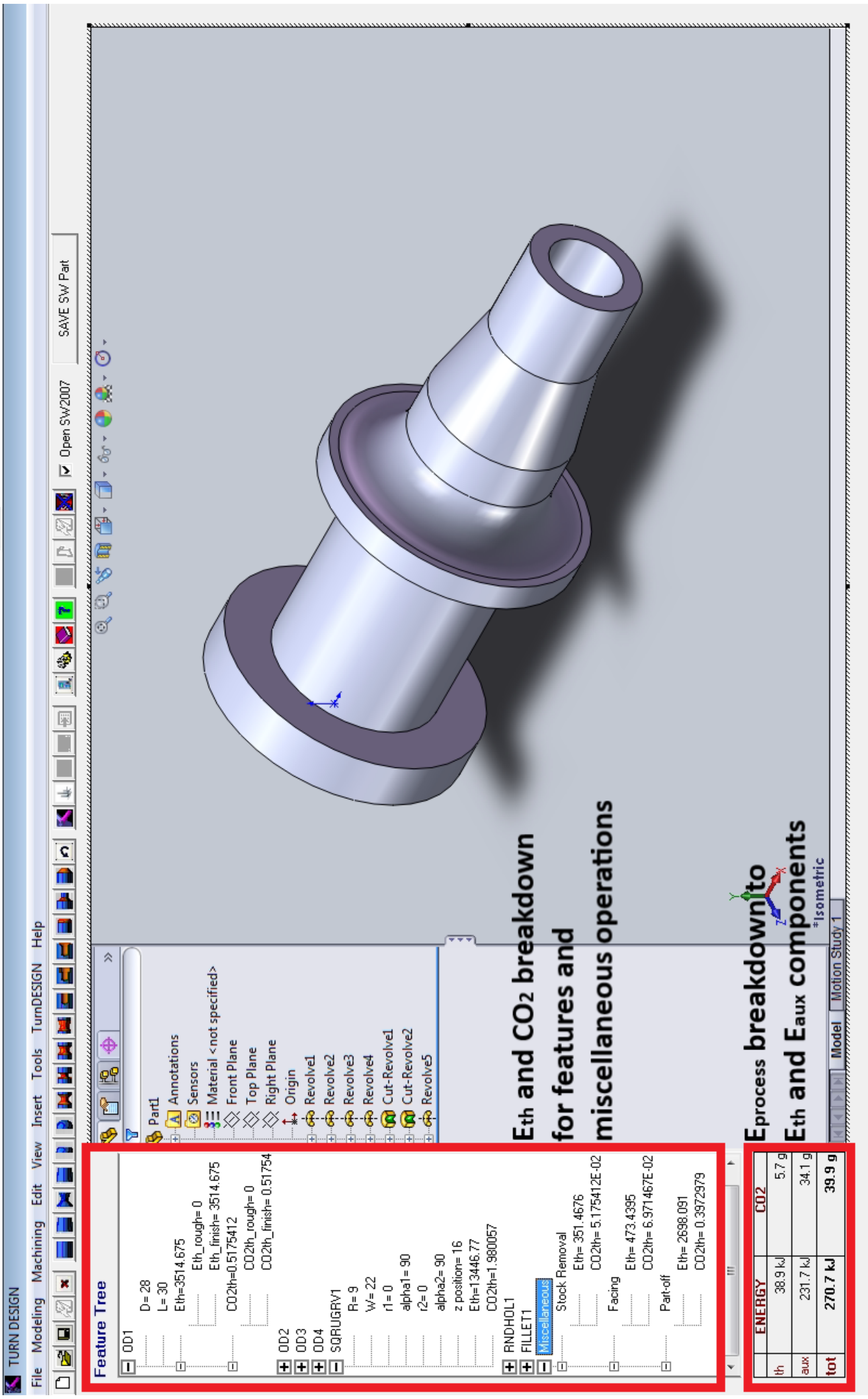

Figure 8.16 Energy and CO_2 outputs on the user interface for SP1-AL6013

estimations illustrating the energy requirement distributions in a user friendly format. This reporting format highlights the energy requirements of individual features, operations and auxiliary equipment, emphasizing components where the energy intensity is high and the areas of potential improvement.

Since theoretical energy estimation is based on features and miscellaneous operations, the breakdown and presentation of the results are grouped by design features, as well. Theoretical energy tab (Figure 8.17) shows the results in four main categories for each feature and miscellaneous operations: removed volumes, specific cutting energy values, theoretical energy requirements and corresponding CO_2 emissions. Each of these values is divided into rough and finish columns where applicable. The removed volume and specific cutting energy categories are used to calculate the energy and carbon emission values as explained in Section 8.2

The auxiliary energy tab categorizes estimation results under each auxiliary component. Depending on the characteristic of the component, usage parameters (usage time, number of uses), average power or energy requirement of that component, estimated auxiliary energy and CO_2 emissions are presented on the left of Figure 8.18. On the right, overall results display the shares of each auxiliary component on the total auxiliary energy requirement, including variable and constant shares. Pie charts visually depict the distribution of auxiliary energy among the components.

The process energy tab (Figure 8.19) data from other tabs to provide a comprehensive breakdown of energy requirement. It presents the total energy needed to machine the part, including both the theoretical and auxiliary components, along with the total CO_2 emissions. The top pie chart visually illustrates the distribution of energy requirements by displaying the proportion of each component in the total process energy. Below, additional pie charts offer a high-level insight into the shares of theoretical and auxiliary energy within the total process energy.

No	Feature	Volume-Rough [mm3]	Volume-Finish [mm3]	Volume-Total [mm3]	ps-Rough [J/mm3]	ps-Finish [J/mm3]
1	OD1	-	2,733	2,733	1.08	1.29
2	OD2	4,524	534	5,058	1.08	1.29
3	OD3	5,047	471	5,519	1.08	1.29
4	OD4	5,529	408	5,938	1.08	1.29
5	SQRUGRV1	-	-	7,948	1.69	-
6	RNDHOL1	-	-	477	1.33	-
7	FILLET1	-307	-	-307	1.08	1.29
No	**Operation**	**Volume-Rough [mm3]**	**Volume-Finish [mm3]**	**Volume-Total [mm3]**	**ps-Rough [J/mm3]**	**ps-Finish [J/mm3]**
1	Facing	-	-	353	1.34	-
2	Stock Removal	-	-	273	1.08	-
3	Parting	-	-	1,847	1.46	-
	TOTAL			**29,839**		

No	Feature	Eth-Rough [J]	Eth-Finish [J]	Eth-Total [J]	CO2-Rough [g]	CO2-Finish [g]	CO2-Total [g]
1	OD1	-	3,515	3,515	-	0.5	0.5
2	OD2	4,892	687	5,579	0.7	0.1	0.8
3	OD3	5,458	606	6,064	0.8	0.1	0.9
4	OD4	5,979	525	6,504	0.9	0.1	1.0
5	SQRUGRV1	-	-	13,447	-	-	2.0
6	RNDHOL1	-	-	633	-	-	0.1
7	FILLET1	-332	-	-332	0.0	-	0.0
No	**Operation**	**Eth-Rough [J]**	**Eth-Finish [J]**	**Eth-Total [J]**	**CO2-Rough [g]**	**CO2-Finish [g]**	**CO2-Total [g]**
1	Facing	-	-	473	-	-	0.1
2	Stock Removal	-	-	351	-	-	0.1
3	Parting	-	-	2,698	-	-	0.4
	TOTAL			**38,932**			**5.7**

Figure 8.17 Theoretical energy tab for SP1-AL6013

Spindle		OP Time [s]	P_aux_var_spindle_av [W]	E_aux_var_spindle [J]	CO2_spindle [g]
1	Facing	7	1,047.5	6,950	1.0
2	Turning - Rough	27	916.5	25,161	3.7
3	Turning - Finish	15	1,047.5	15,865	2.3
4	Drilling	5	1,513.7	7,655	1.1
5	Grooving	47	805.1	38,135	5.6
6	Parting	11	739.3	7,844	1.2
Total		**112**	**-**	**101,611**	**15.0**

Cutting Fluid	ON Time [s]	P_aux_var_fluid_av [W]	E_aux_var_fluid [J]	CO2_fluid [g]
	112	**403.6**	**45,311**	**6.7**

Turret	Tool Change #	E_aux_var_turret_av [J]	E_aux_var_turret [J]	CO2_turret [g]
	6	**229.4**	**1,376**	**0.2**

Chuck	Clamp #	E_aux_var_chuck_av [J]	E_aux_var_chuck [J]	CO2_chuck [g]
	1	**171.5**	**172**	**0.0**

Servo		Time [s]	P_aux_var_servo_av [W]	E_aux_var_servo [J]	CO2_servo [g]
Servo X	Rapid	16	112.6	1,758	0.3
Servo X	Feed	66	7.7	510	0.1
Servo Z	Rapid	18	182.5	3,277	0.5
Servo Z	Feed	32	6.4	202	0.0
Total		**-**	**-**	**5,747**	**0.8**

Lubrication	Lubrication #	E_aux_var_lub_av [J]	E_aux_var_lub [J]	CO2_lub [g]
	0.03	**1,975.5**	**62**	**0.0**

Standby	ON Time [s]	P_aux_cons_sb_av [W]	E_aux_cons_sb [J]	CO2_sb [g]
	112	**690.0**	**77,465**	**11.4**

	E_aux [J]	CO2_aux [g]	% Aux
Variable	154,279	22.7	67
Constant	77,465	11.4	33
TOTAL	**231,743**	**34.1**	**100**

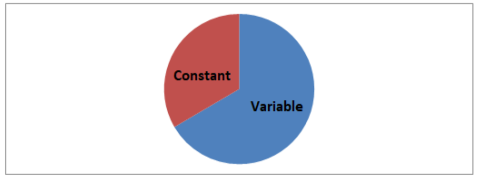

	E_aux [J]	CO2_aux [g]	% Aux
Spindle	101,611	15.0	44
Cutting Fluid	45,311	6.7	20
Turret	1,376	0.2	1
Chuck	172	0.0	0
Servo	5,747	0.8	2
Lubrication	62	0.0	0
Standby	77,465	11.4	33
TOTAL	**231,743**	**34.1**	**100**

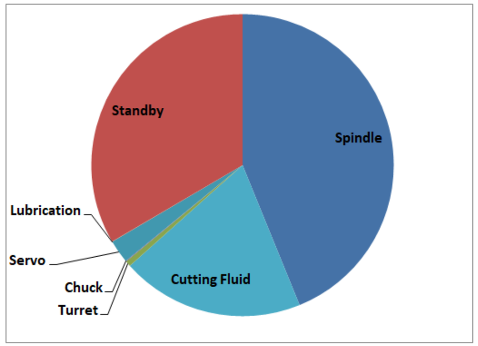

Figure 8.18 Auxiliary energy tab for SP1-AL6013

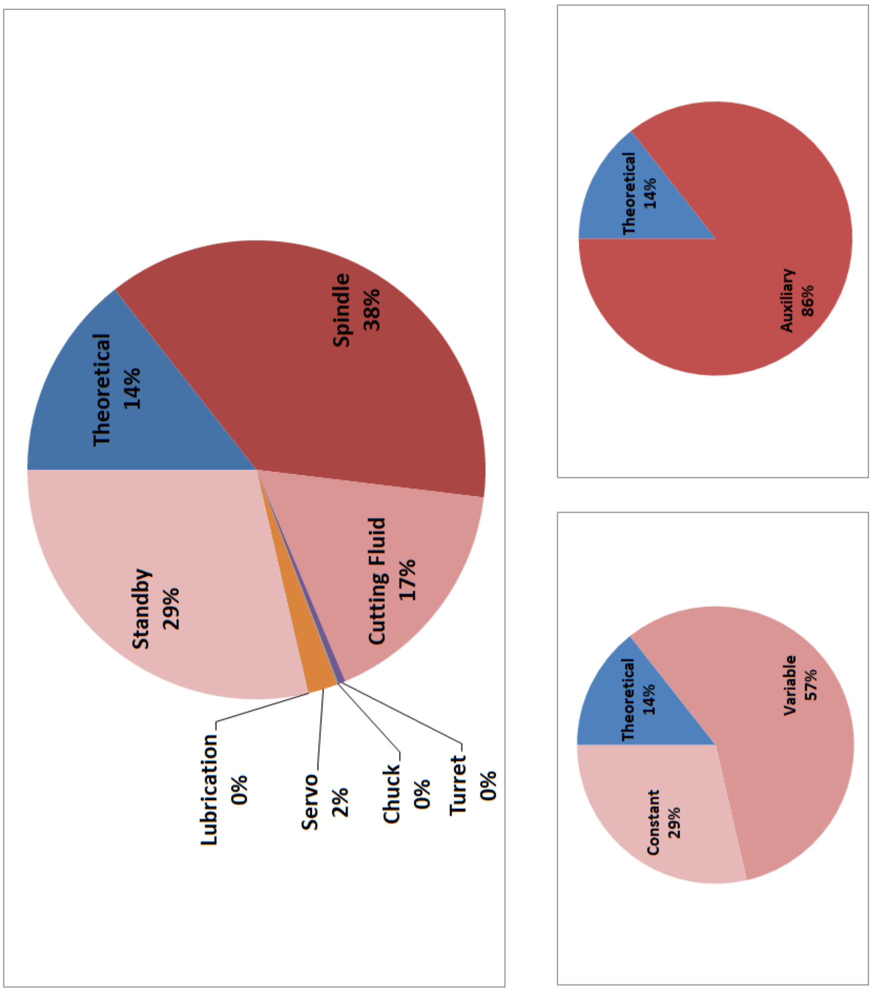

	E [J]	CO2 [g]	%
Theoretical	38,932	5.7	14
Spindle	101,611	15.0	38
Cutting Fluid	45,311	6.7	17
Turret	1,376	0.2	1
Chuck	172	0.0	0
Servo	5,747	0.8	2
Lubrication	62	0.0	0
Standby	77,465	11.4	29
TOTAL	**270,676**	**39.9**	**100**

	E [J]	CO2 [g]	%
Theoretical	38,932	5.7	14
Variable	154,279	22.7	57
Constant	77,465	11.4	29
TOTAL	**270,676**	**39.9**	**100**

	E [J]	CO2 [g]	%
Theoretical	38,932	5.7	14
Auxiliary	231,743	34.1	86
TOTAL	**270,676**	**39.9**	**100**

Figure 8.19 Process energy tab for SP1-AL6013

CHAPTER 9

TEST SET-UP AND VERIFICATION

9.1 Introduction

This chapter is dedicated to verifying the reliability of the developed estimation model. Section 9.2 outlines the test setup and monitoring system utilized in the verification studies. The TP32 CNC Lathe, along with the power measurement system, forms the basis of the test environment. Descriptions of the equipment, data collection and processing techniques to achieve accurate energy monitoring during machining operations are provided.

Section 9.3 focuses on the verification studies conducted with five sample parts. The design, outputs (MPS, Part program, AP224 file) and energy results for each sample part are documented. Estimated energy consumption and carbon footprint values are compared against actual measurements, demonstrating the performance of the model and identifying areas for improvement and future research.

9.2 Test Set-up

Test set-up involves the following three items. Details of them are provided in the following sections:

- Anatool TP32 CNC lathe
- Power Measurement System
- Data Collection and Processing

The general view of the test setup is illustrated in Figure 9.1. It shows the Siemens Sentron PAC3200 power meter (front) and the current transformers (back), which are components of the power measurement system. The Matlab Simulink interface used for data collection is also shown.

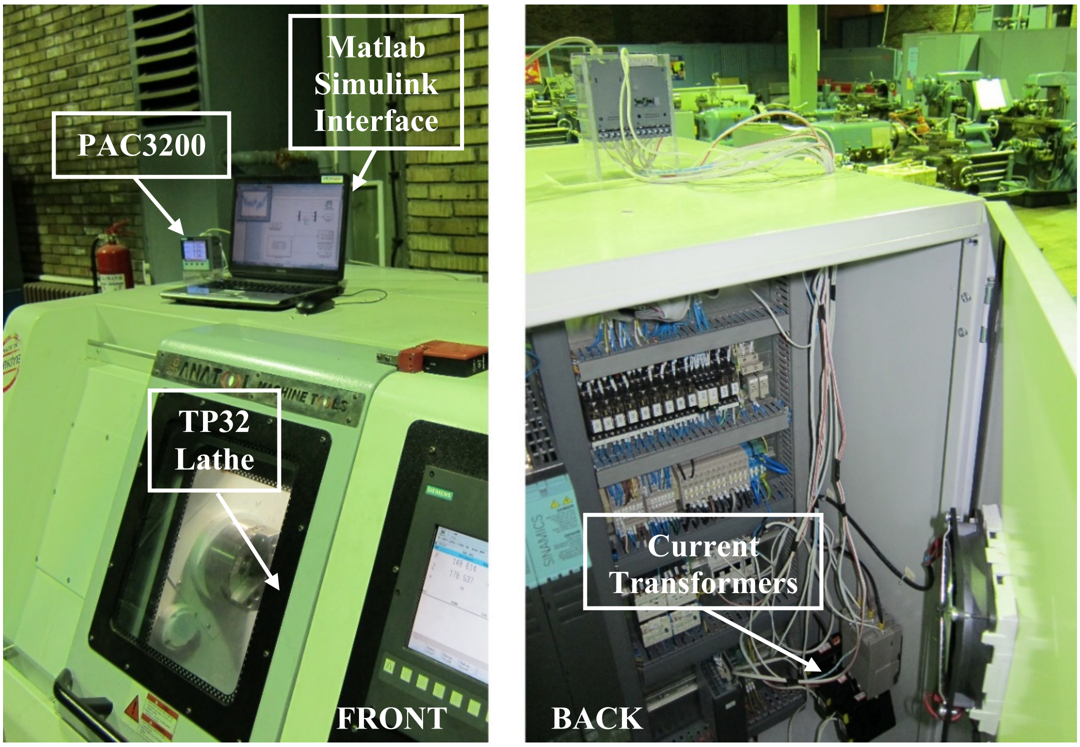

Figure 9.1 Test set-up

9.2.1 TP32 CNC Lathe

The Anatool TP32 is a two-axis lathe in the machine shop of Mechanical Engineering Department at METU. It operates on a Siemens Sinumerik 802D sl controller. The structure of the lathe is displayed in Figure 8.4 and its technical specifications are listed in Table 9.1.

Table 9.1 Technical Specifications of Anatool TP 32 CNC Lathe

Number of Axis	2 (X and Z)
Maximum Turning Diameter	200 mm
Maximum Turning Length	200 mm
Chuck Size	5 inch
Bar Capacity	32 mm
Axis Travel in X-axis	160 mm
Axis Travel in Z-axis	400 mm
Rapid Traverse Rate in X-Z Axes	40000 mm/min
Number of Tools	10
Main Spindle Motor	5.5 kW
Spindle Speed	4500 rpm
Total Nominal/Max. Power	8/15 kW
Nominal/Max. Current	20/40 A
Weight	2100 kg

9.2.2 Power Measurement System

Energy and power requirements during manufacturing are measured using a Siemens Sentron PAC3200 power meter, installed on the TP 32 lathe A connection type of 3P4W (Three-phase measuring, four conductors, unbalanced load, without voltage transformers, with three current transformers, Figure 9.2) is used to collect the necessary parameters from the device.

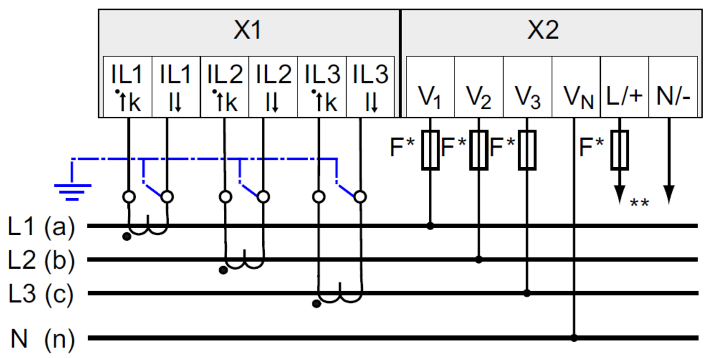

Figure 9.2 3P4W connection for PAC3200 (Siemens, 2008)

Parameters measured by PAC3200 are based on voltage and current inputs. Since PAC3200 is designed for measuring current of 1 A or 5 A, three external current transformers with a conversion ratio of 100A/5A are used. PAC3200 is connected to the internet by the RJ45 Ethernet port embedded on the device. Data is accessed with a PC through the OPC Server of MATLAB Simulink. The structure of the measurement system is illustrated in Figure 9.3.

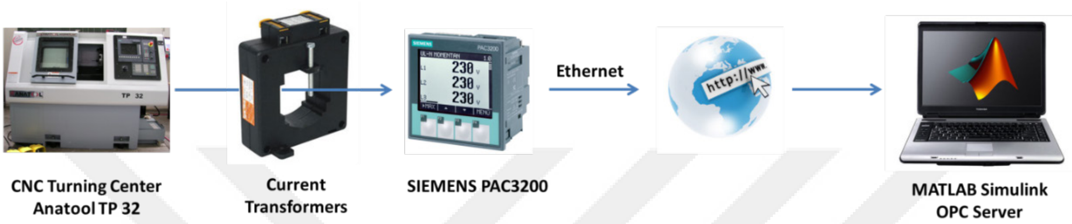

Figure 9.3 Power Measurement System

9.2.3 Data Collection and Processing

Data collection is managed using an OPC server and Matlab Simulink. Figure 9.4 shows the data collection interface in Simulink. The interface includes an OPC Configuration block to establish the link between OPC server and Simulink. The OPC Read block retrieves the following data from the Siemens PAC3200 power meter into the Simulink model:

- Working Hours Counter (s): Tracks the total operational time of the CNC lathe.
- Total Active Power (W): Measures the power consumption during machining.
- Active Energy Import (Wh): Records the total energy consumed.

Using sink blocks, the data is numerically monitored and visualized with a power-time plot on the Simulink interface for real time tracking. After converting active energy (Wh) into joules, all collected data is recorded in the simout matrix for further processing.

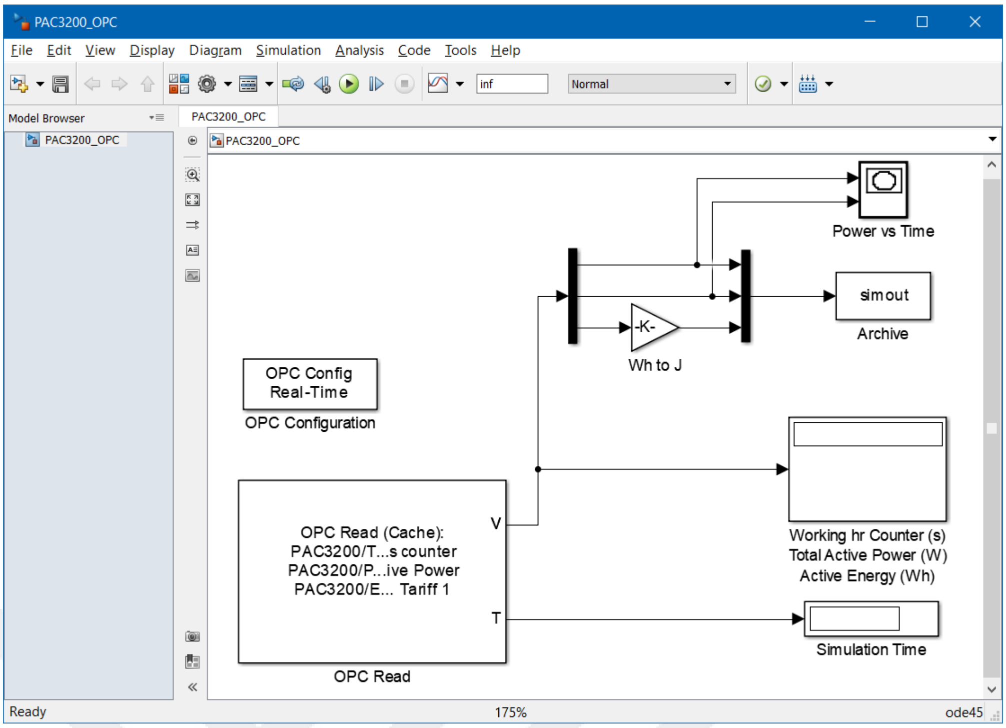

Figure 9.4 Matlab Simulink data collection interface

A Matlab script processes the simout matrix from the Simulink model to handle unique and missing values. Since the working hour and active energy are internal counters that accumulate data over the PAC32000's total lifetime, the script first zeroes the time and energy values relative to their initial entries. It then extracts unique power values from this adjusted matrix, eliminating repeated readings in the same time interval. Interpolation is performed for any missing values. The final results are summarized in a matrix with adjusted time at 0.2 second resolution, including energy and power values. Additionally, the script plots power versus time for visualization and reporting.

9.3 Verification

Verification studies involve measuring the energy requirements of five sample parts (SP) and comparing the findings with the results from the estimation model on

TurnDesign Eco Edition. The overall dimensions and materials of the parts are presented in Table 9.2. To demonstrate the performance of the estimation model for different materials, three samples of SP1 are manufactured using steel, cast iron and aluminum. After manufacturing SP2 and SP3 using aluminum as well, SP1, SP2 and SP3 are used to illustrate the size effect. Pictures of the sample parts after manufacturing are shown in Figure 9.5.

Table 9.2 Sample Parts: Specifications

Name-Material	L (mm)	ϕ_{max} (mm)	V_{rem} (mm^3)	Drawing
SP1-AISI1040	60	28	29839	Figure 9.6
SP1-GG25	60	28	29839	Figure 9.6
SP1-AL6013	60	28	29839	Figure 9.6
SP2-AL6013	60	18	11729	Figure 9.14
SP3-AL6013	50	47	61513	Figure 9.18

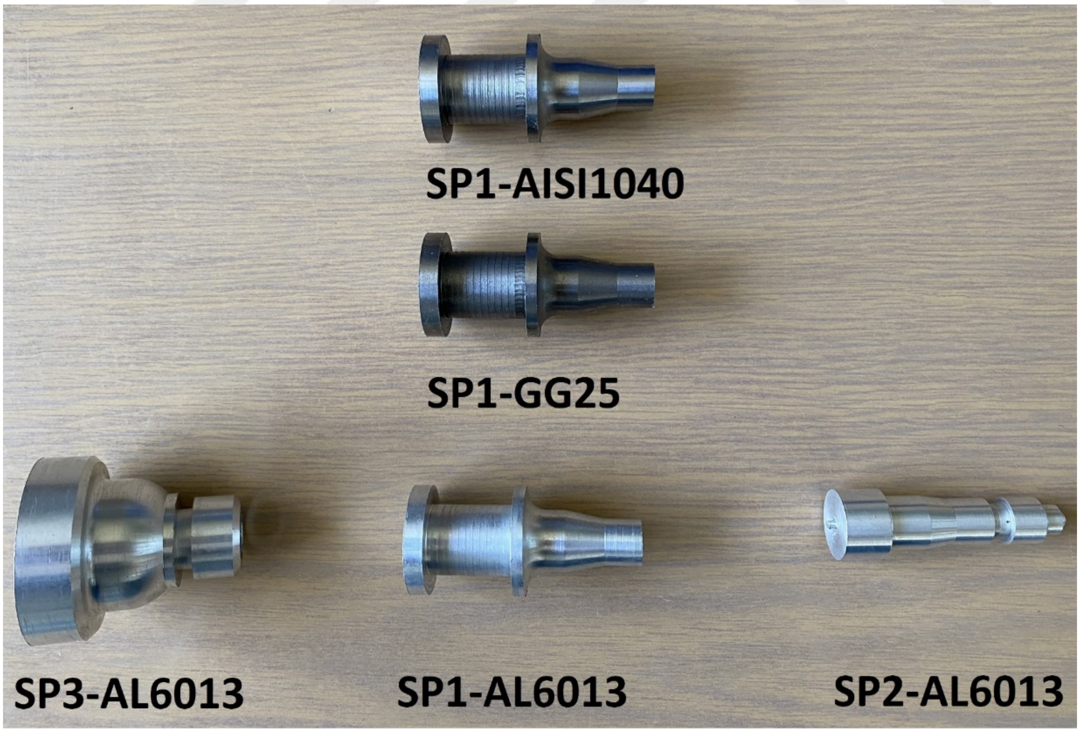

Figure 9.5 Sample Parts: After manufacturing

The performance of the estimation is assessed in terms of theoretical, variable and constant auxiliary energy requirements. To make this assessment, energy measurements corresponding to these categories are necessary. The methodology for measuring these energy requirements is described in Section 9.3.1. Designs of sample parts, outputs of TurnDesign Eco Edition for each sample (AP224 file, manufacturing process sheet and part program) and their energy measurement and estimation results are presented in Sections 9.3.2 to 9.3.4. Finally, a discussion on the results is provided in Section 9.3.5.

9.3.1 Measurement Methodology

As explained in Section 9.2.2, energy requirement by the manufacturing processes will be monitored using Siemens PAC3200 power meter installed on the CNC lathe. Measurements during the manufacture of each sample part provides the process energy ($E_{process}$) and drilling down further into the components of processing energy is not possible with a single measurement. Consequently, a measurement methodology is needed to obtain theoretical and auxiliary energy values.

Equations (8.2) and (8.30) can be combined to find the theoretical and auxiliary energy components of process energy ($E_{process}$):

$$E_{process} = E_{th} + E_{aux\_var} + E_{aux\_cons} \tag{9.1}$$

To measure the E_{aux_cons} component of process energy, the CNC lathe is operated in standby mode for the duration of total cutting time. Since metal is not removed and variable auxiliary energy is not required in this mode, both the theoretical (E_{th}) and variable auxiliary (E_{aux_var}) energy values are zero. Therefore, only the E_{aux_cons} component is read and recorded as the measured process energy value at standby ($E_{process\_sb}$).

$$E_{process\_sb} = \cancel{E_{th}} + \cancel{E_{aux\_var}} + E_{aux\_cons} \quad (9.2)$$

Consequently, constant auxiliary energy of the sample part equals the process energy measured at standby:

$$E_{aux\_cons} = E_{process\_sb} \quad (9.3)$$

Using the part program of each sample part, an air cut is performed to find the auxiliary energy component (E_{aux}) for the measurement data. Since material is not removed and only auxiliary equipment are active during an air cut, theoretical energy requirement is eliminated ($E_{th} = 0$)

$$E_{process\_air} = \cancel{E_{th}} + E_{aux\_var} + E_{aux\_cons} \quad (9.4)$$

The measured value ($E_{process\_air}$) will be equal to the auxiliary energy (E_{aux}) requirement of the part.

$$E_{aux} = E_{process\_air} \quad (9.5)$$

Once E_{aux} is available, the variable part of the auxiliary energy ($E_{aux\text{-}var}$) can be calculated from Equations (9.3) and (9.5):

$$E_{aux\_var} = E_{process\_air} - E_{process\_sb} \quad (9.6)$$

Performing a normal cut will help determine the measured theoretical energy (E_{th}). Substituting Equation (9.5) into (9.1):

$$E_{process\_nomal} = E_{th} + E_{process\_air} \quad (9.7)$$

By subtracting the measured auxiliary energy value ($E_{process\_air}$) from the energy readings of a normal cut ($E_{process\_normal}$), theoretical energy is calculated:

$$E_{th} = E_{process\_normal} - E_{process\_air} \quad (9.8)$$

As a result, taking three measurements (standby mode, air cut, normal cut) and using the Equations (9.3), (9.6) and (9.8), constant auxiliary, variable auxiliary and theoretical energy requirements of a sample part can be determined.

9.3.2 Sample Part 1

SP1 is manufactured using stock dimensions of ϕ30 mm x 73.5 mm which are calculated by TurnDesign Eco Edition based on the maximum diameter and length of the design as explained in Section 6.2. Three SP1 specimens are machined from 1040 carbon steel, GG25 cast iron and Aluminum alloy 6013. The manufacturing processes for SP1 remove 29839 mm^3 corresponding to the 66.5% of the total volume. The following sections present the design information, software outputs and energy results for SP1.

9.3.2.1 Design

The engineering drawing of SP1 is shown in Figure 9.6. The features input on TurnDesign Eco Edition to model SP1, aligned with the drawing, are presented in Table 9.3. Identical design and features are used for all three SP1s. The feature list provided in the table is also an output of the software, as described in Section 4.6 and shown in Figure 4.6.

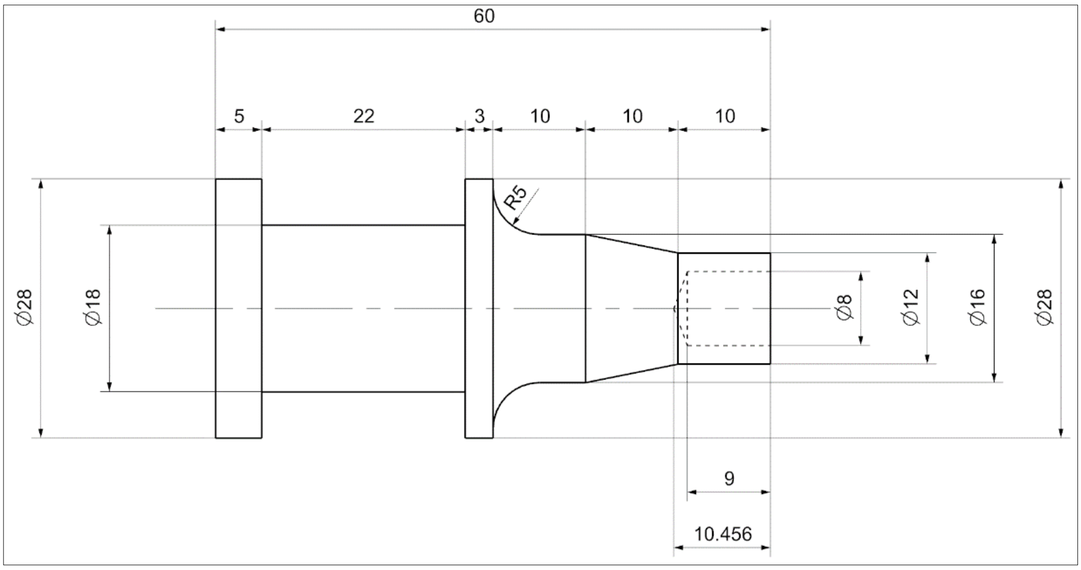

Figure 9.6 Drawing for SP1

Table 9.3 Feature and parameter list for SP1

No	Feature	Parameters	No	Feature	Parameters
1	OD1	D = 28 L = 30	5	SQRUGRV1	R = 9 W = 22 Depth = 5 r1 = 0 alpha1 = 90 r2 = 0 alpha2 = 90 z position = 16
2	OD2	D = 16 L = 10	6	RNDHOL1	D = 8 L = 9 conical bottom alpha = 140 r_tip = 0.0001
3	OD3	D = 16 Df = 12 L = 10	7	FILLET1	1st Feature = OD1 2nd Feature = OD2 r = 5
4	OD4	D = 12 L = 10			

9.3.2.2 Outputs

The first design related output is the TurnDesign Eco Edition interface (Figure 9.7) which is showing the final version of the solid model with high-level energy and carbon emission data. The second output is STEP AP224 file (Table 9.4) containing feature data. The outputs shown in this section are for SP1-AISI1040. Those for SP1-GG25 and SP1-AL6013 follow the same format and are presented in Appendix B.1.

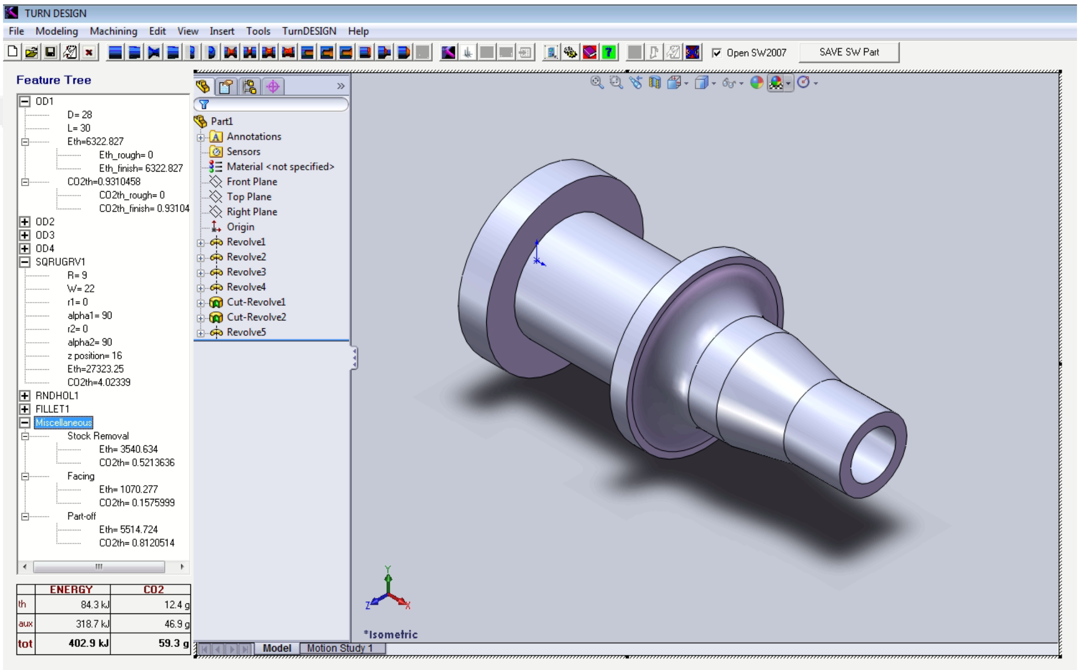

Figure 9.7 TurnDesign Eco Edition interface for SP1-AISI1040

Table 9.4 STEP AP224 file for SP1-AISI1040

```
ISO-10303-21;

HEADER;
FILE_DESCRIPTION(('ISO-10303-224,FEATURE BASED ROTATIONAL PART CREATED BY',
'TurnDESIGN Eco Edition'),'1');
FILE_NAME(('SP1-AISI1040-2024sp.part21','2024-6-22 T23:39:36',
('Designed by: URAL ULUER','METU-ME','ANKARA TURKIYE')
FILE_SCHEMA(('ROTATIONAL PART', 'PART FOR 2-AXIS TURNING'));
ENDSEC;
```

Table 9.4 (continued)

```
DATA;
#1=MATERIAL($,'Steel P1',$,$,$);
#2=OUTER_DIAMETER('OD1',#3,#4,#5,$);
#3=ORIENTATION((0,0,0),(1,0,0,0,1,0,0,0,1));
#4=NUMERIC_PARAMETER('OD1 DIAMETER',MM,28,$);
#5=NUMERIC_PARAMETER('OD1 LENGTH',MM,30,$);
#6=OUTER_DIAMETER('OD2',#7,#8,#9,$);
#7=ORIENTATION((0,0,30),(1,0,0,0,1,0,0,0,1));
#8=NUMERIC_PARAMETER('OD2 DIAMETER',MM,16,$);
#9=NUMERIC_PARAMETER('OD2 LENGTH',MM,10,$);
#10=OUTER_DIAMETER('OD3',#11,#12,#13,#14);
#11=ORIENTATION((0,0,40),(1,0,0,0,1,0,0,0,1));
#12=NUMERIC_PARAMETER('OD3 DIAMETER',MM,16,$);
#13=NUMERIC_PARAMETER('OD3 LENGTH',MM,10,$);
#14=DIAMETER_TAPER(#15);
#15=NUMERIC_PARAMETER('OD3 FINAL DIAMETER',MM,12,$);
#16=OUTER_DIAMETER('OD4',#17,#18,#19,$);
#17=ORIENTATION((0,0,50),(1,0,0,0,1,0,0,0,1));
#18=NUMERIC_PARAMETER('OD4 DIAMETER',MM,12,$);
#19=NUMERIC_PARAMETER('OD4 LENGTH',MM,10,$);
#20=GROOVE('SQRUGRV1',#21,#22,#23,#24);
#21=ORIENTATION((9,0,16),(1,0,0,0,1,0,0,0,1));
#22=DIRECTION(-1,0,0);
#23=NUMERIC_PARAMETER('SQRUGRV1 GROOVE RADIUS',MM,9,$);
#24=SQUARE_U_PROFILE($,#25,#26,#27,#28,#29);
#25=NUMERIC_PARAMETER('SQRUGRV1 WIDTH',MM,22,$);
#26=NUMERIC_PARAMETER('SQRUGRV1 FIRST RADIUS',MM,0,$);
#27=NUMERIC_PARAMETER('SQRUGRV1 FIRST ANGLE',DEGREES,90,$);
#28=NUMERIC_PARAMETER('SQRUGRV1 SECOND RADIUS',MM,0,$);
#29=NUMERIC_PARAMETER('SQRUGRV1 SECOND ANGLE',DEGREES,90,$);
#30=ROUND_HOLE('RNDHOL1',#31,$,#32,#33,$,#34);
#31=ORIENTATION((0,0,60),(1,0,0,0,1,0,0,0,1));
#32=LINEAR_PATH(#35,#36);
#33=NUMERIC_PARAMETER('RNDHOL1 DIAMETER',MM,8,$);
#34=CONICAL_HOLE_BOTTOM(#37,#39);
#35=NUMERIC_PARAMETER('RNDHOL1 DISTANCE',MM,9,$);
#36=DIRECTION(0,0,-1);
#37=NUMERIC_PARAMETER('RNDHOL1 CONICAL BOTTOM TIP ANGLE',MM,140,$);
#38=NUMERIC_PARAMETER('RNDHOL1 CONICAL BOTTOM TIP RADIUS',MM,0.0001,$);
#39=CONSTANT_RADIUS_FILLET('FILLET1','OD1','OD2',#40,$,$);
#40=NUMERIC_PARAMETER('FILLET1 RADIUS',MM,5,$);
ENDSEC;
END-ISO-10303-21;
```

Process planning and part programming outputs for SP1-AISI1040 are shown in Figure 9.8 (Manufacturing Process Sheet) and Table 9.5 (NC code) respectively. MPS displays the tools and parameters used for manufacturing the steel part. Part program is generated based on the parameters of the MPS.

METU DEPARTMENT OF MECHANICAL ENGINEERING	Part Name / No:	Part Name	Machine Tool:	Anatool TP32 CNC Lathe (3500 rpm max)
	By:	Ural Uluer	Stock Dimensions:	D_stock=30 mm L_stock=73.5 mm
	Date:	22.06.2024 / 23:30	Material:	Steel P1

Op No.	Operation Name	Features	Tool (Holder / Insert)	af (mm)	ap (mm)	Cutting Speed (m/min)	Speed (rpm)	Feed (mm/rev)	Feed Rate (mm/min)
1	Facing	-	SDJCR 2020K 11 / DCMT 11 T3 08-PM-GC4235	0.1	0.5	180	**1910**	0.1	**191**
2	Turning - Rough	OD1 FILLET1 OD3 OD4	SDJCR 2020K 11 / DCMT 11 T3 08-PM-GC4235	0.2	1.5	162	**1720**	0.2	**344**
3	Turning - Finish	OD1 FILLET1 OD3 OD4	SDJCR 2020K 11 / DCMT 11 T3 08-PM-GC4235	0.1	0.8	180	**1910**	0.1	**191**
4	Drilling	RNDHOL1	R840-0800-50-A1A	0.1	8	80	**3180**	0.2	**636**
5	Grooving	SQRUGRV1	RF123G20-2020B / N123G2-0300-0002-GF-GC1125	0.05	3	115	**1310**	0.05	**66**
6	Parting	-	N123G30-21A2 / N123G2-0300-0002-CM-GC1125	0.09	3	115	**1220**	0.09	**110**
TURNDESIGN ECO EDITION									

Figure 9.8 Manufacturing process sheet for SP1-AISI1040

Table 9.5 Part Program for SP1-AISI1040

```
;DATE............. 22.06.2024
;TIME............. 23:30
;PROGRAMMER....... Ural Uluer

;D_stock.......... 30 mm
;L_stock.......... 73.5 mm
;MACHINE.......... Anatool TP32 CNC
Lathe


N10 G291
N20 G91
N30 G28 X0
N40 G28 Z0
N50 G90
N60 G21 G18 G95 G40
N70 M07
N80 G54


;-------FACING-------
N90 T01
N100 G97 S1910 M03 F0.1

N110 G00 X34 Z2
N120 G00 X34 Z0
N130 G01 X-1 Z0
N140 G00 X-1 Z2
N150 G00 X34 Z2

N160 G91
N170 G28 X0
N180 G28 Z0
N190 G90


;-------TURNING:ROUGH-------
N200 T01
N210 G97 S1720 M03 F0.2

N220 G00 X34 Z2
```

```
;-------DRILLING-------
N860 T08
N870 G97 S3180 M03 F0.2

N880 G00 X34 Z2
N890 G00 X0 Z2
N900 G01 X0 Z-10.45587
N910 G00 X0 Z2
N920 G00 X34 Z2

N930 G91
N940 G28 X0
N950 G28 Z0
N960 G90


;-------GROOVING-------
N970 T19
N980 G97 S1310 M03 F0.05

N990 G00 X34 Z2
N1000 G00 X34 Z-36
N1010 G00 X30 Z-36

N1020 G01 X18 Z-36        ;Plunge 1
N1030 G00 X30 Z-36

N1040 G00 X30 Z-37.8
N1050 G01 X18 Z-37.8        ;Plunge 2
N1060 G00 X30 Z-37.8

N1070 G00 X30 Z-39.6
N1080 G01 X18 Z-39.6        ;Plunge 3
N1090 G00 X30 Z-39.6

N1100 G00 X30 Z-41.4
N1110 G01 X18 Z-41.4        ;Plunge 4
N1120 G00 X30 Z-41.4

N1130 G00 X30 Z-43.2
N1140 G01 X18 Z-43.2        ;Plunge 5
```

Table 9.5 (continued)

N230 G01 X31 Z2 N240 G01 X31 Z-63 ;Pass 1 N250 G01 X33 Z-62 N260 G00 X33 Z2 N270 G00 X31 Z2 N280 G01 X28 Z2 N290 G01 X28 Z-30 ;Pass 2 N300 G01 X30 Z-29 N310 G00 X30 Z2 N320 G00 X28 Z2 N330 G01 X25 Z2 N340 G01 X25 Z-29.82804 ;Pass 3 N350 G01 X27 Z-28.82804 N360 G00 X27 Z2 N370 G00 X25 Z2 N380 G01 X22 Z2 N390 G01 X22 Z-29.14246 ;Pass 4 N400 G01 X24 Z-28.14246 N410 G00 X24 Z2 N420 G00 X22 Z2 N430 G01 X19 Z2 N440 G01 X19 Z-27.55147 ;Pass 5 N450 G01 X21 Z-26.55147 N460 G00 X21 Z2 N470 G00 X19 Z2 N480 G01 X16 Z2 N490 G01 X16 Z-16 ;Pass 6 N500 G01 X18 Z-15 N510 G00 X18 Z2 N520 G00 X16 Z2 N530 G01 X13.6 Z2 ;Sweep Pass N540 G01 X13.6 Z0 N550 G01 X13.6 Z-10 N560 G01 X17.6 Z-20 N570 G01 X17.6 Z-25 N580 G02 X27.6 Z-30 R5 N590 G01 X29.6 Z-30 N600 G01 X29.6 Z-60 N610 G01 X29.6 Z-63 N620 G01 X34 Z-63 N630 G00 X34 Z2 N640 G91 N650 G28 X0 N660 G28 Z0 N670 G90	N1150 G00 X30 Z-43.2 N1160 G00 X30 Z-45 N1170 G01 X18 Z-45 ;Plunge 6 N1180 G00 X30 Z-45 N1190 G00 X30 Z-46.8 N1200 G01 X18 Z-46.8 ;Plunge 7 N1210 G00 X30 Z-46.8 N1220 G00 X30 Z-48.6 N1230 G01 X18 Z-48.6 ;Plunge 8 N1240 G00 X30 Z-48.6 N1250 G00 X30 Z-50.4 N1260 G01 X18 Z-50.4 ;Plunge 9 N1270 G00 X30 Z-50.4 N1280 G00 X30 Z-52.2 N1290 G01 X18 Z-52.2 ;Plunge 10 N1300 G00 X30 Z-52.2 N1310 G00 X30 Z-54 N1320 G01 X18 Z-54 ;Plunge 11 N1330 G00 X30 Z-54 N1340 G00 X30 Z-55 N1350 G01 X18 Z-55 ;Plunge 12 N1360 G00 X30 Z-55 N1370 G00 X34 Z-55 N1380 G00 X34 Z2 N1390 G91 N1400 G28 X0 N1410 G28 Z0 N1420 G90 ;-------PART-OFF------- N1430 T20 N1440 G97 S1220 M03 F0.09 N1450 G00 X34 Z2 N1460 G00 X34 Z-63 N1470 G01 X-1 Z-63 N1480 G00 X34 Z-63 N1490 G00 X34 Z2 N1500 G91 N1510 G28 X0 N1520 G28 Z0 N1530 G90

Table 9.5 (continued)

;-------TURNING:FINISH------- N680 T01 N690 G97 S1910 M03 F0.1 N700 G00 X34 Z2 N710 G00 X12 Z2 N720 G01 X12 Z0 N730 G01 X12 Z-10 N740 G01 X16 Z-20 N750 G01 X16 Z-25 N760 G02 X26 Z-30 R5 N770 G01 X28 Z-30 N780 G01 X28 Z-60 N790 G01 X28 Z-63 N800 G01 X34 Z-63 N810 G00 X34 Z2 N820 G91 N830 G28 X0 N840 G28 Z0 N850 G90	 N1540 M09 N1550 M30

Detailed energy requirement and carbon emission outputs are presented in the Appendix B.1. Next section summarizes those outputs for comparison with the measured data.

9.3.2.3 Results

Measurement results for **SP1-AISI1040** obtained using the methodology explained in Section 9.3.1 are displayed in Figure 9.9 and Table 9.7. The power consumption from all three measurements are plotted in the figure and the measured energy results are summarized in the table under "Measured" column.

Estimation results for SP1-AISI1040 are detailed in Appendix B.1.1. The energy breakdown for auxiliary equipment and theoretical energy is outlined in Table 9.6. High-level result for theoretical and auxiliary energy categories are shown under the "Estimated" column of Table 9.7.

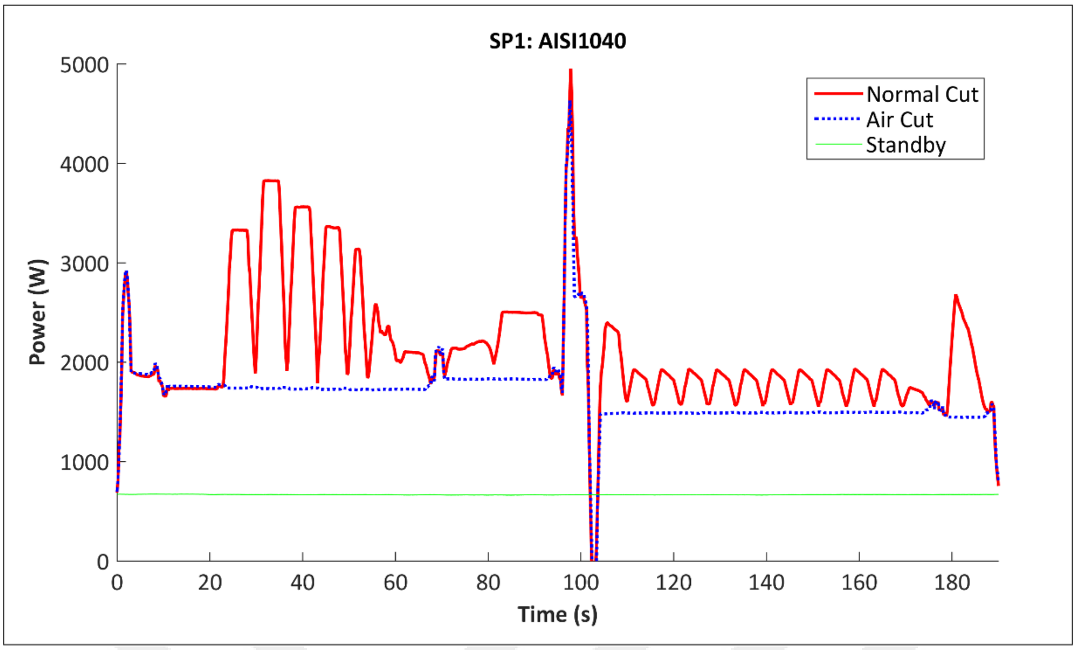

Figure 9.9 Power consumption measurements for SP1-AISI1040

Table 9.6 Energy requirement estimations for SP1-AISI1040

	E [J]	CO_2 [g]	% Share
Theoretical	84,252	12.4	21
Spindle	104,858	15.4	26
Cutting Fluid	75,901	11.2	19
Turret	1,376	0.2	0
Chuck	172	0.0	0
Servo	6,495	1.0	2
Lubrication	103	0.0	0
Standby	129,761	19.1	32
TOTAL	**402,918**	**59.3**	**100**

Based on the comparison table below for SP1-AISI1040, the error between measured and estimated process energy is 0.8 kJ, corresponding to a 0.2% error. This low error is achieved because the underestimation of variable auxiliary energy cancels out the overestimation of variable auxiliary energy.

Table 9.7 Energy results comparison for SP1-AISI1040

	Measured	**Estimated**	**Δ Error**	**% Error**
Time (s)	189.4	188.1	1.3	0.7
E_{th} (kJ)	84.0	84.3	-0.2	-0.3
E_{aux_var} (kJ)	191.8	188.9	2.9	1.5
E_{aux_cons} (kJ)	126.4	129.8	-3.4	-2.7
$E_{process}$ (kJ)	**402.2**	**402.9**	**-0.8**	**-0.2**

Measurement results for **SP1-GG25** obtained using the methodology explained in Section 9.3.1 are shown in Figure 9.10 and Table 9.10. The figure plots the power consumption from all three measurements and the measured energy results are summarized in the "Measured" column of the table.

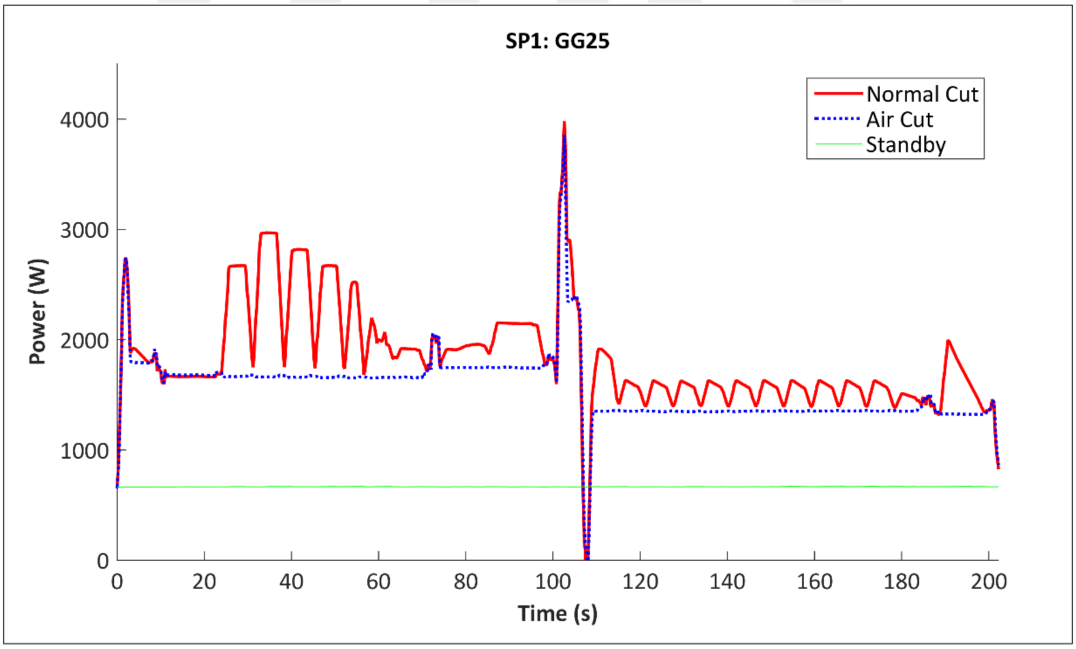

Figure 9.10 Power consumption measurements for SP1-GG25

Estimation results for SP1-GG25 can be found in Appendix B.1.2. The energy breakdown for auxiliary equipment and theoretical energy is outlined in Table 9.8. High-level result for theoretical and auxiliary energy categories are displayed under the "Estimated" column of Table 9.10.

Table 9.8 Energy requirement estimations for SP1-GG25

	E [J]	**CO2 [g]**	**% Share**
Theoretical	57,236	8.4	15
Spindle	94,610	13.9	25
Cutting Fluid	80,872	11.9	21
Turret	1,376	0.2	0
Chuck	172	0.0	0
Servo	6,600	1.0	2
Lubrication	110	0.0	0
Standby	138,260	20.4	36
TOTAL	**379,236**	**55.8**	**100**

The exact composition of the cast iron part used for the verification studies was unknown, so the ps1 and mc values in Table 8.1 could not be directly used in its energy estimations. To determine the correct values, a Brinell hardness test was conducted, resulting in values of 197, 202, 208, 205 and 200 HB (HBW 2.5/187.5) with an average of 202 HB.

The Sandvik Training Handbook (2017b) shows a collection of data for Brinell Hardness and specific cutting energy values, highlighted in the green rectangle on Figure 9.11. Linear regression applied to this data reveals a linear correlation between hardness and specific cutting energy (Table 9.9).

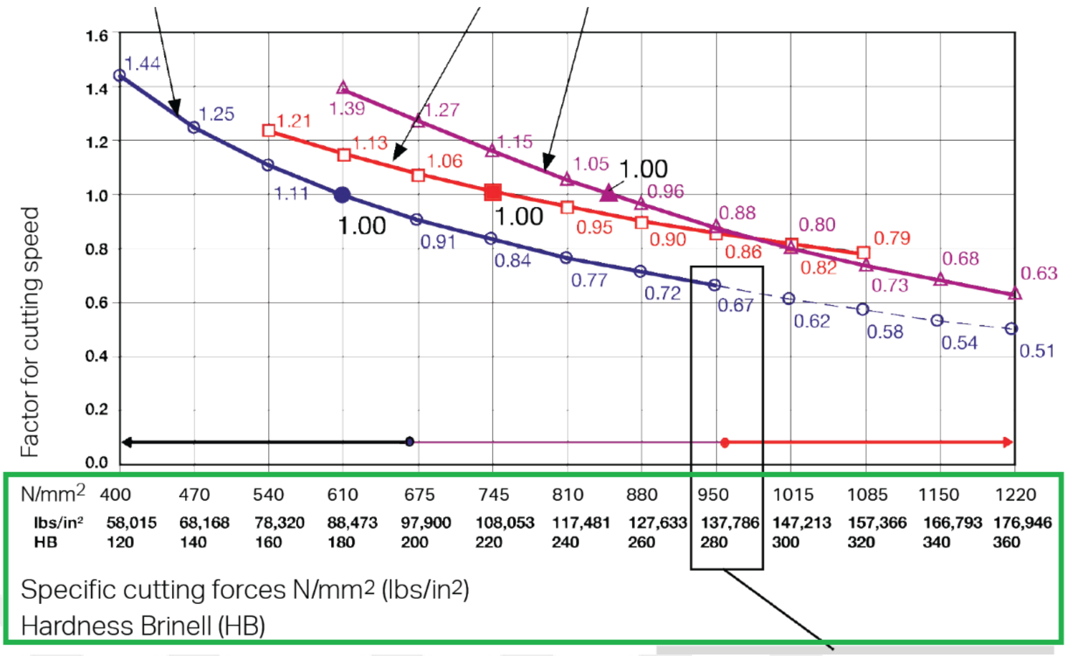

Figure 9.11 Brinell hardness vs. specific cutting energy (Sandvik, 2017b)

Table 9.9 Brinell hardness vs. specific cutting energy

HB	N/mm²	Linear Regression
120	400	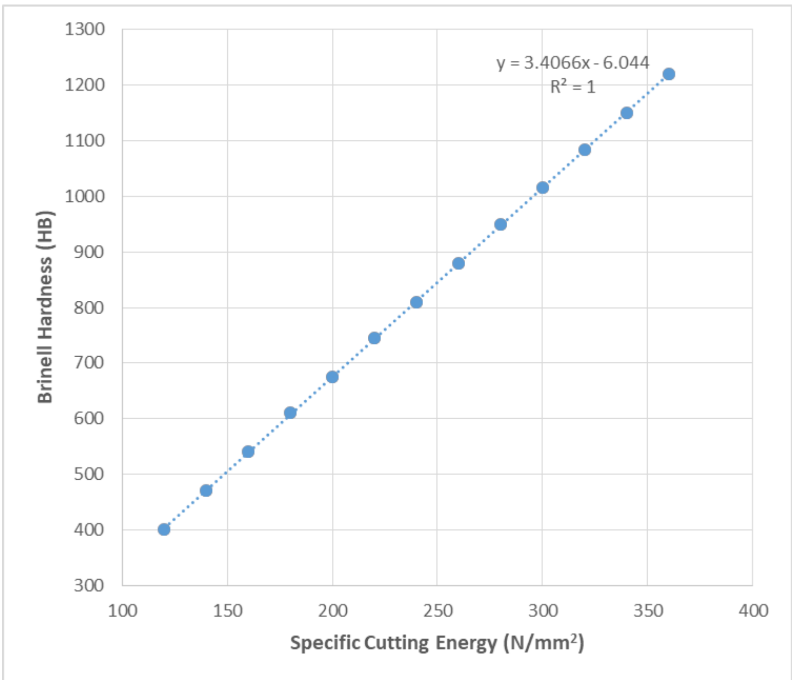
140	470	
160	540	
180	610	
200	675	
220	745	
240	810	
260	880	
280	950	
300	1015	
320	1085	
340	1150	
360	1220	

Applying linear interpolation for a hardness of 202 HB to the cast iron (GG) part using data from Iscar tool catalogues (Figure 9.12: Iscar, 2017a), ps1 is determined to be 1.205 J/mm³ and mc is 0.22.

Based on ISO 513 and VDI 3323 standards

ISO	Material	Condition	Tensile Strength [N/mm²]	Kc1[(1)] [N/mm²]	mc[(2)]	Hardness HB	Material Group No.
K	Gray cast iron (GG)	Ferritic / pearlitic		1150	0.20	180	15
		Pearlitic / martensitic		1350	0.28	260	16
	Nodular cast iron (GGG)	Ferritic		1225	0.25	160	17
		Pearlitic		1350	0.28	250	18
	Malleable cast iron	Ferritic		1225	0.25	130	19
		Pearlitic		1420	0.3	230	20

Figure 9.12 Cast iron material groups (Iscar, 2017a)

For SP1-GG25, the error between measured and estimated process energy turns out to be 8.1 kJ, corresponding to a 2.2% discrepancy. This is mainly due to the overestimation of variable and constant auxiliary energy values.

Table 9.10 Energy results comparison for SP1-GG25

	Measured	Estimated	Δ Error	% Error
Time (s)	201.6	200.4	1.2	0.6
E_{th} (kJ)	56.4	57.2	-0.8	-1.5
E_{aux_var} (kJ)	180.3	183.7	-3.4	-1.9
E_{aux_cons} (kJ)	134.4	138.3	-3.8	-2.9
$E_{process}$ (kJ)	**371.1**	**379.2**	**-8.1**	**-2.2**

Measurement results for **SP1-AL6013** obtained using the methodology explained in Section 9.3.1 are shown in Figure 9.13 and Table 9.12. The figure plots the power consumption from all three measurements and the measured energy results are summarized in the "Measured" column of the table.

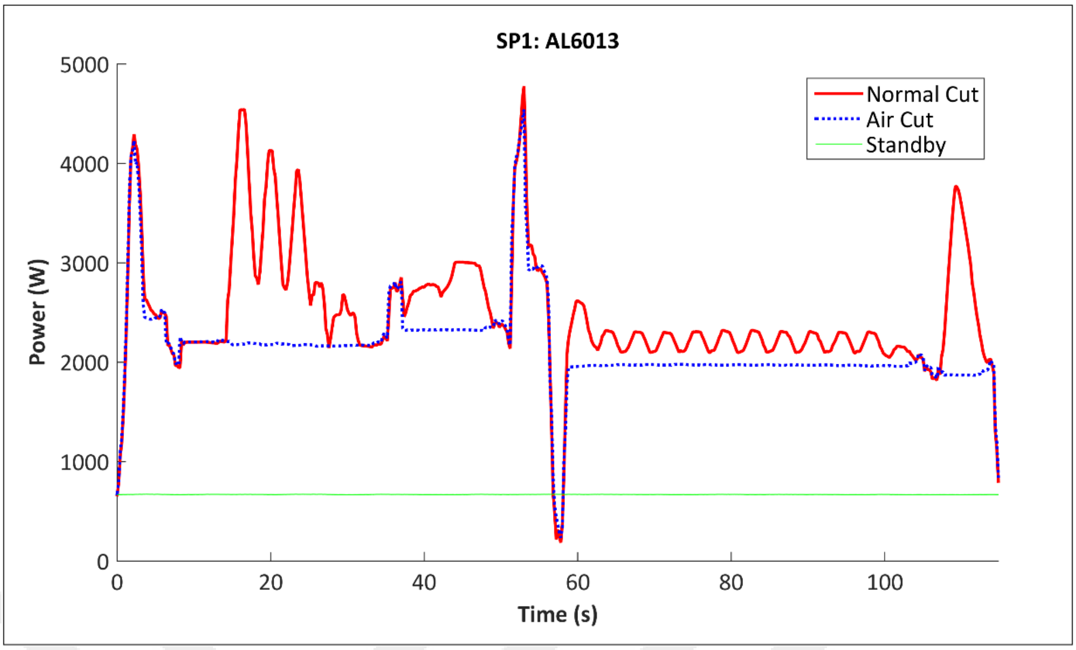

Figure 9.13 Power consumption measurements for SP1-AL6013

Estimation results for SP1-AL6013 can be found in Appendix B.1.3. The energy breakdown for auxiliary equipment and theoretical energy is outlined in Table 9.11. High-level result for theoretical and auxiliary energy categories are displayed under the "Estimated" column of Table 9.12.

Table 9.11 Energy requirement estimations for SP1-AL6013

	E [J]	**CO2 [g]**	**% Share**
Theoretical	38,932	5.7	14
Spindle	101,611	15.0	38
Cutting Fluid	45,311	6.7	17
Turret	1,376	0.2	1
Chuck	172	0.0	0
Servo	5,747	0.8	2
Lubrication	62	0.0	0
Standby	77,465	11.4	29
TOTAL	**270,676**	**39.9**	**100**

For SP1-AL6013, the error between measured and estimated process energy is 15.3 kJ, corresponding to a 5.3% error. The primary source of this discrepancy is the difference between the measured and estimated variable auxiliary energy which is 15.2 kJ.

The first reason for the deviation is the polynomial fit for the spindle (Figure 8.5). From the MPS of SP1-AL6013 (Figure B.10), the most time consuming operations (turning and grooving) operate in the 2200 to 2600 rpm range, where all data points fall above the curve, causing the model to underestimate the true power value by approximately 3 kJ.

The second reason is the deviation in the estimation of the total cutting time value by 2.1s. This creates another source of underestimation for the variable auxiliary energy by around 3 kJ.

Finally, a manual inspection of the measured data reveals a deviation of 100 to 135 W from the ideal estimation results corresponding to a difference of approximately 5 kJ in the oveall variable auxiliary energy. This indicates that the machine is drawing more power than expected during the manufacturing of this sample part. This case shows that the source of discrepancy is not only due to the estimated values but also related to the measured values.

Table 9.12 Energy results comparison for SP1-AL6013

	Measured	**Estimated**	**Δ Error**	**% Error**
Time (s)	114.4	112.3	2.1	1.9
E_{th} (kJ)	39.8	38.9	0.9	2.3
E_{aux_var} (kJ)	169.5	154.3	15.2	9.0
E_{aux_cons} (kJ)	76.6	77.5	-0.8	-1.1
$E_{process}$ (kJ)	**285.9**	**270.7**	**15.3**	**5.3**

9.3.3 Sample Part 2

SP2-AL6013 is manufactured using stock dimensions of ϕ20 mm x 73.5 mm, calculated by TurnDesign Eco Edition based on the design's maximum diameter and length, as explained in Section 6.2. This part is made from Aluminum alloy 6013 by removing 11729 mm^3 which corresponds to 58.8% of the total volume. The following sections present the design information, software outputs and energy results for SP2-AL6013.

9.3.3.1 Design

The engineering drawing of SP2-AL6013 is shown in Figure 9.14. The features used to model SP2-AL6013 on TurnDesign Eco Edition are presented in Table 9.13. As outlined in Section 4.6, this feature list is also generated as an output by the software.

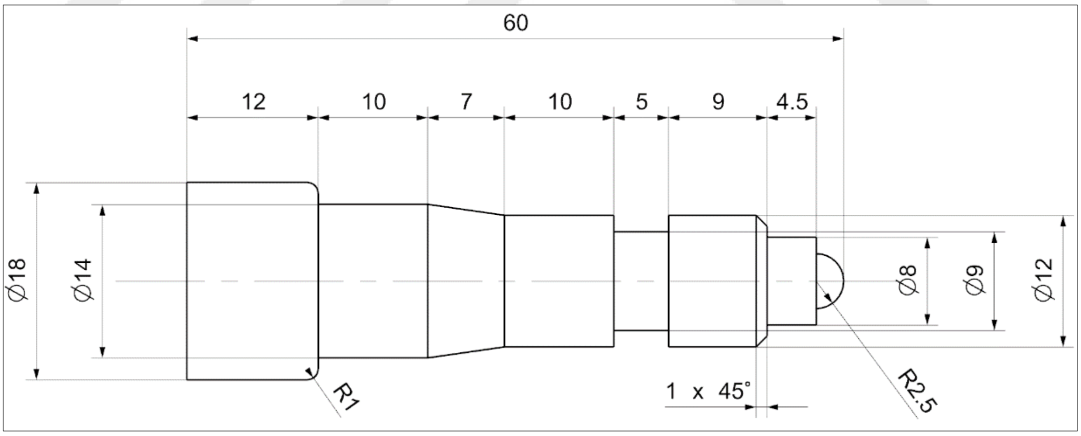

Figure 9.14 Drawing for SP2-AL6013

Table 9.13 Feature and parameter list for SP2-AL6013

No	Feature	Parameters	No	Feature	Parameters
1	OD1	D = 18 L = 12	6	CAP1	R = 2.5 Rf = 0 L = 2.5
2	OD2	D = 14 L = 10	7	SQRUGRV1	R = 4.5 W = 5 Depth = 1.5 r1 = 0 alpha1 = 90 r2 = 0 alpha2 = 90 z position = 41.5
3	OD3	D = 14 Df = 12 L = 7	8	ROUND1	1st Feature = OD1 2nd Feature = EDGE2 r = 1
4	OD4	D = 12 L = 24	9	CHAMFER1	1st Feature = OD4 2nd Feature = EDGE2 D1 = 1 alpha = 45
5	OD5	D = 8 L = 4.5			

9.3.3.2 Outputs

The first design related output is the TurnDesign Eco Edition interface (Figure 9.15), displaying the final version of the solid model along with high-level energy and carbon emission data on the lower left. The second design output is the STEP AP224 file containing all the feature data (Table 9.14) used in the design. The third output is the Excel tab for the feature list, as mentioned in Section 9.3.3.1.

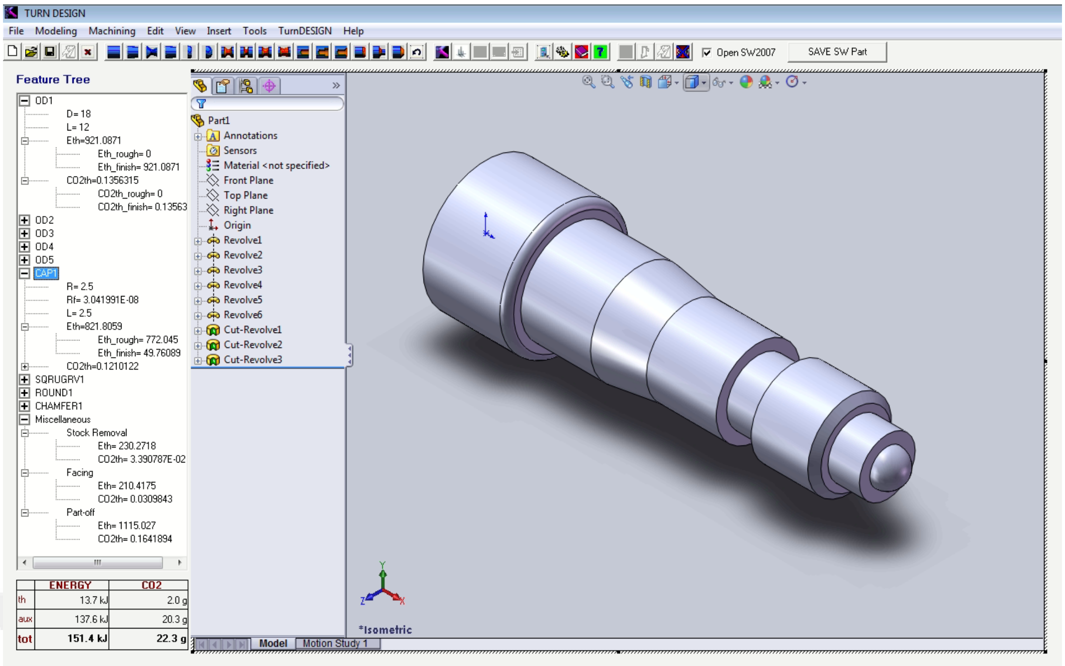

Figure 9.15 TurnDesign Eco Edition interface for SP2-AL6013

Table 9.14 STEP AP224 file for SP2-AL6013

```
ISO-10303-21;

HEADER;
FILE_DESCRIPTION(('ISO-10303-224,FEATURE BASED ROTATIONAL PART CREATED BY',
'TurnDESIGN Eco Edition'),'1');
FILE_NAME(('SP2-AL6013-2024sp.part21','2024-6-23 T01:32:40',
('Designed by: URAL ULUER','METU-ME','ANKARA TURKIYE')
FILE_SCHEMA(('ROTATIONAL PART', 'PART FOR 2-AXIS TURNING'));
ENDSEC;

DATA;
#1=MATERIAL($,'Non-Ferrous Metal N16',$,$,$);
#2=OUTER_DIAMETER('OD1',#3,#4,#5,$);
#3=ORIENTATION((0,0,0),(1,0,0,0,1,0,0,0,1));
#4=NUMERIC_PARAMETER('OD1 DIAMETER',MM,18,$);
#5=NUMERIC_PARAMETER('OD1 LENGTH',MM,12,$);
#6=OUTER_DIAMETER('OD2',#7,#8,#9,$);
#7=ORIENTATION((0,0,12),(1,0,0,0,1,0,0,0,1));
#8=NUMERIC_PARAMETER('OD2 DIAMETER',MM,14,$);
#9=NUMERIC_PARAMETER('OD2 LENGTH',MM,10,$);
#10=OUTER_DIAMETER('OD3',#11,#12,#13,#14);
#11=ORIENTATION((0,0,22),(1,0,0,0,1,0,0,0,1));
#12=NUMERIC_PARAMETER('OD3 DIAMETER',MM,14,$);
#13=NUMERIC_PARAMETER('OD3 LENGTH',MM,7,$);
#14=DIAMETER_TAPER(#15);
#15=NUMERIC_PARAMETER('OD3 FINAL DIAMETER',MM,12,$);
#16=OUTER_DIAMETER('OD4',#17,#18,#19,$);
#17=ORIENTATION((0,0,29),(1,0,0,0,1,0,0,0,1));
```

Table 9.14 (continued)

```
#18=NUMERIC_PARAMETER('OD4 DIAMETER',MM,12,$);
#19=NUMERIC_PARAMETER('OD4 LENGTH',MM,24,$);
#20=OUTER_DIAMETER('OD5',#21,#22,#23,$);
#21=ORIENTATION((0,0,53),(1,0,0,0,1,0,0,0,1));
#22=NUMERIC_PARAMETER('OD5 DIAMETER',MM,8,$);
#23=NUMERIC_PARAMETER('OD5 LENGTH',MM,4.5,$);
#24=REVOLVED_ROUND('CAP1',#25,#26,#27,#28);
#25=ORIENTATION((0,0,57.5),(1,0,0,0,1,0,0,0,1));
#26=DIRECTION(-0.7071068,0,-0.7071068);
#27=NUMERIC_PARAMETER('CAP1 REVOLVED FEATURE RADIUS',MM,3.041991E-08,$);
#28=PARTIAL_CIRCULAR_PROFILE($,#29,#30);
#29=NUMERIC_PARAMETER('CAP1 SWEEP ANGLE',DEGREES,90,$);
#30=NUMERIC_PARAMETER('CAP1 SWEEP RADIUS',MM,2.5,$);
#31=GROOVE('SQRUGRV1',#32,#33,#34,#35);
#32=ORIENTATION((4.5,0,41.5),(1,0,0,0,1,0,0,0,1));
#33=DIRECTION(-1,0,0);
#34=NUMERIC_PARAMETER('SQRUGRV1 GROOVE RADIUS',MM,4.5,$);
#35=SQUARE_U_PROFILE($,#36,#37,#38,#39,#40);
#36=NUMERIC_PARAMETER('SQRUGRV1 WIDTH',MM,5,$);
#37=NUMERIC_PARAMETER('SQRUGRV1 FIRST RADIUS',MM,0,$);
#38=NUMERIC_PARAMETER('SQRUGRV1 FIRST ANGLE',DEGREES,90,$);
#39=NUMERIC_PARAMETER('SQRUGRV1 SECOND RADIUS',MM,0,$);
#40=NUMERIC_PARAMETER('SQRUGRV1 SECOND ANGLE',DEGREES,90,$);
#41=CONSTANT_RADIUS_EDGE_ROUND('ROUND1','OD1','EDGE2',#42,$,$);
#42=NUMERIC_PARAMETER('ROUND1 RADIUS',MM,1,$);
#43=CHAMFER('CHAMFER1',#44,#45);
#44=FIRST_OFFSET('OD4',#46);
#45=SECOND_CHAMFER_OFFSET('EDGE2',#47);
#46=NUMERIC_PARAMETER('CHAMFER1 FIRST_OFFSET',MM,1,$);
#47=CHAMFER_ANGLE(#48);
#48=NUMERIC_PARAMETER('CHAMFER1 ANGLE',DEGREES,45,$);
ENDSEC;
END-ISO-10303-21;
```

Process planning and part programming outputs for SP2-AL6013 are shown in Figure 9.16 (Manufacturing Process Sheet) and Table 9.15 (NC code) respectively. MPS displays the tools and parameters used for manufacturing the aluminum part. Part program is generated based on the parameters of the MPS.

METU DEPARTMENT OF MECHANICAL ENGINEERING	Part Name / No:	Part Name	Machine Tool:	Anatool TP32 CNC Lathe (3500 rpm max)
	By:	Ural Uluer	Stock Dimensions:	D_stock=20 mm L_stock=73.5 mm
	Date:	23.06.2024 / 01:22	Material:	Non-Ferrous Metal N16

Op No.	Operation Name	Features	Tool (Holder / Insert)	af (mm)	ap (mm)	Cutting Speed (m/min)	Speed (rpm)	Feed (mm/rev)	Feed Rate (mm/min)
1	Facing	-	SDJCR 2020K 11 / DCGX 11 T3 08-AL-H10	0.15	0.5	250	3500	0.15	525
2	Turning - Rough	OD1 ROUND1 OD2 OD3 OD4 CHAMFER1 OD5 CAP1	SDJCR 2020K 11 / DCGX 11 T3 08-AL-H10	0.3	2	225	3500	0.3	1050
3	Turning - Finish	OD1 ROUND1 OD2 OD3 OD4 CHAMFER1 OD5 CAP1	SDJCR 2020K 11 / DCGX 11 T3 08-AL-H10	0.15	1	250	3500	0.15	525
4	Grooving	SQRUGRV1	RF123G20-2020B / N123G2-0300-0002-GF-GC1125	0.05	3	190	3500	0.05	175
5	Parting	-	N123G30-21A2 / N123G2-0300-0002-CM-GC1125	0.09	3	190	3020	0.09	272
TURNDESIGN ECO EDITION									

Figure 9.16 Manufacturing process sheet for SP2-AL6013

Table 9.15 Part Program for SP2-AL6013

```
;DATE............. 23.06.2024
;TIME............. 01:22
;PROGRAMMER....... Ural Uluer

;D_stock.......... 20 mm
;L_stock.......... 73.5 mm
;MACHINE..........  Anatool  TP32  CNC
Lathe


N10 G291
N20 G91
N30 G28 X0
N40 G28 Z0
N50 G90
N60 G21 G18 G95 G40
N70 M07
N80 G54


;-------FACING-------
N90 T01
N100 G97 S3500 M03 F0.15

N110 G00 X24 Z2
N120 G00 X24 Z0
N130 G01 X-1 Z0
N140 G00 X-1 Z2
N150 G00 X24 Z2

N160 G91
N170 G28 X0
N180 G28 Z0
N190 G90


;-------TURNING:ROUGH-------
N200 T01
N210 G97 S3500 M03 F0.3

N220 G00 X24 Z2
N230 G01 X20 Z2
N240 G01 X20 Z-63        ;Pass 1
N250 G01 X22 Z-62
N260 G00 X22 Z2
N270 G00 X20 Z2

N280 G01 X16 Z2
N290 G01 X16 Z-48        ;Pass 2
N300 G01 X18 Z-47
N310 G00 X18 Z2
N320 G00 X16 Z2

N330 G01 X12 Z2
N340 G01 X12 Z-7        ;Pass 3
N350 G01 X14 Z-6
N360 G00 X14 Z2
N370 G00 X12 Z2
```

```
;-------TURNING:FINISH-------
N680 T01
N690 G97 S3500 M03 F0.15

N700 G00 X24 Z2
N710 G00 X0 Z2
N720 G01 X0 Z0
N730 G03 X5 Z-2.5 R2.5
N740 G01 X8 Z-2.5
N750 G01 X8 Z-7
N760 G01 X10 Z-7
N770 G01 X12 Z-8
N780 G01 X12 Z-31
N790 G01 X14 Z-38
N800 G01 X14 Z-48
N810 G01 X16 Z-48
N820 G03 X18 Z-49 R1
N830 G01 X18 Z-60
N840 G01 X18 Z-63
N850 G01 X24 Z-63
N860 G00 X24 Z2

N870 G91
N880 G28 X0
N890 G28 Z0
N900 G90


;-------GROOVING-------
N910 T19
N920 G97 S3500 M03 F0.05

N930 G00 X24 Z2
N940 G00 X24 Z-19
N950 G00 X14 Z-19

N960 G01 X9 Z-19        ;Plunge 1
N970 G00 X14 Z-19

N980 G00 X14 Z-20.8
N990 G01 X9 Z-20.8        ;Plunge 2
N1000 G00 X14 Z-20.8

N1010 G00 X14 Z-21
N1020 G01 X9 Z-21        ;Plunge 3
N1030 G00 X14 Z-21

N1040 G00 X24 Z-21
N1050 G00 X24 Z2

N1060 G91
N1070 G28 X0
N1080 G28 Z0
N1090 G90


;-------PART-OFF-------
N1100 T20
```

Table 9.15 (continued)

N380 G01 X8 Z2	N1110 G97 S3020 M03 F0.09
N390 G01 X8 Z-2.5 ;Pass 4	
N400 G01 X10 Z-1.5	N1120 G00 X24 Z2
N410 G00 X10 Z2	N1130 G00 X24 Z-63
N420 G00 X8 Z2	N1140 G01 X-1 Z-63
	N1150 G00 X24 Z-63
N430 G01 X4 Z2	N1160 G00 X24 Z2
N440 G01 X4 Z-0.2087121 ;Pass 5	
N450 G01 X6 Z0.7912878	N1170 G91
N460 G00 X6 Z2	N1180 G28 X0
N470 G00 X4 Z2	N1190 G28 Z0
	N1200 G90
N480 G01 X2 Z2 ;Sweep Pass	
N490 G01 X2 Z0	
N500 G03 X7 Z-2.5 R2.5	N1210 M09
N510 G01 X10 Z-2.5	
N520 G01 X10 Z-7	N1220 M30
N530 G01 X12 Z-7	
N540 G01 X14 Z-8	
N550 G01 X14 Z-31	
N560 G01 X16 Z-38	
N570 G01 X16 Z-48	
N580 G01 X18 Z-48	
N590 G03 X20 Z-49 R1	
N600 G01 X20 Z-60	
N610 G01 X20 Z-63	
N620 G01 X24 Z-63	
N630 G00 X24 Z2	
N640 G91	
N650 G28 X0	
N660 G28 Z0	
N670 G90	

Detailed energy requirement and carbon emission outputs are presented in the Appendix B.2. Next section summarizes those outputs and compares with the measured data.

9.3.3.3 Results

Measurement results for SP2-AL6013 obtained using the methodology explained in Section 9.3.1 are displayed in Figure 9.17 and Table 9.17. The power consumption from all three measurements are plotted in the figure and the measured energy results are summarized in the table under "Measured" column.

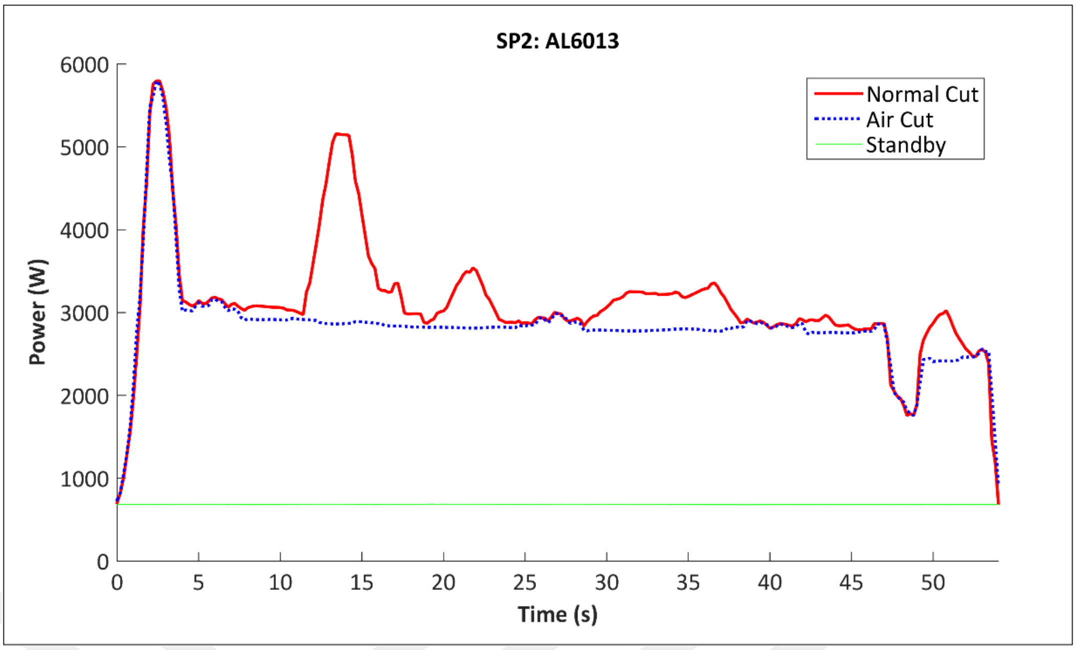

Figure 9.17 Power consumption measurements for SP2-AL6013

Estimation results for SP2-AL6013 are given in Appendix B.2. The energy requirement for auxiliary equipment and theoretical energy is detailed in Table 9.16. High-level result for theoretical and auxiliary energy categories are shown under the "Estimated" column of Table 9.17.

Table 9.16 Energy requirement estimations for SP2-AL6013

	E [J]	**CO2 [g]**	**% Share**
Theoretical	13,741	2.0	9
Spindle	75,825	11.2	50
Cutting Fluid	20,762	3.1	14
Turret	1,147	0.2	1
Chuck	172	0.0	0
Servo	4,184	0.6	3
Lubrication	28	0.0	0
Standby	35,495	5.2	23
TOTAL	**151,354**	**22.3**	**100**

Based on the comparison in Table 9.17 for SP2-AL6013, the error between measured and estimated process energy is 6.0 kJ corresponding to a 3.8% discrepancy. 3.5 kJ of this difference arises from the variable auxiliary energy.

Table 9.17 Energy results comparison for SP2-AL6013

	Measured	**Estimated**	**Δ Error**	**% Error**
Time (s)	53.4	51.4	2.0	3.7
E_{th} (kJ)	15.1	13.7	1.3	8.7
E_{aux_var} (kJ)	105.7	102.1	3.5	3.3
E_{aux_cons} (kJ)	36.6	35.5	1.1	3.0
$E_{process}$ (kJ)	**157.3**	**151.4**	**6.0**	**3.8**

9.3.4 Sample Part 3

SP3-AL6013 is manufactured from stock dimensions of ϕ50 mm x 63.5 mm. Dimensions are calculated by TurnDesign Eco Edition based on the design's maximum diameter and length, as explained in Section 6.2. This part is made from Aluminum alloy 6013 by removing 61513 mm^3 which corresponds to 58.6% of the stock volume. The following sections present the design details, software outputs and energy results for SP3-AL6013.

9.3.4.1 Design

The engineering drawing of SP3-AL6013 is shown in Figure 9.18. The features used to model this sample part on TurnDesign Eco Edition are presented in Table 9.18. As explained in Section 4.6, this feature list is also an output generated by the software.

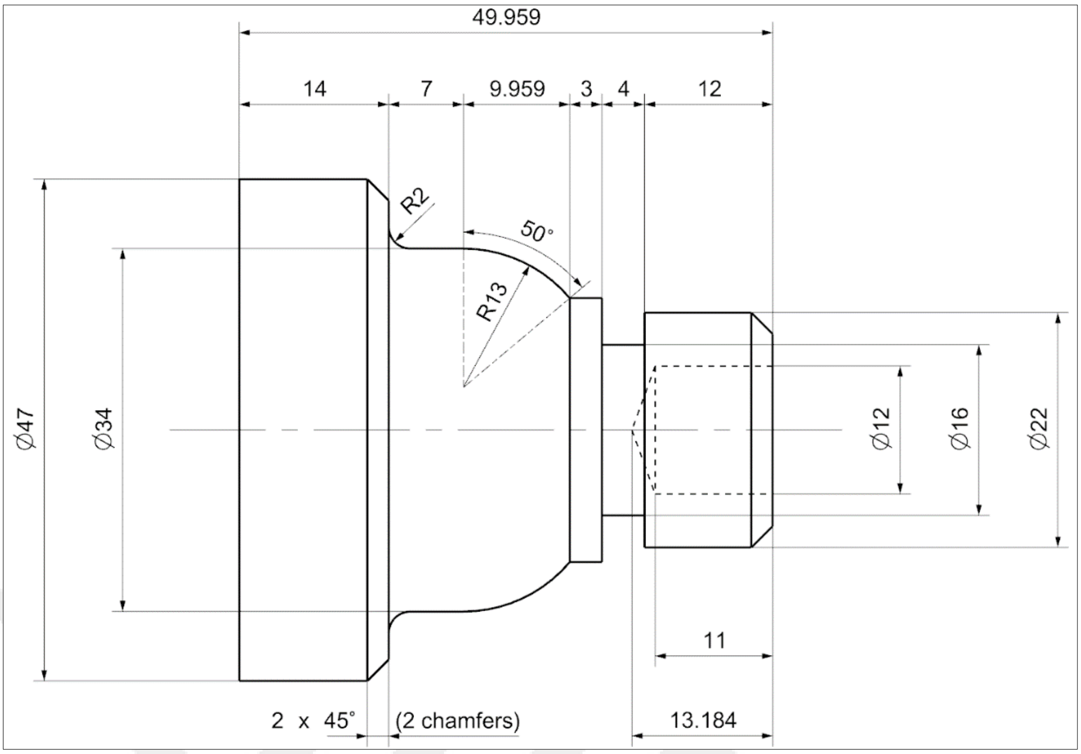

Figure 9.18 Drawing for SP3-AL6013

Table 9.18 Feature and parameter list for SP3-AL6013

No	**Feature**	**Parameters**	**No**	**Feature**	**Parameters**
1	OD1	D = 47 L = 14	6	SQRUGRV1	R = 8 W = 4 Depth = 3 r1 = 0 alpha1 = 90 r2 = 0 alpha2 = 90 z position = 35.95858
2	OD2	D = 34 L = 7	7	RNDHOL1	D = 12 L = 11 conical bottom alpha = 140 r_tip = 0.0001
3	REVRND1	R = 17 Rf = 12.35624 L = 9.958578	8	CHAMFER1	1st Feature = OD1 2nd Feature = EDGE2 D1 = 2 alpha = 45

Table 9.18 (continued)

4	OD3	D = 24.71248 L = 3	9	CHAMFER2	1st Feature = OD4 2nd Feature = EDGE2 D1 = 2 alpha = 45
5	OD4	D = 22 L = 16	10	FILLET1	1st Feature = OD1 2nd Feature = OD2 r = 2

9.3.4.2 Outputs

The first design related output is the TurnDesign Eco Edition interface (Figure 9.19), which displays the final version of the solid model along with high-level energy and carbon emission data. The second design output is the STEP AP224 file containing the feature data (Table 9.19). The third output is the Excel tab for the feature list, as mentioned in Section 9.3.4.1.

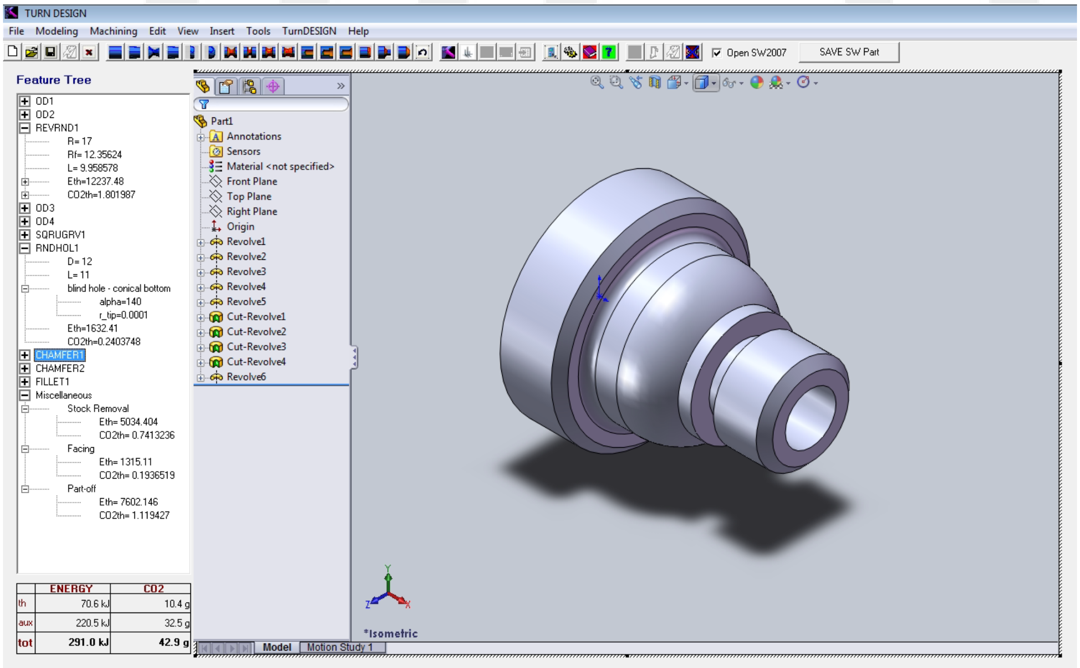

Figure 9.19 TurnDesign Eco Edition interface for SP3-AL6013

Table 9.19 STEP AP224 file for SP3-AL6013

```
ISO-10303-21;

HEADER;
FILE_DESCRIPTION(('ISO-10303-224,FEATURE BASED ROTATIONAL PART CREATED BY',
'TurnDESIGN Eco Edition'),'1');
FILE_NAME(('SP3-AL6013-2024sp.part21','2024-6-23 T01:55:48',
('Designed by: URAL ULUER','METU-ME','ANKARA TURKIYE')
FILE_SCHEMA(('ROTATIONAL PART', 'PART FOR 2-AXIS TURNING'));
ENDSEC;

DATA;
#1=MATERIAL($,'Non-Ferrous Metal N16',$,$,$);
#2=OUTER_DIAMETER('OD1',#3,#4,#5,$);
#3=ORIENTATION((0,0,0),(1,0,0,0,1,0,0,0,1));
#4=NUMERIC_PARAMETER('OD1 DIAMETER',MM,47,$);
#5=NUMERIC_PARAMETER('OD1 LENGTH',MM,14,$);
#6=OUTER_DIAMETER('OD2',#7,#8,#9,$);
#7=ORIENTATION((0,0,14),(1,0,0,0,1,0,0,0,1));
#8=NUMERIC_PARAMETER('OD2 DIAMETER',MM,34,$);
#9=NUMERIC_PARAMETER('OD2 LENGTH',MM,7,$);
#10=REVOLVED_ROUND('REVRND1',#11,#12,#13,#14);
#11=ORIENTATION((0,0,21),(1,0,0,0,1,0,0,0,1));
#12=DIRECTION(-0.9063078,0,-0.4226183);
#13=NUMERIC_PARAMETER('REVRND1 REVOLVED FEATURE RADIUS',MM,12.35624,$);
#14=PARTIAL_CIRCULAR_PROFILE($,#15,#16);
#15=NUMERIC_PARAMETER('REVRND1 SWEEP ANGLE',DEGREES,50,$);
#16=NUMERIC_PARAMETER('REVRND1 SWEEP RADIUS',MM,13,$);
#17=OUTER_DIAMETER('OD3',#18,#19,#20,$);
#18=ORIENTATION((0,0,30.95858),(1,0,0,0,1,0,0,0,1));
#19=NUMERIC_PARAMETER('OD3 DIAMETER',MM,24.71248,$);
#20=NUMERIC_PARAMETER('OD3 LENGTH',MM,3,$);
#21=OUTER_DIAMETER('OD4',#22,#23,#24,$);
#22=ORIENTATION((0,0,33.95858),(1,0,0,0,1,0,0,0,1));
#23=NUMERIC_PARAMETER('OD4 DIAMETER',MM,22,$);
#24=NUMERIC_PARAMETER('OD4 LENGTH',MM,16,$);
#25=GROOVE('SQRUGRV1',#26,#27,#28,#29);
#26=ORIENTATION((8,0,35.95858),(1,0,0,0,1,0,0,0,1));
#27=DIRECTION(-1,0,0);
#28=NUMERIC_PARAMETER('SQRUGRV1 GROOVE RADIUS',MM,8,$);
#29=SQUARE_U_PROFILE($,#30,#31,#32,#33,#34);
#30=NUMERIC_PARAMETER('SQRUGRV1 WIDTH',MM,4,$);
#31=NUMERIC_PARAMETER('SQRUGRV1 FIRST RADIUS',MM,0,$);
#32=NUMERIC_PARAMETER('SQRUGRV1 FIRST ANGLE',DEGREES,90,$);
#33=NUMERIC_PARAMETER('SQRUGRV1 SECOND RADIUS',MM,0,$);
#34=NUMERIC_PARAMETER('SQRUGRV1 SECOND ANGLE',DEGREES,90,$);
#35=ROUND_HOLE('RNDHOL1',#36,$,#37,#38,$,#39);
#36=ORIENTATION((0,0,49.95858),(1,0,0,0,1,0,0,0,1));
#37=LINEAR_PATH(#40,#41);
#38=NUMERIC_PARAMETER('RNDHOL1 DIAMETER',MM,12,$);
#39=CONICAL_HOLE_BOTTOM(#42,#44);
#40=NUMERIC_PARAMETER('RNDHOL1 DISTANCE',MM,11,$);
#41=DIRECTION(0,0,-1);
#42=NUMERIC_PARAMETER('RNDHOL1 CONICAL BOTTOM TIP ANGLE',MM,140,$);
#43=NUMERIC_PARAMETER('RNDHOL1 CONICAL BOTTOM TIP RADIUS',MM,0.0001,$);
#44=CHAMFER('CHAMFER1',#45,#46);
#45=FIRST_OFFSET('OD1',#47);
#46=SECOND_CHAMFER_OFFSET('EDGE2',#48);
#47=NUMERIC_PARAMETER('CHAMFER1 FIRST_OFFSET',MM,2,$);
```

Table 9.19 (continued)

```
#48=CHAMFER_ANGLE(#49);
#49=NUMERIC_PARAMETER('CHAMFER1 ANGLE',DEGREES,45,$);
#50=CHAMFER('CHAMFER2',#51,#52);
#51=FIRST_OFFSET('OD4',#53);
#52=SECOND_CHAMFER_OFFSET('EDGE2',#54);
#53=NUMERIC_PARAMETER('CHAMFER2 FIRST_OFFSET',MM,2,$);
#54=CHAMFER_ANGLE(#55);
#55=NUMERIC_PARAMETER('CHAMFER2 ANGLE',DEGREES,45,$);
#56=CONSTANT_RADIUS_FILLET('FILLET1','OD1','OD2',#57,$,$);
#57=NUMERIC_PARAMETER('FILLET1 RADIUS',MM,2,$);
ENDSEC;
END-ISO-10303-21;
```

Process planning and part programming outputs for SP3-AL6013 are shown in Figure 9.20 (Manufacturing Process Sheet) and Table 9.20 (NC code) respectively. MPS displays the tools and parameters used for manufacturing the steel part. Part program is generated based on the parameters of the MPS.

METU DEPARTMENT OF MECHANICAL ENGINEERING	Part Name / No: Part Name	Machine Tool:	Anatool TP32 CNC Lathe (3500 rpm max)
	By: Ural Uluer	Stock Dimensions:	D_stock=50 mm L_stock=63.45858 mm
	Date: 23.06.2024 / 01:47	Material:	Non-Ferrous Metal N16

Op No.	Operation Name	Features	Tool (Holder / Insert)	af (mm)	ap (mm)	Cutting Speed (m/min)	Speed (rpm)	Feed (mm/rev)	Feed Rate (mm/min)
1	Facing	-	SDJCR 2020K 11 / DCGX 11 T3 08-AL-H10	0.15	0.5	250	**1590**	0.15	**239**
2	Turning - Rough	OD1 CHAMFER1 FILLET1 REVRND1 OD3 OD4 CHAMFER2	SDJCR 2020K 11 / DCGX 11 T3 08-AL-H10	0.3	2	225	**1430**	0.3	**429**
3	Turning - Finish	OD1 CHAMFER1 FILLET1 REVRND1 OD3 OD4 CHAMFER2	SDJCR 2020K 11 / DCGX 11 T3 08-AL-H10	0.15	1	250	**1590**	0.15	**239**
4	Center Drilling	RNDHOL1	HSS Center Drill	0.06	3	55	**3500**	0.12	**420**
5	Drilling	RNDHOL1	R840-1200-50-A1A	0.19	12	120	**3180**	0.38	**1208**
6	Grooving	SQRUGRV1	RF123G20-2020B / N123G2-0300-0002-GF-GC1125	0.05	3	190	**2750**	0.05	**138**
7	Parting	-	N123G30-21A2 / N123G2-0300-0002-CM-GC1125	0.09	3	190	**1210**	0.09	**109**
TURNDESIGN ECO EDITION									

Figure 9.20 Manufacturing process sheet for SP3-AL6013

Detailed energy requirement and carbon emission outputs are presented in Appendix B.3. The estimation values from these outputs are summarized and compared with the measurement data in the next section.

Table 9.20 Part Program for SP3-AL6013

```
;DATE............. 23.06.2024
;TIME............. 01:46
;PROGRAMMER....... Ural Uluer

;D_stock.......... 50 mm
;L_stock.......... 63.45858 mm
;MACHINE.......... Anatool TP32 CNC Lathe


N10 G291
N20 G91
N30 G28 X0
N40 G28 Z0
N50 G90
N60 G21 G18 G95 G40
N70 M07
N80 G54


;-------FACING-------
N90 T01
N100 G97 S1590 M03 F0.15

N110 G00 X54 Z2
N120 G00 X54 Z0
N130 G01 X-1 Z0
N140 G00 X-1 Z2
N150 G00 X54 Z2

N160 G91
N170 G28 X0
N180 G28 Z0
N190 G90


;-------TURNING:ROUGH-------
N200 T01
N210 G97 S1430 M03 F0.3

N220 G00 X54 Z2
N230 G01 X50 Z2
N240 G01 X50 Z-52.95858        ;Pass 1
N250 G01 X52 Z-51.95858
N260 G00 X52 Z2
N270 G00 X50 Z2

N280 G01 X46 Z2
N290 G01 X46 Z-36.45858        ;Pass 2
N300 G01 X48 Z-35.45858
N310 G00 X48 Z2
N320 G00 X46 Z2

N330 G01 X42 Z2
N340 G01 X42 Z-35.95858        ;Pass 3
N350 G01 X44 Z-34.95858
N360 G00 X44 Z2
N370 G00 X42 Z2
```

```
;-------TURNING:FINISH-------
N820 T01
N830 G97 S1590 M03 F0.15

N840 G00 X54 Z2
N850 G00 X18 Z2
N860 G01 X18 Z0
N870 G01 X22 Z-2
N880 G01 X22 Z-16
N890 G01 X24.71248 Z-16
N900 G01 X24.71248 Z-19
N910 G03 X34 Z-28.95858 R13
N920 G01 X34 Z-33.95858
N930 G02 X38 Z-35.95858 R2
N940 G01 X43 Z-35.95858
N950 G01 X47 Z-37.95858
N960 G01 X47 Z-49.95858
N970 G01 X47 Z-52.95858
N980 G01 X54 Z-52.95858
N990 G00 X54 Z2

N1000 G91
N1010 G28 X0
N1020 G28 Z0
N1030 G90


;-------CENTER DRILLING-------
N1040 T04
N1050 G97 S3500 M03 F0.12

N1060 G00 X54 Z2
N1070 G00 X0 Z2
N1080 G01 X0 Z-7
N1090 G00 X0 Z2
N1100 G00 X54 Z2

N1110 G91
N1120 G28 X0
N1130 G28 Z0
N1140 G90


;-------DRILLING-------
N1150 T12
N1160 G97 S3180 M03 F0.38

N1170 G00 X54 Z2
N1180 G00 X0 Z2
N1190 G01 X0 Z-13.18382
N1200 G00 X0 Z2
N1210 G00 X54 Z2

N1220 G91
N1230 G28 X0
N1240 G28 Z0
N1250 G90
```

Table 9.20 (continued)

```
N380 G01 X38 Z2
N390 G01 X38 Z-35.69063        ;Pass 4
N400 G01 X40 Z-34.69063
N410 G00 X40 Z2
N420 G00 X38 Z2

N430 G01 X34 Z2
N440 G01 X34 Z-23.95858        ;Pass 5
N450 G01 X36 Z-22.95858
N460 G00 X36 Z2
N470 G00 X34 Z2

N480 G01 X30 Z2
N490 G01 X30 Z-20.65195        ;Pass 6
N500 G01 X32 Z-19.65195
N510 G00 X32 Z2
N520 G00 X30 Z2

N530 G01 X26 Z2
N540 G01 X26 Z-16        ;Pass 7
N550 G01 X28 Z-15
N560 G00 X28 Z2
N570 G00 X26 Z2

N580 G01 X22 Z2
N590 G01 X22 Z-1        ;Pass 8
N600 G01 X24 Z0
N610 G00 X24 Z2
N620 G00 X22 Z2

N630 G01 X20 Z2        ;Sweep Pass
N640 G01 X20 Z0
N650 G01 X24 Z-2
N660 G01 X24 Z-16
N670 G01 X26.71248 Z-16
N680 G01 X26.71248 Z-19
N690 G03 X36 Z-28.95858 R13
N700 G01 X36 Z-33.95858
N710 G02 X40 Z-35.95858 R2
N720 G01 X45 Z-35.95858
N730 G01 X49 Z-37.95858
N740 G01 X49 Z-49.95858
N750 G01 X49 Z-52.95858
N760 G01 X54 Z-52.95858
N770 G00 X54 Z2

N780 G91
N790 G28 X0
N800 G28 Z0
N810 G90
```

```
;-------GROOVING-------
N1260 T19
N1270 G97 S2750 M03 F0.05

N1280 G00 X54 Z2
N1290 G00 X54 Z-15
N1300 G00 X24 Z-15

N1310 G01 X16 Z-15        ;Plunge 1
N1320 G00 X24 Z-15

N1330 G00 X24 Z-16
N1340 G01 X16 Z-16        ;Plunge 2
N1350 G00 X24 Z-16

N1360 G00 X54 Z-16
N1370 G00 X54 Z2

N1380 G91
N1390 G28 X0
N1400 G28 Z0
N1410 G90

;-------PART-OFF-------
N1420 T20
N1430 G97 S1210 M03 F0.09

N1440 G00 X54 Z2
N1450 G00 X54 Z-52.95858
N1460 G01 X-1 Z-52.95858
N1470 G00 X54 Z-52.95858
N1480 G00 X54 Z2

N1490 G91
N1500 G28 X0
N1510 G28 Z0
N1520 G90

N1530 M09

N1540 M30
```

9.3.4.3 Results

Measurement results for SP3-AL6013 obtained using the methodology explained in Section 9.3.1 are displayed in Figure 9.21 and Table 9.22. The power consumption from all three measurements are plotted in the figure and the measured energy results are summarized in the table under "Measured" column.

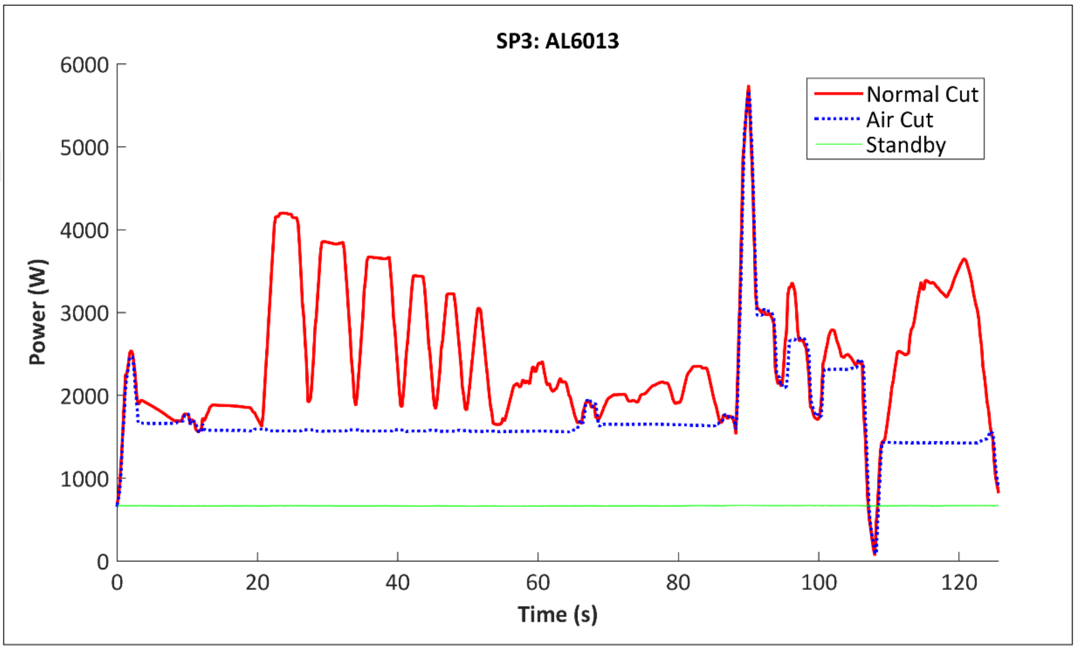

Figure 9.21 Power consumption measurements for SP3-AL6013

Estimation results for SP3-AL6013 are given in Appendix B.3. The energy requirement for auxiliary equipment and theoretical energy is detailed in Table 9.21. High-level result for theoretical and auxiliary energy categories are shown under the "Estimated" column of Table 9.22.

Table 9.21 Energy requirement estimations for SP3-AL6013

	E [J]	CO2 [g]	% Share
Theoretical	70,552	10.4	24
Spindle	75,741	11.2	26
Cutting Fluid	50,385	7.4	17
Turret	1,606	0.2	1
Chuck	172	0.0	0
Servo	6,374	0.9	2
Lubrication	69	0.0	0
Standby	86,139	12.7	30
TOTAL	**291,037**	**42.9**	**100**

Based on the comparison in Table 9.22 for SP3-AL6013, the error between measured and estimated process energy is 16 kJ corresponding to a 5.2% discrepancy. The main difference in the process energy stems from the theoretical energy values, accounting for 19.1 kJ of the discrepancy. To identify the major source of this difference, a breakdown of theoretical energy values is performed, with the results are displayed in Table 9.23.This breakdown result reveals that deviation is concentrated in the parting operation, with a difference of 14.7 kJ between measured and estimated values.

Table 9.22 Energy results comparison for SP3-AL6013

	Measured	Estimated	Δ Error	% Error
Time (s)	125.0	124.8	0.2	0.1
E_{th} (kJ)	89.7	70.6	**19.1**	21.3
E_{aux_var} (kJ)	134.0	134.3	-0.3	-0.2
E_{aux_cons} (kJ)	83.4	86.1	-2.8	-3.3
$E_{process}$ (kJ)	**307.1**	**291.0**	**16.0**	**5.2**

Table 9.23 Breakdown of theoretical energy for SP3-AL6013

	Measured	**Estimated**	**Δ Error**	**% Error**
Facing (kJ)	1.0	1.3	-0.3	-35.8
Turning - Rough (kJ)	57.0	51.4	5.6	9.8
Turning - Finish (kJ)	7.3	6.8	0.5	6.8
Drilling (kJ)	0.4	1.6	-1.2	-301.5
Grooving (kJ)	1.1	1.2	-0.1	-9.2
Parting (kJ)	22.9	8.2	**14.7**	64.3
E_{th} (kJ)	**89.7**	**70.6**	**19.1**	**21.3**

Initially, it was assumed that the reason of the error is using constant rotational speed (n) in the part program instead of constant surface speed. This causes the cutting speed (V_c) to approach zero as the parting tool nears the center of the workpiece, leading to an exponential increase in specific cutting energy. Two models from the literature (Lv et al., 2018) are implemented to involve the effect of increased specific cutting energy in theoretical energy estimation. However, this solution only raised the estimated theoretical parting energy from 7.6 kJ to 9.2 kJ, which did not resolve the error.

Next, the effect of friction force was considered. SP3-AL6013 has a larger diameter compared to the other sample parts, leading to the assumption of higher friction force and consequently higher theoretical energy for the parting operation. Based on findings in the literature (Lokesha et al., 2021), the additional energy requirement was calculated to be 0.3 kJ, which is insufficient to explain the original 14.7 kJ discrepancy.

Subsequently, chatter was suspected as a cause of the high deviation in the parting operation. Chatter experiments were conducted on the same sample part, revealing that the process is stable and there is no chatter.

Finally, two other SP3-AL6013 parts are manufactured by using different feed and cutting speed values for the parting operation than the original one (no1) to observe the effect of cutting parameters on the theoretical energy. Results are presented in Table 9.24.

Table 9.24 Effect of cutting parameters on the error of parting operation

	a_f (mm)	**V_c (m/min)**	**Δ Error**
SP3-AL6013 no1	0.09	190	**14.7**
SP3-AL6013 no2	0.09	470	**7.4**
SP3-AL6013 no3	0.05	470	**11.6**

Results show that even with different cutting conditions, error could be minimized but not eliminated. This suggests there may be issues with either the machine stability or the parting blade or insert. The estimation model of TurnDesign Eco Edition is structured with the assumption that the machine and cutting tools are at in optimal conditions. For the verification studies, the TP32 CNC lathe did not use Sandvik tools with chip breaker designs for aluminum parts and utilized a worn out blade and insert.

While TurnDesign Eco Edition's primary purpose is to provide process energy estimates before manufacturing, this case shows that it can also indicate suboptimal operating conditions of the CNC lathe after manufacturing.

9.3.5 Discussion

The verification studies reveal that the TurnDesign Eco Edition estimation model performs reliably across different materials and dimensions of the sample parts. As illustrated in Table 9.25, the discrepancies between measured and estimated process energy for the sample parts ranged from 0.2% to 5.3%. This shows a high level of accuracy in the estimation model.

The variable auxiliary energy estimations showed discrepancies ranging from -0.3 kJ to 15.2 kJ. The first reason for the deviation is the polynomial fit used for spindle power (Figure 8.5), which slightly underestimates or overestimates power consumption depending on the rotational speeds. Another reason is the underestimated total cutting time values, resulting in lower auxiliary variable energy values. Additionally, the measurements themselves also contribute to these deviations. Trial measurements indicate up to 400 W variations for the same rotational speed. To achieve further accuracy, the cause of these deviations could be investigated in future studies and a sub-model could be integrated into TurnDesign Eco Edition to account for these discrepancies.

The comparison between estimated and measured values also indicates that the model assumes optimal conditions for tools and machine stability. Deviations from these conditions in real-world applications, such as tool wear or suboptimal machine settings, can lead to increased discrepancies, as seen in the parting operation of SP3-AL6013.

Table 9.25 Delta and percent errors for the energy requirements

	SP1-AISI1040		**SP1-GG25**		**SP1-AL6013**		**SP2-AL6013**		**SP3-AL6013**	
Error	**Δ**	**%**	**Δ**	**%**	**Δ**	**%**	**Δ**	**%**	**Δ**	**%**
t	1.3	0.7	1.2	0.6	2.1	1.9	2.0	3.7	0.2	0.1
E_{th}	-0.2	-0.3	-0.8	-1.5	0.9	2.3	1.3	8.7	19.1	21.3
E_{aux_var}	2.9	1.5	-3.4	-1.9	15.2	9.0	3.5	3.3	-0.3	-0.2
E_{aux_cons}	-3.4	-2.7	-3.8	-2.9	-0.8	-1.1	1.1	3.0	-2.8	-3.3
$E_{process}$	**-0.8**	**-0.2**	**-8.1**	**-2.2**	**15.3**	**5.3**	**6.0**	**3.8**	**16.0**	**5.2**

From the summary in Table 9.26, it can be concluded that the theoretical energy component contributed minimally to the overall process energy for all sample parts. It ranges from 9% to 24% of the total process energy, depending on the material and the volume removed. Constant auxiliary energy (standby mode) accounts for 23% to 36% of the total process energy. A sample part with a higher total cutting time results in a higher constant auxiliary energy share. Variable auxiliary energy, which constitutes 46% to 67% of the total process energy, represents a substantial portion of the overall energy consumption for all the sample parts.

A further analysis of the auxiliary energy components in Table 9.26 highlights significant contributors to the total energy consumption. The spindle (25% to 50%), cutting fluid system (14% to 21%) and standby mode (23% to 36%) are the primary consumers of auxiliary energy, consistent across all sample parts. The high energy usage of the spindle and cutting fluid system indicates areas where efficiency improvements could have a substantial impact on reducing overall energy consumption. This insight is critical for optimizing the energy efficiency of CNC machining processes.

Table 9.26 Percent shares of the estimated energy requirements

% Shares	**SP1-AISI1040**	**SP1-GG25**	**SP1-AL6013**	**SP2-AL6013**	**SP3-AL6013**
Theoretical	20.9	15.1	14.4	9.1	24.2
Spindle	26.0	24.9	37.5	50.1	26.0
Cutting Fluid	18.8	21.3	16.7	13.7	17.3
Turret	0.3	0.4	0.5	0.8	0.6
Chuck	0.0	0.0	0.1	0.1	0.1
Servo	1.6	1.7	2.1	2.8	2.2
Lubrication	0.0	0.0	0.0	0.0	0.0
Standby	32.2	36.5	28.6	23.5	29.6
TOTAL	**100**	**100**	**100**	**100**	**100**

CHAPTER 10

CONCLUSION AND FUTURE WORKS

10.1 Conclusion

This study has explored the development of TurnDesign Eco Edition, a comprehensive design software tool that estimates the energy consumption and carbon footprint of rotational parts during the design stage. By focusing on various parts of the CAD/CAM chain, including part design, process planning, part programming and energy usage, the research presents a detailed model that helps improve energy efficiency before manufacturing begins.

TurnDesign Eco Edition not only serves as an estimation model but can also act as a diagnostic instrument that can reveal inefficiencies in the manufacturing process. By identifying areas where energy consumption is higher than expected, such as the auxiliary energy components including spindle power and cutting fluid systems, manufacturers can take targeted actions to optimize these processes.

The main achievement of this research is the creation of an energy estimation model that can accurately predict the energy consumption and carbon emissions for rotational parts. This model combines both theoretical and auxiliary energy components, giving a complete view of the energy needs for different design alternatives. It has been tested and validated using the Anatool TP32 CNC lathe, demonstrating its reliability and practical use in various machining scenarios.

The research introduces a new method for estimating the theoretical energy required based on STEP AP224 features. By using detailed volume calculations and integrating parameters to calculate specific cutting energy, the model predicts the theoretical energy consumption for each feature. This estimation is crucial for understanding the energy demands of machining operations alone, excluding the requirements of auxiliary equipment.

A significant portion of the study is dedicated to auxiliary energy estimation, which includes the energy consumed by spindle assembly, cutting fluid system, servo motors, turret, chuck, lubrication system and standby mode. The research identifies the spindle and cutting fluid systems as the primary consumers of auxiliary energy, highlighting the potential for substantial energy savings through targeted efficiency improvements in these areas. The auxiliary energy model is accounting for both constant and variable energy components and is validated through empirical measurements.

The study extends the energy estimation model to include carbon footprint calculations, linking energy consumption to environmental impact. By converting energy values into corresponding CO_2 emissions, the model provides a critical insight into the sustainability of rotational part designed and CNC turning processes.

The research includes a practical implementation of the energy estimation model in a real-world CNC environment. The model's estimations are compared with actual energy consumption data obtained from Anatool TP32 CNC lathe, demonstrating a high degree of accuracy. This verification confirms the model's applicability in industrial settings and highlights its potential as a tool for improving energy efficiency and reducing carbon emissions in manufacturing.

10.2 Future Work

The developed estimation model revealed some areas for improvement to enhance its functionality. Besides, the study gave an insight into the other research topics mainly complementing the model. The main improvements and future research topics which can be based on this study are discussed below.

Internal turning and threading features and corresponding operations can be incorporated into user input module. This addition will expand the range of part design, making TurnDesign Eco Edition more versatile and comprehensive.

In the process planning module, the current method of calculating stock size based on a formula could be improved by rounding stock sizes to standard values found in a database of available market sizes. This adjustment will make the estimates more practical and aligned with market availability.

Additionally, the material database in the module can be expanded to include all material groups, providing a more extensive range of options for users and enhancing the software's span in energy estimation across various materials.

Another improvement involves the coolant usage assumption. Presently, the software assumes that coolant is on during the entire machining process for all material types. This can be refined to turn off the coolant for specific materials or manufacturing processes where its usage is unnecessary, optimizing energy consumption and improving the accuracy of energy estimates.

For the part programming module, the scope of outer turning operations can be broadened to include Type 2 profiles, which account for both increasing and decreasing contours. Currently, only Type 1 profiles with increasing contours are considered. This will enable the implementation of toolpaths for grooving beyond the current assumption of Square U grooves. Furthermore, toolpaths for groove finishing can be added.

To increase the accuracy of energy estimation module a dedicated study on spindle power consumption characteristics is recommended to further understand the nature of spindle energy use. Such a study would enhance the accuracy of the estimation model, as the spindle is the primary auxiliary equipment with the highest energy demand.

The current energy estimation model does not account for tool wear and its impact on power consumption. Developing and integrating a tool wear model into TurnDesign Eco Edition can more accurately reflect the increasing energy requirements of worn tools, leading to improved energy estimates.

Finally, this entire framework and estimation model can be adapted for CNC vertical machining centers. This adaptation would enable the estimation of energy consumption for prismatic parts using milling operations before their production.

REFERENCES

Amaitik, S.M., Kılıç, S.E., 2005. STEP-Based Feature Modeller for Computer-Aided Process Planning. International Journal of Production Research 43 (15), 3087–3101. https://doi.org/10.1080/00207540500104019

Akkuş, K., Kılıç. S.E., 2012. STEP AP224 Based Feature Modeller with Automatic NC-Code Generation for Rotational Parts. Proceedings of the 15th International Conference on Machine Design and Production (UMTIK2012), 19 - 22 June 2012, Pamukkale, Denizli, Turkey, 2, 763 - 777.

Anatool Machine Tools, 2009. TP 32 CNC Lathe Programming Manual. Ankara, Turkey.

Balogun, V.A., Mativenga, P.T., 2013. Modelling of Direct Energy Requirements in Mechanical Machining Processes. Journal of Cleaner Production 41, 179–186. https://doi.org/10.1016/j.jclepro.2012.10.015

Boettjer, T., Krogshave, J.T., Ramanujan, D., 2021. Machine-Specific Estimation of Milling Energy Consumption in Detailed Design. Journal of Manufacturing Science and Engineering, Transactions of the ASME 143 (8). https://doi.org/10.1115/1.4050179

Boothroyd, G., Knight, W.A., 1989. Fundamentals of Machining and Machine Tools. Marcel Dekker Inc., New York.

Cheng, K., Zhao, G., Wang, W., Liu, Y., 2022. An Estimation Methodology of Energy Consumption for the Intelligent CNC Machining Using STEP-NC. International Journal of Advanced Manufacturing Technology 123 (1–2), 627–644. https://doi.org/10.1007/s00170-022-10194-3

Edem, I.F., Mativenga, P.T., 2017. Modelling of Energy Demand from Computer Numerical Control (CNC) Toolpaths. Journal of Cleaner Production 157, 310–321. https://doi.org/10.1016/j.jclepro.2017.04.096

Gutowski, T., Dahmus, J., Thiriez, A., 2006. Electrical Energy Requirements for Manufacturing Processes. Proceedings of the 13th CIRP International Conference on Life Cycle Engineering, LCE 2006, 623–628.

Hauschild, M., Jeswiet, J., Alting, L., 2005. From Life Cycle Assessment to Sustainable Production: Status and Perspectives. CIRP Annals - Manufacturing Technology 54 (2), 1-21. https://doi.org/10.1016/S0007-8506(07)60017-1

He, Y., Liu, F., Wu, T., Zhong, F.P., Peng, B., 2012. Analysis and Estimation of Energy Consumption for Numerical Control Machining. Proceedings of the Institution of Mechanical Engineers, Part B: Journal of Engineering Manufacture 226 (2), 255–266. https://doi.org/10.1177/0954405411417673

International Standards Organization, 1994. ISO 10303-1 Industrial automation systems and integration - Product data representation and exchange - Part 1: Overview and fundamental principles. Geneva, Switzerland.

International Standards Organization, 2004. ISO 14649-10 Industrial automation systems and integration - Physical device control - Data model for computerized numerical controllers - Part 10: General process data. Geneva, Switzerland.

International Standards Organization, 2006. ISO 10303-224 Industrial Automation Systems and Integration - Product Data Representation and Exchange - Part 224: Application Protocol: Mechanical Product Definition for Process Planning Using Machining Feature. Geneva, Switzerland.

International Standards Organization, 2007. ISO 10303-238 Industrial automation systems and integration - Product data representation and exchange - Part 238: Application protocol: Application interpreted model for computerized numerical controllers. Geneva, Switzerland.

International Standards Organization, 2017. ISO 1832:2017 Indexable inserts for cutting tools - Designation. Geneva, Switzerland.

Iscar, 2017a. Non-Rotating Tool Lines. https://www.iscar.com/Catalogs/publication-2017/Non_Rotating_catalog_06_2017.pdf

Iscar, 2017b. Rotating Tool Lines, https://www.iscar.com/Catalogs/publication-2017/Rotating_Tools_catalog-2017.pdf

Jeswiet, J., Kara, S., 2008. Carbon Emissions and CES^{TM} in Manufacturing. CIRP Annals - Manufacturing Technology 57 (1), 17-20. https://doi.org/10.1016/j.cirp.2008.03.117

Jiang, Z., Gao, D., Lu, Y., Kong, L., Shang, Z., 2019. Electrical Energy Consumption of CNC Machine Tools Based on Empirical Modeling. International Journal of Advanced Manufacturing Technology 100 (9–12), 2255–2267. https://doi.org/10.1007/s00170-018-2808-x

Kolar, M., Vyroubal, J., Smolik, J., 2016. Analytical Approach to Establishment of Predictive Models of Power Consumption of Machine Tools' Auxiliary Units. Journal of Cleaner Production 137, 361–369. https://doi.org/10.1016/j.jclepro.2016.07.092

Kong, D., Choi, S., Yasui, Y., Pavanaskar, S., Dornfeld, D., Wright, P., 2011. Software-Based Tool Path Evaluation for Environmental Sustainability. Journal of Manufacturing Systems 30 (4), 241–247. https://doi.org/10.1016/j.jmsy.2011.08.005

Li, W., Kara, S., 2011. An Empirical Model for Predicting Energy Consumption of Manufacturing Processes: A Case of Turning Process. Proceedings of the Institution of Mechanical Engineers, Part B: Journal of Engineering Manufacture 225 (9), 1636–1646. https://doi.org/10.1177/2041297511398541

Liu, F., Xie, J., Liu, S., 2015. A Method for Predicting the Energy Consumption of the Main Driving System of a Machine Tool in a Machining Process. Journal of Cleaner Production 105, 171–177. https://doi.org/10.1016/j.jclepro.2014.09.058

Lokesha, Nagaraj, P.B., Dinesh, P., 2021. Frictional Force during Machining Process Part 2: Influence of Process Parameters. Materials Today: Proceedings 46, 2468–2470. https://doi.org/10.1016/j.matpr.2021.01.401

Lv, J., Tang, R., Tang, W., Jia, S., Liu, Y., Cao, Y., 2018. An Investigation into Methods for Predicting Material Removal Energy Consumption in Turning. Journal of Cleaner Production 193, 128–139. https://doi.org/10.1016/j.jclepro.2018.05.035

Pawanr, S., Garg, G.K., Routroy, S., 2022. A Novel Approach to Model the Energy Consumption of Machine Tools for Machining Cylindrical Parts. Journal of Manufacturing Processes 84, 28–42. https://doi.org/10.1016/j.jmapro.2022.09.040

Rahimifard, S., Seow, Y., Childs, T., 2010. Minimising Embodied Product Energy to Support Energy Efficient Manufacturing. CIRP Annals - Manufacturing Technology 59 (1), 25–28. https://doi.org/10.1016/j.cirp.2010.03.048

Republic of Turkey, Ministry of Energy and Natural Resources (ETKB), 2007. Energy Efficiency Law (in Turkish). https://www.mevzuat.gov.tr/MevzuatMetin/1.5.5627.pdf (accessed 12 January 2024).

Republic of Turkey, Ministry of Energy and Natural Resources (ETKB), 2008. Regulation on Increasing Efficiency in the usage of Energy Sources and Energy (in Turkish). https://www.mevzuat.gov.tr/MevzuatMetin/yonetmelik/7.5.15437.pdf (accessed 12 January 2024).

Republic of Turkey, Ministry of Energy and Natural Resources (ETKB), 2008. National Energy Efficiency Action Plan. https://enerji.gov.tr//Media/Dizin/EVCED/tr/EnerjiVerimlili%C4%9Fi/UlusalEnerjiVerimlili%C4%9FiEylemPlan%C4%B1/Belgeler/NEEAP.pdf (accessed 12 January 2024).

Sandvik Coromant, 2009. Main Catalogue.

Sandvik Coromant, 2017a. Turning Tools. www.sandvik.coromant.com/en-us/downloads/

Sandvik Coromant, 2017b. Training Handbook. www.sandvik.coromant.com/en-us/downloads/

Sandvik Coromant, 2017c. Turning Handbook. www.sandvik.coromant.com/en-us/downloads/

Sandvik Coromant, 2017d. Solid Round Tools. www.sandvik.coromant.com/en-us/downloads/

SECO Tools, 2012. MN2012 - Turning in: Machining Navigator Catalogue

SECO Tools, 2015. MN2015 - Holemaking in: Machining Navigator Catalogue

SECO Tools, 2023. Catalog & Technical Guide 2023.1

Shah, J.J., Rogers, M.T., 1988. Functional Requirements and Conceptual Design of the Feature-Based Modelling System. Computer-Aided Engineering Journal 5(1), 9-15. https://doi.org/10.1049/cae.1988.0004

Siemens AG, 2008. Power Monitoring Device SENTRON PAC3200 Manual. https://support.industry.siemens.com/cs/attachments/26504150/A5E01168664B-04_EN-US_122016_201612221316360495.pdf (accessed 27 May 2024)

Smid, P., 2008. CNC Programming Handbook, 3rd Edition. Industrial Press Inc., New York.

Turkish Electricity Transmission Company (TEİAŞ), 2022a. Electrical Characteristics by Turkey's Installed Capacity and Gross Generation (1970-2022). https://webim.teias.gov.tr/file/5c948b1a-7784-42ab-84d9-c7599a150c28?download (accessed 12 January 2024)

Turkish Electricity Transmission Company (TEİAŞ), 2022b. The Distribution of Gross Electricity Generation by Primary Energy Resources and the Electric Utilities in Turkey (2022). https://webim.teias.gov.tr/file/26116654-2d11-49f0-b2f3-8faf607ff4c1?download (accessed 11 May 2024)

Turkish Statistical Institute (TurkStat), 2023. National Inventory Report 1990 - 2021. https://unfccc.int/sites/default/files/resource/tur-2023-nir-14apr23.zip (accessed 13 January 2024)

World Business Council for Sustainable Development (WBCSD), World Resources Institute (WRI), 2004. Greenhouse Gas Protocol: A Corporate Accounting and Reporting Standard, Revised Edition. https://ghgprotocol.org/sites/default/files/standards/ghg-protocol-revised.pdf (accessed 9 May 2024).

Zhao, G., Cheng, K., Wang, W., Liu, Y., Dan, Z., 2022. A Milling Cutting Tool Selection Method for Machining Features Considering Energy Consumption in the STEP-NC Framework. International Journal of Advanced Manufacturing Technology 120 (5–6), 3963–3981. https://doi.org/10.1007/s00170-022-08964-0

APPENDIX A

VOLUME CALCULATIONS FOR MATERIAL REMOVAL

A.1 Outer Diameter

$$V_{rem} = \frac{\pi}{4}(D_{max}^2 - D^2) \cdot L \qquad \text{(A.1)}$$

where D_{max} is the maximum diameter value for the current design.

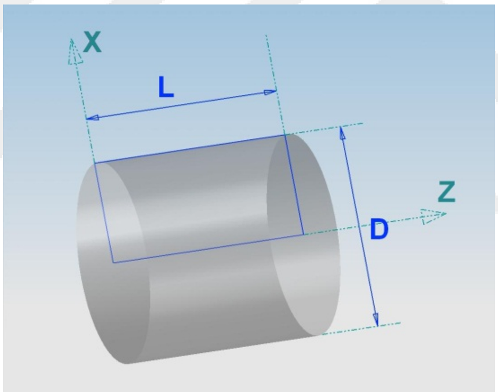

Figure A.1 Outer Diameter (Akkuş and Kılıç, 2012)

A.2 Tapered Outer Diameter

$$V_{rem} = \frac{\pi}{4} D_{max}^2\, L - \frac{\pi}{12}\,(D^2 + D\, D_F + D_F^2)\;L \qquad \text{(A.2)}$$

If α is used, for decreasing taper D_F can be calculated using the following equation:

$$D_F = D - 2\, L \tan\alpha \qquad \text{(A.3)}$$

If α is used, for increasing taper D_F can be calculated using the following equation:

$$D_F = D + 2\,L\,tan(\pi - \alpha) \tag{A.4}$$

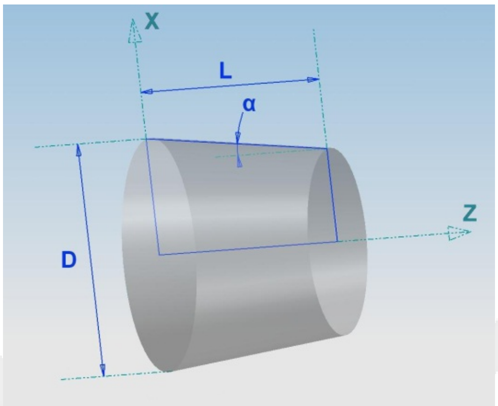

Figure A.2 Tapered Outer Diameter (Akkuş and Kılıç, 2012)

A.3 Revolved Flat

$$V_{rem} = \frac{\pi}{4} D_{max}^2\, L - \frac{\pi}{3}\,(R^2 + R\,R_F + R_F^2)\;L \tag{A.5}$$

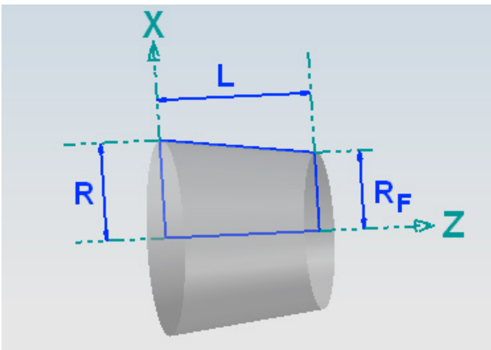

Figure A.3 Revolved Flat (Akkuş and Kılıç, 2012)

A.4 Revolved Round

Length and the final radius of the feature can be calculated using the following two equations:

$$L = r\ sin\alpha \tag{A.6}$$

$$R_F = R - r + r\ cos\alpha \tag{A.7}$$

Sweep angle α can be found by:

$$\alpha = cos^{-1}\left(\frac{r + R_F - R}{r}\right) \tag{A.8}$$

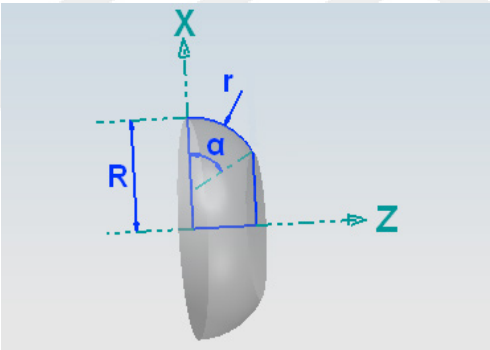

Figure A.4 Revolved Round (Akkuş and Kılıç, 2012)

The volume removed for Revolved Round feature is found by breaking it down into three components:

$$V_{rem} = V_{rec} - V_{trap} - V_{seg} \tag{A.9}$$

$$V_{rec} = \pi\ \frac{D_{max}^2}{4}\ r\ sin\alpha \tag{A.10}$$

where D_{max} is the maximum diameter value for the current design.

$$V_{trap} = \frac{\pi}{3}\,(R^2 + R\,R_F + R_F^2)\;r\,sin\alpha \tag{A.11}$$

The volume generated by 360 degree rotation of the circular segment is calculated using Equations (A.43) to (A.14).

$$V_{seg} = 2\pi\,\bar{r}_{seg}\,A_{seg} \tag{A.12}$$

$$\bar{r}_{seg} = \frac{4r}{3}\,\frac{sin^3\,(\alpha/2)}{(\alpha - sin\,\alpha)}\;sin(\frac{\pi}{2} - \frac{\alpha}{2}) + R - r \tag{A.13}$$

$$A_{seg} = \frac{r^2}{2}\,(\alpha - sin\alpha) \tag{A.14}$$

A.5 Spherical Cap

Spherical cap is essentially a derivative of Revolved Round where R=r and α=90°.

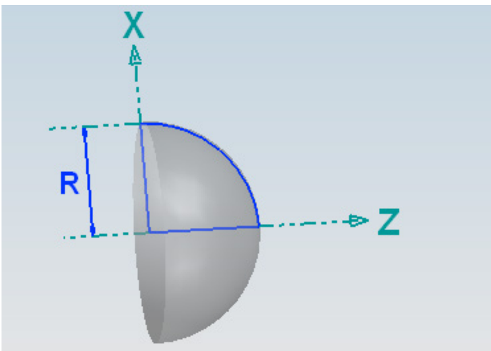

Figure A.5 Spherical Cap (Akkuş and Kılıç, 2012)

$$V_{rec} = \pi\,\frac{D_{max}^2}{4}\,R \tag{A.15}$$

$$V_{trap} = \frac{\pi}{3} R^3 \tag{A.16}$$

$$\bar{r}_{seg} = \frac{4}{3} R \frac{1}{4} \frac{1}{\pi/2-1} = \frac{R}{3} \frac{1}{\pi/2-1} \tag{A.17}$$

$$A_{seg} = \frac{R^2}{2}(\pi/2 - 1) \tag{A.18}$$

$$V_{seg} = 2\pi \frac{R^2}{2} \frac{R}{3} = \frac{\pi}{3} R^3 \tag{A.19}$$

$$V_{rem} = \pi \frac{D_{max}^2}{4} R - \frac{2\pi}{3} R^3 \tag{A.20}$$

A.6 Rounded U Groove

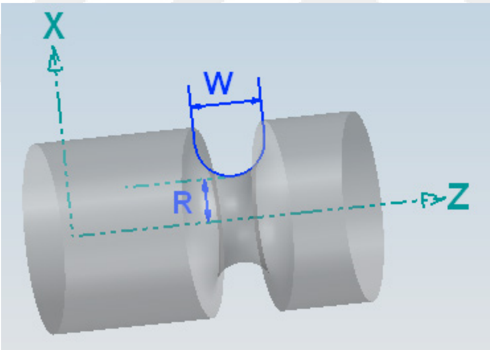

Figure A.6 Rounded U Groove (Akkuş and Kılıç, 2012)

$$V_{rem} = V_{rec} + V_{sc} \tag{A.21}$$

where V_{rec} is the volume generated by the 360 degree revolution of the rectangular area and V_{sc} is the volume generated by the semicircular area.

$$V_{rec} = \pi \left(\frac{D^2}{4} - R^2 - RW - \frac{W^2}{4}\right) W \tag{A.22}$$

$$V_{sc} = 2\pi \, \bar{r}_{sc} \, A_{sc} \tag{A.23}$$

$$\bar{r}_{sc} = \frac{W}{2} + R - \frac{4}{3\pi} \frac{W}{2} \tag{A.24}$$

$$\bar{r}_{sc} = \frac{W}{2} + R - \frac{2}{3} \frac{W}{\pi} \tag{A.25}$$

$$A_{sc} = \frac{\pi \, W^2}{8} \tag{A.26}$$

$$V_{sc} = 2 \, \pi \, \bar{r}_{sc} \, A_{sc} \tag{A.27}$$

A.7 Partial Circular Groove

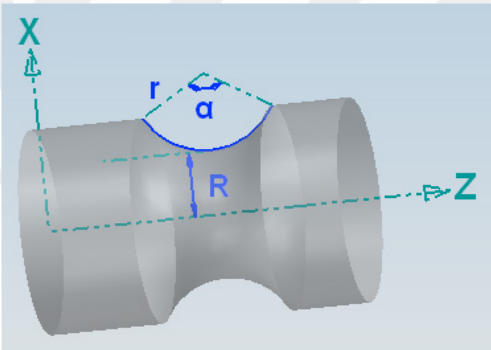

Figure A.7 Partial Circular Groove (Akkuş and Kılıç, 2012)

The volume removed is equal to the volume generated when the segment is revolved 360 degrees around the centerline.

$$V_{rem} = V_{seg} \tag{A.28}$$

$$\bar{r}_{seg} = R + r - \frac{4r}{3} \frac{\sin^3(\alpha/2)}{(\alpha - \sin\alpha)} \tag{A.29}$$

$$A_{seg} = \frac{r^2}{2}\,(\alpha - sin\,\alpha) \qquad (A.30)$$

$$V_{seg} = 2\pi\,\bar{r}_{seg}\,A_{seg} \qquad (A.31)$$

A.8 Square U Groove

$$V_{rem} = V_{cyl1} - V_{cyl2} - V_{trap1} - V_{trap2} - V_{tri1} + V_{seg1} - V_{tri2} + V_{seg2} \qquad (A.32)$$

Total length of the feature is calculated as follows:

$$L = W + \frac{D/2 - R}{tan\,\alpha_1} + \frac{D/2 - R}{tan\,\alpha_2} = W + (D/2 - R)(\frac{\cos\alpha_1}{sin\,\alpha_1} + \frac{cos\alpha_2}{sin\,\alpha_2}) \qquad (A.33)$$

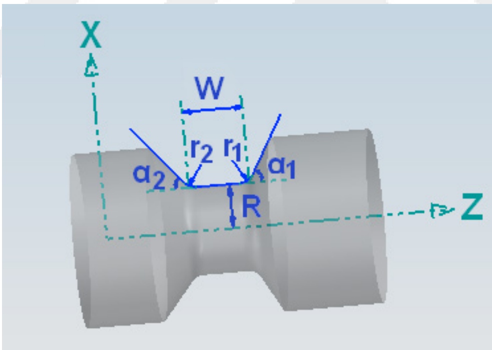

Figure A.8 Square U Groove (Akkuş and Kılıç, 2012)

The outer volumes V_{cyl1}, V_{cyl2}, V_{trap1} and V_{trap2} are found from the following equations:

$$V_{cyl1} = \frac{\pi}{4} D^2 \left[W + (D/2 - R)\left(\frac{cos\,\alpha_1}{sin\,\alpha_1} + \frac{cos\alpha_2}{sin\,\alpha_2}\right)\right] \qquad (A.34)$$

$$V_{cyl2} = \pi\ R^2\ W \qquad (A.35)$$

$$V_{trap1} = \frac{\pi}{12} \left(D^2 + 2DR + 4R^2\right) \frac{D/2 - R}{tan\, \alpha_1} \tag{A.36}$$

$$V_{trap2} = \frac{\pi}{12} \left(D^2 + 2DR + 4R^2\right) \frac{D/2 - R}{tan\, \alpha_2} \tag{A.37}$$

The volume generated by 360 degree rotation of the internal triangular area is calculated using Equations (A.38) to (A.42):

$$V_{tri2} = 2\pi \;\; \bar{r}_{tri2} \, . \; A_{tri2} \tag{A.38}$$

$$\bar{r}_{tri2} = \frac{2}{3} \, r_2 \, \frac{sin^2(\alpha_2/2)}{cos(\alpha_2/2)} \;\; cos(\alpha_2/2) + R \tag{A.39}$$

$$\bar{r}_{tri2} = \frac{2}{3} \, r_2 \;\; sin^2 \, (\alpha_2/2) + R \tag{A.40}$$

$$A_{tri2} = \frac{1}{2} \;\; 2 \, r_2 \, sin \, (\alpha_2/2) \;\; r_2 \frac{sin^2(\alpha_2/2)}{cos(\alpha_2/2)} \tag{A.41}$$

$$A_{tri2} = r_2^2 \; \frac{sin^3(\alpha_2/2)}{cos(\alpha_2/2)} \tag{A.42}$$

The volume generated by 360 degree rotation of the circular segment is calculated using Equations (A.43) to (A.45):

$$V_{seg2} = 2\pi \;\; \bar{r}_{seg2} \;\; A_{seg2} \tag{A.43}$$

$$\bar{r}_{seg2} = \left[\frac{r_2}{cos(\alpha_2/2)} - \frac{4r_2}{3} \; \frac{sin^3(\alpha_2/2)}{\alpha_2 - sin\, \alpha_2} \right] cos(\alpha_2/2) + R \tag{A.44}$$

$$A_{seg2} = \frac{r_2^2}{2} \; (\alpha_2 - sin\, \alpha_2) \tag{A.45}$$

To calculate V_{tri1} and V_{seg1} all subscripts "2" in the Equations (A.38) to (A.45) should be changed to "1".

A.9 Vee Groove

Volume removed for Vee Groove feature can be found by:

$$V_{rem} = V_{tri1} - V_{tri2} + V_{seg} \tag{A.46}$$

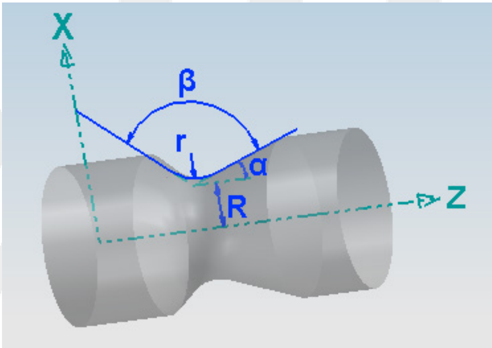

Figure A.9 Vee Groove (Akkuş and Kılıç, 2012)

The total length of the feature is:

$$L = \frac{D/2-R}{tan(\pi-\alpha-\beta)} + \frac{D/2-R}{tan\alpha} \tag{A.47}$$

The volume obtained when the first triangular section is rotated around the centerline can be calculated using Equations (A.48) to (A.52):

$$V_{tri1} = 2\pi\ \bar{r}_{tri1} \,.\, A_{tri1} \tag{A.48}$$

$$A_{tri1} = \frac{1}{2}\ L\ (D/2 - R) \tag{A.49}$$

$$A_{tri1} = \frac{(D/2-R)^{\ 2}}{2}\left[\frac{1}{tan(\pi-\alpha-\beta)} + \frac{1}{tan\ \alpha}\right] \tag{A.50}$$

$$\bar{r}_{tri1} = R + \frac{2}{3}\left(\frac{D}{2} - R\right) \tag{A.51}$$

$$\bar{r}_{tri1} = \frac{R+D}{3} \tag{A.52}$$

The volume obtained when the second triangular section formed at the tip of the first triangle is rotated at 360 degrees can be calculated using Equations (A.53) to (A.56):

$$V_{tri2} = 2\pi\ \ \bar{r}_{tri2}\ .\ A_{tri2} \tag{A.53}$$

$$\bar{r}_{tri2} = R + \frac{2}{3}r\ \frac{cos^2(\beta/2)}{sin(\beta/2)}\ sin(\ \alpha + \beta/2) \tag{A.54}$$

$$A_{tri2} = \frac{1}{2}\ 2\ r\ \ cos(\beta/2)\ \ r\ \frac{cos^2(\beta/2)}{sin(\beta/2)} \tag{A.55}$$

$$A_{tri2} = r^2\,\frac{cos^3(\beta/2)}{sin(\beta/2)} \tag{A.56}$$

The volume generated by 360 degree rotation of the circular segment is calculated using Equations (A.57) to (A.59):

$$V_{seg} = 2\pi\ \ \bar{r}_{seg}\ .\ A_{seg} \tag{A.57}$$

$$\bar{r}_{seg} = \left[\frac{r}{sin(\beta/2)} - \frac{4r}{3}\ \ \frac{sin^3(\pi/2-\beta/2)}{\pi-\beta-sin(\pi-\beta)}\right]\ sin\ (\alpha + \beta/2) + R \tag{A.58}$$

$$A_{seg} = \frac{r}{2}\,[\ \pi - \beta - sin\ (\pi - \beta)\ ] \tag{A.59}$$

A.10 Round Hole

Bottom Condition 1: Through

$$V_{rem} = \frac{\pi}{4} D^2 L_{max} \tag{A.60}$$

Bottom Condition 2: Flat

$$V_{rem} = \frac{\pi}{4} D^2 L \tag{A.61}$$

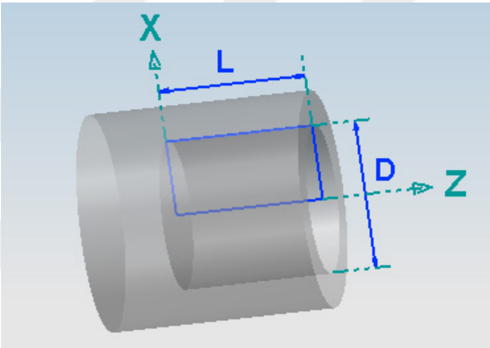

Figure A.10 Round Hole: Flat Bottom (Akkuş and Kılıç, 2012)

Bottom Condition 3:Conical

The volume removed for the conical bottom condition is broken down into two components. V_{rec} is used for calculating the cylindrical volume. V_{tri} is used to calculate the conical volume based on the 360 degree revolution of the triangular area at the end of the cylindrical part.

$$V_{rem} = V_{rec} + V_{tri} \tag{A.62}$$

$$V_{tri} = V_{tri1} - V_{tri2} + V_{seg} \tag{A.63}$$

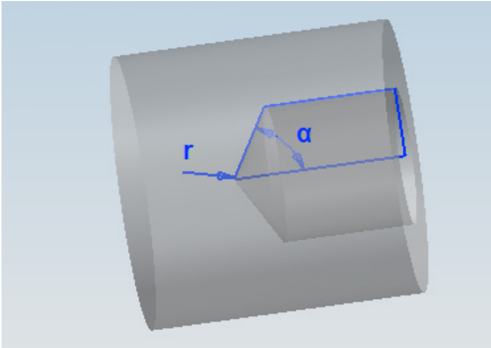

Figure A.11 Round Hole: Conical Bottom (Akkuş and Kılıç, 2012)

$$V_{rec} = \frac{\pi}{4}\, D^2\, L \tag{A.64}$$

V_{tri1} and V_{tri2} are found from the volume of a cone formula in Equations (A.65) and (A.66):

$$V_{tri1} = \frac{\pi}{12}\, \pi\, D^2 \frac{D/2}{tan(\alpha/2)} = \frac{\pi}{24}\, \frac{D^3}{tan(\alpha/2)} \tag{A.65}$$

$$V_{tri2} = \frac{\pi}{12}\, 4\, r^2\, cos^2(\alpha/2)\; r\, \frac{cos^2(\alpha/2)}{sin(\alpha/2)} = \frac{\pi}{3}\, r^3\, \frac{cos^4(\alpha/2)}{sin(\alpha/2)} \tag{A.66}$$

The volume of a circular segment is found using the following equations:

$$V_{seg} = \frac{\pi}{3}\; h_{seg}^2(3r - h_{seg}) \tag{A.67}$$

$$V_{seg} = \frac{\pi}{3}\; [r^2 - 2r^2\, sin(\alpha/2) + r^2\, sin^2(\alpha/2)]\; [2r\; + r\; sin(\alpha/2)] \tag{A.68}$$

$$V_{seg} = \frac{\pi}{3}\, [2r^3 - 3r^3\, sin(\alpha/2) + r^3\, sin^3(\alpha/2)] \tag{A.69}$$

$$V_{seg} = \frac{\pi}{3} r^3\, [2 - 3\, sin(\alpha/2) + sin^3(\alpha/2)] \tag{A.70}$$

Bottom Condition 4 and 5: Flat with Radius and Flat with Taper

Flat bottoms with radius and with taper conditions are neglected in this study since turning cannot produce such hole geometries. These conditions are specific to milling. However, a basic volume calculation is included for completeness.

$$V_{rem} = \frac{\pi}{4} D^2 L \tag{A.71}$$

Bottom Condition 6: Spherical

The volume removed for a spherical bottom condition is broken down into two components. V_{rec} is the volume generated by the 360 degree revolution of the cylindrical part and V_{sc} is the volume generated by the semicircular area.

$$V_{rem} = V_{rec} + V_{sc} \tag{A.72}$$

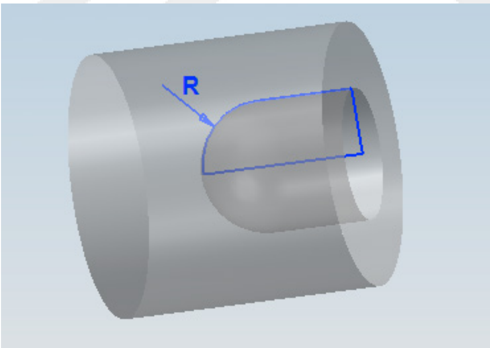

Figure A.12 Round Hole: Spherical Bottom (Akkuş and Kılıç, 2012)

$$V_{rec} = \frac{\pi}{4} D^2 (L - D/2) \tag{A.73}$$

$$V_{sc} = \frac{2}{3} \pi \frac{D^3}{8} = \frac{\pi}{12} D^3 \tag{A.74}$$

A.11 Counterbored Hole

Based on STEP AP224 definition, a counterbored hole has a larger hole (D_1, L_1) and a smaller hole (D_2, L_2).

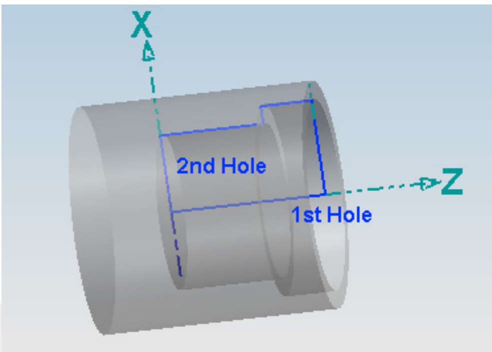

Figure A.13 Counterbored Hole (Akkuş and Kılıç, 2012)

Bottom Condition 1: Through

$$V_{rem} = V_{rec1} + V_{rec2} \quad \text{(A.75)}$$

$$V_{rec1} = \frac{\pi}{4} D_1^2\, L_1 \quad \text{(A.76)}$$

$$V_{rec2} = \frac{\pi}{4} D_2^2\, (L_{max} - L_1) \quad \text{(A.77)}$$

Bottom Condition 2: Flat

$$V_{removed} = V_{rec1} + V_{rec2} \quad \text{(A.78)}$$

$$V_{rec1} = \frac{\pi}{4} D_1^2\, L_1 \quad \text{(A.79)}$$

$$V_{rec2} = \frac{\pi}{4} D_2^2 \, L_2 \tag{A.80}$$

Bottom Condition 3:Conical

$$V_{rem} = V_{rec1} + V_{rec2} + V_{tri1} - V_{tri2} + V_{seg} \tag{A.81}$$

$$V_{rec1} = \frac{\pi}{4} D_1^2 \, L_1 \tag{A.82}$$

$$V_{rec2} = \frac{\pi}{4} D_2^2 \, L_2 \tag{A.83}$$

$$V_{tri1} = \frac{\pi}{24} \, \frac{D_2^3}{tan(\alpha/2)} \tag{A.84}$$

$$V_{tri2} = \frac{\pi}{3} \, r^3 \, \frac{cos^4(\alpha/2)}{sin(\alpha/2)} \tag{A.85}$$

$$V_{seg} = \frac{\pi}{3} r^3 \, [2 - 3\,sin(\alpha/2) + sin^3(\alpha/2)] \tag{A.86}$$

Bottom Condition 4 and 5: Flat with Radius and Flat with Taper

Flat bottoms with radius and with taper conditions are neglected in this study since turning cannot produce such hole geometries. These conditions are specific to milling. However, a basic volume calculation is included for completeness.

$$V_{rem} = V_{rec1} + V_{rec2} \tag{A.87}$$

$$V_{rec1} = \frac{\pi}{4} D_1^2 \, L_1 \tag{A.88}$$

$$V_{rec2} = \frac{\pi}{4} D_2^2 \, L_2 \tag{A.89}$$

Bottom Condition 6: Spherical

$$V_{rem} = V_{rec1} + V_{rec2} + V_{sc} \quad \text{(A.90)}$$

$$V_{rec1} = \frac{\pi}{4} D_1^2 \, L_1 \quad \text{(A.91)}$$

$$V_{rec2} = \frac{\pi}{4} D_2^2 \, (L_2 - D_2/2) \quad \text{(A.92)}$$

$$V_{sc} = \frac{\pi}{12} \; D_2^3 \quad \text{(A.93)}$$

A.12 Countersunk Hole

Based on STEP AP224 definition, a countersunk hole has a tapered hole (D_1, L_1, D_2 or α) and a constant diameter hole (D_2, L_2).

Bottom Condition 1: Through

$$V_{rem} = V_{trap} + V_{rec} \quad \text{(A.94)}$$

$$V_{trap} = \frac{\pi}{12} (D_1^2 + D_1 \, D_2 + D_2^2) \, L_1 \quad \text{(A.95)}$$

$$V_{rec} = \frac{\pi}{4} D_2^2 \, (L_{max} - L_1) \quad \text{(A.96)}$$

Bottom Condition 2: Flat

$$V_{rem} = V_{trap} + V_{rec} \quad \text{(A.97)}$$

$$V_{trap} = \frac{\pi}{12} (D_1^2 + D_1 \, D_2 + D_2^2) \, L_1 \quad \text{(A.98)}$$

$$V_{rec} = \frac{\pi}{4} D_2^2\, L_2 \tag{A.99}$$

Bottom Condition 3:Conical

$$V_{rem} = V_{trap} + V_{rec} + V_{tri1} - V_{tri2} + V_{seg} \tag{A.100}$$

$$V_{trap} = \frac{\pi}{12} (D_1^2 + D_1\, D_2 + D_2^2)\, L_1 \tag{A.101}$$

$$V_{rec} = \frac{\pi}{4} D_2^2\, L_2 \tag{A.102}$$

$$V_{tri1} = \frac{\pi}{24}\ \frac{D_2^3}{tan(\alpha/2)} \tag{A.103}$$

$$V_{tri2} = \frac{\pi}{3}\, r^3\ \frac{cos^4(\alpha/2)}{sin(\alpha/2)} \tag{A.104}$$

$$V_{seg} = \frac{\pi}{3} r^3\, [2 - 3\, sin(\alpha/2) + sin^3(\alpha/2)] \tag{A.105}$$

Bottom Condition 4 and 5: Flat with Radius and Flat with Taper

Flat bottoms with radius and with taper conditions are neglected in this study since turning cannot produce such hole geometries. These conditions are specific to milling. However, a basic volume calculation is included for completeness.

$$V_{rem} = V_{trap} + V_{rec} \tag{A.106}$$

$$V_{trap} = \frac{\pi}{12} (D_1^2 + D_1\, D_2 + D_2^2)\, L_1 \tag{A.107}$$

$$V_{rec} = \frac{\pi}{4} D_2^2\, L_2 \tag{A.108}$$

Bottom Condition 6: Spherical

$$V_{removed} = V_{trap} + V_{rec} + V_{sc} \quad \text{(A.109)}$$

$$V_{trap} = \frac{\pi}{12}(D_1^2 + D_1\,D_2 + D_2^2)L_1 \quad \text{(A.110)}$$

$$V_{rec} = \frac{\pi}{4}D_2^2\,(L_2 - D_2/2) \quad \text{(A.111)}$$

$$V_{sc} = \frac{\pi}{12}\;D_2^3 \quad \text{(A.112)}$$

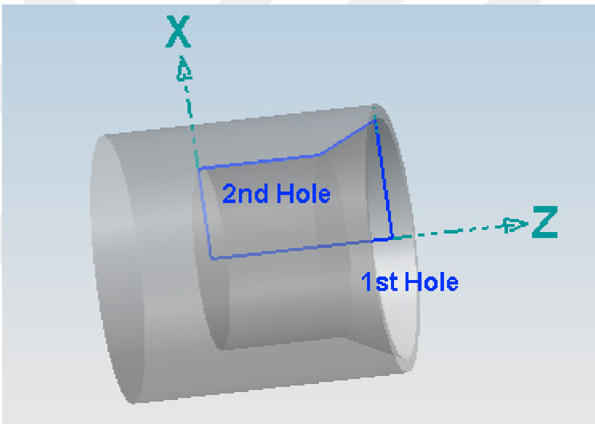

Figure A.14 Countersunk Hole (Akkuş and Kılıç, 2012)

A.13 Fillet

Angles for the first (γ) and the second (β) features are calculated by Equations (A.113) and (A.114):

$$\gamma = tan^{-1}\left(\frac{D_1 - D}{2L_1}\right) \quad \text{(A.113)}$$

$$\beta = tan^{-1}\left(\frac{D_2 - D}{2L_2}\right) \quad (A.114)$$

where L_1 and L_2 are the lengths of the first and the second features, on which the fillet is applied and D is the diameter at the intersection of the features. The profile angle (α) is calculated using the following equation:

$$\pi - \alpha + \beta + \gamma = \pi \quad \Rightarrow \quad \alpha = \beta + \gamma \quad (A.115)$$

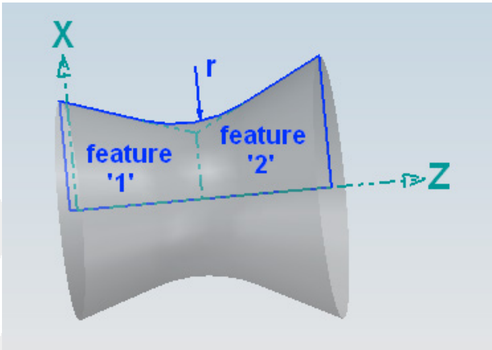

Figure A.15 Fillet (Akkuş and Kılıç, 2012)

When a fillet is created, it adds a volume to the part (V_{added}) which was previously removed. V_{added} is broken down into two volumes:

$$V_{added} = V_{tri} - V_{seg} \quad (A.116)$$

The volume obtained when the triangular section is rotated around the centerline can be calculated using Equations (A.117) to (A.119):

$$V_{tri} = 2\pi \ \bar{r}_{tri} \ A_{tri} \quad (A.117)$$

$$\bar{r}_{tri} = \frac{D}{2} + \frac{2}{3} r \frac{sin^2(\alpha/2)}{cos(\alpha/2)} \ sin\left(\frac{\pi}{2} - \frac{\alpha}{2} + \beta\right) \quad (A.118)$$

$$A_{tri} = \frac{1}{2}\ 2\, r\ sin(\alpha/2)\ \ r\frac{sin^2(\alpha/2)}{cos(\alpha/2)} \tag{A.119}$$

$$A_{tri} = r^2\ \frac{sin^3(\alpha/2)}{cos(\alpha/2)} \tag{A.120}$$

The volume generated by 360 degree rotation of the circular segment is calculated using Equations (A.121) to (A.123):

$$V_{seg} = 2\pi\ \bar{r}_{seg}\ A_{seg} \tag{A.121}$$

$$\bar{r}_{seg} = \left[\frac{r}{cos(\alpha/2)} - \frac{4r}{3}\ \frac{sin^3(\alpha/2)}{(\alpha - sin\alpha)}\right]\ sin\left(\frac{\pi}{2} - \frac{\alpha}{2} + \beta\right) + D_2 \tag{A.122}$$

$$A_{seg} = r^2\,(\alpha - sin\alpha) \tag{A.123}$$

A.14 Edge Round

Angles for the first (γ) and the second (β) features are calculated by Equations (A.124) and (A.125):

$$\gamma = tan^{-1}\left(\frac{D - D_1}{2L_1}\right) \tag{A.124}$$

$$\beta = tan^{-1}\left(\frac{D - D_2}{2L_2}\right) \tag{A.125}$$

where L_1 and L_2 are the lengths of the first and the second features, on which the edge round is applied and D is the diameter at the intersection of the features. The profile angle (α) is calculated using the following equation:

$$\frac{\pi}{2} - \gamma + \frac{\pi}{2} - \beta + \alpha = \pi \qquad \Rightarrow \qquad \alpha = \gamma + \beta \tag{A.126}$$

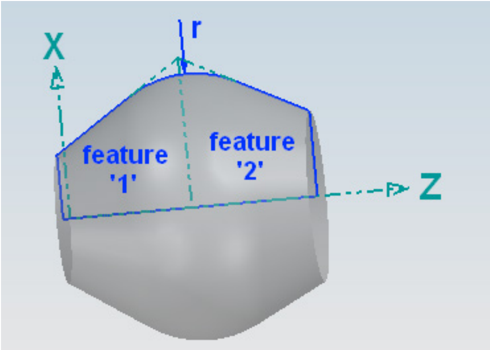

Figure A.16 Edge Round (Akkuş and Kılıç, 2012)

Volume removed for the edge round is divided into two components: V_{tri} and V_{seg}:

$$V_{rem} = V_{tri} - V_{seg} \tag{A.127}$$

The volume obtained when the triangular section is rotated around the centerline can be calculated using Equations (A.128) to (A.131):

$$V_{tri} = 2\pi\, \bar{r}_{tri}\, A_{tri} \tag{A.128}$$

$$\bar{r}_{tri} = \frac{D}{2} - \left[\frac{r}{cos(\alpha/2)} - \frac{r}{3}\,\frac{sin^2(\alpha/2)}{cos(\alpha/2)} - r\,cos(\alpha/2)\right]\, sin\left(\frac{\alpha}{2} + \frac{\pi}{2} - \beta\right) \tag{A.129}$$

$$A_{tri} = \frac{1}{2}\, 2\, r\, sin(\alpha/2)\;\; r\, \frac{sin^2(\alpha/2)}{cos(\alpha/2)} \tag{A.130}$$

$$A_{tri} = r^2\, \frac{sin^3(\alpha/2)}{cos(\alpha/2)} \tag{A.131}$$

The volume generated by 360 degree rotation of the circular segment is calculated using Equations (A.132) to (A.134):

$$V_{seg} = 2\pi\, \bar{r}_{seg}\, A_{seg} \tag{A.132}$$

$$\bar{r}_{seg} = \frac{D}{2} - \left[\frac{r}{cos(\alpha/2)} - \frac{4r}{3}\frac{sin^3\ (\alpha/2)}{(\alpha - sin\alpha)}\right] sin\left(\frac{\alpha}{2} + \frac{\pi}{2} - \beta\right) \quad \text{(A.133)}$$

$$A_{seg} = \frac{r^2}{2}(\alpha - sin\alpha) \quad \text{(A.134)}$$

A.15 Chamfer

Angles for the first (γ) and the second (β) features are calculated by Equations (A.135) and (A.136):

$$\gamma = \tan^{-1}\left(\frac{D_1 - D}{2L_1}\right) \quad \text{(A.135)}$$

$$\beta = tan^{-1}\left(\frac{D_2 - D}{2L_2}\right) \quad \text{(A.136)}$$

where L_1 and L_2 are the lengths of the first and the second features, on which the chamfer is applied and D is the diameter at the intersection of the features.

Volume added (V_{added}) is equal to the volume generated when the triangular section is rotated around the centerline can be calculated using Equations (A.138) to (A.140):

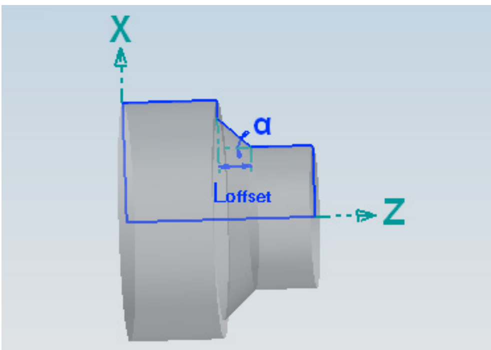

Figure A.17 Chamfer (Akkuş and Kılıç, 2012)

$$V_{added} = V_{tri} \tag{A.137}$$

$$V_{tri} = 2\pi\ \bar{r}_{tri}\, A_{tri} \tag{A.138}$$

$$\bar{r}_{tri} = \frac{D}{2} + \frac{2}{3}\, L_{offset}\, sin\alpha\, sin\left(\frac{\pi}{2} - \gamma + \alpha\right) \tag{A.139}$$

$$A_{tri} = \frac{1}{2}\ \left[L_{offset}\, cos\alpha + \frac{L_{offset}\, sin\alpha}{tan(\gamma+\beta-\alpha)}\right] L_{offset}\, sin\alpha \tag{A.140}$$

APPENDIX B

VERIFICATION OUTPUTS

B.1 Sample Part 1

B.1.1 SP1-AISI1040

No	Feature	Volume-Rough [mm3]	Volume-Finish [mm3]	Volume-Total [mm3]	ps-Rough [J/mm3]	ps-Finish [J/mm3]
1	OD1	-	2,171	2,171	2.47	2.91
2	OD2	4,448	422	4,871	2.47	2.91
3	OD3	4,960	372	5,331	2.47	2.91
4	OD4	5,429	322	5,750	2.47	2.91
5	SQRUGRV1	-	-	7,948	3.44	-
6	RNDHOL1	-	-	477	2.95	-
7	FILLET1	-307	-	-307	2.47	2.91
No	Operation	Volume-Rough [mm3]	Volume-Finish [mm3]	Volume-Total [mm3]	ps-Rough [J/mm3]	ps-Finish [J/mm3]
1	Facing	-	-	353	3.03	-
2	Stock Removal	-	-	1,397	2.47	-
3	Parting	-	-	1,847	2.99	-
	TOTAL			29,839		

No	Feature	Eth-Rough [J]	Eth-Finish [J]	Eth-Total [J]	CO2-Rough [g]	CO2-Finish [g]	CO2-Total [g]
1	OD1	-	6,323	6,323	-	0.9	0.9
2	OD2	10,968	1,229	12,197	1.6	0.2	1.8
3	OD3	12,228	1,083	13,311	1.8	0.2	2.0
4	OD4	13,385	937	14,321	2.0	0.1	2.1
5	SQRUGRV1	-	-	27,323	-	-	4.0
6	RNDHOL1	-	-	1,409	-	-	0.2
7	FILLET1	-758	-	-758	-0.1	-	-0.1
No	Operation	Eth-Rough [J]	Eth-Finish [J]	Eth-Total [J]	CO2-Rough [g]	CO2-Finish [g]	CO2-Total [g]
1	Facing	-	-	1,070	-	-	0.2
2	Stock Removal	-	-	3,541	-	-	0.5
3	Parting	-	-	5,515	-	-	0.8
	TOTAL			84,252			12.4

Figure B.1 Theoretical energy estimation breakdown for SP1-AISI1040

Spindle		OP Time [s]	P_aux_var_spindle_av [W]	E_aux_var_spindle [J]	CO2_spindle [g]
1	Facing	9	688.8	6,537	1.0
2	Turning - Rough	58	603.7	35,305	5.2
3	Turning - Finish	27	688.8	18,531	2.7
4	Drilling	5	1,331.4	7,283	1.1
5	Grooving	73	430.1	31,533	4.6
6	Parting	14	393.7	5,669	0.8
Total		**188**	**-**	**104,858**	**15.4**

Cutting Fluid	ON Time [s]	P_aux_var_fluid_av [W]	E_aux_var_fluid [J]	CO2_fluid [g]
	188	**403.6**	**75,901**	**11.2**

Turret	Tool Change #	E_aux_var_turret_av [J]	E_aux_var_turret [J]	CO2_turret [g]
	6	**229.4**	**1,376**	**0.2**

Chuck	Clamp #	E_aux_var_chuck_av [J]	E_aux_var_chuck [J]	CO2_chuck [g]
	1	**171.5**	**172**	**0.0**

Servo		Time [s]	P_aux_var_servo_av [W]	E_aux_var_servo [J]	CO2_servo [g]
Servo X	Rapid	16	112.6	1,765	0.3
Servo X	Feed	118	7.7	912	0.1
Servo Z	Rapid	18	182.5	3,354	0.5
Servo Z	Feed	73	6.4	465	0.1
Total		**-**	**-**	**6,495**	**1.0**

Lubrication	Lubrication #	E_aux_var_lub_av [J]	E_aux_var_lub [J]	CO2_lub [g]
	0.05	**1,975.5**	**103**	**0.0**

Standby	ON Time [s]	P_aux_cons_sb_av [W]	E_aux_cons_sb [J]	CO2_sb [g]
	188	**690.0**	**129,761**	**19.1**

	E_aux [J]	CO2_aux [g]	% Aux
Variable	188,905	27.8	59
Constant	129,761	19.1	41
TOTAL	**318,666**	**46.9**	**100**

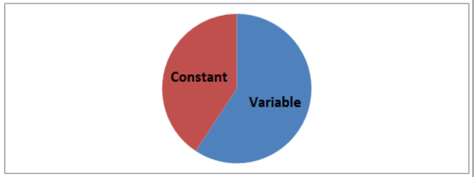

	E_aux [J]	CO2_aux [g]	% Aux
Spindle	104,858	15.4	33
Cutting Fluid	75,901	11.2	24
Turret	1,376	0.2	0
Chuck	172	0.0	0
Servo	6,495	1.0	2
Lubrication	103	0.0	0
Standby	129,761	19.1	41
TOTAL	**318,666**	**46.9**	**100**

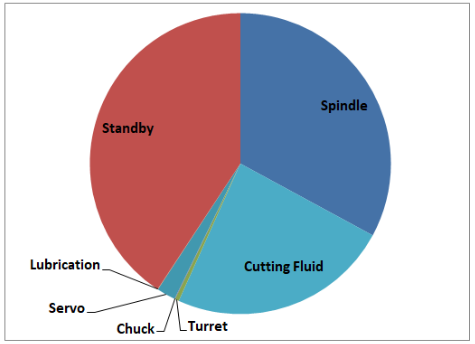

Figure B.2 Auxiliary energy estimation breakdown for SP1-AISI1040

	E [J]	CO2 [g]	%
Theoretical	84,252	12.4	21
Spindle	104,858	15.4	26
Cutting Fluid	75,901	11.2	19
Turret	1,376	0.2	0
Chuck	172	0.0	0
Servo	6,495	1.0	2
Lubrication	103	0.0	0
Standby	129,761	19.1	32
TOTAL	**402,918**	**59.3**	**100**

	E [J]	CO2 [g]	%
Theoretical	84,252	12.4	21
Variable	188,905	27.8	47
Constant	129,761	19.1	32
TOTAL	**402,918**	**59.3**	**100**

	E [J]	CO2 [g]	%
Theoretical	84,252	12.4	21
Auxiliary	318,666	46.9	79
TOTAL	**402,918**	**59.3**	**100**

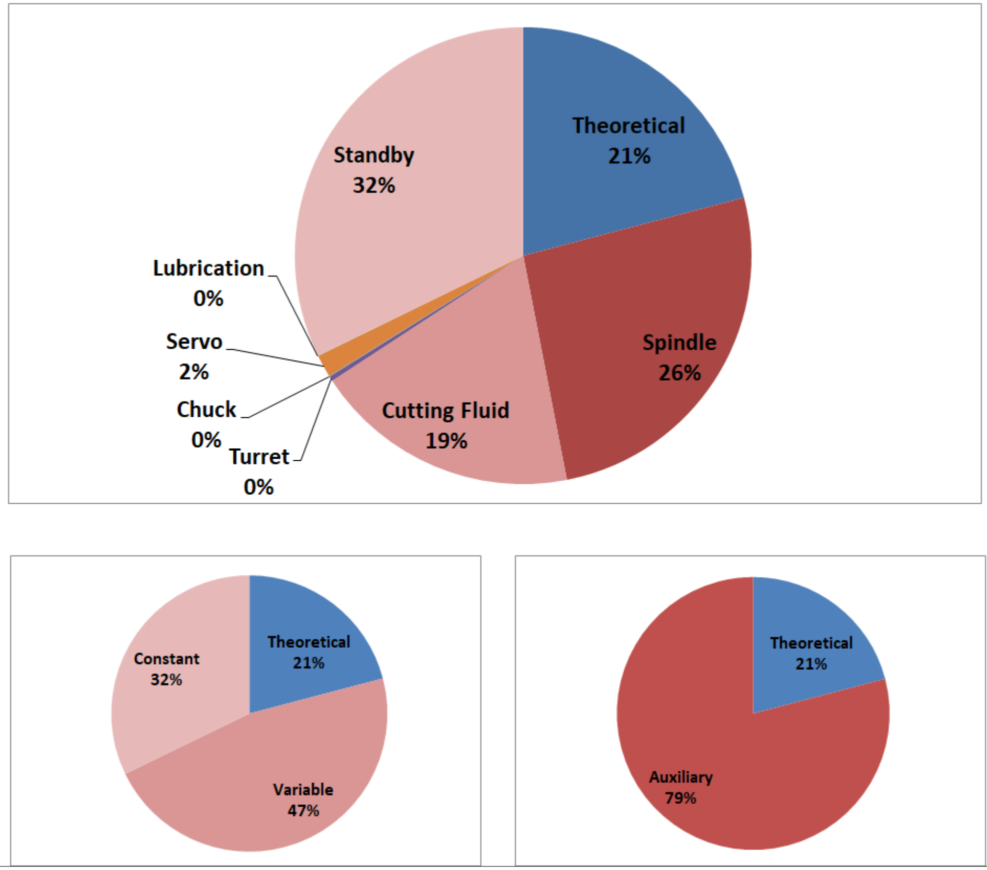

Figure B.3 Process energy estimation breakdown for SP1-AISI1040

B.1.2 SP1-GG25

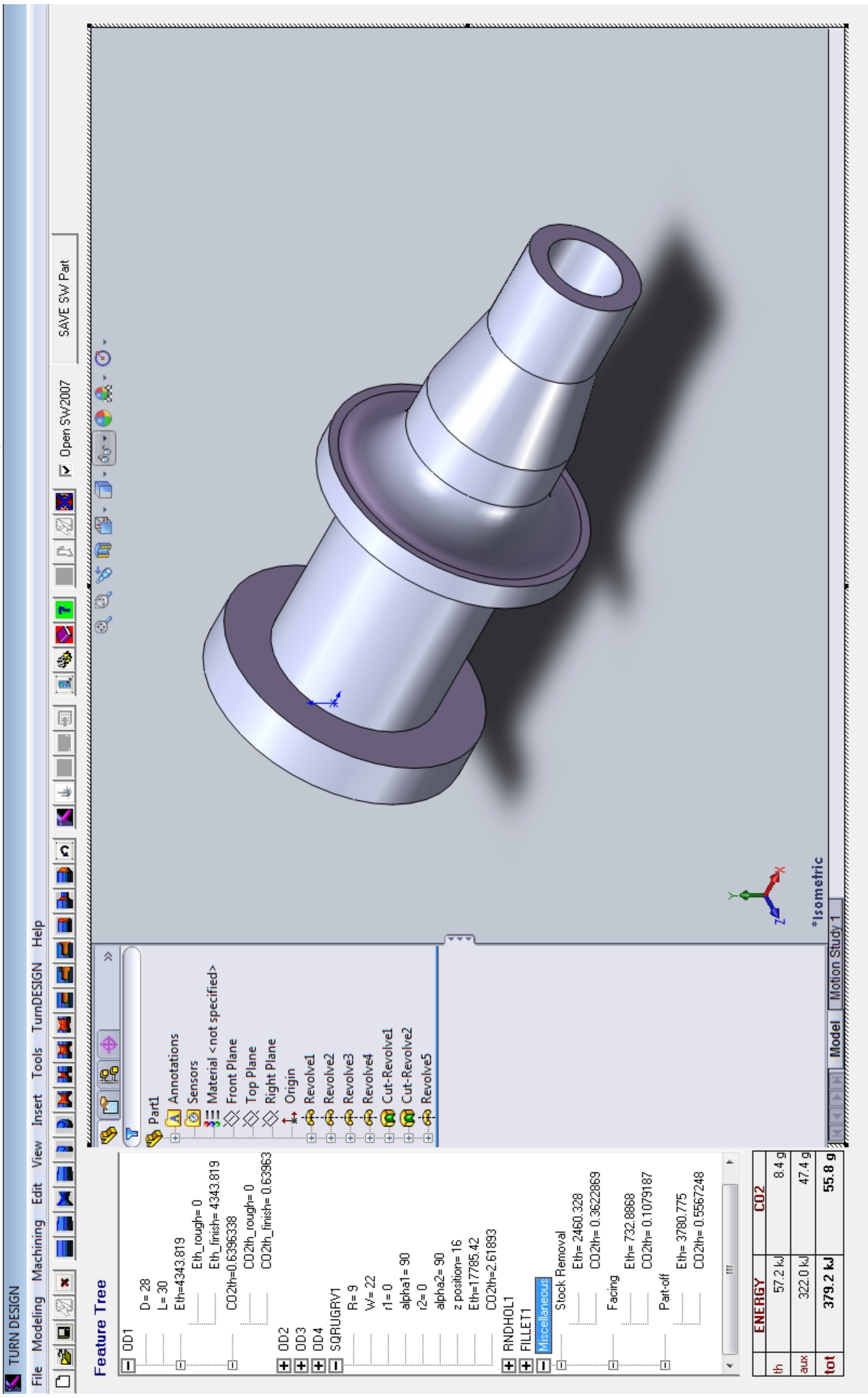

Figure B.4 TurnDesign Eco Edition interface for SP1-GG25

Table B.1 STEP AP224 file for SP1-GG25

```
ISO-10303-21;

HEADER;
FILE_DESCRIPTION(('ISO-10303-224,FEATURE BASED ROTATIONAL PART CREATED BY',
'TurnDESIGN Eco Edition'),'1');
FILE_NAME(('SP1-GG25-2024sp.part21','2024-6-23 T00:54:31',
('Designed by: URAL ULUER','METU-ME','ANKARA TURKIYE')
FILE_SCHEMA(('ROTATIONAL PART', 'PART FOR 2-AXIS TURNING'));
ENDSEC;

DATA;
#1=MATERIAL($,'Cast Iron K12',$,$,$);
#2=OUTER_DIAMETER('OD1',#3,#4,#5,$);
#3=ORIENTATION((0,0,0),(1,0,0,0,1,0,0,0,1));
#4=NUMERIC_PARAMETER('OD1 DIAMETER',MM,28,$);
#5=NUMERIC_PARAMETER('OD1 LENGTH',MM,30,$);
#6=OUTER_DIAMETER('OD2',#7,#8,#9,$);
#7=ORIENTATION((0,0,30),(1,0,0,0,1,0,0,0,1));
#8=NUMERIC_PARAMETER('OD2 DIAMETER',MM,16,$);
#9=NUMERIC_PARAMETER('OD2 LENGTH',MM,10,$);
#10=OUTER_DIAMETER('OD3',#11,#12,#13,#14);
#11=ORIENTATION((0,0,40),(1,0,0,0,1,0,0,0,1));
#12=NUMERIC_PARAMETER('OD3 DIAMETER',MM,16,$);
#13=NUMERIC_PARAMETER('OD3 LENGTH',MM,10,$);
#14=DIAMETER_TAPER(#15);
#15=NUMERIC_PARAMETER('OD3 FINAL DIAMETER',MM,12,$);
#16=OUTER_DIAMETER('OD4',#17,#18,#19,$);
#17=ORIENTATION((0,0,50),(1,0,0,0,1,0,0,0,1));
#18=NUMERIC_PARAMETER('OD4 DIAMETER',MM,12,$);
#19=NUMERIC_PARAMETER('OD4 LENGTH',MM,10,$);
#20=GROOVE('SQRUGRV1',#21,#22,#23,#24);
#21=ORIENTATION((9,0,16),(1,0,0,0,1,0,0,0,1));
#22=DIRECTION(-1,0,0);
#23=NUMERIC_PARAMETER('SQRUGRV1 GROOVE RADIUS',MM,9,$);
#24=SQUARE_U_PROFILE($,#25,#26,#27,#28,#29);
#25=NUMERIC_PARAMETER('SQRUGRV1 WIDTH',MM,22,$);
#26=NUMERIC_PARAMETER('SQRUGRV1 FIRST RADIUS',MM,0,$);
#27=NUMERIC_PARAMETER('SQRUGRV1 FIRST ANGLE',DEGREES,90,$);
#28=NUMERIC_PARAMETER('SQRUGRV1 SECOND RADIUS',MM,0,$);
#29=NUMERIC_PARAMETER('SQRUGRV1 SECOND ANGLE',DEGREES,90,$);
#30=ROUND_HOLE('RNDHOL1',#31,$,#32,#33,$,#34);
#31=ORIENTATION((0,0,60),(1,0,0,0,1,0,0,0,1));
#32=LINEAR_PATH(#35,#36);
#33=NUMERIC_PARAMETER('RNDHOL1 DIAMETER',MM,8,$);
#34=CONICAL_HOLE_BOTTOM(#37,#39);
#35=NUMERIC_PARAMETER('RNDHOL1 DISTANCE',MM,9,$);
#36=DIRECTION(0,0,-1);
#37=NUMERIC_PARAMETER('RNDHOL1 CONICAL BOTTOM TIP ANGLE',MM,140,$);
#38=NUMERIC_PARAMETER('RNDHOL1 CONICAL BOTTOM TIP RADIUS',MM,0.0001,$);
#39=CONSTANT_RADIUS_FILLET('FILLET1','OD1','OD2',#40,$,$);
#40=NUMERIC_PARAMETER('FILLET1 RADIUS',MM,5,$);
ENDSEC;
END-ISO-10303-21;
```

METU DEPARTMENT OF MECHANICAL ENGINEERING	**Part Name / No:** **By:** **Date:**	Part Name Ural Uluer 23.06.2024 / 00:42	**Machine Tool:** Anatool TP32 CNC Lathe **(3500 rpm max)** **Stock Dimensions:** D_stock=30 mm L_stock=73.5 mm **Material:** Cast Iron K12

Op No.	Operation Name	Features	Tool (Holder / Insert)	af (mm)	ap (mm)	Cutting Speed (m/min)	Speed (rpm)	Feed (mm/rev)	Feed Rate (mm/min)
1	Facing	-	SDJCR 2020K 11 / DCMT 11 T3 08-KM-GC3215	0.1	0.5	170	**1800**	0.1	**180**
2	Turning - Rough	OD1 FILLET1 OD3 OD4	SDJCR 2020K 11 / DCMT 11 T3 08-KM-GC3215	0.2	1.5	153	**1620**	0.2	**324**
3	Turning - Finish	OD1 FILLET1 OD3 OD4	SDJCR 2020K 11 / DCMT 11 T3 08-KM-GC3215	0.1	0.8	170	**1800**	0.1	**180**
4	Drilling	RNDHOL1	R840-0800-50-A1A	0.11	8	70	**2790**	0.22	**614**
5	Grooving	SQRUGRV1	RF123G20-2020B / N123G2-0300-0003-GM-GC1125	0.06	3	90	**1020**	0.06	**61**
6	Parting	-	N123G30-21A2 / N123G2-0300-0002-CM-GC1125	0.09	3	90	**950**	0.09	**86**
TURNDESIGN ECO EDITION									

Figure B.5 Manufacturing process sheet for SP1-GG25

Table B.2 Part Program for SP1-GG25

;DATE............. 23.06.2024 ;TIME............. 00:42 ;PROGRAMMER....... Ural Uluer ;D_stock.......... 30 mm ;L_stock.......... 73.5 mm ;MACHINE.......... Anatool TP32 CNC Lathe N10 G291 N20 G91 N30 G28 X0 N40 G28 Z0 N50 G90 N60 G21 G18 G95 G40 N70 M07 N80 G54 ;-------FACING------- N90 T01 N100 G97 S1800 M03 F0.1 N110 G00 X34 Z2 N120 G00 X34 Z0 N130 G01 X-1 Z0 N140 G00 X-1 Z2 N150 G00 X34 Z2 N160 G91 N170 G28 X0 N180 G28 Z0 N190 G90 ;-------TURNING:ROUGH------- N200 T01 N210 G97 S1620 M03 F0.2 N220 G00 X34 Z2 N230 G01 X31 Z2 N240 G01 X31 Z-63 ;Pass 1 N250 G01 X33 Z-62 N260 G00 X33 Z2 N270 G00 X31 Z2 N280 G01 X28 Z2 N290 G01 X28 Z-30 ;Pass 2 N300 G01 X30 Z-29 N310 G00 X30 Z2 N320 G00 X28 Z2 N330 G01 X25 Z2 N340 G01 X25 Z-29.82804 ;Pass 3 N350 G01 X27 Z-28.82804 N360 G00 X27 Z2 N370 G00 X25 Z2	;-------DRILLING------- N860 T08 N870 G97 S2790 M03 F0.22 N880 G00 X34 Z2 N890 G00 X0 Z2 N900 G01 X0 Z-10.45587 N910 G00 X0 Z2 N920 G00 X34 Z2 N930 G91 N940 G28 X0 N950 G28 Z0 N960 G90 ;-------GROOVING------- N970 T19 N980 G97 S1020 M03 F0.06 N990 G00 X34 Z2 N1000 G00 X34 Z-36 N1010 G00 X30 Z-36 N1020 G01 X18 Z-36 ;Plunge 1 N1030 G00 X30 Z-36 N1040 G00 X30 Z-37.8 N1050 G01 X18 Z-37.8 ;Plunge 2 N1060 G00 X30 Z-37.8 N1070 G00 X30 Z-39.6 N1080 G01 X18 Z-39.6 ;Plunge 3 N1090 G00 X30 Z-39.6 N1100 G00 X30 Z-41.4 N1110 G01 X18 Z-41.4 ;Plunge 4 N1120 G00 X30 Z-41.4 N1130 G00 X30 Z-43.2 N1140 G01 X18 Z-43.2 ;Plunge 5 N1150 G00 X30 Z-43.2 N1160 G00 X30 Z-45 N1170 G01 X18 Z-45 ;Plunge 6 N1180 G00 X30 Z-45 N1190 G00 X30 Z-46.8 N1200 G01 X18 Z-46.8 ;Plunge 7 N1210 G00 X30 Z-46.8 N1220 G00 X30 Z-48.6 N1230 G01 X18 Z-48.6 ;Plunge 8 N1240 G00 X30 Z-48.6 N1250 G00 X30 Z-50.4 N1260 G01 X18 Z-50.4 ;Plunge 9 N1270 G00 X30 Z-50.4

Table B.2 (continued)

```
N380 G01 X22 Z2
N390 G01 X22 Z-29.14246         ;Pass 4
N400 G01 X24 Z-28.14246
N410 G00 X24 Z2
N420 G00 X22 Z2

N430 G01 X19 Z2
N440 G01 X19 Z-27.55147         ;Pass 5
N450 G01 X21 Z-26.55147
N460 G00 X21 Z2
N470 G00 X19 Z2

N480 G01 X16 Z2
N490 G01 X16 Z-16         ;Pass 6
N500 G01 X18 Z-15
N510 G00 X18 Z2
N520 G00 X16 Z2

N530 G01 X13.6 Z2         ;Sweep Pass
N540 G01 X13.6 Z0
N550 G01 X13.6 Z-10
N560 G01 X17.6 Z-20
N570 G01 X17.6 Z-25
N580 G02 X27.6 Z-30 R5
N590 G01 X29.6 Z-30
N600 G01 X29.6 Z-60
N610 G01 X29.6 Z-63
N620 G01 X34 Z-63
N630 G00 X34 Z2

N640 G91
N650 G28 X0
N660 G28 Z0
N670 G90


;-------TURNING:FINISH-------
N680 T01
N690 G97 S1800 M03 F0.1

N700 G00 X34 Z2
N710 G00 X12 Z2
N720 G01 X12 Z0
N730 G01 X12 Z-10
N740 G01 X16 Z-20
N750 G01 X16 Z-25
N760 G02 X26 Z-30 R5
N770 G01 X28 Z-30
N780 G01 X28 Z-60
N790 G01 X28 Z-63
N800 G01 X34 Z-63
N810 G00 X34 Z2

N820 G91
N830 G28 X0
N840 G28 Z0
N850 G90
```

```
N1280 G00 X30 Z-52.2
N1290 G01 X18 Z-52.2        ;Plunge 10
N1300 G00 X30 Z-52.2

N1310 G00 X30 Z-54
N1320 G01 X18 Z-54        ;Plunge 11
N1330 G00 X30 Z-54

N1340 G00 X30 Z-55
N1350 G01 X18 Z-55        ;Plunge 12
N1360 G00 X30 Z-55

N1370 G00 X34 Z-55
N1380 G00 X34 Z2

N1390 G91
N1400 G28 X0
N1410 G28 Z0
N1420 G90


;-------PART-OFF-------
N1430 T20
N1440 G97 S950 M03 F0.09

N1450 G00 X34 Z2
N1460 G00 X34 Z-63
N1470 G01 X-1 Z-63
N1480 G00 X34 Z-63
N1490 G00 X34 Z2

N1500 G91
N1510 G28 X0
N1520 G28 Z0
N1530 G90


N1540 M09

N1550 M30
```

No	Feature	Volume-Rough [mm3]	Volume-Finish [mm3]	Volume-Total [mm3]	ps-Rough [J/mm3]	ps-Finish [J/mm3]
1	OD1	-	2,171	2,171	1.72	2.00
2	OD2	4,448	422	4,871	1.72	2.00
3	OD3	4,960	372	5,331	1.72	2.00
4	OD4	5,429	322	5,750	1.72	2.00
5	SQRUGRV1	-	-	7,948	2.24	-
6	RNDHOL1	-	-	477	1.99	-
7	FILLET1	-307	-	-307	1.72	2.00
No	Operation	Volume-Rough [mm3]	Volume-Finish [mm3]	Volume-Total [mm3]	ps-Rough [J/mm3]	ps-Finish [J/mm3]
1	Facing	-	-	353	2.07	-
2	Stock Removal	-	-	1,397	1.72	-
3	Parting	-	-	1,847	2.05	-
TOTAL				**29,839**		

No	Feature	Eth-Rough [J]	Eth-Finish [J]	Eth-Total [J]	CO2-Rough [g]	CO2-Finish [g]	CO2-Total [g]
1	OD1	-	4,344	4,344	-	0.6	0.6
2	OD2	7,640	845	8,485	1.1	0.1	1.2
3	OD3	8,518	744	9,262	1.3	0.1	1.4
4	OD4	9,324	644	9,967	1.4	0.1	1.5
5	SQRUGRV1	-	-	17,785	-	-	2.6
6	RNDHOL1	-	-	947	-	-	0.1
7	FILLET1	-528	-	-528	-0.1	-	-0.1
No	Operation	Eth-Rough [J]	Eth-Finish [J]	Eth-Total [J]	CO2-Rough [g]	CO2-Finish [g]	CO2-Total [g]
1	Facing	-	-	733	-	-	0.1
2	Stock Removal	-	-	2,460	-	-	0.4
3	Parting	-	-	3,781	-	-	0.6
TOTAL				**57,236**			**8.4**

Figure B.6 Theoretical energy estimation breakdown for SP1-GG25

Spindle		OP Time [s]	P_aux_var_spindle_av [W]	E_aux_var_spindle [J]	CO2_spindle [g]
1	Facing	10	639.2	6,281	0.9
2	Turning - Rough	62	560.1	34,549	5.1
3	Turning - Finish	28	639.2	18,081	2.7
4	Drilling	6	1,120.3	6,176	0.9
5	Grooving	78	315.3	24,583	3.6
6	Parting	17	288.7	4,940	0.7
Total		**200**	**-**	**94,610**	**13.9**

Cutting Fluid	ON Time [s]	P_aux_var_fluid_av [W]	E_aux_var_fluid [J]	CO2_fluid [g]
	200	**403.6**	**80,872**	**11.9**

Turret	Tool Change #	E_aux_var_turret_av [J]	E_aux_var_turret [J]	CO2_turret [g]
	6	**229.4**	**1,376**	**0.2**

Chuck	Clamp #	E_aux_var_chuck_av [J]	E_aux_var_chuck [J]	CO2_chuck [g]
	1	**171.5**	**172**	**0.0**

Servo		Time [s]	P_aux_var_servo_av [W]	E_aux_var_servo [J]	CO2_servo [g]
Servo X	Rapid	16	112.6	1,765	0.3
Servo X	Feed	128	7.7	988	0.1
Servo Z	Rapid	18	182.5	3,354	0.5
Servo Z	Feed	77	6.4	493	0.1
Total		**-**	**-**	**6,600**	**1.0**

Lubrication	Lubrication #	E_aux_var_lub_av [J]	E_aux_var_lub [J]	CO2_lub [g]
	0.06	**1,975.5**	**110**	**0.0**

Standby	ON Time [s]	P_aux_cons_sb_av [W]	E_aux_cons_sb [J]	CO2_sb [g]
	200	**690.0**	**138,260**	**20.4**

	E_aux [J]	CO2_aux [g]	% Aux
Variable	183,740	27.1	57
Constant	138,260	20.4	43
TOTAL	**322,000**	**47.4**	**100**

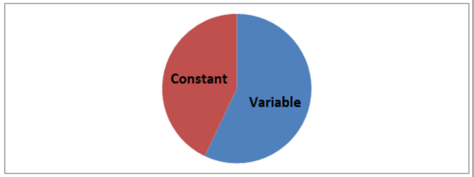

	E_aux [J]	CO2_aux [g]	% Aux
Spindle	94,610	13.9	29
Cutting Fluid	80,872	11.9	25
Turret	1,376	0.2	0
Chuck	172	0.0	0
Servo	6,600	1.0	2
Lubrication	110	0.0	0
Standby	138,260	20.4	43
TOTAL	**322,000**	**47.4**	**100**

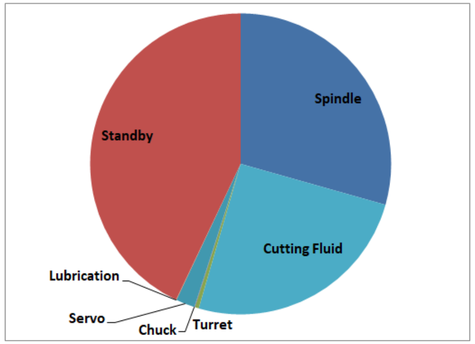

Figure B.7 Auxiliary energy estimation breakdown for SP1-GG25

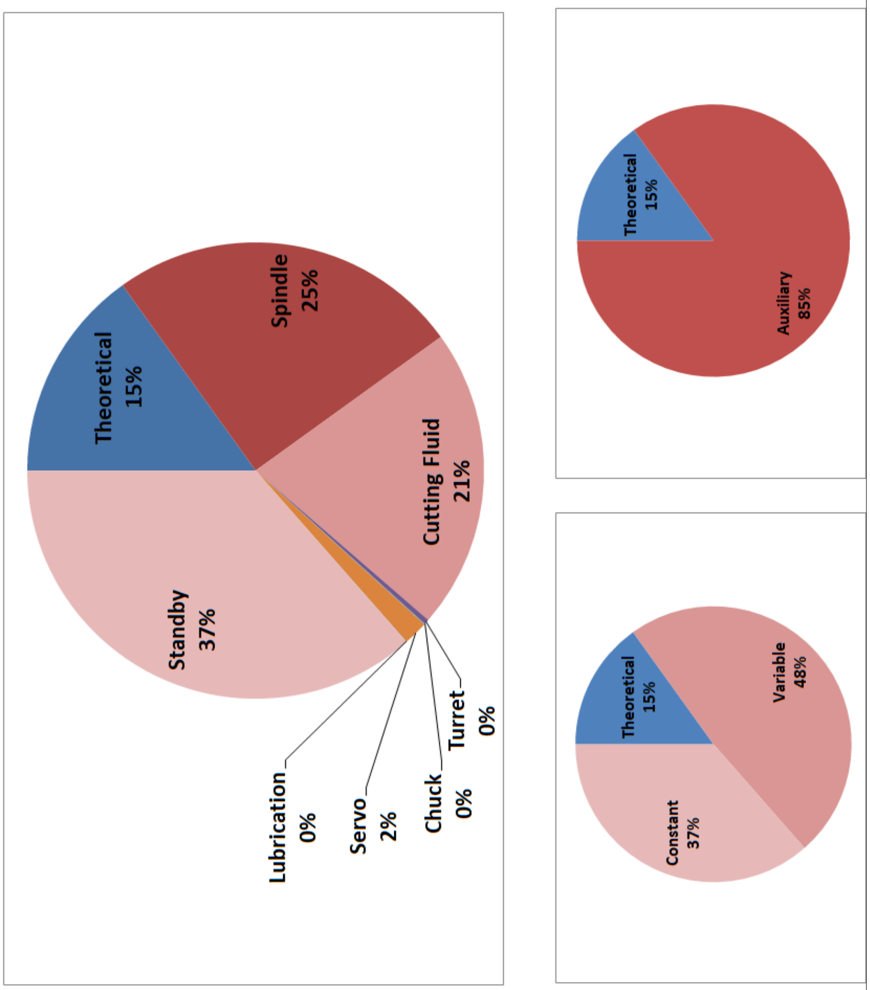

	E [J]	CO2 [g]	%
Theoretical	57,236	8.4	15
Spindle	94,610	13.9	25
Cutting Fluid	80,872	11.9	21
Turret	1,376	0.2	0
Chuck	172	0.0	0
Servo	6,600	1.0	2
Lubrication	110	0.0	0
Standby	138,260	20.4	36
TOTAL	**379,236**	**55.8**	**100**

	E [J]	CO2 [g]	%
Theoretical	57,236	8.4	15
Variable	183,740	27.1	48
Constant	138,260	20.4	36
TOTAL	**379,236**	**55.8**	**100**

	E [J]	CO2 [g]	%
Theoretical	57,236	8.4	15
Auxiliary	322,000	47.4	85
TOTAL	**379,236**	**55.8**	**100**

Figure B.8 Process energy estimation breakdown for SP1-GG25

B.1.3 SP1-AL6013

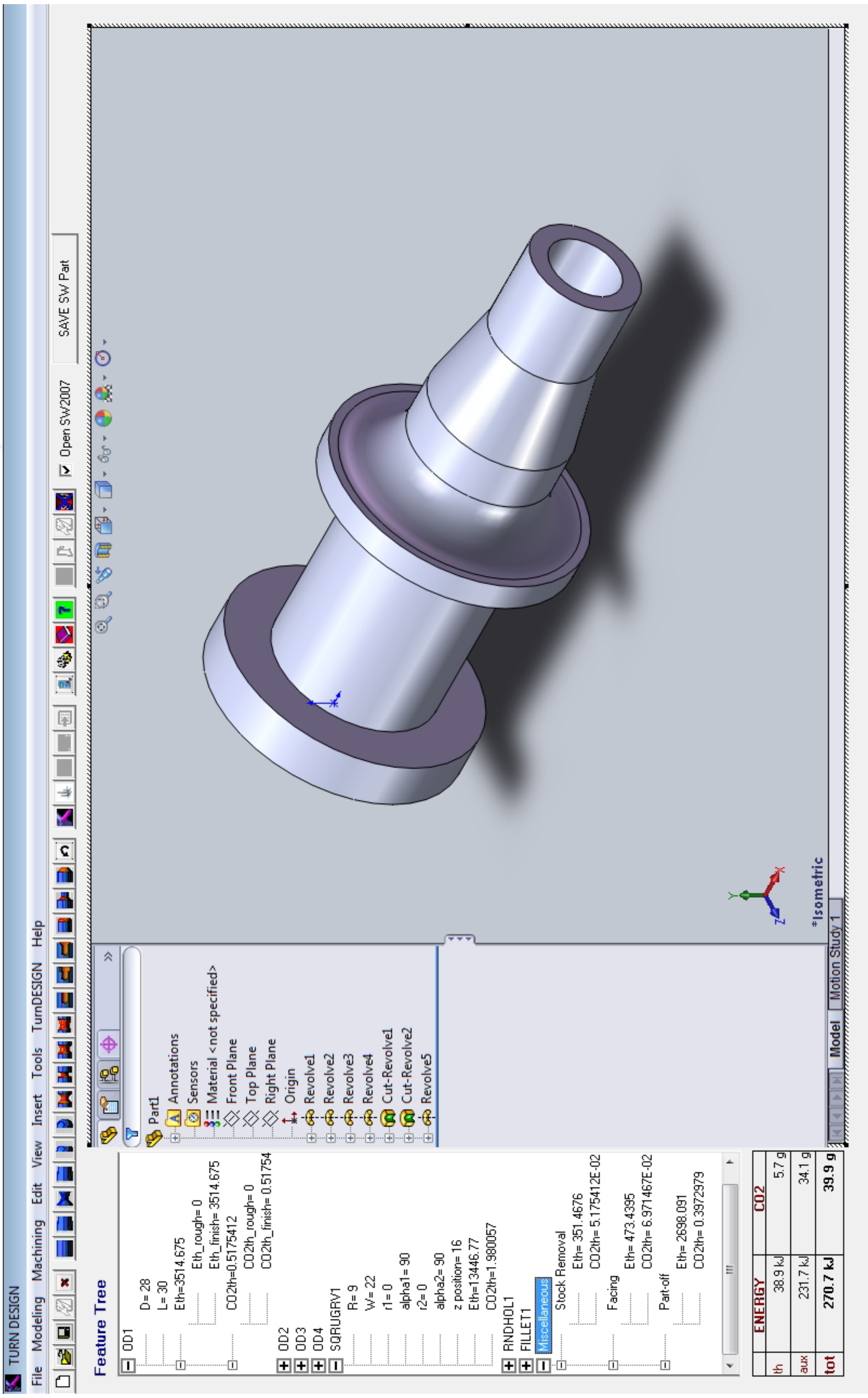

Figure B.9 TurnDesign Eco Edition interface for SP1-AL6013

Table B.3 STEP AP224 file for SP1-AL6013

```
ISO-10303-21;

HEADER;
FILE_DESCRIPTION(('ISO-10303-224,FEATURE BASED ROTATIONAL PART CREATED BY',
'TurnDESIGN Eco Edition'),'1');
FILE_NAME(('SP1-AL6013-2024sp.part21','2024-6-23 T00:25:41',
('Designed by: URAL ULUER','METU-ME','ANKARA TURKIYE')
FILE_SCHEMA(('ROTATIONAL PART', 'PART FOR 2-AXIS TURNING'));
ENDSEC;

DATA;
#1=MATERIAL($,'Non-Ferrous Metal N16',$,$,$);
#2=OUTER_DIAMETER('OD1',#3,#4,#5,$);
#3=ORIENTATION((0,0,0),(1,0,0,0,1,0,0,0,1));
#4=NUMERIC_PARAMETER('OD1 DIAMETER',MM,28,$);
#5=NUMERIC_PARAMETER('OD1 LENGTH',MM,30,$);
#6=OUTER_DIAMETER('OD2',#7,#8,#9,$);
#7=ORIENTATION((0,0,30),(1,0,0,0,1,0,0,0,1));
#8=NUMERIC_PARAMETER('OD2 DIAMETER',MM,16,$);
#9=NUMERIC_PARAMETER('OD2 LENGTH',MM,10,$);
#10=OUTER_DIAMETER('OD3',#11,#12,#13,#14);
#11=ORIENTATION((0,0,40),(1,0,0,0,1,0,0,0,1));
#12=NUMERIC_PARAMETER('OD3 DIAMETER',MM,16,$);
#13=NUMERIC_PARAMETER('OD3 LENGTH',MM,10,$);
#14=DIAMETER_TAPER(#15);
#15=NUMERIC_PARAMETER('OD3 FINAL DIAMETER',MM,12,$);
#16=OUTER_DIAMETER('OD4',#17,#18,#19,$);
#17=ORIENTATION((0,0,50),(1,0,0,0,1,0,0,0,1));
#18=NUMERIC_PARAMETER('OD4 DIAMETER',MM,12,$);
#19=NUMERIC_PARAMETER('OD4 LENGTH',MM,10,$);
#20=GROOVE('SQRUGRV1',#21,#22,#23,#24);
#21=ORIENTATION((9,0,16),(1,0,0,0,1,0,0,0,1));
#22=DIRECTION(-1,0,0);
#23=NUMERIC_PARAMETER('SQRUGRV1 GROOVE RADIUS',MM,9,$);
#24=SQUARE_U_PROFILE($,#25,#26,#27,#28,#29);
#25=NUMERIC_PARAMETER('SQRUGRV1 WIDTH',MM,22,$);
#26=NUMERIC_PARAMETER('SQRUGRV1 FIRST RADIUS',MM,0,$);
#27=NUMERIC_PARAMETER('SQRUGRV1 FIRST ANGLE',DEGREES,90,$);
#28=NUMERIC_PARAMETER('SQRUGRV1 SECOND RADIUS',MM,0,$);
#29=NUMERIC_PARAMETER('SQRUGRV1 SECOND ANGLE',DEGREES,90,$);
#30=ROUND_HOLE('RNDHOL1',#31,$,#32,#33,$,#34);
#31=ORIENTATION((0,0,60),(1,0,0,0,1,0,0,0,1));
#32=LINEAR_PATH(#35,#36);
#33=NUMERIC_PARAMETER('RNDHOL1 DIAMETER',MM,8,$);
#34=CONICAL_HOLE_BOTTOM(#37,#39);
#35=NUMERIC_PARAMETER('RNDHOL1 DISTANCE',MM,9,$);
#36=DIRECTION(0,0,-1);
#37=NUMERIC_PARAMETER('RNDHOL1 CONICAL BOTTOM TIP ANGLE',MM,140,$);
#38=NUMERIC_PARAMETER('RNDHOL1 CONICAL BOTTOM TIP RADIUS',MM,0.0001,$);
#39=CONSTANT_RADIUS_FILLET('FILLET1','OD1','OD2',#40,$,$);
#40=NUMERIC_PARAMETER('FILLET1 RADIUS',MM,5,$);
ENDSEC;
END-ISO-10303-21;
```

METU DEPARTMENT OF MECHANICAL ENGINEERING	**Part Name / No:**	Part Name	**Machine Tool:**	Anatool TP32 CNC Lathe **(3500 rpm max)**
	By:	Ural Uluer	**Stock Dimensions:**	D_stock=30 mm L_stock=73.5 mm
	Date:	23.06.2024 / 00:04	**Material:**	Non-Ferrous Metal N16

Op No.	Operation Name	Features	Tool (Holder / Insert)	af (mm)	ap (mm)	Cutting Speed (m/min)	Speed (rpm)	Feed (mm/rev)	Feed Rate (mm/min)
1	Facing	-	SDJCR 2020K 11 / DCGX 11 T3 08-AL-H10	0.15	0.5	250	**2650**	0.15	**398**
2	Turning - Rough	OD1 FILLET1 OD3 OD4	SDJCR 2020K 11 / DCGX 11 T3 08-AL-H10	0.3	2	225	**2390**	0.3	**717**
3	Turning - Finish	OD1 FILLET1 OD3 OD4	SDJCR 2020K 11 / DCGX 11 T3 08-AL-H10	0.15	1	250	**2650**	0.15	**398**
4	Drilling	RNDHOL1	R840-0800-50-A1A	0.14	8	120	**3500**	0.28	**980**
5	Grooving	SQRUGRV1	RF123G20-2020B / N123G2-0300-0002-GF-GC1125	0.05	3	190	**2160**	0.05	**108**
6	Parting	-	N123G30-21A2 / N123G2-0300-0002-CM-GC1125	0.09	3	190	**2020**	0.09	**182**
TURNDESIGN ECO EDITION									

Figure B.10 Manufacturing process sheet for SP1-AL6013

Table B.4 Part Program for SP1-AL6013

```
;DATE............. 23.06.2024
;TIME............. 00:04
;PROGRAMMER....... Ural Uluer

;D_stock.......... 30 mm
;L_stock.......... 73.5 mm
;MACHINE.......... Anatool TP32 CNC
Lathe


N10 G291
N20 G91
N30 G28 X0
N40 G28 Z0
N50 G90
N60 G21 G18 G95 G40
N70 M07
N80 G54


;-------FACING-------
N90 T01
N100 G97 S2650 M03 F0.15

N110 G00 X34 Z2
N120 G00 X34 Z0
N130 G01 X-1 Z0
N140 G00 X-1 Z2
N150 G00 X34 Z2

N160 G91
N170 G28 X0
N180 G28 Z0
N190 G90


;-------TURNING:ROUGH-------
N200 T01
N210 G97 S2390 M03 F0.3

N220 G00 X34 Z2
N230 G01 X30 Z2
N240 G01 X30 Z-63        ;Pass 1
N250 G01 X32 Z-62
N260 G00 X32 Z2
N270 G00 X30 Z2

N280 G01 X26 Z2
N290 G01 X26 Z-29.89898        ;Pass 2
N300 G01 X28 Z-28.89898
N310 G00 X28 Z2
N320 G00 X26 Z2

N330 G01 X22 Z2
N340 G01 X22 Z-29        ;Pass 3
N350 G01 X24 Z-28
N360 G00 X24 Z2
N370 G00 X22 Z2
```

```
;-------DRILLING-------
N810 T08
N820 G97 S3500 M03 F0.28

N830 G00 X34 Z2
N840 G00 X0 Z2
N850 G01 X0 Z-10.45587
N860 G00 X0 Z2
N870 G00 X34 Z2

N880 G91
N890 G28 X0
N900 G28 Z0
N910 G90


;-------GROOVING-------
N920 T19
N930 G97 S2160 M03 F0.05

N940 G00 X34 Z2
N950 G00 X34 Z-36
N960 G00 X30 Z-36

N970 G01 X18 Z-36        ;Plunge 1
N980 G00 X30 Z-36

N990 G00 X30 Z-37.8
N1000 G01 X18 Z-37.8        ;Plunge 2
N1010 G00 X30 Z-37.8

N1020 G00 X30 Z-39.6
N1030 G01 X18 Z-39.6        ;Plunge 3
N1040 G00 X30 Z-39.6

N1050 G00 X30 Z-41.4
N1060 G01 X18 Z-41.4        ;Plunge 4
N1070 G00 X30 Z-41.4

N1080 G00 X30 Z-43.2
N1090 G01 X18 Z-43.2        ;Plunge 5
N1100 G00 X30 Z-43.2

N1110 G00 X30 Z-45
N1120 G01 X18 Z-45        ;Plunge 6
N1130 G00 X30 Z-45

N1140 G00 X30 Z-46.8
N1150 G01 X18 Z-46.8        ;Plunge 7
N1160 G00 X30 Z-46.8

N1170 G00 X30 Z-48.6
N1180 G01 X18 Z-48.6        ;Plunge 8
N1190 G00 X30 Z-48.6

N1200 G00 X30 Z-50.4
N1210 G01 X18 Z-50.4        ;Plunge 9
N1220 G00 X30 Z-50.4
```

Table B.4 (continued)

N380 G01 X18 Z2 N390 G01 X18 Z-25 ;Pass 4 N400 G01 X20 Z-24 N410 G00 X20 Z2 N420 G00 X18 Z2 N430 G01 X14 Z2 N440 G01 X14 Z-10 ;Pass 5 N450 G01 X16 Z-9 N460 G00 X16 Z2 N470 G00 X14 Z2 N480 G01 X14 Z2 ;Sweep Pass N490 G01 X14 Z0 N500 G01 X14 Z-10 N510 G01 X18 Z-20 N520 G01 X18 Z-25 N530 G02 X28 Z-30 R5 N540 G01 X30 Z-30 N550 G01 X30 Z-60 N560 G01 X30 Z-63 N570 G01 X34 Z-63 N580 G00 X34 Z2 N590 G91 N600 G28 X0 N610 G28 Z0 N620 G90 ;-------TURNING:FINISH------- N630 T01 N640 G97 S2650 M03 F0.15 N650 G00 X34 Z2 N660 G00 X12 Z2 N670 G01 X12 Z0 N680 G01 X12 Z-10 N690 G01 X16 Z-20 N700 G01 X16 Z-25 N710 G02 X26 Z-30 R5 N720 G01 X28 Z-30 N730 G01 X28 Z-60 N740 G01 X28 Z-63 N750 G01 X34 Z-63 N760 G00 X34 Z2 N770 G91 N780 G28 X0 N790 G28 Z0 N800 G90	N1230 G00 X30 Z-52.2 N1240 G01 X18 Z-52.2 ;Plunge 10 N1250 G00 X30 Z-52.2 N1260 G00 X30 Z-54 N1270 G01 X18 Z-54 ;Plunge 11 N1280 G00 X30 Z-54 N1290 G00 X30 Z-55 N1300 G01 X18 Z-55 ;Plunge 12 N1310 G00 X30 Z-55 N1320 G00 X34 Z-55 N1330 G00 X34 Z2 N1340 G91 N1350 G28 X0 N1360 G28 Z0 N1370 G90 ;-------PART-OFF------- N1380 T20 N1390 G97 S2020 M03 F0.09 N1400 G00 X34 Z2 N1410 G00 X34 Z-63 N1420 G01 X-1 Z-63 N1430 G00 X34 Z-63 N1440 G00 X34 Z2 N1450 G91 N1460 G28 X0 N1470 G28 Z0 N1480 G90 N1490 M09 N1500 M30

No	Feature	Volume-Rough [mm3]	Volume-Finish [mm3]	Volume-Total [mm3]	ps-Rough [J/mm3]	ps-Finish [J/mm3]
1	OD1	-	2,733	2,733	1.08	1.29
2	OD2	4,524	534	5,058	1.08	1.29
3	OD3	5,047	471	5,519	1.08	1.29
4	OD4	5,529	408	5,938	1.08	1.29
5	SQRUGRV1	-	-	7,948	1.69	-
6	RNDHOL1	-	-	477	1.33	-
7	FILLET1	-307	-	-307	1.08	1.29
No	**Operation**	**Volume-Rough [mm3]**	**Volume-Finish [mm3]**	**Volume-Total [mm3]**	**ps-Rough [J/mm3]**	**ps-Finish [J/mm3]**
1	Facing	-	-	353	1.34	-
2	Stock Removal	-	-	273	1.08	-
3	Parting	-	-	1,847	1.46	-
TOTAL				**29,839**		

No	Feature	Eth-Rough [J]	Eth-Finish [J]	Eth-Total [J]	CO2-Rough [g]	CO2-Finish [g]	CO2-Total [g]
1	OD1	-	3,515	3,515	-	0.5	0.5
2	OD2	4,892	687	5,579	0.7	0.1	0.8
3	OD3	5,458	606	6,064	0.8	0.1	0.9
4	OD4	5,979	525	6,504	0.9	0.1	1.0
5	SQRUGRV1	-	-	13,447	-	-	2.0
6	RNDHOL1	-	-	633	-	-	0.1
7	FILLET1	-332	-	-332	0.0	-	0.0
No	**Operation**	**Eth-Rough [J]**	**Eth-Finish [J]**	**Eth-Total [J]**	**CO2-Rough [g]**	**CO2-Finish [g]**	**CO2-Total [g]**
1	Facing	-	-	473	-	-	0.1
2	Stock Removal	-	-	351	-	-	0.1
3	Parting	-	-	2,698	-	-	0.4
TOTAL				**38,932**			**5.7**

Figure B.11 Theoretical energy estimation breakdown for SP1-AL6013

Spindle		OP Time [s]	P_aux_var_spindle_av [W]	E_aux_var_spindle [J]	CO2_spindle [g]
1	Facing	7	1,047.5	6,950	1.0
2	Turning - Rough	27	916.5	25,161	3.7
3	Turning - Finish	15	1,047.5	15,865	2.3
4	Drilling	5	1,513.7	7,655	1.1
5	Grooving	47	805.1	38,135	5.6
6	Parting	11	739.3	7,844	1.2
Total		**112**	**-**	**101,611**	**15.0**

Cutting Fluid	ON Time [s]	P_aux_var_fluid_av [W]	E_aux_var_fluid [J]	CO2_fluid [g]
	112	**403.6**	**45,311**	**6.7**

Turret	Tool Change #	E_aux_var_turret_av [J]	E_aux_var_turret [J]	CO2_turret [g]
	6	**229.4**	**1,376**	**0.2**

Chuck	Clamp #	E_aux_var_chuck_av [J]	E_aux_var_chuck [J]	CO2_chuck [g]
	1	**171.5**	**172**	**0.0**

Servo		Time [s]	P_aux_var_servo_av [W]	E_aux_var_servo [J]	CO2_servo [g]
Servo X	Rapid	16	112.6	1,758	0.3
Servo X	Feed	66	7.7	510	0.1
Servo Z	Rapid	18	182.5	3,277	0.5
Servo Z	Feed	32	6.4	202	0.0
Total		**-**	**-**	**5,747**	**0.8**

Lubrication	Lubrication #	E_aux_var_lub_av [J]	E_aux_var_lub [J]	CO2_lub [g]
	0.03	**1,975.5**	**62**	**0.0**

Standby	ON Time [s]	P_aux_cons_sb_av [W]	E_aux_cons_sb [J]	CO2_sb [g]
	112	**690.0**	**77,465**	**11.4**

	E_aux [J]	CO2_aux [g]	% Aux
Variable	154,279	22.7	67
Constant	77,465	11.4	33
TOTAL	**231,743**	**34.1**	**100**

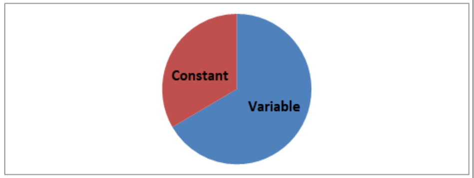

	E_aux [J]	CO2_aux [g]	% Aux
Spindle	101,611	15.0	44
Cutting Fluid	45,311	6.7	20
Turret	1,376	0.2	1
Chuck	172	0.0	0
Servo	5,747	0.8	2
Lubrication	62	0.0	0
Standby	77,465	11.4	33
TOTAL	**231,743**	**34.1**	**100**

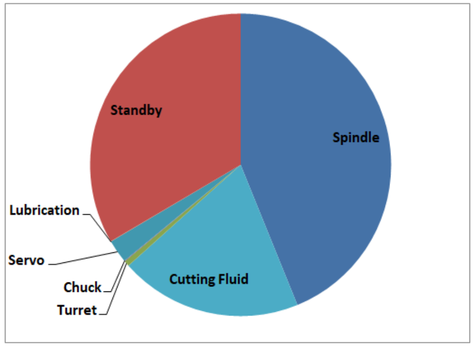

Figure B.12 Auxiliary energy estimation breakdown for SP1-AL6013

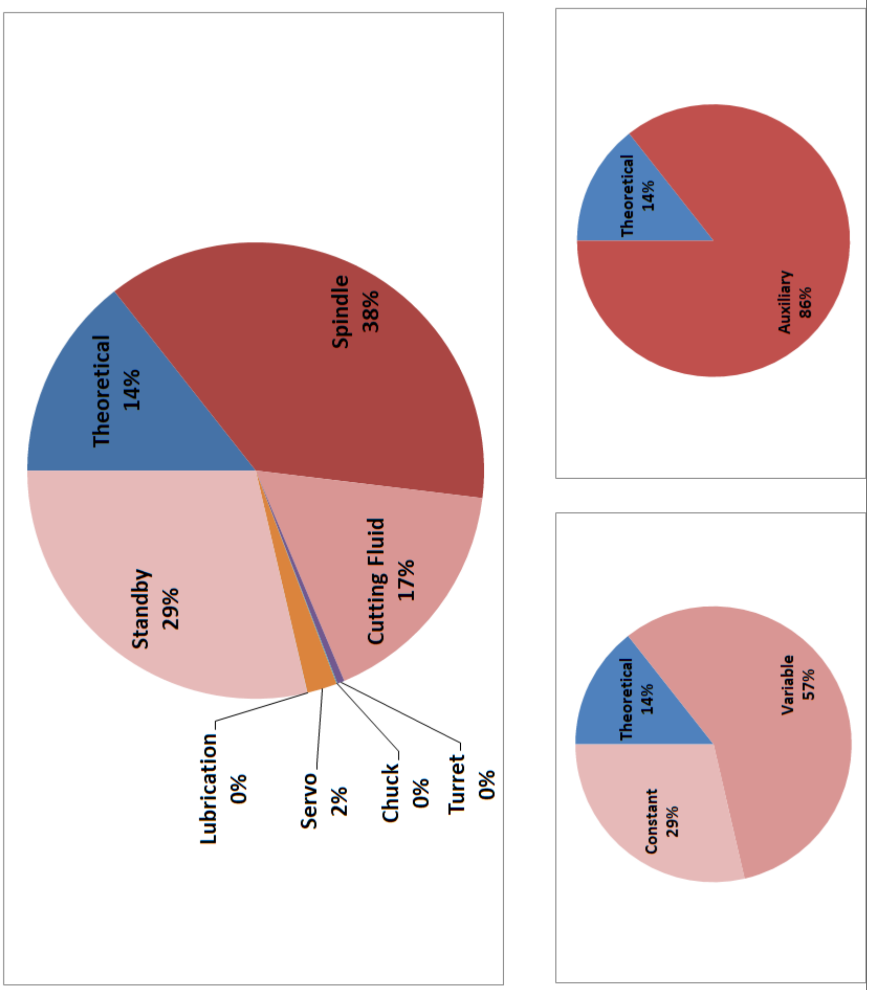

	E [J]	CO2 [g]	%
Theoretical	38,932	5.7	14
Spindle	101,611	15.0	38
Cutting Fluid	45,311	6.7	17
Turret	1,376	0.2	1
Chuck	172	0.0	0
Servo	5,747	0.8	2
Lubrication	62	0.0	0
Standby	77,465	11.4	29
TOTAL	**270,676**	**39.9**	**100**

	E [J]	CO2 [g]	%
Theoretical	38,932	5.7	14
Variable	154,279	22.7	57
Constant	77,465	11.4	29
TOTAL	**270,676**	**39.9**	**100**

	E [J]	CO2 [g]	%
Theoretical	38,932	5.7	14
Auxiliary	231,743	34.1	86
TOTAL	**270,676**	**39.9**	**100**

Figure B.13 Process energy estimation breakdown for SP1-AL6013

B.2 Sample Part 2

No	Feature	Volume-Rough [mm3]	Volume-Finish [mm3]	Volume-Total [mm3]	ps-Rough [J/mm3]	ps-Finish [J/mm3]
1	OD1	-	716	716	1.08	1.29
2	OD2	1,131	471	1,602	1.08	1.29
3	OD3	960	308	1,268	1.08	1.29
4	OD4	3,845	980	4,825	1.08	1.29
5	OD5	1,060	127	1,188	1.08	1.29
6	CAP1	714	39	753	1.08	1.29
7	SQRUGRV1	-	-	247	1.69	-
8	ROUND1	12	-	12	1.08	1.29
9	CHAMFER1	18	-	18	1.08	1.29
No	**Operation**	**Volume-Rough [mm3]**	**Volume-Finish [mm3]**	**Volume-Total [mm3]**	**ps-Rough [J/mm3]**	**ps-Finish [J/mm3]**
1	Facing	-	-	157	1.34	-
2	Stock Removal	-	-	179	1.08	-
3	Parting	-	-	763	1.46	-
	TOTAL			**11,729**		

No	Feature	Eth-Rough [J]	Eth-Finish [J]	Eth-Total [J]	CO2-Rough [g]	CO2-Finish [g]	CO2-Total [g]
1	OD1	-	921	921	-	0.1	0.1
2	OD2	1,223	606	1,829	0.2	0.1	0.3
3	OD3	1,038	396	1,434	0.2	0.1	0.2
4	OD4	4,158	1,260	5,418	0.6	0.2	0.8
5	OD5	1,147	164	1,310	0.2	0.0	0.2
6	CAP1	772	50	822	0.1	0.0	0.1
7	SQRUGRV1	-	-	419	-	-	0.1
8	ROUND1	13	-	13	0.0	-	0.0
9	CHAMFER1	19	-	19	0.0	-	0.0
No	**Operation**	**Eth-Rough [J]**	**Eth-Finish [J]**	**Eth-Total [J]**	**CO2-Rough [g]**	**CO2-Finish [g]**	**CO2-Total [g]**
1	Facing	-	-	210	-	-	0.0
2	Stock Removal	-	-	230	-	-	0.0
3	Parting	-	-	1,115	-	-	0.2
	TOTAL			**13,741**			**2.0**

Figure B.14 Theoretical energy estimation breakdown for SP2-AL6013

Spindle		OP Time [s]	P_aux_var_spindle_av [W]	E_aux_var_spindle [J]	CO2_spindle [g]
1	Facing	5	1,513.7	8,145	1.2
2	Turning - Rough	18	1,513.7	27,797	4.1
3	Turning - Finish	13	1,513.7	19,275	2.8
4	Grooving	7	1,513.7	11,217	1.7
5	Parting	8	1,243.3	9,391	1.4
Total		**51**	**-**	**75,825**	**11.2**

Cutting Fluid	ON Time [s]	P_aux_var_fluid_av [W]	E_aux_var_fluid [J]	CO2_fluid [g]
	51	**403.6**	**20,762**	**3.1**

Turret	Tool Change #	E_aux_var_turret_av [J]	E_aux_var_turret [J]	CO2_turret [g]
	5	**229.4**	**1,147**	**0.2**

Chuck	Clamp #	E_aux_var_chuck_av [J]	E_aux_var_chuck [J]	CO2_chuck [g]
	1	**171.5**	**172**	**0.0**

Servo		Time [s]	P_aux_var_servo_av [W]	E_aux_var_servo [J]	CO2_servo [g]
Servo X	Rapid	12	112.6	1,302	0.2
Servo X	Feed	20	7.7	155	0.0
Servo Z	Rapid	14	182.5	2,599	0.4
Servo Z	Feed	20	6.4	128	0.0
Total		**-**	**-**	**4,184**	**0.6**

Lubrication	Lubrication #	E_aux_var_lub_av [J]	E_aux_var_lub [J]	CO2_lub [g]
	0.01	**1,975.5**	**28**	**0.0**

Standby	ON Time [s]	P_aux_cons_sb_av [W]	E_aux_cons_sb [J]	CO2_sb [g]
	51	**690.0**	**35,495**	**5.2**

	E_aux [J]	CO2_aux [g]	% Aux
Variable	102,118	15.0	74
Constant	35,495	5.2	26
TOTAL	**137,613**	**20.3**	**100**

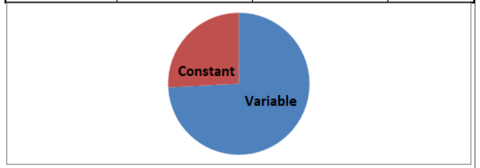

	E_aux [J]	CO2_aux [g]	% Aux
Spindle	75,825	11.2	55
Cutting Fluid	20,762	3.1	15
Turret	1,147	0.2	1
Chuck	172	0.0	0
Servo	4,184	0.6	3
Lubrication	28	0.0	0
Standby	35,495	5.2	26
TOTAL	**137,613**	**20.3**	**100**

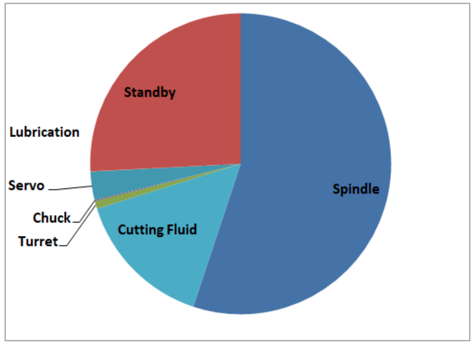

Figure B.15 Auxiliary energy estimation breakdown for SP2-AL6013

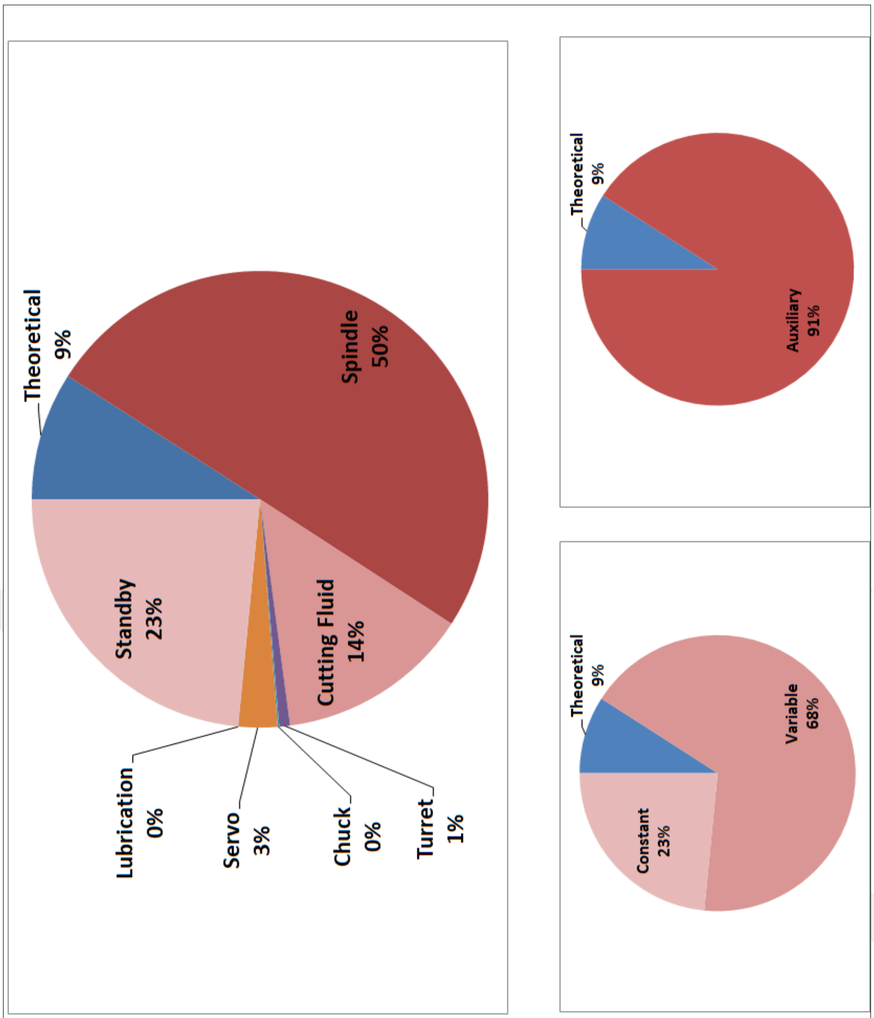

	E [J]	CO2 [g]	%
Theoretical	13,741	2.0	9
Spindle	75,825	11.2	50
Cutting Fluid	20,762	3.1	14
Turret	1,147	0.2	1
Chuck	172	0.0	0
Servo	4,184	0.6	3
Lubrication	28	0.0	0
Standby	35,495	5.2	23
TOTAL	**151,354**	**22.3**	**100**

	E [J]	CO2 [g]	%
Theoretical	13,741	2.0	9
Variable	102,118	15.0	67
Constant	35,495	5.2	23
TOTAL	**151,354**	**22.3**	**100**

	E [J]	CO2 [g]	%
Theoretical	13,741	2.0	9
Auxiliary	137,613	20.3	91
TOTAL	**151,354**	**22.3**	**100**

Figure B.16 Process energy estimation breakdown for SP2-AL6013

B.3 Sample Part 3

No	Feature	Volume-Rough [mm3]	Volume-Finish [mm3]	Volume-Total [mm3]	ps-Rough [J/mm3]	ps-Finish [J/mm3]
1	OD1	-	2,111	2,111	1.08	1.29
2	OD2	6,075	770	6,845	1.08	1.29
3	REVRND1	10,120	1,006	11,127	1.08	1.29
4	OD3	3,976	242	4,218	1.08	1.29
5	OD4	22,934	1,156	24,090	1.08	1.29
6	SQRUGRV1	-	-	716	1.69	-
7	RNDHOL1	-	-	1,326	1.23	-
8	CHAMFER1	287	-	287	1.08	1.29
9	CHAMFER2	130	-	130	1.08	1.29
10	FILLET1	-94	-	-94	1.08	1.29
No	**Operation**	**Volume-Rough [mm3]**	**Volume-Finish [mm3]**	**Volume-Total [mm3]**	**ps-Rough [J/mm3]**	**ps-Finish [J/mm3]**
1	Facing	-	-	982	1.34	-
2	Stock Removal	-	-	4,570	1.08	-
3	Parting	-	-	5,205	1.46	-
TOTAL				**61,513**		

No	Feature	Eth-Rough [J]	Eth-Finish [J]	Eth-Total [J]	CO2-Rough [g]	CO2-Finish [g]	CO2-Total [g]
1	OD1	-	2,715	2,715	-	0.4	0.4
2	OD2	6,569	990	7,559	1.0	0.1	1.1
3	REVRND1	10,943	1,294	12,237	1.6	0.2	1.8
4	OD3	4,299	312	4,611	0.6	0.0	0.7
5	OD4	24,799	1,487	26,286	3.7	0.2	3.9
6	SQRUGRV1	-	-	1,212	-	-	0.2
7	RNDHOL1	-	-	1,632	-	-	0.2
8	CHAMFER1	310	-	310	0.0	-	0.0
9	CHAMFER2	140	-	140	0.0	-	0.0
10	FILLET1	-102	-	-102	0.0	-	0.0
No	**Operation**	**Eth-Rough [J]**	**Eth-Finish [J]**	**Eth-Total [J]**	**CO2-Rough [g]**	**CO2-Finish [g]**	**CO2-Total [g]**
1	Facing	-	-	1,315	-	-	0.2
2	Stock Removal	-	-	5,034	-	-	0.7
3	Parting	-	-	7,602	-	-	1.1
TOTAL				**70,552**			**10.4**

Figure B.17 Theoretical energy estimation breakdown for SP3-AL6013

Spindle		OP Time [s]	P_aux_var_spindle_av [W]	E_aux_var_spindle [J]	CO2_spindle [g]
1	Facing	11	547.2	6,008	0.9
2	Turning - Rough	54	479.5	25,705	3.8
3	Turning - Finish	21	547.2	11,501	1.7
4	Center Drilling	6	1,513.7	8,602	1.3
5	Drilling	5	1,331.4	6,933	1.0
6	Grooving	8	1,099.4	9,209	1.4
7	Parting	20	389.7	7,784	1.1
Total		**125**	**-**	**75,741**	**11.2**

Cutting Fluid	ON Time [s]	P_aux_var_fluid_av [W]	E_aux_var_fluid [J]	CO2_fluid [g]
	125	**403.6**	**50,385**	**7.4**

Turret	Tool Change #	E_aux_var_turret_av [J]	E_aux_var_turret [J]	CO2_turret [g]
	7	**229.4**	**1,606**	**0.2**

Chuck	Clamp #	E_aux_var_chuck_av [J]	E_aux_var_chuck [J]	CO2_chuck [g]
	1	**171.5**	**172**	**0.0**

Servo		Time [s]	P_aux_var_servo_av [W]	E_aux_var_servo [J]	CO2_servo [g]
Servo X	Rapid	17	112.6	1,970	0.3
Servo X	Feed	55	7.7	421	0.1
Servo Z	Rapid	20	182.5	3,588	0.5
Servo Z	Feed	62	6.4	395	0.1
Total		**-**	**-**	**6,374**	**0.9**

Lubrication	Lubrication #	E_aux_var_lub_av [J]	E_aux_var_lub [J]	CO2_lub [g]
	0.03	**1,975.5**	**69**	**0.0**

Standby	ON Time [s]	P_aux_cons_sb_av [W]	E_aux_cons_sb [J]	CO2_sb [g]
	125	**690.0**	**86,139**	**12.7**

	E_aux [J]	CO2_aux [g]	% Aux
Variable	134,345	19.8	61
Constant	86,139	12.7	39
TOTAL	**220,485**	**32.5**	**100**

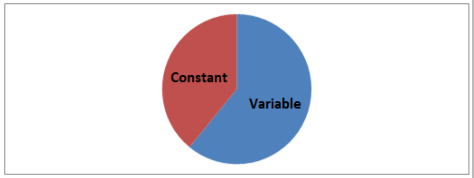

	E_aux [J]	CO2_aux [g]	% Aux
Spindle	75,741	11.2	34
Cutting Fluid	50,385	7.4	23
Turret	1,606	0.2	1
Chuck	172	0.0	0
Servo	6,374	0.9	3
Lubrication	69	0.0	0
Standby	86,139	12.7	39
TOTAL	**220,485**	**32.5**	**100**

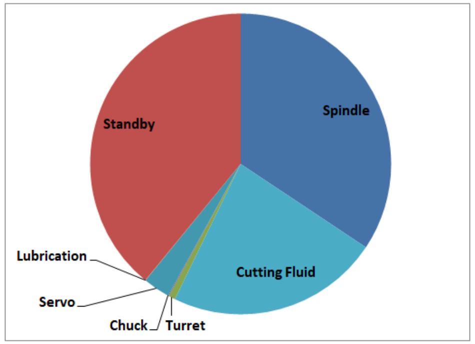

Figure B.18 Auxiliary energy estimation breakdown for SP3-AL6013

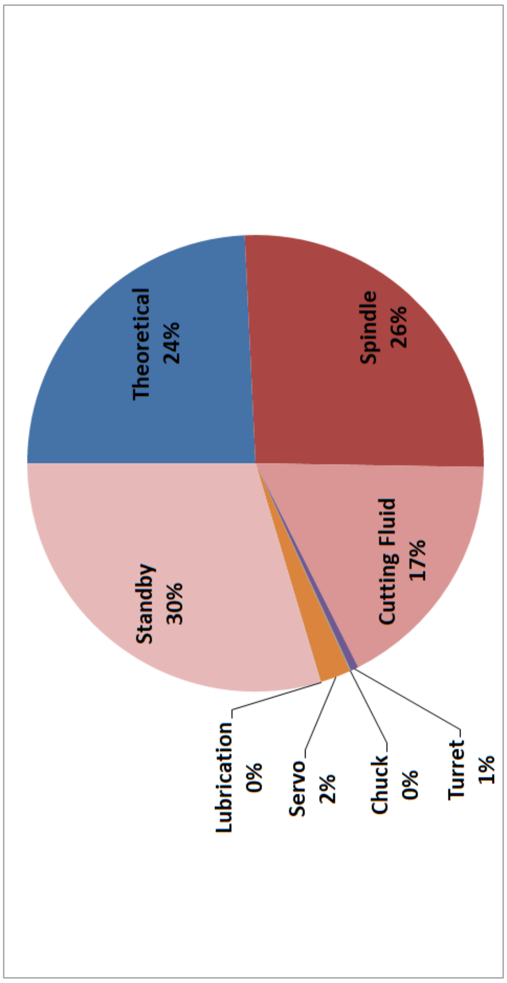

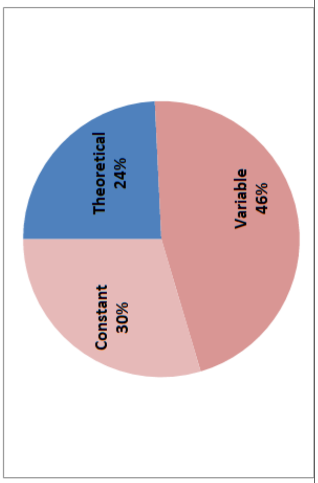

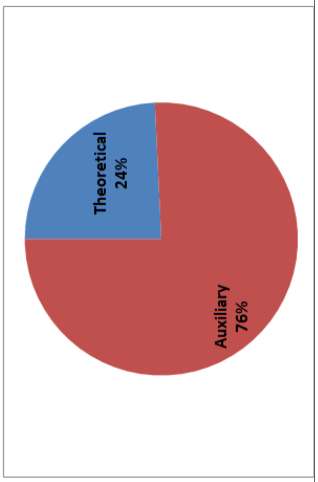

	E [J]	CO2 [g]	%
Theoretical	70,552	10.4	24
Spindle	75,741	11.2	26
Cutting Fluid	50,385	7.4	17
Turret	1,606	0.2	1
Chuck	172	0.0	0
Servo	6,374	0.9	2
Lubrication	69	0.0	0
Standby	86,139	12.7	30
TOTAL	**291,037**	**42.9**	**100**

	E [J]	CO2 [g]	%
Theoretical	70,552	10.4	24
Variable	134,345	19.8	46
Constant	86,139	12.7	30
TOTAL	**291,037**	**42.9**	**100**

	E [J]	CO2 [g]	%
Theoretical	70,552	10.4	24
Auxiliary	220,485	32.5	76
TOTAL	**291,037**	**42.9**	**100**

Figure B.19 Process energy estimation breakdown for SP3-AL6013

CURRICULUM VITAE

M. URAL ULUER

EDUCATION

Degree	**Institution**	**Year of Graduation**
Ph.D.	METU Mechanical Engineering	2024
M.Sc.	METU Mechanical Engineering	2007
B.Sc.	METU Mechanical Engineering	2003
High School	TED Ankara College	1998

WORK EXPERIENCE

Year	**Place**	**Enrollment**
2010 - Present	METU Mechanical Engineering	Instructor
2004 - 2010	METU Mechanical Engineering	Teaching Assistant

AWARDS

2018, Excellence in Education Award, Prof. Dr. Mustafa N. Parlar Education and Research Foundation

2017, Instructor of the Year Award, Prof. Dr. Mustafa N. Parlar Education and Research Foundation

2016, Instructor of the Year Award, Prof. Dr. Mustafa N. Parlar Education and Research Foundation

SELECTED PAPERS AND PRESENTATIONS

Uluer, M.U., Ünver, H.Ö., Akkök, M., & Kılıç, S.E. (2016). An Investigation into Power and Energy Requirements for the Auxiliary Components of a CNC Lathe. Proceedings of the 17th International Conference on Machine Design and Production, 2, 611-628, 12 - 15 July 2016, Bursa, Turkey.

Uluer, M.U., Ünver, H.Ö., Gök, G., Fescioğlu-Ünver, N., & Kılıç, S.E. (2016). A Framework for Energy Reduction in Manufacturing Process Chains (E-MPC) and a Case Study from the Turkish Household Appliance Industry. Journal of Cleaner Production, 112, 3342 - 3360.

Altıntaş, R.S., Uluer, M.U., Ünver, H.Ö., & Kılıç, S.E. (2013). A Theoretical Energy Consumption Prediction Model for Prismatic Parts Using STEP AP224 Features. Proceedings of the 11th Global Conference on Sustainable Manufacturing, 655 - 660, 23 - 25 September 2013, Berlin, Germany.

Uluer, M.U., Ünver, H.Ö., Akkuş, K., & Kılıç, S.E. (2013). A Model for Predicting Theoretical Process Energy Consumption of Rotational Parts Using STEP AP224 Features. Proceedings of the 20th CIRP International Conference on Life Cycle Engineering, 141 - 146, 17 - 19 April 2013, Singapore.

Uluer, M.U., Ünver, H.Ö., & Kılıç, S.E. (2012). An Eco-Tracking System for Environmentally Conscious Manufacturing. Proceedings of the 15th International Conference on Machine Design and Production, 2, 845 - 855, 19 - 22 June 2012, Pamukkale, Denizli, Turkey.

Ünver, H.Ö., Uluer, M.U., Altın, A., Taşcıoğlu, Y., & Kılıç, S.E. (2012). An Eco-Improvement Methodology for Reduction of Product Embodied Energy in Discrete Manufacturing. Proceedings of the 19th CIRP International Conference on Life Cycle Engineering, 405 - 410, 23 - 25 May 2012, Berkeley, USA.

Uluer, M.U., Gök, G., Ünver, H.Ö., & Kılıç, S.E. (2011). Towards a Decision Support Framework for Sustainable Manufacturing. Proceedings of the 9th Global Conference on Sustainable Manufacturing, 88-93, 28 - 30 September 2011, Saint Petersburg, Russia.